

**LINEAR AND CROSSLINKED POLY(N-ISOPROPYLACRYLAMIDE-CO-MONOITACONATE)S: SYNTHESIS, CHARACTERIZATION AND INVESTIGATION OF SOLUTION BEHAVIOUR**

**Ph.D. Thesis by  
Yalçın YILDIZ, M.Sc.**

**Department: Polymer Science and Technology**

**Programme: Polymer Science and Technology**

**FEBRUARY 2008**

**LINEAR AND CROSSLINKED POLY(N-ISOPROPYLACRYLAMIDE-CO-MONOITACONATE)S: SYNTHESIS, CHARACTERIZATION AND INVESTIGATION OF SOLUTION BEHAVIOUR**

**Ph.D. Thesis by  
Yalçın YILDIZ, M.Sc.  
515992008**

**Date of submission : 8 February 2008**

**Date of defence examination: 10 July 2008**

**Supervisors (Chairmans): Prof. Dr. Nurseli UYANIK  
Prof. Dr. Candan ERBİL**

**Members of the Examining Committee Prof.Dr. Tuncer ERCİYES (I.T.U.)  
Prof.Dr. Oğuz OKAY (I.T.U.)  
Prof.Dr. Ayten KUNTMAN (I.U.)  
Prof.Dr. Hüseyin YILDIRIM (Y.T.U.)  
Assoc. Prof.Dr. Özlem CANKURTARAN (Y.T.U)**

**FEBRUARY 2008**

**İSTANBUL TEKNİK ÜNİVERSİTESİ ★ FEN BİLİMLERİ ENSTİTÜSÜ**

**DOĞRUSAL VE ÇAPRAZ BAĞLI POLİ(N-İZOPROPİLAKRİLAMİT-KO-MONOİTAKONİK ASİT ESTER)LERİ: SENTEZİ, KARAKTERİZAYONU VE ÇÖZELTİ ÖZELLİKLERİNİN İNCELENMESİ**

**DOKTORA TEZİ**  
**Y. Kimyager Yalçın YILDIZ**  
**515992008**

**Tezin Enstitüye Verildiği Tarih : 8 Şubat 2008**

**Tezin Savunulduğu Tarih : 10 Temmuz 2008**

**Tez Danışmanları : Prof. Dr. Nurseli UYANIK**  
**Prof. Dr. Candan ERBİL**

**Diğer Jüri Üyeleri : Prof.Dr. Tuncer ERCİYES (İ.T.Ü.)**

**Prof.Dr. Oğuz OKAY (İ.T.Ü.)**

**Prof.Dr. Ayten KUNTMAN (İ.Ü.)**

**Prof.Dr. Hüseyin YILDIRIM (Y.T.Ü.)**

**Doç.Dr. Özlem CANKURTARAN (Y.T.Ü.)**

**ŞUBAT 2008**

## ACKNOWLEDGEMENTS

I would like to express my thankfulness and appreciation to my supervisors, especially Prof. Dr. Candan ERBİL and Prof. Dr. Nurseli UYANIK. Their continuous support and wide knowledge have been of great value for me. Their understanding, encourage and guidance have provided an invaluable contribution for the present dissertation.

I would like to express my sincere thanks to the thesis committee Prof. Dr. Ayten KUNTMAN, late Prof. Dr. Muhammed MUSTAFAYEV and Prof. Dr. Tuncer ERCİYES for their beneficial reviews, and productive advices during the preparation of this thesis.

I also would like to thank Prof. Dr. A.Sezai SARAÇ for permission to use UV-vis and FTIR facilities.

I wish to thank Dr. Fevzi Ç. CEBECİ, Dr. A. RIZA ERDEM, M.Sc. Hüseyin YALÇINKAYA, and M.Sc. Argun GÖKÇEÖREN for their precious contribution and their friendships.

My special thanks are to FLOKSER TEKSTİL SAN. TİC. A.Ş., Başar YILDIZ, M. Cenap CETİNTAŞ and MERVE MOCAN for their invaluable support.

I owe my loving thanks to my wife Yasemin GÜLER YILDIZ and my family, without their hearted support and understanding; it would have been impossible for me to finish this dissertation.

February 2008

Yalçın YILDIZ

## TABLE OF CONTENTS

<b>LIST OF ABBREVIATIONS .....</b>	<b>vii</b>
<b>LIST OF TABLES.....</b>	<b>ix</b>
<b>LIST OF FIGURES.....</b>	<b>x</b>
<b>LIST OF SYMBOLS .....</b>	<b>xvi</b>
<b>SUMMARY .....</b>	<b>xviii</b>
<b>ÖZET.....</b>	<b>xxiv</b>
<b>1. INTRODUCTION .....</b>	<b>1</b>
<b>2. THEORY.....</b>	<b>5</b>
2.1. Polymers as Linear Free Chains in Solution .....	7
2.2. Polymeric Gels .....	8
2.2.1. Defects in gels .....	9
2.3. Lower Critical Solution Temperature (LCST) .....	11
2.3.1. Determination of LCST by UV-VIS spectrophotometer .....	13
2.3.2. Determination of LCST by differential scanning calorimetry .....	13
2.3.3. Determination of LCST by light-scattering .....	14
2.4. Importance of Lower Critical Solution Temperature .....	14
2.4.1. LCST of modified temperature-sensitive polymers .....	16
2.5. Swelling and Volume Phase Transitions of Gels .....	19
2.5.1. Flory-Rehner theory (FH Theory).....	20
2.5.2. Fundamental interactions and gel phase transitions.....	22
2.6. Applications .....	26
2.6.1. Mechanical devices .....	27
2.6.2. Solvent purification.....	27
2.6.3. Pharmaceutical applications.....	28
2.7. Mechanical Strength of the Gels .....	34
<b>3. EXPERIMENTAL SECTION .....</b>	<b>36</b>
3.1. Materials.....	36
3.1.1. N-isopropylacrylamide (NIPAAm).....	36
3.1.2. Itaconic acid (IA) .....	36
3.1.3. N,N,N',N'- tetramethylethylene diamine (TEMED) .....	37
3.1.4. Potassium persulfate (K <sub>2</sub> S <sub>2</sub> O <sub>8</sub> ).....	37
3.1.5. N,N'-methylenebisacrylamide (BIS) .....	37
3.1.6. Azobis(isobutyronitrile) (AIBN).....	38
3.1.7. Dimethyl itaconate (DMI).....	38

3.1.8.	$\alpha,\omega$ -acryloxyorganofunctional poly(dimethylsiloxane) vinyl terminated PDMS (VTPDMS) .....	38
3.1.9.	$\alpha,\omega$ -acryloxyorganofunctional poly(dimethylsiloxane) vinyl terminated PDMS (VTPDMS) .....	39
3.1.10.	Acetyl chloride (AcCl) .....	39
3.1.11.	Theophylline (THP) .....	39
3.1.12.	Chloroform (CHCl <sub>3</sub> ) .....	40
3.1.13.	1,4-Dioxane .....	40
3.1.14.	Benzene (C <sub>6</sub> H <sub>6</sub> ) .....	40
3.1.15.	n-Heptane .....	40
3.1.16.	Methanol (MetOH) .....	41
3.1.17.	Octyl alcohol (C <sub>8</sub> H <sub>18</sub> O) .....	41
3.1.18.	Cetyl alcohol (C <sub>16</sub> H <sub>34</sub> O) .....	41
3.1.19.	Butyl alcohol (C <sub>4</sub> H <sub>10</sub> O) .....	42
3.1.20.	Sodium chloride (NaCl) .....	42
3.1.21.	Potassium chloride (KCl) .....	42
3.1.22.	Potassium dihydrogen phosphate (KH <sub>2</sub> PO <sub>4</sub> ) .....	42
3.1.23.	Disodium hydrogen phosphate (Na <sub>2</sub> HPO <sub>4</sub> ) .....	42
3.1.24.	Citric acid monohydrate (C <sub>6</sub> H <sub>8</sub> O <sub>7</sub> .H <sub>2</sub> O) .....	42
3.1.25.	Phosphoric acid (H <sub>3</sub> PO <sub>4</sub> ) .....	42
3.1.26.	Boric acid (H <sub>3</sub> BO <sub>3</sub> ) .....	42
3.1.27.	Sodium hydroxide (NaOH) .....	43
3.1.28.	Hydrochloric acid (HCl) .....	43
3.1.29.	Distilled-deionized water (DDW) .....	43
3.1.30.	Phosphate buffer (PBS) .....	43
3.1.31.	Citrate buffer (CB) .....	43
3.2.	Experimental Set-up and Equipment .....	44
3.2.1.	Thermostated water bath .....	44
3.2.2.	Vacuum oven .....	44
3.2.3.	Oven .....	44
3.2.4.	Digital compass .....	44
3.2.5.	Tubes .....	44
3.2.6.	FT-IR specrophotometer .....	44
3.2.7.	UV-visible spectrophotometer .....	44
3.2.8.	Compressive testing .....	45
3.2.9.	Conductometer and pH-meter .....	45
3.2.10.	Differential scanning calorimetry (DSC) .....	45
3.2.11.	Gel permeation chromatography (GPC) .....	45
3.3.	Synthesis and Characterization of Crosslinked and Linear PNIPAAm .....	46
3.3.1.	Synthesis of PNIPAAm hydrogels crosslinked with VTPDMS .....	46
3.3.2.	Synthesis of monoesters of itaconic acid .....	49
3.3.3.	Synthesis of PNIPAAm/monoitaconate copolymer hydrogels crosslinked with BIS .....	51
3.3.4.	Synthesis of linear PNIPAAm, its copolymers and terpolymers with itaconic acid, its monoitaconates and dimethyl itaconate .....	52
3.4.	Drug Loading and Release .....	54
3.4.1.	Standard absorbance curve .....	54
3.4.2.	Drug loading and drug delivery system (DDS) preparation .....	54
3.4.3.	Drug release study .....	54
3.5.	Characterization methods .....	55

3.5.1.	Measurements of gel diameter .....	55
3.5.2.	Gravimetric and volumetric measurement .....	55
3.5.3.	Compression-strain measurements .....	56
3.5.4.	Measurement of swelling kinetics.....	57
3.5.6.	Determination of monoitaconate content in linear NIPAAm copolymers .....	59
3.5.7.	Cloud point measurements .....	59
<b>4.</b>	<b>RESULTS AND DISCUSSION.....</b>	<b>60</b>
4.1.	Compressive Elastic Moduli of Poly(NIPAAm) Hydrogels Crosslinked with VTPDMS.....	60
4.2.	Synthesis and Characterization of Monoitaconates .....	71
4.3.	Compressive Elastic Moduli of NIPAAm Copolymer Hydrogel: the Effects of Crosslinker Concentration, Temperature and, Type and Concentration of Monoitaconates on the Swelling Equilibria and Mechanical Properties. ..	74
4.4.	Drug release of Theophylline from PNIPAAm and its Copolymer Hydrogels Crosslinked with BIS and VTPDMS.....	99
4.5.	Solution Behavior of NIPAAm/Monoitaconate Copolymers and NIPAAm/Itaconic Acid/Dimethyl Itaconate Terpolymers.....	110
4.5.1.	Cloud point (LCST) measurements .....	117
<b>5.</b>	<b>CONCLUSION.....</b>	<b>129</b>
	<b>REFERENCES.....</b>	<b>132</b>
	<b>BIOGRAPHY .....</b>	<b>145</b>

## LIST OF ABBREVIATIONS

<b>NIPAAm</b>	: N-isopropylacrylamide
<b>PNIPAAm</b>	: poly(N-isopropylacrylamide)
<b>LCST</b>	: Lower Critical Solution Temperature
<b>KPS</b>	: Potassium Persulfate
<b>APS</b>	: Ammonium Persulfate
<b>AIBN</b>	: Azobis(isobutyronitrile)
<b>THF</b>	: Tetrahydrofuran
<b>TEMED</b>	: N,N,N',N'-tetramethylethylenediamine
<b>AAm</b>	: Acrylamide
<b>SP</b>	: Smart Polymer
<b>CP</b>	: Critical Point
<b>DSC</b>	: Differential Scanning Calorimetry
<b>LS</b>	: Light Scattering
<b>FT-IR</b>	: Fourier Transform Infrared Spectrometer
<b>NMR</b>	: Nuclear Magnetic Resonance
<b>DLS</b>	: Dynamic Light Scattering
<b>DOAM</b>	: Di-n-octylacrylamide
<b>DPAM</b>	: Di-n-propylacrylamide
<b>DDAM</b>	: Di-n-dodecylacrylamide
<b>PAA</b>	: poly(acrylic acid)
<b>PMcA</b>	: poly(methacrylic acid)
<b>PIA</b>	: poly(itaconic acid)
<b>BIS</b>	: N,N'-methylenebisacrylamide
<b>ETAS</b>	: Ethyltriacetoxysilane
<b>FH</b>	: Flory-Huggins Theory
<b>POE</b>	: poly(oxyethylene)
<b>PVME</b>	: poly(vinylmethylether)
<b>PVP</b>	: poly(vinylpyrrolidinone)
<b>PAAm</b>	: poly(acrylamide)

<b>DMI</b>	: Dimethyl Itaconate
<b>IA</b>	: Itaconic Acid
<b>AA</b>	: Acrylic Acid
<b>DMF</b>	: N,N'-dimethylformamide
<b>PDMS</b>	: poly(dimethylsiloxane)
<b>VTPDMS</b>	: Vinyl terminated poly(dimethylsiloxane)
<b>GLY</b>	: octa functional glyoxal bis(diallyl acetal)
<b>PDEAAm</b>	: poly(N,N'-diethylacrylamide)
<b>PEO</b>	: poly(ethylene oxide)
<b>PPO</b>	: poly(propylene oxide)
<b>PMA</b>	: poly(methacrylic acid)
<b>DDS</b>	: Drug Delivery System
<b>THP</b>	: Theophylline
<b>DDW</b>	: Distilled-deionized Water
<b>GPC</b>	: Gel Permission Chromatography
<b>MMI</b>	: Mono Methyl Itaconate
<b>MBuI</b>	: Mono Butyl Itaconate
<b>MCeI</b>	: Mono Cetyl Itaconate
<b>MOcI</b>	: Mono Octyl Itaconate
<b>PDMI</b>	: poly(dimethyl itaconate)
<b>PBS</b>	: Phosphate Buffer Saline
<b>CB</b>	: Citrate Buffer
<b>MetOH</b>	: Methanol
<b>HB</b>	: Hydrogel with BIS
<b>HP</b>	: Hydrogel with PDMS
<b>DSR</b>	: Deswelling Ratio
<b>SR</b>	: Swelling Ratio
<b>SR<sub>eq</sub></b>	: Swelling Ratio of the gel at equilibrium

## LIST OF TABLES

	<u>Page number</u>
<b>Table 3.1</b> : Synthesis Conditions, Melting Points and Yields of Monoitaconates.....	50
<b>Table 4.1</b> : Polymerization Conditions, Polymer Volume Fractions ( $v_{2r}, v_{2s}$ ), Compression Moduli (G) and Polymer-water Interaction Parameters ( $\chi$ ) at Swelling Equilibria at 25°C for Neutral PNIPAAm Hydrogels Prepared in the Presence of two Different Crosslinker.....	61
<b>Table 4.2</b> : Swollen Diameters of the Samples Given in Tables 4.1.....	70
<b>Table 4.3</b> : Type and Comonomer Concentration of Monoitaconates in NIPAAm Hydrogels ( $T=23\pm 2^\circ\text{C}$ ).....	74
<b>Table 4.4</b> : Polymer Volume Fractions ( $v_{2r}, v_{2s}$ ), Compression Moduli (G) and Polymer-water Interaction Parameters ( $\chi$ ) at 23°C for PNIPAAm, NIPAAm/IA, and NIPAAm/monoitaconate (MBuI, MOcI, MCeI) Hydrogels Prepared Using BIS ( $2.50\times 10^{-2}$ mol/L and $3.75\times 10^{-2}$ mol/L) and AIBN as Crosslinker and Initiator.....	82
<b>Table 4.5</b> : Polymer Volume Fractions ( $v_{2r}, v_{2s}$ ), Compression Moduli (G) and Polymer-water Interaction Parameters ( $\chi$ ) at 37 °C for PNIPAAm, and NIPAAm/monoitaconate (MBuI, MOcI, MCeI) Hydrogels Prepared Using BIS ( $2.50\times 10^{-2}$ mol/L and $3.75\times 10^{-2}$ mol/L) and AIBN as Crosslinker and Initiator.....	83
<b>Table 4.6</b> : Polymer Volume Fractions ( $v_{2r}, v_{2s}$ ), Compression Moduli (G) and Polymer-water Interaction Parameters ( $\chi$ ) at 23 °C and 37 °C for PNIPAAm and NIPAAm/MOcI Hydrogels Prepared Using BIS and $\text{K}_2\text{S}_2\text{O}_8$ as Crosslinker and Initiator..	94
<b>Table 4.7</b> : Initial Slope ( $k_{sr}$ ), Diffusional Exponent (n) and Diffusion Parameter (k) Values of PNIPAAm and PNIPAAm/IA Copolymeric Hydrogels at 25°C in DDW.....	112
<b>Table 4.8</b> : Initial Slope ( $k_{sr}$ ), Diffusional Exponent (n) and Diffusion Parameter (k) Values of PNIPAAm and PNIPAAm/IA Copolymeric Hydrogels at 25°C in pH 7.50 Phosphate Buffer	113
<b>Table 4.9</b> : Synthesis Conditions, GPC and DSC Results of PNIPAAm, PDMI and NIPAAm/monoitaconate Copolymers.....	123
<b>Table 4.10</b> : DSC Results of NIPAAm Copolymers and Terpolymers.....	125
<b>Table 4.11</b> : Feed and Copolymer Compositions of NIPAAm Copolymers	127
<b>Table 4.12</b> : pH and Solvent Dependence of LCST for PNIPAAm, NIPAAm/IA and NIPAAm/MBuI Copolymers, Containing 10.0 mol % of Comonomer in the Feed.....	131

## LIST OF FIGURES

	<u>Page number</u>
<b>Figure 1.1</b> : Gel is Defined as a Cross-linked Polymer Network Swollen With a Liquid. Gels Undergo Reversible Volume Transition in Response to Changes in External Conditions.....	2
<b>Figure 2.1</b> : Classification of the Polymers by Their Physical Form: (i) Linear Free Chains in Solution Where Polymer Undergoes a Reversible Collapse After an External Stimulus is Applied; (ii) Covalently Cross-linked Reversible Gels Where Swelling or Shrinking of the Gels can be Triggered by Environmental Change; and (iii) Chain Adsorbed or Surface-grafted Form, Where the Polymer Reversibly Swells or Collapses on Surface, Once an External Parameter is Changed.....	7
<b>Figure 2.2</b> : Schematic of Crosslinking Polymerization Process of PNIPAAm.....	9
<b>Figure 2.3</b> : Schematic Illustration of Thermo-sensitive Polymers.....	11
<b>Figure 2.4</b> : Schematic Illustration for Networks of NIPAAm Gels as – Synthesized in Water and DMF.....	12
<b>Figure 2.5</b> : Ionic Interaction.....	22
<b>Figure 2.6</b> : Hydrophobic Interaction.....	23
<b>Figure 2.7</b> : (a) Van der Waals and (b) Hydrogen Bonding Interactions....	24
<b>Figure 2.8</b> : The Left Part Shows Isotherms for a Van Der Waals Gas Near a Critical. The Right Part Shows Isobars for a Gel Near a Critical Point.....	25
<b>Figure 2.9</b> : Schematic Illustration of Oral Colon-specific Drug Delivery Using Biodegradable and pH-sensitive Hydrogels. The Azoaromatic Moieties in the Cross-links are Designated by –N=N-.....	31
<b>Figure 2.10</b> : Schematic Illustration of the Novel, Thermo-responsive DDS to Give a Positive Drug Release by Modulating the External Temperature.....	33
<b>Figure 3.1</b> : Structural Formula of N-isopropylacrylamide.....	36
<b>Figure 3.2</b> : Structural Formula of Itaconic Acid.....	36
<b>Figure 3.3</b> : Structural Formula of N,N,N',N'- Tetramethylethylene Diamine.....	37
<b>Figure 3.4</b> : Structural Formula of N,N'-methylenebisacrylamide.....	37
<b>Figure 3.5</b> : Structural Formula of Azobis(isobutyronitrile).....	38
<b>Figure 3.6</b> : Structural Formula of Dimethyl Itaconate.....	38
<b>Figure 3.7</b> : Structural Formula of $\alpha,\omega$ -acryloxyorganofunctional Poly(dimethylsiloxane).....	39
<b>Figure 3.8</b> : Structural Formula of $\alpha,\omega$ -acryloxyorganofunctional Poly(dimethylsiloxane).....	39
<b>Figure 3.9</b> : Structural Formula of Acetyl Chloride.....	39

<b>Figure 3.10 :</b>	Structural Formula of Theophylline.....	40
<b>Figure 3.11 :</b>	Structural Formula of 1,4-Dioxane.....	40
<b>Figure 3.12 :</b>	Structural Formula of n-Heptane.....	41
<b>Figure 3.13 :</b>	Structural Formula of Methanol.....	41
<b>Figure 3.14 :</b>	Structural Formula of Octyl Alcohol.....	41
<b>Figure 3.15 :</b>	Structural Formula of Cetyl Alcohol.....	41
<b>Figure 3.16 :</b>	Structural Formula of Butyl Alcohol.....	42
<b>Figure 3.17 :</b>	Photograph of Compressive Testing Machine.....	45
<b>Figure 4.1 :</b>	Compression Process of Sample HB11 in Table 4.1: (a) Initial (F = 0.0 N) and (b) Final States (F = 5.0 N).....	62
<b>Figure 4.2 :</b>	Compression Process of Sample HP1 in Table 4.1: (a) Initial (F = 0.0 N) and (b) Final States(F = 5.0 N).....	62
<b>Figure 4.3 :</b>	Measured Force, F (N) as a Function of Compression (mm) for Samples HB10 – HB13 Given in Table 4.1.....	64
<b>Figure 4.4 :</b>	Measured Force, F (N) as a Function of Compression (mm) for Samples HP1, HP3 – HP5 Given in Table 4.1.....	64
<b>Figure 4.5 :</b>	Measured Force, F (N) as a Function of Compression (mm) for Samples HP2, HP7 – HP9 Given in Table 4.1.....	66
<b>Figure 4.6 :</b>	Compression Stress-strain Curves (Pressure (Pa) vs. $-(\lambda-\lambda^{-2})$ ) for Samples HB10 – HB13 Given in Table 4.1.....	67
<b>Figure 4.7 :</b>	Compression Stress-strain Curves (Pressure (Pa) vs. $-(\lambda-\lambda^{-2})$ ) for Samples HP1, HP3 – HP5 Given in Table 4.....	68
<b>Figure 4.8 :</b>	Compression Stress-strain Curves (Pressure (Pa) vs. $-(\lambda-\lambda^{-2})$ ) for Samples HP2, HP7 – HP9 Given in Table 4.1.....	69
<b>Figure 4.9 :</b>	FTIR Spectra of (a) IA, (b) MbuI and (c) MceI.....	72
<b>Figure 4.10 :</b>	Potentiometric Titration Curves of (a) MMI and (b) IA.....	73
<b>Figure 4.11 :</b>	Conductometric Titration Curves of (a) MMI and (b) IA.....	73
<b>Figure 4.12 :</b>	Temperature Dependence of the Volume Swelling Ratios of the PNIPAAm and Ionic NIPAAm/IA Copolymer Gels Identified in Table 4.3.....	75
<b>Figure 4.13 :</b>	Temperature Dependence of the Volume Swelling Ratios of the PNIPAAm and NIPAAm/DMI Copolymer Gels Identified in Table 4.3.....	76
<b>Figure 4.14 :</b>	Temperature Dependence of the Volume Swelling Ratios of the PNIPAAm and NIPAAm/MMI Copolymer Gels Identified in Table 4.3.....	76
<b>Figure 4.15 :</b>	Temperature Dependence of the Volume Swelling Ratios of the PNIPAAm, NIPAAm/IA, NIPAAm/MMI, NIPAAm/MbuI, NIPAAm/DMI Gels Having 1.0 mole % of Comonomer, Which is Identified in Table 4.3.....	77
<b>Figure 4.16 :</b>	Temperature Dependence of the Volume Swelling Ratios of the PNIPAAm, NIPAAm/IA, NIPAAm/MMI, NIPAAm/DMI Copolymer Gels Having 2.50 mole % of Comonomer, Which is Identified in Table 4.3.....	78
<b>Figure 4.17 :</b>	Temperature Dependence of the Volume Swelling Ratios of the PNIPAAm, NIPAAm/IA, NIPAAm/MMI, NIPAAm/DMI Copolymer Gels Having 5.0 mole % of Comonomer, Which is Identified in Table 4.3.....	79

<b>Figure 4.18 :</b>	Temperature Dependence of the Volume Swelling Ratios of the PNIPAAm, NIPAAm/IA, NIPAAm/MMI, NIPAAm/DMI Copolymer Gels Having 10.0 mole % of Comonomer, Which is Identified in Table 4.3.....	79
<b>Figure 4.19 :</b>	Temperature Dependence of the Volume Swelling Ratios of the Effect of Crosslinker type and Concentration on the Swelling Behavior of PNIPAAm Hydrogels.....	80
<b>Figure 4.20 :</b>	Photographs of PNIPAAm Hydrogels Crosslinked with BIS and Equilibrated in DDW: (a) Sample HB11, (b) Sample HB12.....	81
<b>Figure 4.21 :</b>	Photograph Showing the Morphology of PNIPAAm Hydrogel Crosslinked with VTPDMS and Equilibrated in DDW: (a) Sample HP2, (b) Sample HP1.....	81
<b>Figure 4.22 :</b>	Measured Force, F (N) as a Function of Compression (mm) for Samples HB35, HB36, HB37, HB38, HB39, HB40, and HB41 are Given in Table 4.4. (Tswelling= 23°C).....	84
<b>Figure 4.23 :</b>	Measured Force, F (N) as a Function of Compression (mm) for Samples HB35, HB36, HB37, HB38, HB39, HB40, HB41 Given in Table 4.5 (Tswelling= 37°C).....	85
<b>Figure 4.24 :</b>	Compression Stress-strain Curves (Pressure (Pa) vs. $-(\lambda-\lambda^{-2})$ ) for Samples HB35, HB36, HB37, HB38, HB39, HB40, and HB41 are Given in Table 4.4. (Tswelling= 23°C).....	86
<b>Figure 4.25 :</b>	Compression Stress-strain Curves (Pressure (Pa) vs. $-(\lambda-\lambda^{-2})$ ) for Samples HB35, HB36, HB37, HB38, HB39, HB40, and HB41, Given in Table 4.5. (Tswelling = 37°C).....	86
<b>Figure 4.26 :</b>	Series of Photograph Showing the Morphology of PNIPAAm Hydrogels Equilibrated in DDW 37°C, (a) HB36, (b) HB37, (c) HB38, (d) HB39, (e) HB40, (f) HB41.....	87
<b>Figure 4.27 :</b>	Measured Force, F (N) as a Function of Compression (mm) for Samples HB42, HB43, HB44, HB45, HB46, HB47, HB48 Given in Table 4.4 (Tswelling= 23°C).....	88
<b>Figure 4.28 :</b>	Measured Force, F (N) as a Function of Compression (mm) for Samples HB42, HB43, HB44, HB45, HB46, HB47, HB48 Given in Table 4.5 (Tswelling= 37°C).....	89
<b>Figure 4.29 :</b>	Compression Stress-strain Curves (Pressure (Pa) vs. $-(\lambda-\lambda^{-2})$ ) for Samples HB42, HB43, HB44, HB45, HB46, HB47, and HB48 Given in Table 4.4. (Tswelling = 23°C).....	90
<b>Figure 4.30 :</b>	Compression Stress-strain Curves (Pressure (Pa) vs. $-(\lambda-\lambda^{-2})$ ) for Samples HB42, HB43, HB44, HB45, HB46, HB47, and HB48 Given in Table 4.5. (Tswelling= 37°C).....	90
<b>Figure 4.31 :</b>	Series of Photograph Showing the Morphology of NIPAAm/monoitaconate Hydrogels Crosslinked with $3.75 \times 10^2$ mol/L Concentration of BIS in DDW at 37°C: (a) HB42, (b) HB43, (c) HB45, (d) HB46, (e) HB47, (g) HB48...	91
<b>Figure 4.32 :</b>	Measured Force, F (N) as a Function of Compression (mm) for Samples HB35, HB42, HB49, HB50 Given in Table 4.4 (Tswelling = 23°C).....	92
<b>Figure 4.33 :</b>	Compression Stress-strain Curves (Pressure (Pa) vs. $-(\lambda-\lambda^{-2})$ ) for Samples HB35, HB42, HB49, and HB40 Given in Table 4.4. (Tswelling= 23°C).....	93

<b>Figure 4.34 :</b>	Measured Force, F (N) as a Function of Compression (mm) for Samples HB11, HB51, HB52, HB53, and HB54 Given in Table 4.6. (Tswelling= 23°C).....	95
<b>Figure 4.35 :</b>	Measured Force, F (N) as a Function of Compression (mm) for Samples HB11, HB51, HB52, HB53, HB54 Given in Table 4.16 (Tswelling = 37°C).....	96
<b>Figure 4.36 :</b>	Compression Stress-strain Curves (Pressure (Pa) vs. $-(\lambda-\lambda^{-2})$ ) for Samples HB11, HB51, HB52, HB53, and HB54 Given in Table 4.6. (Tswelling = 23°C).....	97
<b>Figure 4.37 :</b>	Compression Stress-strain Curves (Pressure (Pa) vs. $-(\lambda-\lambda^{-2})$ ) for Samples HB51, HB52, HB53, and HB54 Given in Table 4.6. (Tswelling = 37°C).....	97
<b>Figure 4.38 :</b>	Series of Photograph Showing the Morphology of PNIPAAm Hydrogels in DDW at 37°C, (a) HB51, (b) HB52, (c) HB53, (d) HB 54.....	98
<b>Figure 4.39 :</b>	Percentage Mass Swelling as a Function of Time for the Series of NIPAAm Hydrogels at 25°C in pH 7.5 Phosphate Buffer.....	100
<b>Figure 4.40 :</b>	The Plot of Percentage Mass Swelling Versus Square Root of Time for NIPAAm Hydrogels at 25°C in pH 7.5 Phosphate Buffer.....	101
<b>Figure 4.41 :</b>	Percentage Mass Swelling as a Function of Time for the Series of NIPAAm Hydrogels at 25°C in Distilled Water.....	102
<b>Figure 4.42 :</b>	The Plot of Percentage Mass Swelling Versus Square Root of Time for NIPAAm Hydrogels at 25°C in Distilled Water.....	103
<b>Figure 4.43 :</b>	The Plot of ln F vs ln t for the Series of NIPAAm Hydrogels at Different Comonomer Concentration at 25°C in Distilled Water.....	103
<b>Figure 4.44 :</b>	The Plot of ln F vs ln t for the Series of NIPAAm Hydrogels at Different Comonomer Concentration at 25°C in pH 7.5 Phosphate Buffer.....	104
<b>Figure 4.45 :</b>	Deswelling Ratio as a Function of Time for the NIPAAm and NIPAAm/IA Copolymeric Hydrogels (Sample HB12, HP1, HB16, HP3, and HP6) at 37°C in DDW.....	105
<b>Figure 4.46 :</b>	The Standart Calibration Curve of the Absorbance as a Function of the Theophylline Concentration at 266 nm.....	106
<b>Figure 4.47 :</b>	Absorbance (at 266 nm) vs Time of Theophylline Release (C=0.1 g/L) for the PNIPAAm and NIPAAm/IA Copolymer hydrogels.....	107
<b>Figure 4.48 :</b>	Absorbance (at 266 nm) vs Time of Theophylline Release (C=0.1 g/L) for the PNIPAAm, NIPAAm/IA, NIPAAm/MBuI, NIPAAm/MOcI and NIPAAm/MCeI Copolymer Hydrogels.....	107
<b>Figure 4.49 :</b>	Absorbance (at 266 nm) vs Time of Theophylline Release (C=0.3 g/L) for the PNIPAAm and NIPAAm/IA Copolymer Hydrogels.....	108
<b>Figure 4.50 :</b>	Absorbance (at 266 nm) vs Time of Theophylline Release (C=0.3 g/L) for the PNIPAAm, NIPAAm/IA, NIPAAm/MBuI, NIPAAm/MOcI and NIPAAm/MCeI Copolymer Hydrogels.....	109

<b>Figure 4.51 :</b>	DSC Thermograms of NIPAAm/IA (L-16), NIPAAm/MOCl (L-19), NIPAAm/MCeI (L-20) Copolymers Containing 5.0 mole % of Comonomer in the Feed.....	113
<b>Figure 4.52 :</b>	DSC Thermograms of NIPAAm/IA (L-4), NIPAAm/DMI/IA Terpolymers Containing 10.0 mole % of Total Comonomer Content in the Feed.....	113
<b>Figure 4.53 :</b>	FTIR Spectrum of PNIPAAm.....	115
<b>Figure 4.54 :</b>	FT-IR Spectra of NIPAAm/IA Copolymers. IA Content in the Feed (a) 2.5 mole %, (b) 5.0 mole %, (c) 7.5 mole % (in 1,4-Dioxane).....	116
<b>Figure 4.55 :</b>	FTIR Spectra of NIPAAm/DMI/IA Terpolymers. (a) PNIPAm, (b) 2.5 mole % of IA+7.5 mole % of DMI, (c) 5.0 mol % of IA+5.0 mole % of DMI (in 1,4-Dioxane).....	117
<b>Figure 4.56 :</b>	Absorbance of the NIPAAm/IA (a) and NIPAAm/MBuI (b) Copolymer Solutions as a Function of Temperature (in DDW and in CB at pH4; Comonomer Content: 10.0 mol %, in the Feed).....	120
<b>Figure 4.57 :</b>	Absorbances ( $\lambda = 400$ nm) of the NIPAAm/IA (10 mole % of IA) (L-4); NIPAAm/DMI/IA (9.0 mole% of IA+1.0 mole % of DMI) (L-13) and 1.0 mole % of IA+9.0 mole % of DMI (L-15) Copolymer and Terpolymer Solutions as a Function of Temperature (in DDW at pH4 in 1,4-Dioxane).....	121
<b>Figure 4.58 :</b>	Absorbances ( $\lambda = 400$ nm) of the NIPAAm/IA (10 mole % of IA) (L-4); NIPAAm/DMI/IA (9.0 mole% of IA+1.0 mole % of DMI) (L-13) and 1.0 mole % of IA+9.0 mole % of DMI (L-15) Copolymer and Terpolymer Solutions as a Function of Temperature (in CB at pH4, in 1,4-Dioxane).....	122
<b>Figure 4.59 :</b>	Changes in Cloud Points as a Function of pH for Solutions of the PNIPAAm, and NIPAAm/monoester and NIPAAm/diester of IA Copolymers (measured as visual, in DDW). The Samples are Described in Tables 4.9.....	122
<b>Figure 4.60 :</b>	Changes in Cloud Points as a Function of Comonomer Content of the NIPAAm/IA, NIPAA/DMI and NIPAAm/DMI/IA Copolymers and Terpolymers (measured as visual, in DDW). The Samples are Described in Tables 4.9-4.11 (L-21) 1.0 % IA, (L-22) 2.5 % IA; (L-16) 5.0 mole % of IA; (L-23) 7.5 mole % of IA; (L-4) 10.0 mole % of IA ; (L-13) 9.0 mole % of IA-1.0 mole % of DMI; (L-27) 7.5 mole % of IA-2.5 mole % of DMI; (L-14) 5.0 mole % of IA-5.0 mole % of DMI; (L-28) 2.5 mole % of IA-7.5 mole % of DMI; (L-15) 1.0 mole % of IA-9.0 mole % of DMI; (L-8) 10.0 mole % of DMI; (L-17) 5.0 mole % of DMI; (L-29) 1.0 mole % of DMI.....	123
<b>Figure 4.61 :</b>	Changes in Cloud Points as a Function of pH for Solutions of the NIPAAm/IA Copolymers (measured as visual, in DDW). The Samples are Described in Tables 4.9-4.11.....	125

<b>Figure 4.62 :</b>	Changes in LCSTs as a Function of pH for the Aqueous Solutions of PNIPAAm (L-2), NIPAAm/IA (L-21), NIPAAm/MOCl (L-24), NIPAAm/MOCl (L-25, 2.5 mole % of MOCl) and NIPAAm/MCeI (L-26) Copolymers Containing 1.0 mole % of Comonomer (except Sample L-25) in the Feed (measured as visual, in DDW). Copolymer Compositions of the Samples are Described in Table 4.1.....	125
<b>Figure 4.63 :</b>	Changes in Cloud Points as a Function of pH for Solutions of the PNIPAAm, NIPAAm/IA, NIPAA/DMI and NIPAAm/DMI/IA Copolymers and Terpolymers (measured as visual, in DDW). The Samples are Described in Tables 4.9-4.11.....	126
<b>Figure 4.64 :</b>	Effect of MOCl and MCeI Contents on the LCSTs of the Polymers PNIPAAm (measured as visual in DDW at pH 4). The Polymer Compositions of Samples L-2 (PNIPAAm), L-19 (1.0 mole % of MOCl, in the feed), L-25 (2.5 mole % of MOCl, in the feed) and L-26 (1.0 mole % of MCeI, in the feed) are Described in Table 4.10.....	127

## LIST OF SYMBOLS

$\Delta G$	: Gibbs free energy change
$\Delta G_{\text{mix}}$	: Gibbs free energy change of mixing
$\Delta G_{\text{el}}$	: Gibbs free energy change of elastic deformation
$\Delta G_i$	: Gibbs free energy change of electrostatic interactions
$\mu_1$	: Chemical potential of solvent inside the gel
$\mu_1^0$	: Chemical potential of solvent outside the gel
$k$	: Boltzman constant
$T$	: Temperature
$n_1$	: Number of swelling agent molecules in the solution
$n_2$	: Number of polymer molecules in the solution
$v_1$	: Volume fraction of solvent
$v_{2s}$	: Polymer volume fraction of the swollen chains in the swollen state
$v_{2r}$	: Polymer volume fraction in the gel
$\chi$	: Polymer-solvent interaction parameter
$\nu$	: Number of network chains
$\phi$	: Number of junction
$M_c$	: Average molecular weight between crosslinking points
$d$	: Equilibrium diameter of the gel
$d_0$	: Original diameter of the gel
$\nu_e$	: Crosslinking density
$\pi$	: Osmotic pressure
$W_\infty$	: Equilibrium water content
$\tau$	: Applied force per unit area of the sample
$F$	: Force
$A_0$	: Area
$G$	: Compression moduli
$w_1$	: Weight of dry gel sample
$w_2$	: Solvent absorbed by the sample during swelling
$\rho_1$	: Density of the solvent

<b><math>\rho_2</math></b>	: Density of the dry gel
<b>S%</b>	: Mass swelling percentages
<b><math>m_0</math></b>	: Mass of the dry gel at the beginning (t=0)
<b><math>m_t</math></b>	: Mass of the swollen/shrunken gel at time t
<b><math>m_{t,eq}</math></b>	: Mass of the swollen gel at equilibrium
<b><math>k_{sr}</math></b>	: Swelling rate
<b>t</b>	: Time
<b>F</b>	: Fractional uptake
<b><math>M_\infty</math></b>	: Maximum amount absorbed
<b>n</b>	: Diffusional exponent
<b>D</b>	: Diffusion coefficient
<b><math>m_p</math></b>	: Mass of the dry polymer
<b><math>m_s</math></b>	: Absorbed solvent
<b><math>V_2^0</math></b>	: Volume fraction of the polymer at the gel preparation
<b><math>T_g</math></b>	: Glass transition temperature
<b>Mw</b>	: Weight average molecular weight
<b>Mn</b>	: Number average molecular weight
<b><math>V_s</math></b>	: Volume after equilibrium swelling
<b><math>V_r</math></b>	: Volume before equilibrium swelling
<b><math>\chi_s</math></b>	: Entropic contributions to the polymer-water interaction parameter
<b>A</b>	: Absorbance
<b>C:</b>	: Concentration

# LINEAR AND CROSSLINKED POLY(N-ISOPROPYLACRYLAMIDE-CO-MONOITACONATE)S: SYNTHESIS, CHARACTERIZATION AND INVESTIGATION OF SOLUTION BEHAVIOUR

## SUMMARY

The temperature-sensitive and pH-sensitive polymers have many applications for various purposes. Temperature-sensitive polymers exhibit lower critical solution temperature (LCST) behaviour where phase separation is induced by surpassing a certain temperature threshold. LCST is a phase transition behavior of materials. The LCST of linear polymer in a solvent, in which the polymer are soluble at the low temperatures but separate into an aggregated phase when the temperature is raised above their characteristic LCST (in Figure 1a). The LCST definition can also be used for gels. The LCST of crosslinked polymer (a gel) in a solvent, in which the polymer swells at the low temperatures but shrink when the temperature is raised above their characteristic LCST (in Figure 1b). PNIPAAm (Poly(N-isopropyl acrylamide)) is the most popular member of this class of polymers has also attracted wide interest in biomedical applications that exhibits LCST in aqueous solutions which lies between 32°C and 34 °C, which is close body temperature. PNIPAAm linear chains and hydrogels expand or swell when they are cooled below LCSTs or their phase transition temperatures in the case of the crosslinked structures while they collapse and shrink when they are heated above the indicated temperatures, respectively.

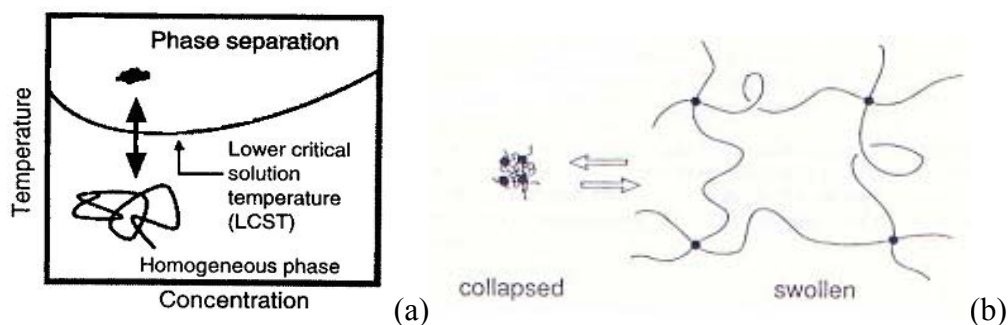


**Figure 1:** Schematic Illustration of LCST for Thermo-sensitive Polymers a) linear, b) gel

PNIPAAm has become the most popular member of a class of polymers that exhibits inverse solubility in aqueous solutions. This property is contrary to the solution behavior of most polymers in organic solvents under atmospheric pressure near room temperature. Its macromolecular transition from a hydrophilic to a hydrophobic structure occurs at a temperature, which is known as the lower critical solution temperature (LCST). This temperature, being a function of the micro-structure of the polymer chains lies between 32°C and 34°C. PNIPAAm has been used in many

forms including single chains, macroscopic gels, micro gels, latexes, thin films, membranes, coatings and fibers. Moreover, wide ranges of disciplines have examined PNIPAAm, encompassing chemistry, physics, rheology, biology and photography.

The effects of initiator, comonomer and crosslinker type and concentration, synthesis-solvent composition, temperature and pH on the physical properties and solution behaviours of linear and crosslinked NIPAAm copolymers have been investigated.

Non-ionic NIPAAm (N-isopropylacrylamide) homopolymer gels, NIPAAm/DMI, (dimethyl itaconate) NIPAAm/IA (itaconic acid), NIPAAm/MMI (monomethyl itaconate), NIPAAm/MBuI (monobutyl itaconate), NIPAAm/MCeI (monocetyl itaconate), and NIPAAm/MOCl (monoocetyl itaconate) copolymer hydrogels containing hydrophobic (DMI), hydrophilic (IA), and amphiphilic (MMI, MBuI, MCeI, and MOCl) comonomers were prepared by free radical polymerizations using potassium persulfate (KPS)-N,N,N',N'-tetramethyl ethylene diamine (TEMED) redox pair and AIBN as initiator, in the presence of hydrophilic (N,N'-methylene bis(acrylamide, BIS) and hydrophobic (vinyl terminated poly(dimethylsiloxane), VTPDMS) crosslinking agents. It was observed that the synthesis-solvent composition (40/60 v/v % of water/methanol mixture and 1,4-dioxane (D)) and initiator concentration significantly affected the properties of the NIPAAm gels.

The effect of hydrophobic crosslinker, i.e., VTPDMS on the compression moduli of neutral and ionic NIPAAm copolymer hydrogels attained equilibrium swollen state in distilled-deionized water was investigated. For mechanical strength analysis, conventional rubber elasticity and swelling theories for networks formed in the presence of diluents were adopted. The second one deals with neutral polymer chains. From the swelling and compression measurements, effective crosslinking density  $\nu_e$ , average molecular weight between crosslinks  $M_c$  and polymer-water interaction parameter  $\chi$ , which can be used to characterize the structures of the hydrogels, were calculated. It was revealed that the compressive elastic moduli of VTPDMS-crosslinked neutral NIPAAm hydrogels were 50 times higher than those of the ones crosslinked with conventional tetra functional monomer, i.e., BIS in 1,4-dioxane. The lower mechanical responses of the neutral NIPAAm hydrogels crosslinked with Tegomer V-Si 2150, having half of the dimethylsiloxane units in the molecular structure of Tegomer V-Si 2250 supported the importance of the nature of secondary forces, being highly effected on the degree of physical crosslinkings.

For both Tegomer V-Si 2250 and Tegomer V-Si 2150, the compression moduli of the ionic NIPAAm hydrogels were decreased sharply, with increasing IA content. As to these results, it can be discussed the electrostatic repulsive forces between the ionized carboxyl groups of IA units destroyed the strong intramolecular hydrophobic interactions arising from the dimethylsiloxane units of VTPDMS chains. Therefore, to obtain the most productive combinations of the hydrophilic component which absorbed large amount of water and the hydrophobic component, which improved the mechanical performance, it is necessary to designate the materials having the right balance of repulsive and attractive forces, being responsible for swelling and mechanical behaviors of the networks.

Figure 2. shows the effect of comonomer type on the compression moduli of NIPAAm hydrogels. It is seen that the mechanical strength of the samples containing

2.50 and 5.0 mole % of monoesters of IA in the feed and crosslinked with BIS ( $2.50 \times 10^{-2}$  mol/L) increase with temperature and alkyl chain length in the order of MCEI > MOcI > MBuI. It means that both the temperature ( $37^\circ\text{C}$ ) being higher than the LCST ( $\sim 32^\circ\text{C} - 34^\circ\text{C}$ ), and the increase in the length of the alkyl chain results in an increase of hydrophobicity and so the mechanical strength of the gels.

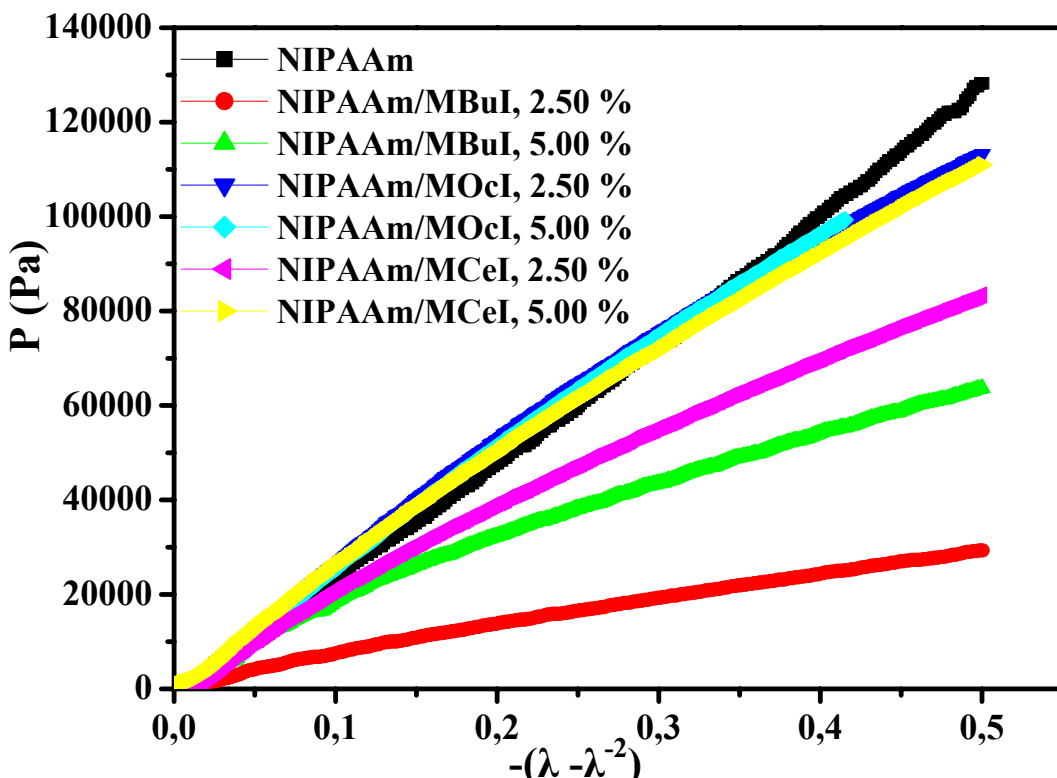


**Figure 2** : Compression Stress-strain Curves (Pressure (Pa) vs.  $-(\lambda-\lambda^{-2})$ ) for NIPAAm, NIPAAm/MBuI, NIPAAm/MOcI, NIPAAm/MCEI Hydrogels, ( $T_{\text{swelling}} = 37^\circ\text{C}$ ).

The compression moduli of the NIPAAm hydrogels containing 5.0 mole % of MOcI crosslinked with concentrated solution of BIS ( $3.75 \times 10^{-2}$  mol/L) were highly greater than those of the ones synthesized with  $2.5 \times 10^{-2}$  mol/L concentration of BIS. The results also support that both covalent bonds (primary interactions) between the NIPAAm chains and hydrophobic interactions resulting from the hydrophobic octyl chains (secondary interactions) describes the optimum conditions of crosslinker concentration and n-alkyl chain length.

PNIPAAm, PDMI and, copolymers and terpolymers of NIPAAm with IA, DMI, MMI, MBuI, MOcI and MCEI were obtained by free radical solution polymerization using AIBN and KPS/TEMED redox pair, as initiator in 1,4-Dioxane and in MetOH/DDW mixture (MetOH/DDW: 60/40, v/v %) with a total monomer concentration of 0,7 mol/L.

From the comparison of the feed compositions of the copolymers with the corresponding copolymer compositions, obtained from the acid-base titrations it was seen that the reactivities of monoitaconates were higher than that of IA and increased with increasing length of alkyl chain. DSC to see how the introduction of hydrophobic alkyl chains affects the Tgs of NIPAAm chains conducted thermal analysis. In the case of NIPAAm/IA and NIPAAm/MMI copolymers, the presence of

the carboxylic groups forming hydrogen bonds increases the  $T_g$  while the monoalkyl and dialkyl itaconates such as MBuI, MOcI, MCEI and DMI lead to a decrease in  $T_g$ s of copolymer and terpolymer because of the destructions of intermolecular interactions (resulting from the  $-COOH$  and  $-COO^-$  groups) through the longer alkyl spacers.

The hydrophilic/hydrophobic balance of the copolymers and terpolymers and their LCSTs could be adjusted sensitively by controlling alkyl chain lengths, comonomer (or comonomers) contents and combinations. With increasing length of hydrophobic alkyl chains in the mono-N-alkylitaconates, intramolecular interactions between the carboxyl groups were suppressed and LCSTs increased.

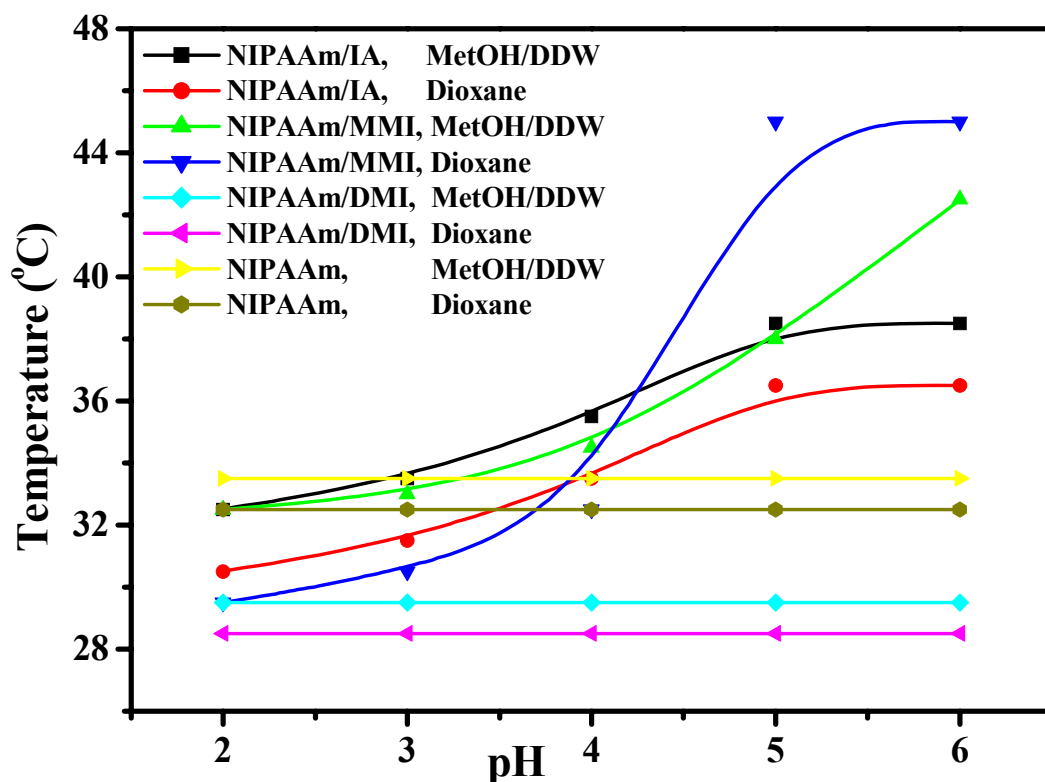


**Figure 3.** Changes in Cloud Points as a Function of pH for Solutions of the PNIPAAm, and NIPAAm/monoester and NIPAAm/diester of IA Copolymers (measured as visual, in DDW).

Figures 3 show temperature vs pH curves of PNIPAAm, NIPAAm/DMI, NIPAAm/IA and NIPAAm/MMI copolymers synthesized in two different media. The combination of pH-sensitive and/or hydrophobically modified comonomers such as IA and MMI, hydrophobic comonomer DMI and thermo-sensitive monomer, NIPAAm in the copolymer structures leads to a polymer that respond to both temperature and pH. Both the pure PNIPAAm chains (NIPAAm (MetOH/DDW), NIPAAm (D) in Figure 3) and the NIPAAm/DMI copolymer chains (NIPAAm/DMI (MetOH/DDW), NIPAAm/DMI (D) in Figure 3) show pH-independent phase transitions. In the case of DMI comonomer, the presence of the methyl groups in the chain structure results in a decrease in LCST.

The sensitivity of NIPAAm copolymers (NIPAAm/MMI and NIPAAm/IA copolymers in Figure 3) and terpolymers to change in pH and temperature suggest

that they could be useful in biotechnology and drug delivery applications where small changes in pH and temperature.

Further, the temperature vs. volume swelling ratio (Figure 4) and mass swelling vs time curves of the NIPAAm copolymer hydrogels crosslinked with VTPDMS and/or BIS indicate that the one having 2.5 mole % of IA in the feed can be suggested for drug release experiments because of discontinuous and larger volume change during the phase transition.

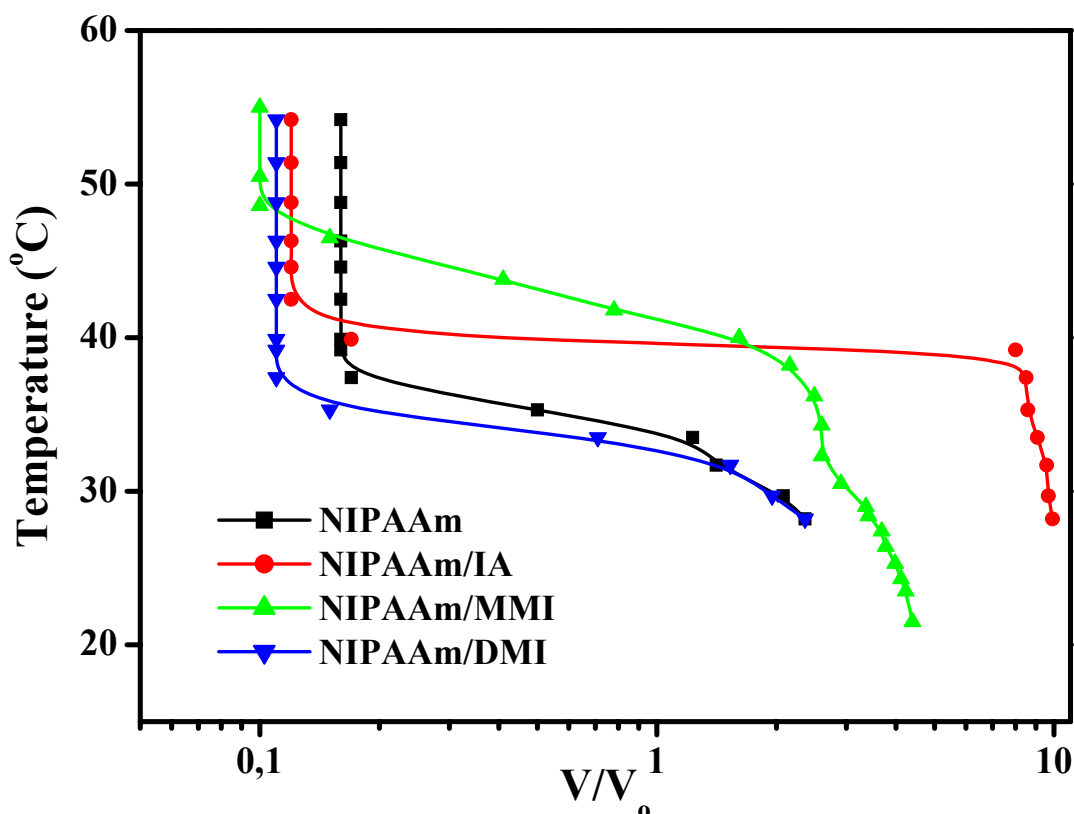


**Figure 4:** Temperature Dependence of the Volume Swelling Ratios of the PNIPAAm, NIPAAm/IA, NIPAAm/MMI, NIPAAm/DMI Copolymer Gels Having 2.50 mole % of Comonomer.

Equilibrium percentage mass swelling in both water and phosphate buffer of NIPAAm crosslinked with BIS was higher than the NIPAAm hydrogel crosslinked with VTPDMS. This result supports the effect of hydrophobic crosslinker on the diffusion process of solvent in to the hydrogel. For the samples containing ionizable comonomer IA, equilibrium percentage mass swelling increased with increasing repulsive forces resulting from  $-\text{COO}^-$  groups. In the presence of VTPDMS as crosslinker, the percentages in water were higher than in phosphate buffer.

PNIPAAm, NIPAAm/IA and NIPAAm/monoitaconate copolymer hydrogels were used for drug release experiments. Both Theophylline concentration and composition of the hydrogels affects the drug loading/release capacities and mechanisms of hydrogels (Figure 5).

The results of drug release experiments of NIPAAm copolymer hydrogel crosslinked with BIS and containing 2.50 mol % of MOcI in the feed as hydrophilic crosslinker

and hydrophobically modified ionizable comonomer, respectively, gave the most optimum conditions like its mechanical strength and LCST measurement results.

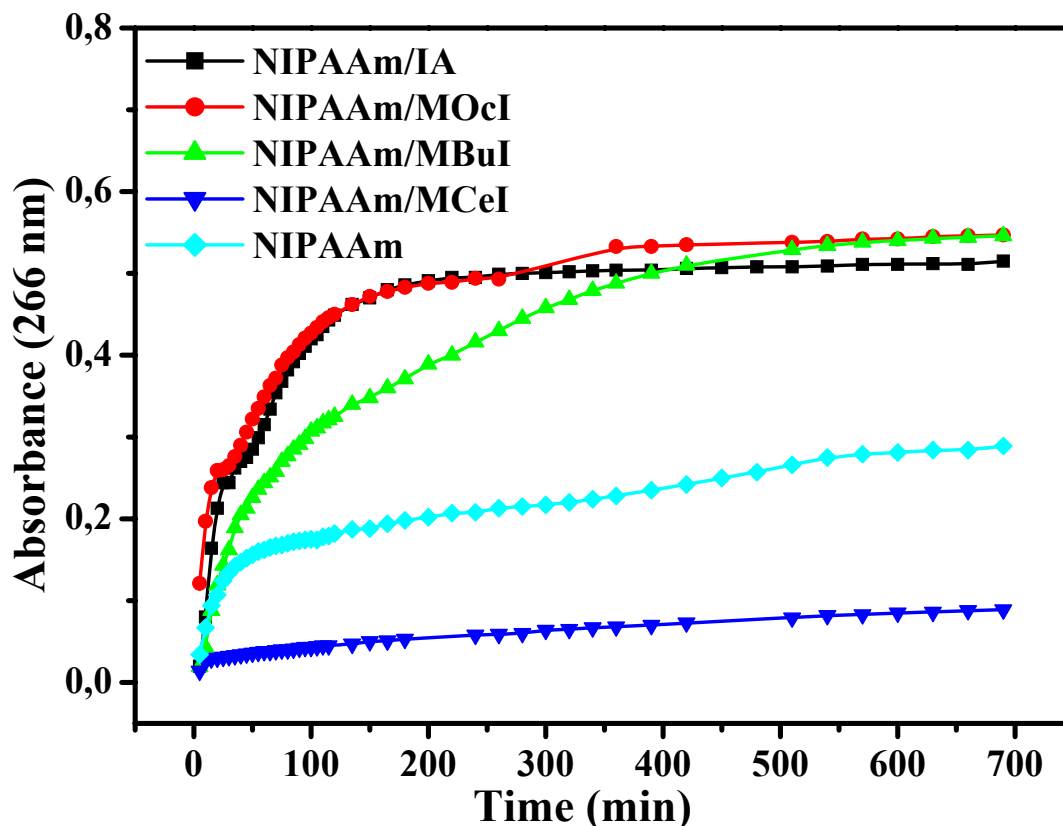


**Figure 5.** Absorbance (at 266 nm) vs Time Curves of Theophylline Release ( $C=0.1$  g/L) for the PNIPAAm, NIPAAm/IA, NIPAAm/MBuI, NIPAAm/MOCl and NIPAAm/MCEI Copolymer Hydrogels Crosslinked with BIS

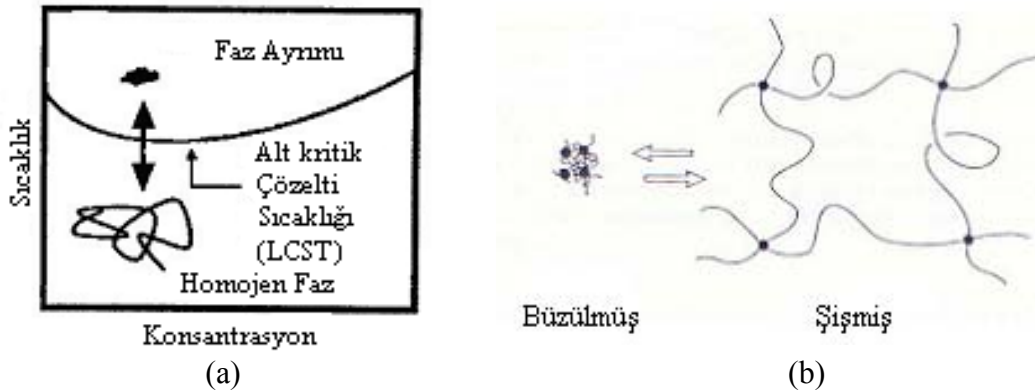
PNIPAAm hydrogel crosslinked with VTPDMS has the lowest drug release capacity because of the unressemble structure to drug molecules. This means that Theohylline, being a water-soluble drug and having hydrophilic structure does not prefer to intermolecular interaction with hydrophobic dimethyl siloxane groups and so drug loading/release capacity decrease. The presence of hydrophilic and ionizable IA molecules in the structures of NIPAAm hydrogels increases the release capacities and rates of hydrogels crosslinked with BIS or VTPDMS because repulsive forces between the  $-COO^-$  groups controls the shrinking rate at  $37^\circ C$  and so the drug molecules do not trap in the polymeric network.

As a result, linear and crosslinked NIPAAm copolymer hydrogel especially having higher mechanical strength, which is containing 2.5 mole % of MOCl in the feed to sensitive to change in pH and temperature and having 2.5 mole % of IA in the feed can be suggest that they could be useful in biotechnology and drug delivery applications because of discontinuous and larger volume change during the phase transition.

## DOĞRUSAL VE ÇAPRAZ BAĞLI POLİ(N-İZOPROPİLAKRİLAMİT-KO-MONOİTAKONİK ASİT ESTER)LERİ: SENTEZİ, KARAKTERİZASYONU VE ÇÖZELTİ DAVRANIŞININ İNCELENMESİ

### ÖZET

Sıcaklık ve pH duyarlı polimerlerin çok farklı uygulamaları vardır. Sıcaklığa duyarlı polimerler faz ayrımına neden olan eşik sıcaklığını aştığında alt kritik çözelti sıcaklığı (LCST) davranışı gösterir. LCST, malzemelerin faz geçiş davranışıdır. Çözücü içindeki doğrusal polimer, düşük sıcaklıkta çözünür fakat sıcaklık, polimerin karakteristik LCST değerinin üzerine çıktığında faz ayrımı sonucu topaklanmalar olur (Şekil 1a). LCST tanımı aynı zamanda jeller için de kullanılır. Çözücü içindeki çapraz bağlı polimer (jel), düşük sıcaklıkta şişer fakat sıcaklık polimerin karakteristik LCST değerinin üzerine çıktığında büzülür (Şekil 1b). PNIPAAm (Poli(N-izopropil akrilamit) sulu çözeltilerde 32°C-34°C gibi vücut sıcaklığına yakın bir LCST davranışı gösterdiği için özellikle biyomedikal uygulamalar olmak üzere bu sınıftaki polimerlerin en popüler üyesidir. PNIPAAm doğrusal zincirleri ve hidrojelleri LCST değerinin altına soğutulduğunda gevşer veya şişerken LCST değerinin üzerinde bir sıcaklığa ısıtıldığında çökme veya büzülme davranışı gösterir.



**Şekil 1:** Isıl Duyarlı Polimerlerin LCST' nin Şematik Gösterimi, a) Doğrusal, b) Jel

PNIPAAm, sulu çözeltilerde ters çözünürlük davranışı gösteren polimerler içinde önemli yer tutmaktadır. Bu özellik, birçok polimerin oda sıcaklığında ve atmosfer basıncı altında organik çözücülerdeki çözünürlük davranışına tamamen zıt düşmektedir. LCST, hidrofilik yapıdan hidrofobik yapıya doğru belirli bir sıcaklıkta makromoleküler geçiş olarak bilinmektedir. PNIPAAm doğrusal zincirler, makroskobik jeller, lateks, ince filmler, membranlar, kaplama ve fiberler gibi birçok değişik formda kullanılmaktadır.

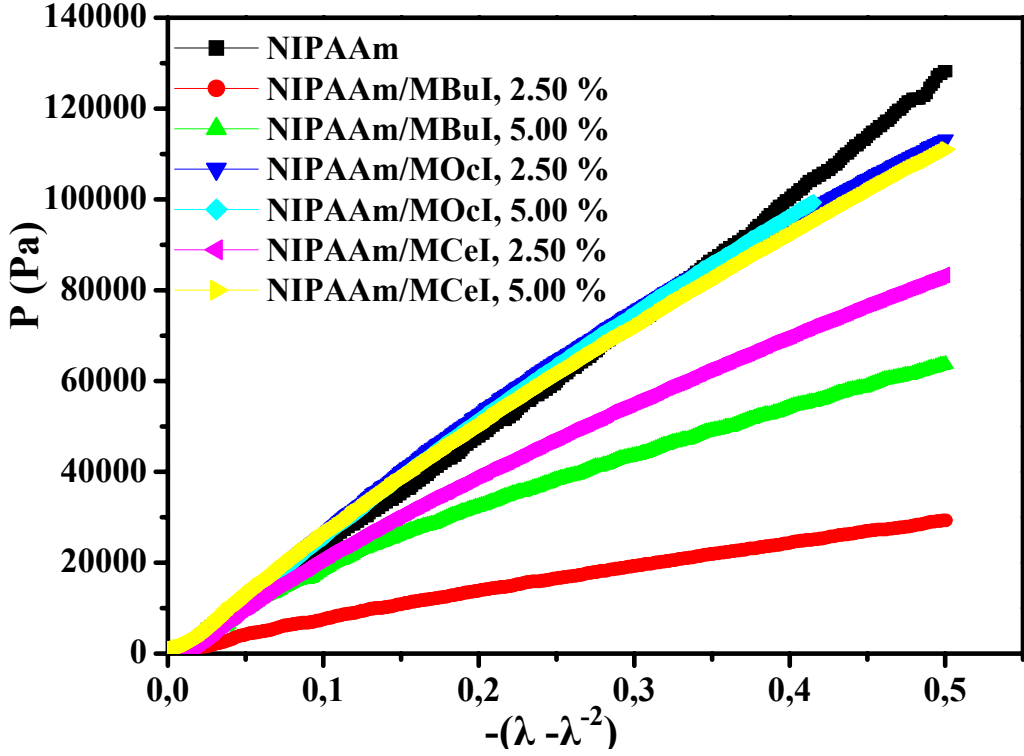
Bu çalışmada, başlatıcı, komonomer ve çapraz bağlayıcı türü ve konsantrasyonunun, sentez-çözücü bileşiminin, sıcaklığın ve pH'ın doğrusal ve çapraz bağlı NIPAAm kopolimerlerinin fiziksel özellikleri ve çözelti davranışları üzerine etkileri incelenmiştir.

İyonik olmayan NIPAAm homopolimer jelleri ile, hidrofobik (DMI), hidrofilik (IA) ve amphilik (MMI, MBuI, MCEI ve MOcI) komonomerler içeren NIPAAm/DMI, (dimetil itakonat) NIPAAm/IA (itakonik asit), NIPAAm/MMI (monometil itakonat), NIPAAm/MBuI (monobutil itakonat), NIPAAm/MCEI (monosetil itakonat), ve NIPAAm/MOcI (monooktil itakonat) kopolimer hidrojelleri, hidrofilik N,N'-metilenbis(akrilamit) (BIS) ve hidrofobik (vinil sonlu poli(dimetilsiloksan), VTPDMS) çapraz bağlayıcılar varlığında, başlatıcı olarak potasyum persulfat (KPS)-N,N,N',N'-tetrametiletildiamin (TEMED) redoks çifti ve AIBN kullanılarak serbest radikal çözelti polimerizasyonu ile elde edildi. Sentez-çözücü bileşiminin (hacimce % 40/60 su/metanol ve 1,4-dioksan) ve başlatıcı konsantrasyonunun NIPAAm jellerinin özelliklerini önemli derecede etkilediği gözlenmiştir.

Destile-deiyonize su içinde denge şişme durumundaki nötral ve iyonik NIPAAm kopolimer hidrojellerinin sıkıştırma modülüne, hidrofobik çapraz bağlayıcının (VTPDMS) etkisi incelendi. Mekanik dayanım analizi için, ağ yapı için geçerli olan kauçuk elastisitesi ve şişme teorisi uygulandı. Hidrojellerin yapısını karakterize edebilmek için kullanılan parametrelerden, etkin çapraz bağ yoğunluğu  $v_e$ , iki çapraz bağ noktası arasındaki ortalama molekül ağırlığı  $M_c$  ve polimer-su etkileşim parametresi  $\chi$ , şişme ve sıkıştırma ölçümlerinden elde edilen veriler kullanılarak hesaplandı. VTPDMS ile çapraz bağlı NIPAAm jellerinin sıkıştırma modüllerinin, yaygın olarak kullanılan dört fonksiyonlu BIS ile 1,4-dioksan da sentezlenmiş jellere oranla 50 kat daha fazla olduğu görüldü. Tegomer V-Si 2250'nin molekül yapısının yarısı kadar dimetilsiloksan birimlerine sahip Tegomer V-Si 2150 ile çapraz bağlı nötral NIPAAm jellerinin düşük mekanik özelliklere sahip olması ikincil kuvvetlerin fiziksel çapraz bağlanma derecesini artırmakta ne kadar etkili olduğunu desteklemektedir.

Tegomer V-Si 2250 ve Tegomer V-Si 2150 nin her ikisi ile de sentezlenmiş iyonik NIPAAm hidrojellerinin sıkıştırma modülleri, IA içeriğinin artmasıyla keskin bir şekilde azalmaktadır. IA birimlerindeki iyonlaşabilen karboksil grupları arasındaki elektrostatik itme kuvvetleri, VTPDMS zincirlerindeki dimetilsiloksan birimlerinden kaynaklanan moleküllerarası hidrofobik etkileşimlerin artmasıyla yok olmaktadır. Ağ yapının mekanik ve şişme davranışlarına karşı sorumlu olan dengedeki itici ve çekici kuvvetlere sahip malzemelerin dizaynı için, yüksek miktarlarda su absorplayabilen hidrofilik bileşenler ile mekanik performansı iyileştiren hidrofobik bileşenin en uygun kombinasyonu gereklidir.

Şekil 2'de NIPAAm hidrojellerinin sıkıştırma modüllerine komonomer türünün etkisi görülmektedir. Şekilden görüldüğü gibi % 2.5 ve % 5.0 mol itakonik asit monoesterleri içeren ve  $2.5 \times 10^{-2}$  mol/L konsantrasyonda BIS kullanılarak sentezlenen NIPAAm hidrojellerinin sıkıştırma modülleri alkil zincirlerinin uzunluğunun artmasına paralel olarak MCEI>MOcI>MBuI sıralamasına göre beklendiği şekilde artış göstermiştir. Sıcaklığın (37°C) LCST (~32°C–34°C) değerinden yüksek olması ve alkil zincir uzunluğunun artması sonucu olarak hidrofobluk artmış ve dolayısıyla hidrojellerin mekanik dayanımlarında artmıştır.



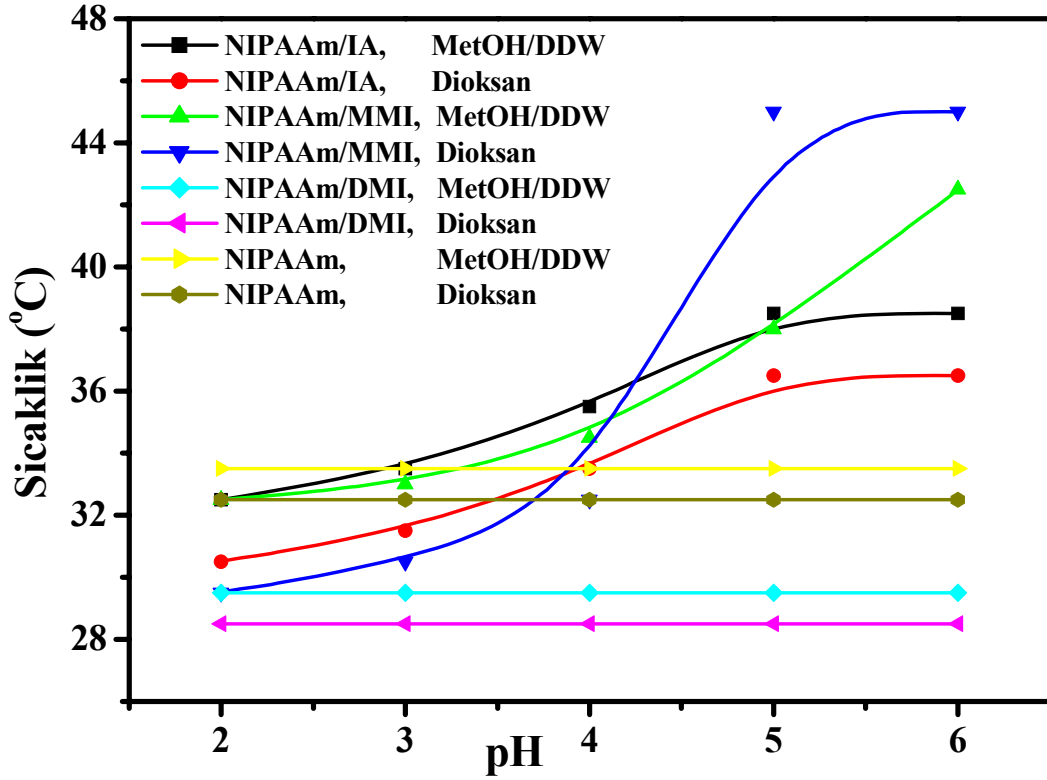
**Şekil 2 :** NIPAAm, NIPAAm/MBuI, NIPAAm/MOCl, NIPAAm/MCeI Hidrojel Örnekleri İçin Basınç (Pa) vs.  $-(\lambda-\lambda^{-2})$  Grafiği, ( $T_{şişme} = 37^{\circ}\text{C}$ ).

% 5 mol MOCl içeren ve  $3.75 \times 10^{-2}$  mol/L BIS konsantrasyonunda hazırlanan NIPAAm hidrojelinin sıkıştırma modülü ve çapraz bağ yoğunluğu,  $2.50 \times 10^{-2}$  mol/L BIS konsantrasyonunda hazırlanan bütün hidrojellerinkinden çok yüksektir. Bu sonuç, hidrofobik oktil zincirlerinden dolayı (ikincil etkileşim) NIPAAm zincirleri arasındaki kovalent bağların (birincil etkileşim) ve hidrofobik etkileşimlerin, çapraz bağlayıcı konsantrasyonu ve alkil zincirlerinin uzunluğunun uygun koşullarının sağlanmasına bağlı olduğunu göstermiştir.

PNIPAAm, Poli(dimetil itakonot) (PDMI) ve IA, DMI, MMI, MBuI, MOCl ve MCeI kullanılarak, AIBN ve KPS/TEMED redox başlatıcı çifti eşliğinde 1,4-dioksan ve metanol/su çözücü karışımında, toplam monomer konsantrasyonu 0.7 mol/L sabit tutularak, NIPAAm'ın serbest radikal çözelti polimerizasyonu ile doğrusal kopolimerleri ve terpolimerleri sentezlendi

Kopolimerlerin başlangıç bileşimleri ile asit-baz titrasyonu ile hesaplanan bileşimler karşılaştırıldığında, IA monoesterlerinin IA'e göre reaktiviteleri çok daha yüksektir ve alkil gruplarının zincir uzunluğu ile paralel bir artış göstermiştir. DSC ile hidrofobik alkil zincirlerinin NIPAAm kopolimerlerinin  $T_g$ 'leri üzerindeki etkileri incelenmiştir. NIPAAm/IA ve NIPAAm/MMI kopolimerlerinde karboksil gruplarının hidrojen bağı oluşturması ile  $T_g$  artarken, MBuI, MOCl, MCeI ve DMI gibi mono ve dialkil itakonotlar, terpolimer ve kopolimerlerin  $T_g$  değerlerinin düşük çıkmasına neden olmuştur.

Kopolimer ve terpolimerlerin hidrofilik/hidrofobik dengeleri ve bunların LCST'leri alkil zincir uzunlukları, komonomer içeriği ve kombinasyonu ile hassas olarak ayarlanabilmektedir. Mono-N-alkilitakonotlardaki hidrofobik alkil zincirlerinin uzunluğunun artması ile birlikte karboksil grupları arasındaki molekülic etkileşimler bastırılmakta ve LCST değeri artmaktadır.



**Şekil 3.** PNIPAAm, NIPAAm/IA Monoesterleri ve NIPAAm/IA Diesterli Kopolimer Örneklerinin Sulu Çözeltilerinin Bulutlanma Noktalarının pH ile Değişim Eğrileri (Ölçümler Görsel Olarak Yapılmıştır).

İki farklı ortamda sentezlenen PNIPAAm, NIPAAm/DMI, NIPAAm/IA ve NIPAAm/MMI kopolimerinin sıcaklık vs pH eğrileri Şekil 3'te verilmiştir. pH duyarlı ve/veya IA ve MMI gibi hidrofobik olarak iyileştirilmiş komonomer, hidrofobik komonomer DMI ve sıcaklığa duyarlı monomer NIPAAm'ın yapıda bulunması polimerlerin sıcaklık ve pH duyarlı olmasına neden olmaktadır. PNIPAAm homopolimer zincirleri (NIPAAm (MetOH/DDW), NIPAAm (Dioksan), Şekil 3) ve NIPAAm/DMI kopolimer zincirlerinin (NIPAAm/DMI (MetOH/DDW), NIPAAm/DMI (Dioksan) Şekil 3) her ikisinde pH tan bağımsız bir faz geçişi göstermektedir. DMI komonomerinin zincir yapısındaki metil grupları LCST değerinin düşmesine neden olmaktadır.

NIPAAm kopolimerleri (NIPAAm/MMI ve NIPAAm/IA kopolimerleri, Şekil 3) ve terpolimerlerinin, pH ve sıcaklık değişimlerine duyarlılığı bunların biyoteknoloji ve ilaç salım uygulamalarında kullanımını uygun kılmaktadır.

VTPDMS ve/veya BIS ile çapraz bağlı NIPAAm kopolimer hidrojelinin sıcaklık vs. hacim şişme oranı (Şekil 4) ve ağırlık şişme vs. zaman eğrilerinde görüldüğü gibi % 2.50 mol IA içeren hidrojelinde faz geçişi sırasında süresiz hacim değişimine sahip olması bu hidrojelinde ilaç salım deneyleri için önerilmesini sağlamıştır.

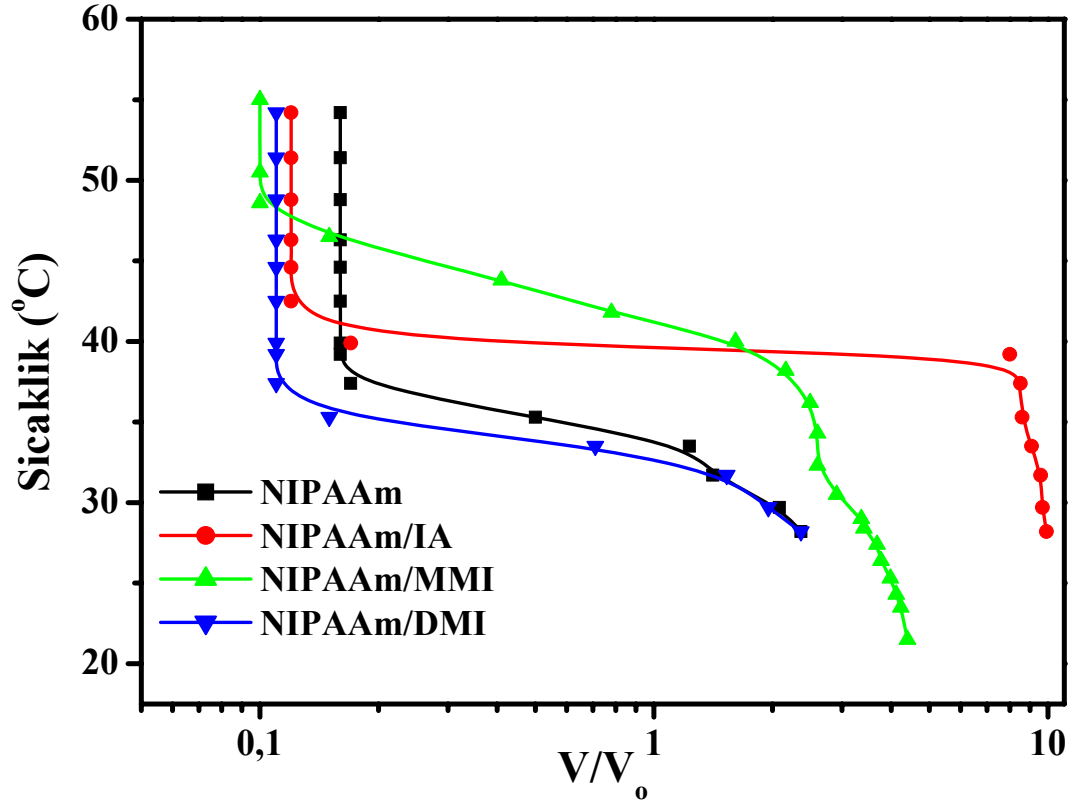
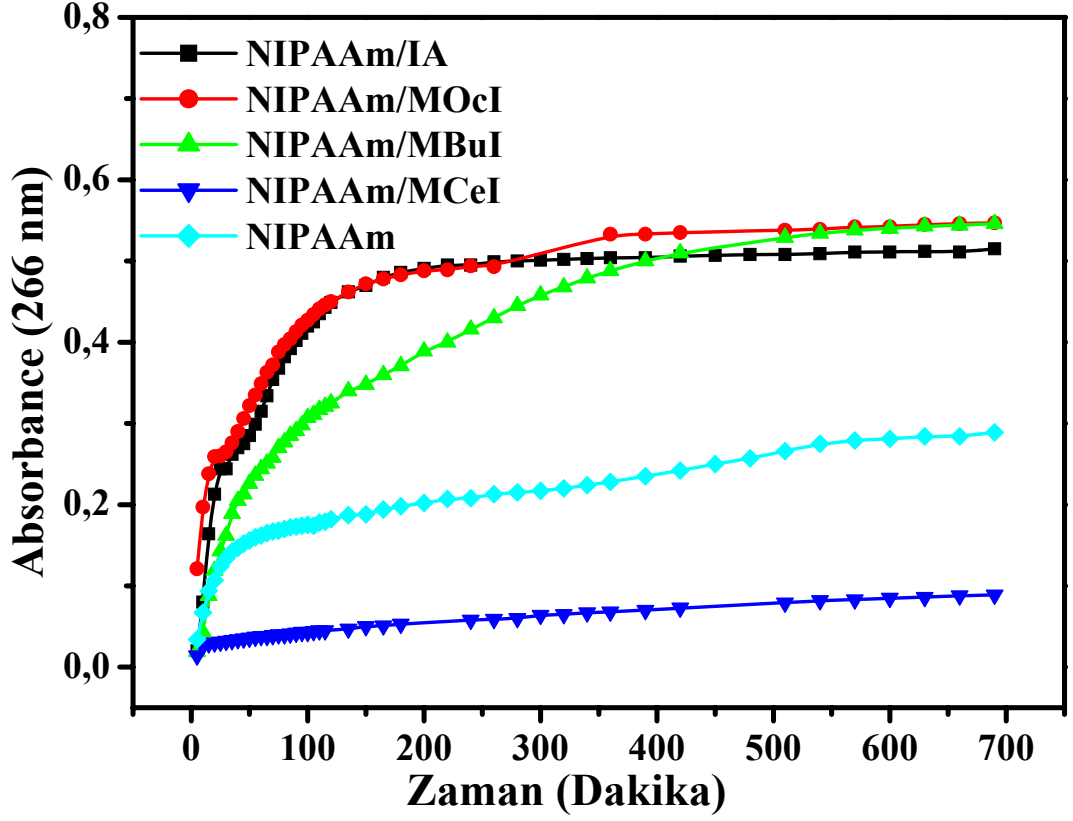


**Figure 4:** PNIPAAm ve % 2.50 mol Komonomer İçeren NIPAAm/IA, NIPAAm/MMI ve NIPAAm/DMI Kopolimer Hidrojellerinin Sıcaklığa Bağlı Hacim Şişme Oranları.

Su ve fosfat tamponun her ikisinde de BIS ile çapraz bağlı PNIPAAm' in denge ağırlık şişmesi, VTPDMS ile çapraz bağlı PNIPAAm'in den daha büyüktür. Bu sonuç, hidrojel içine çözücü difüzyonu prosesine hidrofobik çapraz bağlayıcı etkisini desteklemektedir. İyonlaşabilen komonomer (IA) içeren örneklerde,  $-COO^-$  grubundan kaynaklanan çekici kuvvetlerin artmasıyla birlikte denge ağırlık şişme yüzdesi de artmaktadır.

PNIPAAm, NIPAAm/IA ve NIPAAm/monoitakonat kopolimer hidrojelleri ilaç salım deneylerinde kullanılmıştır. Tiyofilin konsantrasyonu ve hidrojellerin bileşiminin hidrojinin ilaç yükleme/salım kapasitelerini ve mekanizmalarını etkilemektedir (Şekil 5).

BIS ile çapraz bağlı ve % 2.5 mol MOCl içeren NIPAAm kopolimer hidrojel ile, mekanik dayanım ve LCST ölçüm sonuçlarında olduğu gibi, ilaç salım deneyleri sonucunda da en uygun sonuçlar elde edilmiştir.



**Şekil 5.** C=0.1 g/L Konsantrasyonda Tiyofilin Yükleme Yapılan BIS ile Çapraz Bağlı PNIPAAm, NIPAAm/IA, NIPAAm/MBuI, NIPAAm/MOcI ve NIPAAm/MCEI Kopolimer Hidrojellerinin pH=7.5 Fosfat Tampon daki Salım Sırasındaki Zaman Karşı Absorbans Değişimi.

VTPDMS ile çapraz bağlı PNIPAAm hidrojel, ilaç molekülünün farklı bir yapıya sahip olmasından dolayı en düşük ilaç salım kapasitesine sahiptir. Tiyofilin suda çözünebilir bir ilaçtır ve hidrofilik bir yapıya sahip olduğu için hidrofobik dimetil siloksan grupları ile moleküller arası etkileşim yapmayı tercih etmez, bunun sonucu olarak da ilaç yükleme/salım kapasitesi düşüktür. NIPAAm hidrojelinin yapısında hidrofilik ve iyonlaşabilen IA molekülleri varlığında, BIS ve VTPDMS ile çapraz bağlı olan hidrojellere göre salım kapasitesi daha yüksektir.  $-COO^-$  grupları arasındaki itici kuvvetler  $37^{\circ}C$  de büzülme kontrol etmekte ve dolayısıyla ilaç moleküllerinin polimerik ağ yapısı içinde hapsolmesini engellemektedir.

Sonuç olarak, bu çalışmada sentezlenen pH ve sıcaklık değişimlerine duyarlı doğrusal ve çapraz bağlı NIPAAm kopolimerlerinden, özellikle mekanik dayanımı yüksek ve LCST değeri pH ile kontrol edilebilen % 2.50 MOcI içeren NIPAAm kopolimeri ile yüksek hacim şişme oranı ve süresiz faz geçişi gösteren % 2.50 IA içeren NIPAAm hidrojel biyoteknoloji ve ilaç salım uygulamaları için önerilebilir.

## 1. INTRODUCTION

Poly(N-isopropyl acrylamide) (PNIPAAm) has become the most popular member of a class of polymers that exhibits inverse solubility in aqueous solutions. This property is contrary to the solution behavior of most polymers in organic solvents under atmospheric pressure near room temperature. Its macromolecular transition from a hydrophilic to a hydrophobic structure occurs at a temperature, which is known as the lower critical solution temperature (LCST). This temperature, being a function of the micro-structure of the polymer chains lies between 30°C and 35°C. PNIPAAm has been used in many forms including single chains, macroscopic gels, micro gels, latexes, thin films, membranes, coatings and fibers. Moreover, wide ranges of disciplines have examined PNIPAAm, encompassing chemistry, physics, rheology, biology and photography.

PNIPAAm has been synthesized by a variety of techniques. Free radical initiation in organic solvents and aqueous media is only one of these experimental methods. Various initiators and solvents such as potassium persulfate (KPS), ammonium persulfate (APS), azobis(isobutyronitrile) (AIBN), benzoylperoxide, laurylperoxide and water, methanol, benzene, 1,4-dioxane, tetrahydrofuran (THF), respectively, have been used in free radical polymerization produced in organic solvents and in aqueous media.

Redox polymerization of NIPAAm typically uses APS or KPS as the initiator and N,N,N',N' tetramethylethylenediamine (TEMED) as the accelerator.

PNIPAAm, its linear copolymers and hydrogels that respond environmental stimuli such as light, temperature, electric field, pH, ionic strength, solvent composition and addition of small solutes are defined as stimuli-responsive polymers. Materials based on these polymers have several potential applications, ranging from valves and switches to intelligent drug delivery systems. PNIPAAm has also attracted wide interest in biomedical applications because it exhibits a well-defined LCST in water around 32 °C. PNIPAAm linear chains and hydrogels expand or swell when they are cooled below LCSTs or their phase transition temperatures in the case of the cross-

linked structures while they collapse and shrink when they are heated above the indicated temperatures, respectively. This behavior arises from the hydrophobic/hydrophilic balance of PNIPAAm chains due to the presence of isopropyl(-CH(CH<sub>3</sub>)<sub>2</sub>) and amide (O=C-NH) groups.

Hydrogels are three-dimensional and hydrophilic polymer networks capable of imbibing large amounts of water or biological liquids (Figure 1.1). Hydrogels resemble natural living tissue due to their high water content and soft touch. Their mechanical properties are similar to those of natural rubbers. They have high deformability and nearly complete recoverability. Depending upon the solvent, temperature, and other environmental conditions, the polymer chains can either repel each other and be swollen, or attract each other and be very compact.

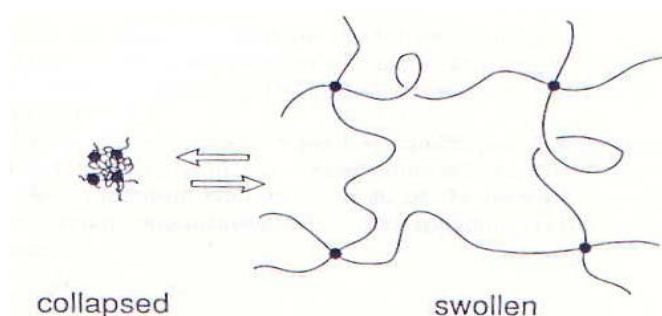


**Figure 1.1 :** Gel is Defined as a Cross-linked Polymer Network Swollen with a Liquid. Gels Undergo Reversible Volume Transition in Response to Changes in External Conditions.

Recently, a great attention has been paid to the effect of the lower critical solution temperature (LCST) in solutions of linear macromolecules and in polymer gels. Crosslinked structures undergo a discontinuous or continuous phase transition in response to temperature, pH-value, solvent composition; these effects were intensively investigated to understand the relation between phase transition and biological interactions. Further, particularly for industrial applications, the LCSTs of copolymers have to be accurately predicted by synthesis parameters such as comonomer composition. LCST can also be controlled by other parameters, such as pH-value, ionic strength, solvent composition and temperature.

The reason for the phase transition from coil to globule conformation for linear chains and from swollen to shrinking state for crosslinked structures, which change drastically the chemical and physical properties can be explained by a good balance between hydrophilic and hydrophobic interactions in the polymer. The LCST of

PNIPAAm can be varied by the copolymerization of the NIPAAm monomer with hydrophilic or hydrophobic comonomers. This means that the LCSTs of the PNIPAAm copolymers are strongly influenced by the nature of the comonomers. Hydrophobic compounds lower the LCST and hydrophilic compounds raise it. It has been shown that the LCST phenomenon disappears when a hydrophilic compound contains more than a certain amount of comonomer.

Inverse temperature-sensitive hydrogels are made of hydrophobic polymer chains and used for biomedical applications such as selective membranes, enzyme activity controlling and drug delivery systems.

It is known that synthesis method and temperature, synthesis-solvent composition, type and concentration of initiator; monomer, comonomer and crosslinker have important effects on both swelling and mechanical properties of NIPAAm hydrogels. The combination of large swelling and high mechanical performance within the same gel structure is important for both industrial and biomechanical applications. The formation of hydrophobically modified copolymers, nanocomposite gels and double networks by incorporation of hydrophobic components into the hydrogel structure can be given as the main examples of the methods, which are used to improve the mechanical properties.

Many pharmacologically active compounds employed in drug delivery systems are amphiphilic or hydrophobic molecules. The synthesis of polymers containing both hydrophobic and hydrophilic and/or weakly acidic monomers is an alternative to obtain amphiphilic systems that could place in hydrophobic substances.

Common carboxylic acid monomers, such as acrylic acid (AA), methacrylic acid (MAA) and itaconic acid (IA), have been copolymerized with NIPAAm to form random copolymers with both thermo- and pH-sensitive properties, being variables that change in typical physiological, biological and chemical systems.

Itaconic acid has two carboxyl groups. This means that two ester groups can be introduced into itaconic acid. It is possible to change one of two ester groups to modify hydrophilic/hydrophobic balance of homopolymer and copolymers and to study the thermo- and pH-responsive behaviours of polymers in aqueous solutions.

Although there are different alternatives to find a compromise between composition and solution behaviours of NIPAAm polymers, very little information is available on

the systematic variation of the properties of its copolymers and terpolymers using monomers containing both hydrophilic and hydrophobic groups.

In this study, taking into account the above literature results, we have attempted to investigate the effect of monomer purity, initiator concentration, hydrophobic and ionizable comonomers, and synthesis-solvent composition on the swelling behaviour of NIPAAm gels. For this purpose, NIPAAm gels, initiated with two different initiator concentrations, in water, and NIPAAm/DMI (dimethyl itaconate) and NIPAAm/IA and NIPAAm/monoesters of IA copolymer hydrogels in water/methanol mixtures were synthesized and their volume phase transitions were examined. Conventional swelling theory was used to calculate the physical parameters and characterize the interactions between the polymer and solvent molecules.

Hydrogels composed of NIPAAm, BIS, vinyl terminated poly(dimethyl siloxane) (VTPDMS) (commercial product) and IA as hydrophobic monomer, hydrophilic crosslinker, hydrophobic crosslinker and weakly ionizable comonomer, respectively, were prepared to investigate the effect of hydrophobic component, i.e., VTPDMS on the compression moduli of the samples attained equilibrium swollen state in distilled-deionized water at 25°C. For mechanical strength analysis, conventional rubber elasticity and swelling theories for networks formed in the presence of diluent were adopted. The second one deals with neutral polymer chains. From the swelling and compression measurements, effective crosslinking density  $\nu_e$ , average molecular weight between crosslinks  $M_c$  and polymer-water interaction parameter  $\chi$ , which can be used to characterize the structures of the hydrogels, were calculated.

Monoitaconates containing methyl, butyl, octyl and cetyl groups were synthesized. The copolymers and terpolymers (NIPAAm/IA/DMI) containing these monoitaconates were obtained by free-radical solution polymerization of NIPAAm. Their molecular structures and solution properties were investigated using FTIR, GPC, UV-visible spectroscopy, and DSC and acid-base titrations. The dependence of their thermosensitivity on pH-value of solution has been discussed taking into account the polymer structures and their hydrophilic/hydrophobic balance.

## 2. THEORY

The synthetic polymers can be classified into different categories based on their chemical properties. Out of these, some special types of polymers which are coined with different names have their own special chemical properties. These names are “stimuli-responsive polymers” [1] or “smart polymers (SP)” [2,3] or “intelligent polymers” [4] or “environmental-sensitive polymers” [5]. The characteristic features of these polymers are their ability to respond to very slight changes in the surrounding environment. When a polymer has both hydrophilic and hydrophobic constituents shows these characteristic features. Poly(N-isopropylacrylamide) (PNIPAAm) is the most studied environmental-sensitive polymer. These polymers undergo fast and reversible changes in a discontinuous or continuous phase transitions as a response to the environment. The environmental trigger can be either change in temperature [6], in electric field, in magnetic field, or pH shift, increase in ionic strength [7], presence of certain metabolic chemicals [8], addition of an oppositely charged polymer [9] and polycation–polyanion complex formation [10].

PNIPAAm has been synthesized by a variety of techniques. Free radical initiation in organic solvents [11,12] and aqueous media [13-17] is only one of these experimental methods. Various initiators and solvents such as KPS, APS, AIBN, benzoylperoxide, laurylperoxide and water, methanol, benzene, dioxane, THF, respectively, have been used in free radical polymerization produced in organic solvents and in aqueous media. Redox polymerization of NIPAAm typically uses APS or KPS as the initiator and either TEMED as the accelerator [14-17].

The temperature-sensitive and pH- sensitive polymers have many applications for various purposes. Temperature-sensitive polymers exhibit lower critical solution temperature (LCST) behavior where phase separation is induced by surpassing a certain temperature threshold. PNIPAAm is the most popular member of this class of polymers that exhibits LCST in aqueous solutions which lies between 30°C and 35°C. Polymers of this type undergo a thermally induced, reversible phase transition; they are soluble in a solvent (generally in water) at low temperatures but become

insoluble as the temperature rises above the LCST [18]. The LCST corresponds to the region in the phase diagram at which the enthalpy contribution of water hydrogen-bonded to the polymer chain becomes less than the entropic gain of the system as a whole and thus is largely dependent on the hydrogen-bonding capabilities of the constituent monomer units. In principle, the LCST of a given polymer can be “tuned” as desired by variation in hydrophilic or hydrophobic constituent in monomer structure or comonomer content. pH-sensitive polymers effect on the LCST depending on the protonation/deprotonation events on the molecule. The pH-induced phase transition of pH-sensitive polymer tends to be very sharp and usually switches within 0.2–0.3 unit of pH. The polymer systems which have these kinds of responses are useful in bio-related applications such as drug delivery [5,19], bioseparation [2], chromatography [4,20,21] and cell culture [22]. Some systems have been developed to combine two or more stimuli responsive mechanisms into one polymer system.

Environmental-sensitive polymers can be either linear or crosslinked structure. A crosslinked polymer has a three dimensional network structure known as gel. A gel can retain a large amount of solvent inside its structure. These materials are known as organogels if the solvent retained is an organic one. A hydrogel is a gel that occludes water. Hydrogels have become of major interest because polymers are increasingly used in medical applications. Hydrogels have become of major interest because polymers are increasingly used in medical applications and used nowadays for membranes, catheters, contact lenses, and drug-delivery systems [23,24].

Environmental-sensitive polymers or SPs can be categorized into three classes according to their physical forms (Figure 2.1). They are (i) linear free chains in solution, where polymer undergoes a reversible collapse after an external stimulus is applied, (ii) covalently cross-linked gels and reversible or physical gels, which can be either microscopic or macroscopic networks and for which swelling behavior is environmentally triggered and (iii) chain adsorbed or surface-grafted form, where the polymer reversibly swells or collapses on a surface, converting the interface from hydrophilic to hydrophobic and vice versa, once a specific external parameter is modified. SPs in all the three forms—in solution, as hydrogels and on surfaces can be conjugated with biomolecules, thereby widening their potential scope of use in many interesting ways.

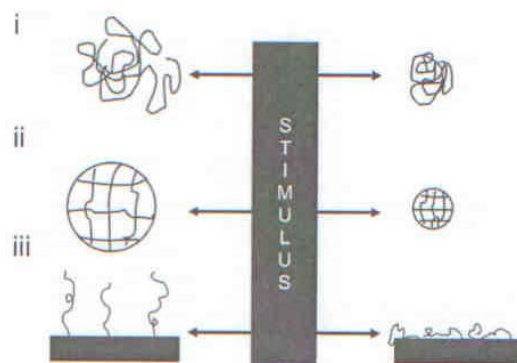


**Figure 2.1** : Classification of the Polymers by Their Physical Form: (i) Linear Free Chains in Solution Where Polymer Undergoes a Reversible Collapse After an External Stimulus is Applied; (ii) Covalently Cross-linked Reversible Gels Where Swelling or Shrinking of the Gels can be Triggered by Environmental Change; and (iii) Chain Adsorbed or Surface-grafted Form, Where the Polymer Reversibly Swells or Collapses on Surface, Once an External Parameter is Changed.

### 2.1. Polymers as Linear Free Chains in Solution

Environmental-sensitive polymers, which have both hydrophilic and hydrophobic constituents, accommodate either ionic or non-ionic groups. The most common non-ionic SP is PNIPAAm, which is soluble in polar solvent. Studies on solution behavior of PNIPAAm involve in water and in water/methanol mixture generally. In aqueous solution, the delicate balance between hydrophobic–hydrophilic conditions controls phase transition of the polymer.

Ionic polymers contain groups that ionize when placed in contact with a polar solvent. Their ability to respond to changes in the external environment is one of the most important properties utilized in many applications. The charged groups in the polymer ionize under favorable external conditions, and the resulting repulsion between the groups causes shrinking chain to expand. They may be classified according to the nature of the charges present in the polymer as anionic, cationic and amphiphilic networks. When ionized cationic polymers carry positive charges like ammonium ( $\text{NH}_4$ ) or amino groups ( $-\text{NH}_3^+$ ), owing to their ability to swell in an acidic environment, their diffusional properties are profoundly affected. First-order phase transition in positively ionized acrylic acid (AA) gels was observed by Hirokawa et al [25].

## 2.2. Polymeric Gels

Polymeric gel is physically and chemically cross-linked network of polymer chains, within which low molecular weight liquid is immobilized and the amount of solvent present within the network is much higher than the amount of polymer constituting the network. Polymeric hydrogels have a series of particular characteristic: they are hydrophilic, insoluble in water, soft, elastic and swell with water, keeping their shape but increasing in volume, until reaching a physical chemical equilibrium. Based on the response to the surrounding medium conditions, hydrogels can be categorized into two classes: (a) conventional hydrogels (b) stimuli-responsive hydrogels. The stimuli-responsive hydrogels demonstrates sensitivity towards various external stimuli such as pH, temperature, light, ions, electric field, etc. In such class of polymeric gels, the pH and temperature responsive gels have shown great potential in various biotechnological applications [5]. Poly(N-isopropylacrylamide) PNIPAAm is a well known reversibly thermo-sensitive polymer which exhibits a lower critical solution temperature (LCST) in an aqueous solution generally at 32°C (Figure 2.2). Dry hydrogels (xerogels) are crystalline [26,27]. These characteristics are related to several factors:

- (a) the hydrophilic character is due to water-soluble chemical groups –OH, –COOH, –CONH<sub>2</sub>, –CONH, –SO<sub>3</sub>H;
- (b) the existence of a polymeric network implies their insolubility;
- (c) the softness and elasticity are determined by the hydrophilic monomer and the low density of crosslinking; and
- (d) the conservation of shape in the swollen form is the result of the overall balance between dispersive and cohesive intermolecular forces (which allow the absorption of water) [28].

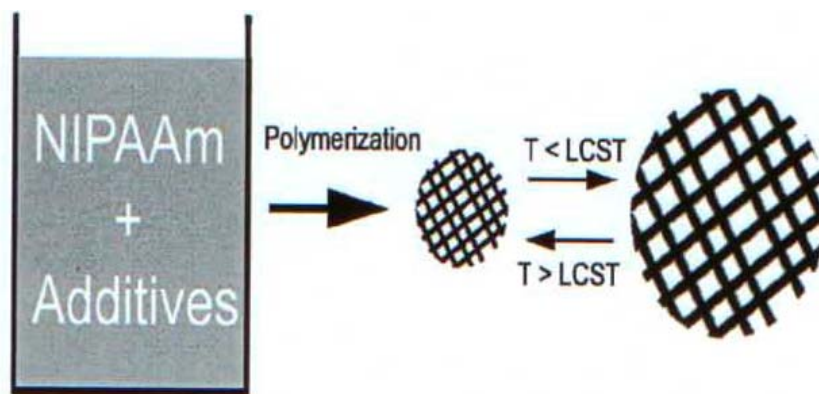


**Figure 2.2 :** Schematic of Crosslinking Polymerization Process of PNIPAAm.

Hydrogels are three-dimensional and hydrophilic polymer networks capable of imbibing large amounts water or biological liquids. Hydrogels resemble natural living tissue due to their high water content and soft touch. Their mechanical properties are similar to those of natural rubbers. It has high deformability and nearly complete recoverability. Depending upon the solvent, temperature, and other environmental conditions, the polymer chains can either repel each other and be swollen, or attract each other and be very compact.

NIPAAm is the major building block for temperature-sensitive microgels. The monomer is available from specialty chemical distributors. With a structure close to acrylamide (AAm), many of the properties of NIPAAm are similar to those of AAm. In aqueous solution it undergoes rapid free radical polymerization in water to give high molecular weight polymers at rates similar to that of AAm [13,29-31]. Like AAm, NIPAAm is a suspected carcinogen and neurotoxin, however, unlike AAm, NIPAAm has an intense odor so monomer contamination is easy to detect.

### 2.2.1. Defects in gels

The structure of many an ideal network should be topologically similar to an ideal lattice. A network with the functionality four corresponds to a simple cubic lattice. The lattice sites correspond to the network cross-links, and the bonds between adjacent sites correspond to flexible polymer chains of equal length. There are many defects in a real polymer network, including dangling chains, loops, entanglements, and large polymers trapped inside the gel [32]. Also, since the gelation process quenches the randomness of the structure, there are permanent structural fluctuations in the network. Many properties of gels, including permeability [33], elasticity [34],

swelling ratio [35], and solvent molecules diffusion rate [36], etc. are directly dependent on the defects of the network.

Pusey & van Megen [37] showed that for some gels the collective diffusion coefficient determined from the time-averaged correlation function of scattered light could be larger than the real value of the diffusion coefficient.

Solvent-phobic cross-link molecules tend to aggregate to form clusters upon a free radical copolymerization process. This effect has been reported in the case of poly(acrylamide) and poly(acrylamide)-derivative gels with cross-linking molecules N,N'-methylene-bis-acrylamide (BIS) [38-40] and poly(dimethyl siloxane) gels, with ethyl triacetoxy silane (ETAS) as cross-link molecules [41]. This aggregation causes the formation of structural inhomogeneities and makes the gel more permeable [42-44]. Gels prepared with relatively high BIS or ETAS concentrations become opaque because of the frozen density fluctuations. It is interesting to point out that although the numerical value of the elastic modulus depends on the cross-link concentration, the power law relation between the elastic modulus and the network concentration is preserved [45,46].

The networks made by cross-linking polymers, rather than starting with monomers, have many entanglements. The entanglements of the network chains effectively increase the number of cross-links [47-49]. The high frequency response of a polymer melt of entangled long chains is similar to that of a gel system [47].

The pendent (side) chains exist practically in all the gels made by different methods. Although the equilibrium swelling ratio in a good solvent is relatively insensitive to the concentration of the pendent chains, the elasticity and other properties [50-52] crucially depend on the pendent chain concentration. The loops in a network can be effectively treated as pendent chains.

A uniform distribution of the cross-link molecules in a network at preparation can become non-uniform and inhomogeneous upon swelling in good solvent [53,54]. This phenomenon was experimentally observed by Bastide et al, using SANS technique [55]. Candau and co-workers reported another type of inhomogeneity in the partially ionized poly(acrylic acid) gel [56] also probed by SANS.

### 2.3. Lower Critical Solution Temperature (LCST)

LCST is a phase transition behavior of materials. The LCST of linear polymer in a solvent, in which the polymer are soluble at the low temperatures but separate into an aggregated phase when the temperature is rased above their characteristic LCST. The LCST defination can also be used for gels. The LCST of crosslinked polymer (a gel) in a solvent, in which the polymer swells at the low temperatures but shrink when the temperature is rased above their characteristic LCST (Figure 2.3).

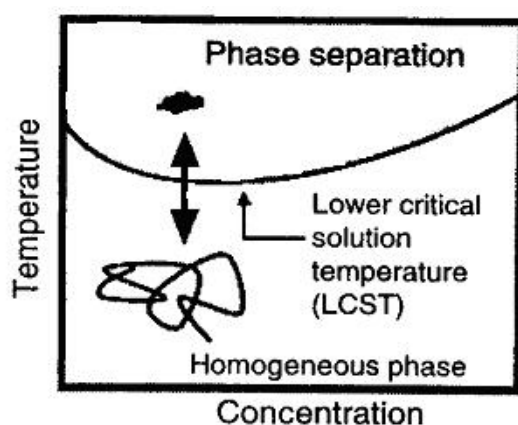


**Figure 2.3 :** Schematic Illustration of Thermo-sensitive Polymers

Aqueous solutions of thermoresponsive polymers are characterized by an inverse dissolution behavior, their isobaric phase diagrams presenting a LCST [21,22,57,58]. The solutions are homogenous at low temperature and a phase separation appears when the temperature exceeds a definite value. The LCST is the minimum of the phase diagram of the system, and in the practical cases to be treated in the following, the phase separation temperatures at which the phase transition occurs, also called demixtion, will be denoted “Td” or critical point (CP). PNIPAAm gained its popularity mainly because of the sharpness of its phase transition, and the easiness to vary its phase separation temperature by co-polymerization [58,59], addition of salts [60-62], or addition of surfactants [25,63] to the polymer solution. When PNIPAAm heated above 32 °C, the polymer becomes hydrophobic and precipitates out from solution and below LCST it becomes completely soluble because of hydrophilic state and forms a clear solution.

The effects of synthesis-solvent composition, initiator concentration, comonomer type monomer purity on the volume swelling ratios, and polymer-solvent interactions have been investigated as a function of temperature. Non-ionic NIPAAm

homopolymer gels, poly(NIPAAm-co-DMI) (P(NIPAAm-co-DMI)) and poly(NIPAAm (IA)) (P(NIPAAm-co-IA)) gels containing hydrophobic (DMI) and hydrophilic (IA) comonomers were prepared by free radical polymerization using KPS, TEMED (redox initiator) in the presence of an BIS cross-linking agent. The synthesis-solvent composition (40/60 v/v % mixture of water/methanol and water) and initiator concentration employed significantly affected the proper of the NIPAAm gels. The transition temperatures of P(NIPAAm-co-IA) gels synthesized in water/methanol mixture were higher than that of the gel obtained in water [64]. Tokuyama et al [65] reported that to elucidate the effects of synthesis-solvent on the network structure of NIPAAm hydrogels. NIPAAm hydrogels were synthesized in four synthesis-solvents: water, ethanol, acetone and N,N-dimethylformamide (DMF) (Figure 2.4). The swelling and elastic properties of those hydrogels were investigated.

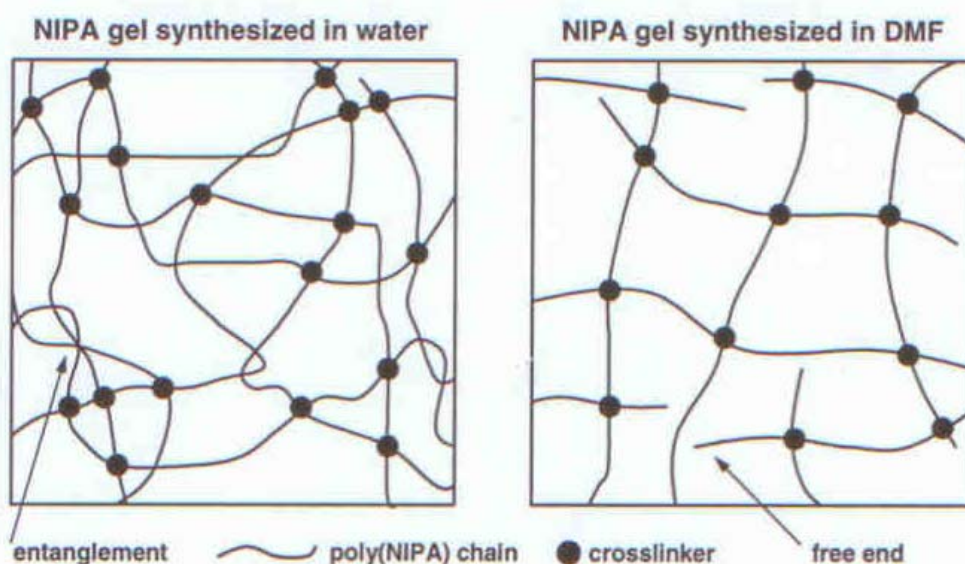


**Figure 2.4 :** Schematic Illustration for Networks of NIPAAm Gels as –Synthesized in Water and DMF.

Water-soluble block copolymers were prepared from the non-ionic monomer of N-isopropylacrylamide (NIPAAm) and the zwitterionic monomer 3-[N-(3-methacrylamidopropyl)- N,N-dimethyl] ammonio-propane sulfonate (SPP) by sequential free radical polymerization via the reversible addition–fragmentation chain transfer (RAFT) process. Such block copolymers with two hydrophilic blocks exhibit double thermoresponsive behavior in water: the PNIPAAm block shows a LCST, whereas the poly-SPP block exhibits an upper critical solution temperature.

Heskins and Guillet [34] published a study simple visual observation of macroscopic phase separation upon heating (LCST). Therefore, the LCST is commonly known as the cloud point due to this method [35].

Many researchers have somewhat quantified the method determining LCST by various methods. The phase transition behavior of PNIPAAm aqueous solutions has been investigated by a wide variety of experimental techniques including light scattering (LS) [66-69], calorimetry [14,16,71-76], viscometry [76,77], FT-IR spectroscopy [72], NMR spectroscopy [78], electron microscope [79], fluorescence [80-82], small-angle neutron scattering [83,84], and UV turbidimetry [75,85].

### **2.3.1. Determination of LCST by UV-VIS spectrophotometer**

The standard UV-VIS spectrophotometry is the most commonly used method by determining the LCST [50,86-90]. The main difference among the mentioned works for the same polymer comes from the selected wavelength of observation. Fixed wavelengths such as 500 nm [36,91] or 600 nm [17,88] or computer-averaging turbidity from 400 to 800 nm [50,86] has been employed. The wavelength of the measurement determines the minimum size of precipitated particle detected; nevertheless, for binary aqueous solutions of PNIPAAm, there seems to be no particular advantage to any particular wavelength in the UV-VIS spectrum. However, when certain additives are added to the system [36,88,91], the precipitated aggregate's size can be equal to or less than that of the wavelength of the light used, leading to clear, "turbid" solutions. Therefore, the observation of LCST may be a function of the wavelength chosen. Consequently, it may be very difficult to assign an LCST based on cloud point measurements [91], and more precise dynamic light scattering [89] must be used to observe the precipitation process.

### **2.3.2. Determination of LCST by differential scanning calorimetry**

When the physical and/or chemical transitions occur with temperature can be measured by differential scanning calorimetry (DSC). Heskins and Guillet [34] were the first report than an endotherm can be observed at LCST upon heating aqueous solutions of PNIPAAm. Their measured transition heats varied with concentration; this was attributed to the energy required to break hydrogen bonds between polymer and water molecules. However the instrument they employed was not sensitive enough for precise measurements; an instrument such as that typically used in

biological studies [90] is required. The latter type of calorimeter has recently been extensively utilized to observe PNIPAAm solutions [90,91]. Schild and Tirrell [91] have demonstrated that the transition is detected by DSC is in excellent agreement with results from visual cloud point measurements.

### **2.3.3. Determination of LCST by light-scattering**

If polymer molecules are dissolved in a solvent the light scattered by the polymer far exceeds that scattered by the solvent and is a measure of molecular dimension. Experiments using light as a probe offer information on the size, shape, and interactions of macromolecules [38,39]. Much more structural information is available than can be obtained with the simple turbidimetric, cloud point measurements discussed above. Initial studies employing more sophisticated light scattering apparatus concentrated on the determining weight average molecular weight of PNIPAAm [34,92]. Heskins and Guillet reported that the apparent molecular weight increased 4.5 times upon increasing the temperature from 25°C to 33°C, and suggested a simple aggregation phenomenon was present. More recent measurements [36,41-43] have employed dynamic as well as static light scattering to much more dilute solutions to attempt to detect coil-to-globule transition [44]. In this case at the LCST instead of intermolecular polymer-polymer bonds replacing polymer-water interactions because the neighboring chains are so distant intramolecular polymer-polymer bonds form, thereby collapsing the chain. Theoretically, one would ultimately attain a hard sphere.

## **2.4. Importance of Lower Critical Solution Temperature**

Temperature-sensitive polymers have been the subjects of many investigations due to the characteristic features of these kinds of polymers. Taylor and Cerankowski showed that incorporation of more hydrophobic groups led to a lower LCST for polymers including PNIPAAm [93]. It is also known that PNIPAAm's tacticity has a major influence on PNIPAAm's LCST [94,95]. Other solution components can exert a significant and predictable effect on a PNIPAAm's LCST. However, the effect of end groups on LCSTs and the effect of degree of polymerization on LCST are less clear. In the case of PNIPAAm, reports variously say that LCSTs increase, decrease, or remain unchanged with molecular weight. Works by Fujishige et al. [96],

Tiktopulo et al. [97], Takei et al. [98], and Ding et al. [99], report no appreciable change in LCST with changes in the molecular weight of PNIPAAm. In contrast, reports by Tong and co-workers [100,101] suggest that LCSTs increase with increasing molecular weight. Finally, Baltes et al. [102] and Scield and Tirrell [16] reported that LCSTs decrease with increasing molecular weight. A very recent report by Xia et al. using PNIPAAm samples prepared by atom radical polymerization, suggest that a combination of polymer-solvent interactions and end-groups effects are both important [103]. Furyk et al. [104] reported that PNIPAAm synthesis and measure very little differences in LCST with a great precision to provide more definitive results as to how changes in molecular weight of PNIPAAm affect LCSTs. The results described that LCSTs of high – molecular weight PNIPAAm samples are not affected by molecular weight, end group structure, or polydispersity until low molecular-weight samples are examined. In cases where changes in LCST for PNIPAAm samples begin to be observed, they have been able to show that these effects are most simply ascribed to the effect of the polymers end group structure.

At the LCST, hydrophobic forces (due to interaction of  $-N-(CH_3)_2$  groups) causing water insolubility, are balanced by H-bonding among water,  $-HN-$ , and/or  $-CO$  groups responsible for maintenance of water solubility [105]. Increases in the LCST can achieve by incorporation of ionic co-monomers of formulation with salt and surfactants [16,19,106]. The reason is that changes in pH, for example, can alter repulsive forces between ionic co-monomers and thereby further enhance changes in the extent of swelling of the co-polymer. Decreases in LCST values can be attained by incorporation of hydrophobic co-monomers, such as methacrylic acid [25] and more recently, molecules such as N-tert-butylacrylamide (NtBAAm) [107].

The behavior of PNIPAAm in water and the effect of various factors such as solvent composition [108], structure of the group in the side chains [109], addition of cosolutes (salt, surfactants) [110] were investigated extensively. The molecular reason of the phenomenon of phase separation in PNIPAAm is believed to be the hydrophilic/hydrophobic between various groups on the polymer chain. Rearrangement of hydrogen bonds between polymer-solvent systems in combination with hydrophobic interactions of flexible side groups on the polymer chain strongly affects the temperature of phase separation [111].

PNIPAAm lattices show the traditional LCST characteristic [29,30,112] as they expand and swell when cooled below the LCST, and they shrink and collapse when heated above the LCST. Hydrogels prepared from crosslinked PNIPAAm, undergo analogous swelling and shrinking volume transition [113]. These temperature-induced volume changes have been used to develop novel “smart” gels, which promise applications in controlled release technology, bioseparation, robotics [114], and drug design [115], or photographic films [116]. For these purposes, the polymers have been applied as single chains [117], macroscopic gels [118], microgels [30], or lattice [119].

PNIPAAm forms swollen hydrogels of crosslinked species due to the presence of both hydrophilic amide group and hydrophilic isopropyl groups in its side chains. Xue et al. [120] study is the synthesis novel copolymeric thermosensitive hydrogels of NIPA with the double alkyl chain acrylamide monomers di-n-propylacrylamide (DPAM), di-n-octylacrylamide (DOAM) and di-n-dodecylacrylamide (DDAM), respectively. These comonomers were chosen because (1) it has been reported for hydrophobically modified polyacrylamide [121] that for a similar hydrophobe level, double-chain hydrophobes considerably enhance the thickening efficiency with respect to single chain hydrophobes. This indicates that there is a much stronger hydrophobic interaction between acrylamide derivatives containing two alkyl chains than those containing only one alkyl chain. (2) Introduction of a hydrophobic component also improves the mechanical strength of hydrogels [122].

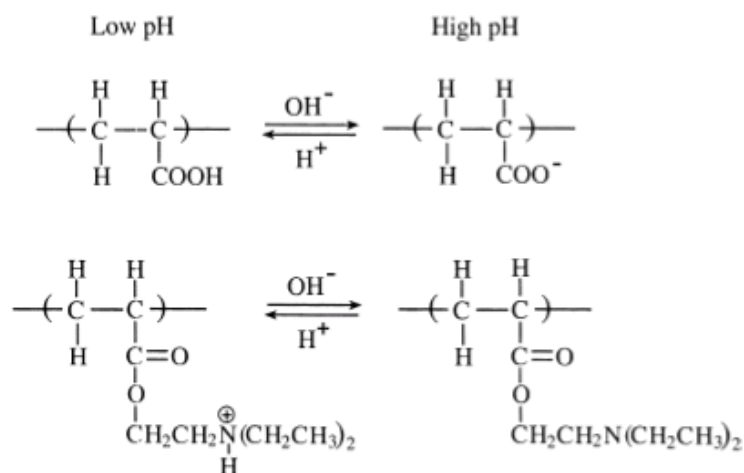
#### **2.4.1. LCST of modified temperature-sensitive polymers**

Modification of temperature-sensitive polymers can be done by changing hydrophilic and/or hydrophobic constituent of polymers or by copolymerization. These kinds of modifications affect the LCST value either lowering or raising.

Fluorocarbon-modified hydrophilic polymers form strong associations, even with low hydrophobe contents [123]. Li et al [81] reported that hydrophobically associating PNIPAAm containing low amounts (0.06 – 0.08 mol %) of fluorocarbon (CF<sub>3</sub>(F<sub>2</sub>)-) side chains shows much more pronounced hydrophobic association in an aqueous solution than do the corresponding hydrogen-substituted ones.

The development of systems with respect to phase transition (determining LCST) and pH sensitivity has been achieved by random and block copolymerization

employing hydrophobic and hydrophilic monomers containing ionizing groups. Following this strategy, NIPAAm has been copolymerized with different monomers to change their phase transition temperatures [124]. The copolymerization with ionic comonomers is an interesting approach because it makes it possible to adjust the thermosensitivity close to that of human body temperature [125]. The polymers with a large number of ionizable groups are known as polyelectrolytes. Scheme 2.1 shows structures of examples of anionic and cationic polyelectrolytes and their pH-dependent ionization. PAA becomes ionized at high pH, while poly(N,N'-diethylaminoethylmethacrylate) (PDEAEM) becomes ionized at low pH. As shown in Scheme 2.1, cationic polyelectrolytes, such as PDEAEM, dissolve more, or swell more if crosslinked, at low pH due to ionization. On the other hand, polyanions, such as PAA, dissolve more at high pH.



**Scheme 2.1.** pH-dependent Ionization of Polyelectrolytes. PAA (top) and PDEAEM (bottom).

The combination of both hydrophobic and ionic comonomers produces PNIPAAm-based hydrophobically modified polyelectrolytes. It is known that the polymers containing both temperature and pH-sensitive constituents exhibit pH-dependent phase transitions when the solution pH is varied. Temperature-sensitive PNIPAAm copolymerized with pH-sensitive monomers containing an ionisable group, such as AA and methacrylic acid (MeA) [85,126-128]. Erbil et al. studied the effects of the variation of both pH of the aqueous environment and itaconic acid (IA) comonomer content within the chain on the LCST of the copolymers are examined by cloud-point

measurements [129]. The results showed that changing in coil-globule transitions of pH- and temperature sensitive NIPAAm-IA copolymers.

AA is the most commonly employed comonomer for this purpose. The copolymerization with ionizing comonomers AA [130], the grafting or preformed polymers is also used as an alternative method to impart pH sensitivity to the polymeric system [131,132]. This grafting procedure has been used by Chen and Hoffman [133] to prepare P(NIPAAm-g-AA). This polymer maintained the ability to phase separate at physiological pH (7.4), remaining its cloud temperature as 32°C.

The LCST of PNIPAAm was investigated by copolymerization with charged [134] or uncharged [80]. Djokpe et al synthesized a series of statically copolymers of PNIPAAm and N-isopropylmethacrylamide. These products were investigated in terms of cloud points and composition and compared with different physical mixtures of NIPAAm and NIPAAm homopolymers [111]. The LCST of PNIPAAm copolymers is strongly influenced by the nature of the comonomer. Hydrophobic compounds lower the LCST and hydrophilic compounds raise it. It has been shown that the LCST phenomenon disappears when a hydrophilic compound contain more than a certain amount of comonomer [21]. The copolymerization of NIPAAm with a monomer bearing a carboxylic group makes it possible to change the hydrophilicity of the polymer by altering the pH-value, resulting in a change in the LCST [135]. Modified PNIPAAm copolymers by right balancing of hydrophobic and hydrophilic monomers [136] were prepared for the applications of PNIPAAm in biotechnology, drug release, film technology, water treatment, and so on, hydrophobically [80,137-142] and hydrophilically [71,83,84,126,143,144].

The hydrophobic modification of the polymer chains modulates the swelling and shrinking behavior of the gels and, thus, may be used to influence the pharmaceutical applicability of these gels [137,138,142,145,146]. Polyelectrolyte gels are networks made of ionic macromolecules swollen in water or aqueous fluids. They are interesting for various biological applications, e.g., because of the known negative charge on the surface of blood cells, blood vessel walls, and other tissue types [147]. However, the polyelectrolyte gels are also interesting in their own right. The most striking characteristic is that they can absorb up to several hundred times their own weight of water, while retaining coherence and elasticity [126,148]. Shibayama et al. [72,74] have shown that in a swollen PNIPAAm gel there are two types of water

molecules. 10-15 water molecules per NIPAAm segment are associated with the phase transition and about 1-3 water molecules per polymer segment may be considered as the lower limit for the hydrophobic hydration. Ethyl and tert-butyl methacrylate have recently been employed by Jones et al [149] to synthesize amphiphilic polymers for oral administration of hydrophobic drugs [149,150].

NIPAAm copolymer gels were synthesized by free radical crosslinking copolymerization of NIPAAm with each of AA, IA, and maleic acid (MA), the difference being both between configurations and carboxyl group numbers, and pK values, in the presence of BIS. The influence of comonomer concentrations, BIS content, and comonomer type (AA, IA, and MA) on the external views was examined.

The synthesis and characterization of a new heterogeneous, thermally reversible hydrogel prepared from mixture of NIPAAm monomer and vinyl terminated polydimethylsiloxane (VTPDMS) macromer [151,152]. It is interesting that this hydrogel has the same LCST as the homopolymer of NIPAAm, independent of VTPDMS content, and also that at higher silicone contents it exhibits an enhanced rate of shrinking when heated through the LCST. From these observations, it was postulated that incorporation of an ionic monomer into this hydrogel might result in a gel whose swelling is very sensitive to pH, especially above the LCST of PNIPAAm.

## **2.5. Swelling and Volume Phase Transitions of Gels**

The quantitative treatment of the rubber network was started 1934 by Guth & Mark [88] and Kuhn [153,154], and was extended later by James, Flory, and others [17,155]. Their efforts resulted in the Phantom Network Theory [156] and the Affine Network Theory [157,158]. Both theories give similar results on the rubber elasticity.

The first mean-field treatment of gel network systems was given independently by Flory and Huggins [159]. In 1968, based on the Flory-Huggins theory, Dusek & Patterson predicted a volume phase transition of the network system between a dense phase and a dilute phase [160]. In 1973 Tanaka et al. were able to observe the density fluctuations of polymer network using dynamic light scattering spectroscopy [161]. In 1977, they observed the critical behavior and phase transition of polyacrylamide gels [162].

### 2.5.1. Flory-Rehner theory (FH Theory)

The Flory-Rehner theory has been widely used to explain the swelling process of the gels [158,163]. According to this theory, the free energy change ( $\Delta G$ ) involved in the mixing of pure solvent with the initially pure, amorphous, unstrained polymeric network is conveniently considered to equal to the sum of the individual free energy terms, i.e., the ordinary free energy change of mixing ( $\Delta G_{\text{mix}}$ ), the free energy of elastic deformation ( $\Delta G_{\text{el}}$ ), and in the case of ionic network, the free energy of electrostatic interactions ( $\Delta G_i$ );

$$\Delta G = \Delta G_{\text{mix}} + \Delta G_{\text{el}} + \Delta G_i \quad (2.1)$$

When a non-ionic polymeric network is placed in a swelling agent, there are two contributions to the free energy of the system, mixing and elastic-refractive free energies as expressed as  $\Delta G_{\text{mix}}$  and  $\Delta G_{\text{el}}$ , respectively. Total free energy

$$\Delta G = \Delta G_{\text{mix}} + \Delta G_{\text{el}} \quad (2.2)$$

By taking the derivative of each term in this equation with respect to the number of molecules of swelling agent in the system, a relationship between the chemical potential contributions and total chemical potential can be derived for equilibrium conditions:

$$\mu_1 - \mu_1^0 = (\Delta\mu_1)_{\text{mix}} + (\Delta\mu_1)_{\text{el}} = 0 \quad (2.3)$$

where  $\mu_1$  is the chemical potential of the swelling agent in the polymer-swelling agent mixture, and  $\mu_1^0$  is the chemical potential of the pure swelling agent. The first term in the right-hand side of the equation (2.1), for the mixing of polymer chains with the solvent can be given in terms of the Flory- Huggins relationship:

$$\Delta G_{\text{mix}} = kT [n_1 \ln v_1 + n_2 \ln v_{2s} + \chi n_1 v_{2s}] \quad (2.4)$$

In equation (2,4)  $n_1$  is the number of swelling agent molecules in the solution,  $v_1$  is the volume fraction of solvent,  $n_2$  is the number of polymer molecules in the solution and  $v_{2s}$  is the polymer volume fraction of the swollen chains in the swollen state. Equation (2,4) may be differentiated to give equation (2,5):

$$(\Delta\mu_1)_{mix} = RT \left[ \ln(1 - v_{2s}) + v_{2s} + \chi(v_{2s})^2 \right] \quad (2.5)$$

Expression of  $\Delta G_{el}$  for a phantom network is given in equation (2,6) below [38]

$$\Delta G_{el} = \left( \frac{3\nu kT}{2} \right) \left[ \left( \frac{v_{2r}}{v_{2s}} \right)^{2/3} - 1 \right] - \mu kT \ln \left( \frac{v_{2r}}{v_{2s}} \right) \quad (2,6)$$

where  $\nu$  is the number of network chains,  $\mu$  is the number of junctions,  $v_{2r}$  is the polymer volume fraction in the gels immediately after preparation (relaxed state) and  $v_{2s}$  is the polymer volume fraction of the swollen gels (swollen state). Differentiation of equation (2,6) with respect to the number of moles of solvent and substitution in equation (2,3) together with equation (2,5), one obtains for a phantom network

$$\ln(1 - v_{2s}) + v_{2s} + \chi(v_{2s})^2 + B \left( \frac{v_{2s}}{v_{2r}} \right)^{1/3} = 0 \quad (2,7)$$

where

$$B = \left( 1 - \frac{2}{\phi} \right) \left( \frac{V_1}{\nu M_c} \right) \quad (2.8)$$

and  $\phi$  is the functionality at the cross-linking site. In the highly swollen state, a real network exhibits properties closer to those of the phantom network model. Consequently, equation (2,7) is a more realistic representation for equilibrium swelling. Thus, equation (2,7) may be used to estimate the average chain length between cross-links, especially at the high degrees of expansion obtained in the swelling experiments [66]. Using equation (2,8) and solving equation (2,6) for  $M_c$  leads to

$$M_c = - \frac{\left[ \left( 1 - \frac{2}{\phi} \right) V_1 (v_{2r}^{2/3} v_{2s}^{1/3}) \right]}{\nu \left[ \ln(1 - v_{2s}) + v_{2s} + \chi(v_{2s})^2 \right]} \quad (2,9)$$

This derived equation using the phantom network model is valid for neutral and non-ionic structures and Bahar et al. using several network samples with different cross-

link densities had proved that equation (2,9) leads to an estimate of  $\chi$  as a function of  $v_{2s}$  as well [47].

### 2.5.2. Fundamental interactions and gel phase transitions

Amiya & Tanaka showed the volume phase transition is general in all kinds of polymer networks [42]. The volume of a gel can change either continuously or discontinuously upon a change of the environmental conditions such as temperature and solvent composition. For practical reasons, the transition has been observed in water or a mixture of water and other solvents such as alcohol and acetone.

The volume phase transition is a result of a competitive balance between a repulsive force that acts to expand the polymer network and an attractive force that acts to shrink the network. The most effective repulsive force is the electrostatic interaction between the polymer charges of the same kind. It can be imposed upon a gel by introducing ionization into the network. The osmotic pressure by counter ions adds to the expanding pressure. The attractive forces can be Van der Waals, hydrophobic interaction, ion-ion interactions between opposite kinds of charges and hydrogen bonding.

#### 2.5.2.1. Ionic interactions

A frequently used means of varying the degree of the discontinuity of the gel phase transition is the ionization of the network (Figure 2.5). The greater the ionization, the larger the volume changes at a discontinuous transition. Ionizable polymer networks can be obtained by several ways; copolymerizing ionizable molecules into the network [127], hydrolysis [164], and light illumination [151]. Ionized network are sensitive to pH [51,52], salt [52,53], electric field [54,55,165], and light [166].

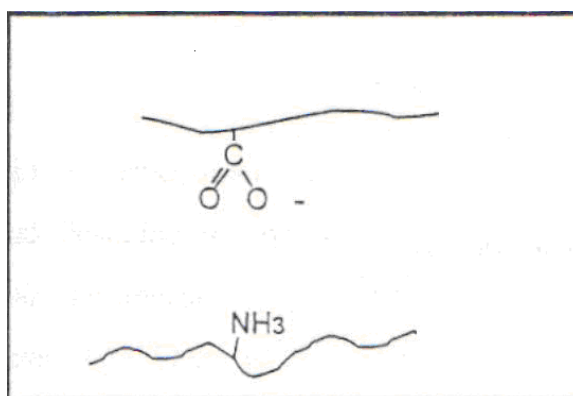


**Figure 2.5 :** Ionic Interaction.

Once the ionized gels are prepared, the degree of ionization can be controlled in several ways, including introducing deassociable chemicals into the network, and varying pH [56,167] and salt concentration [168,169]. Ionization contributes to the free energy of the network in two ways [48,49]. In the FH theory, the mobile counterions are confined inside the gel by the Donnan potential barrier [168]. These mobile counterions exert a gas-like pressure on the wall of Donnan charge bilayer. Screened electrostatic interaction among charges account for another means of enhancing free energy in the polymer network.

### 2.5.2.2. Hydrophobic interactions

The hydrophobic interaction arises between non-polar molecules in water, which is a polar solvent (Figure 2.6). A hydrophobic group is shielded by water molecules, which form a cage around the group [170-172]. The water molecules in the cage are arranged in a certain order and may be considered frozen. When the temperature is increased, the cage of frozen water molecules is partially melted and the protection of the hydrophilic groups becomes weakened. This is the reason why the hydrophobic interaction increases as the temperature is increased. The entropy decrease due to the network collapse is compensated by the larger entropy decrease associated with the melting of the cage. Therefore, the entropy of the collapsed gel increases upon heating.

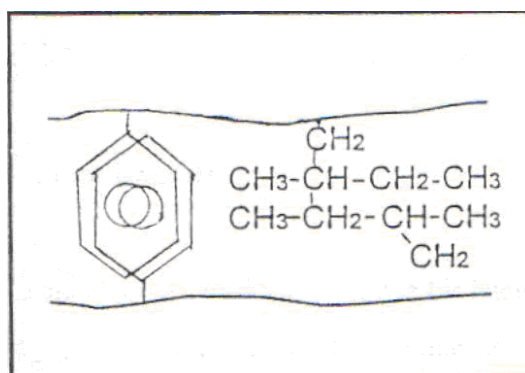


**Figure 2.6 :** Hydrophobic Interaction.

A thermally induced gel phase transition in pure water has been observed in several systems, including poly(N,N-diethylacrylamide) [173] and PNIPAAm [91], and other systems [174]. Introducing small additives such as alcohol, DMSO, and DMF can also weaken the hydrophobic interaction. In water these molecules form hydrates and effectively reduce the available water molecules for the cage. This effect has

been observed by several groups [14,175,176]. The hydrophobic interaction can also be modified using surfactants [177,178].

### 2.5.2.3. Van Der Waals and hydrogen-bonding interactions

Phase transition of hydrophilic networks in water has also been observed. Overcoming the hydrophilic interaction between polymers and solvent by the chain-chain attraction induces the phase transition. This is achieved by mixing water with other solvents such as alcohol, acetone, DMSO, etc. to enhance the Van der Waals interaction (Figure 2.7a).

Another important attractive interaction is hydrogen bonding (Figure 2.7b). It is known that polymer complexes are formed between poly(acrylic acid) and some polybases such as poly(oxyethylene) (POE), poly(vinylmethylether) (PVME), and poly(vinylpyrrolidone) (PVP) [179]. Based on this principle, Okano and his colleagues developed an interpenetrating polymer network of poly(acrylic acid) and poly(acrylamide) and observed a sharp swelling of the gel upon increasing the temperature [127]. The phase transition of the gel was recently observed by Ilmain et al [180], who slightly ionized the gel developed by Okana's group [181]. The mechanisms of the polymer complexation and the gel phase transition are believed to be the same, where the zipping effect seems to play an important role in enhancing the attractive interaction.

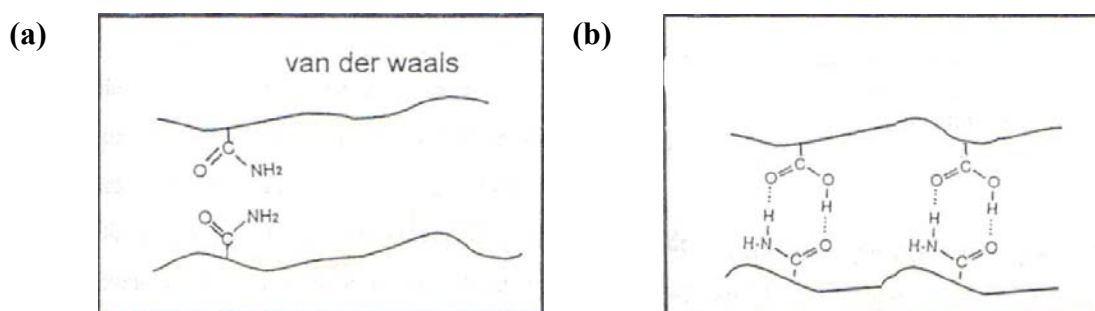


**Figure 2.7 :** (a) Van der Waals and (b) Hydrogen Bonding Interactions.

### 2.5.2.4. Critical behavior of gels

Associated with the volume phase transition of gel network systems, gels show critical behavior near the critical point at which the discontinuity of the volume change disappears. The study of the critical point is of great theoretical and practical interest. For some gels, a large change in volume is obtained by small changes in the

surrounding environment, such as temperature or pH. These gels are called critical gels or super-critical gels due to their resemblance to gases at and beyond their critical point. Critical gels are close to another type of critical point under normal pressure and temperature. Figure 2.8 shows the similarity in behavior for a van der Waals gas and a gel near the critical points, although the physical and chemical background of each system is different. It was known decades ago that the critical exponents of many systems couldn't be explained by the classical mean-field theories [182]. The discrepancy was not understood until the renormalization group theory was introduced [183]. According to the renormalization group theory, the critical exponents are related to only a few parameters of the system and are independent of the details. Totally different systems can belong to the same universality class and have identical exponents. It is therefore important to determine the critical exponents and the possible universality class to which the system may belong.

The state of a gel is determined by three variables; the reduced temperature  $\tau$ , the osmotic pressure  $\pi$ , and the network density  $\phi$ . In most gel experiments, the gels are immersed in a large volume of solvent, thus the external osmotic pressure is kept at zero. Depending on the chemical and physical composition of the network, the zero external pressure can be higher or lower than the critical osmotic pressure of the network. If it is higher, the isobar curve is continuous, and if lower, it is discontinuous.

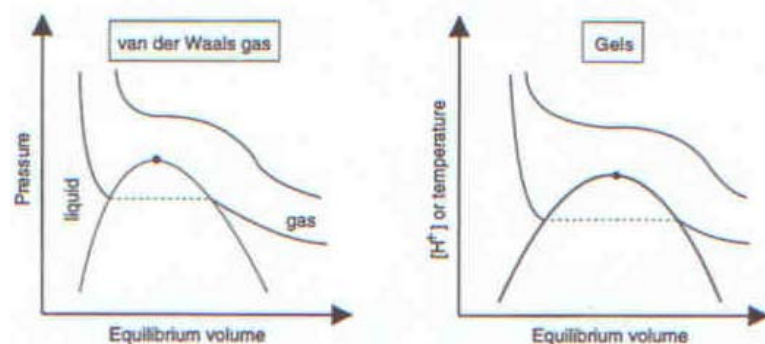


**Figure 2.8 :** The Left Part Shows Isotherms for a Van Der Waals Gas Near a Critical. The Right Part Shows Isobars for a Gel Near a Critical Point.

Fixing any one of the three variables at the critical value, and varying one of the other two can conveniently approach the critical point of a gel. One can fix the gel volume and approach the critical point from the positive osmotic pressure region.

Approaching from the negative osmotic pressure domain results in gel shrinkage. Or one can choose a system that has a critical osmotic pressure  $\pi_c=0$  and approach the critical point along the isobar path by varying the temperature [127,184]. The  $\pi_c=0$  condition can be achieved by changing the chemical or physical structure of the network or solvent [91]. For NIPA gel we find that for BIS=2.6, the critical osmotic pressure is approximately zero.

The critical density fluctuations of poly(acrylamide) (PAAm) gel were first observed in the scattered light intensity by Tanaka et al. [162] and Hochberg et al. [185]. The NMR study [186] of PAAm gels in an acetone/water mixture showed that the proton-lattice relaxation time diverges and the effective diffusion coefficient approaches zero near the critical acetone concentration. Near the critical point, the shear modulus is proportional to the density of the network and does not show any anomaly [91,187]. The bulk modulus, in contrast, approaches zero at the critical point.

## **2.6. Applications**

Gels exist widely in biological systems and food products, often as thickening agents, e.g. starch and gelatin [188]. The use of gels as a sieving matrix in electrophoresis and chromatography has been established for several decades [189]. The hydrolic fracturing technique used in the petroleum and natural gas industry uses gels to open and crack rocks and soils [190]. The gel beads mixed with soil can effectively control the moisture necessary for plants [191]. The organic solvent (oil) based gels have been used to seal electric components and keep them from corrosion by water moisture. The ability of gel to exchange gas and moisture with the eye makes long-wearing soft contact lenses possible [192]. The swelling property of the gel network makes the material ideal to be used in the absorption technologies. Well-known examples are baby diapers and sanitary napkins. In all these applications, however, only the swelling properties of gels are used.

Reversible volume transitions in response to various types of stimuli indicate that gels can be used as smart materials, and have attracted industrial scientists, engineers, and medical doctors to the gel research.

### **2.6.1. Mechanical devices**

The concentration and expansion of gel fibers provides a means of converting chemical energy into a mechanical energy, which can be used to develop artificial muscles and actuators. The early work on this subject was pioneered by Steinberg et al. [193] and Sussman & Katchalsky [194], using contraction and relaxation of collagen fibers, which can be induced by changing solvent condition. Recent studies have shown that the efficiency of a gel engine increases with the load and the degree of crosslinking [195]. Cross-linked poly(vinyl alcohol) fiber can induce a high strength reaction [196]. De Rossi and his colleagues have developed an artificial sphincter using electric-sensitive gels [197]. A group in the Toyota Research Laboratories developed an interesting fish made of gels that swims in water driven by an electric field [198]. They also developed a three-finger hand that can pick up a quail egg. Suzuki devised a model gel arm that can raise a Coke bottle [199]. Osada and his groups devised a seesaw balance that oscillates in response to the shrinking and swelling of gels driven by an electric field [200-204].

### **2.6.2. Solvent purification**

When a gel swells from the shrunken state to the swollen state, it can absorb a tremendous amount of solvent. The final swelling ratio depends on the solvent [202]. In the case of a mixed solvent, however, the degree of absorption depends on the chemical structure and molecular weight of the solvent molecules to be absorbed. It was found that the absorption efficiency of a gel decreases as the molecular weight of the solvent increases. Such a selective absorption provides a way of using polymer gels to extract solvents from aqueous solutions [203]. The absorbed solvent can be disposed of or collected by squeezing the gel using the collapsing phase transition.

It is also possible to design the network with strong selective absorption ability. Kokufuto et al, showed that hydrophobic gels can be used to extract detergent molecules [205]. This concept can also be used in designing oil cleaning products using hydrophobic gels.

### 2.6.3. Pharmaceutical applications

The diffusion of a large guest molecule trapped in a gel network depends on the state and the structure of the network [205-210]. Naturally diffusion is prohibited when the gel is collapsed, but enhanced when the gel is swollen. Based on this principle, specific condition-sensitive, therefore target-sensitive, drug delivery systems have been designed [211].

Varying the state of the gel can control the activity of enzymes trapped in a gel matrix. Hoffman and his colleagues have shown that temperature cycling of thermal hydrogels can enhance the enzyme productivity dramatically [211-214]. It was also shown that the swelling behavior of a gel network can also be modified by the existence of the trapped enzymes [214]. Kokufuta et al. designed a gel using poly(N-isopropyleacrylamide) in which some enzymes are incorporated that undergoes a phase transition when the enzymatic reaction takes place [215].

There are basically two kinds of drug-release mechanisms related to gel volume change. One acts by squeezing, where the drug is released because of the fast initial shrinking of network [211]. In the swollen state, the drug molecules are dissolved in the solvent and remain inside the gel because of the small diffusion rate. When the gel shrinks suddenly, the drug molecules are squeezed out together with solvent, thus causing a drug release burst.

The other mechanism relates to a hydrophobic drug trapped in hydrophobic network, in which the drug diffusion rate and crystallization degree are strongly dependent on the network density [216-219]. Siegel et al. observed a similar result using pH as the controlling parameter [218]. In the collapsed state, the diffusion rate is low and the crystallization of the drug molecules is high, which results in the off state of the release. The swollen state provides a freer environment for the drug molecules and they can diffuse out easily.

Using hydrogel membranes, Siegel & Firestone showed that it is possible to design human implantable self-regulating insulin delivery systems that are sensitive to glucose concentration [219]. Grimshaw & Grodzinsky reported that it is possible to selectively control the transport of proteins across polyelectrolyte gel membranes [220].

### **2.6.3.1. Environmental-sensitive hydrogels for drug delivery and controlled release systems**

Polymeric systems that modify their structure and, in consequence, their properties in response to changes in the physical and chemical characteristics of the physiological medium are very promising candidates to achieve optimum control of the moment and rate of drug release. In this sense, smart polymer hydrogels that experience reversible phase transitions have attracted special attention. PNIPAAm hydrogel is one of the most widely studied examples of gel systems that undergo a temperature-controlled volume phase transition. The gel is swollen at temperatures lower than 33°C and collapses when the temperature is raised. Hydrogels based on NIPAAm and its copolymers have been used to develop temperature-modulated drug release systems. The release of a drug entrapped in the polymer network depends strongly on the permeability of the network, i.e. on the degree of swelling of the gel. Therefore, the swelling/ collapse process can be used to switch the release of the drug on and off, presenting a pulsatile release control.

Additionally, the presence of ionic components may provide pH-sensitive hydrogels, which are particularly useful, for example, in the delivery of drugs or peptides to a specific site in the gastrointestinal tract or in response to small changes in the pH of blood stream or tissues in a pathological situation, such as a clot or cancer. It has been observed in vitro that the combination of pH- and temperature-responsiveness is particularly useful to optimize the control of drug release. However, the dependence of the critical temperature on the composition of the gel is sometimes an obstacle to the efficient combination of pH and temperature-sensitive components, although the design of new monomers or synthetic routes can help to overcome this problem.

The relationship between the swelling response and the drug release rate, and in particular the influence of cross-linking density on the mesh size, has received considerable attention. However, there is still little information about the contribution of hydrogel flexibility, distribution of comonomers or presence of ions in the medium to this process and, especially, to the uptake of drugs by the hydrogels. Most of the smart hydrogels developed for drug delivery act as reservoirs that do not interact effectively with the drug. The incorporation of a comonomer that could establish a reversible bond with the drug, breakable under specific environmental conditions, would contribute to controlling the release process. In this

sense, the utility of phase transitions to achieve reversible, and even specific, molecular adsorption based on multiple-point interaction with a component of the hydrogel has been recently shown. These hydrogels consist of a main component, which allows the gel to swell and shrink reversibly in response to environmental changes, and a minor monomer component able to establish electrostatic interactions with a multicharged target molecule. These minor functional components develop affinity for the target when they can come close to each other (collapsed state) to form a binding site (receptor), but when they are separated (swollen state), the affinity diminishes. Therefore, the affinity of the hydrogel for a given drug may be modulated by the reversible phase transition. These previous papers used strong acids or bases as functional components, with a degree of ionization, and, in consequence, an affinity for the target molecule, almost independent of pH.

Hydrogels have been used extensively in the development of the smart drug delivery systems. A hydrogel is a network of hydrophilic polymers that can swell in water and hold large amounts of water while maintaining the structure. Hydrogels can protect the drug from hostile environments, e.g. the presence of enzymes and low pH in the stomach. Hydrogels can also control drug release by changing the gel structure in response to environmental stimuli. Hydrogels containing such 'sensor' properties can undergo reversible volume phase transitions upon only minute changes in the environmental condition. The types of environment-sensitive hydrogels are also called 'Intelligent' or 'smart' hydrogels [221]. Many physical and chemical stimuli have been applied to induce various responses of the smart hydrogel systems. The physical stimuli include temperature, electric fields, solvent composition, and light, pressure, sound and magnetic fields, while chemical or biochemical stimuli include pH, ions and specific molecular recognition events [222,223]. Smart hydrogels have been used in diverse applications, such as in making artificial muscles [224-228], chemical valves [200], immobilization of enzymes and cells [211,213,229-235], and concentrating dilute solutions in bioseparation [236,237,238-241]. Environment-sensitive hydrogels are ideal candidates for developing self-regulated drug delivery systems.

pH-sensitive hydrogels have been most frequently used to develop controlled release formulations for oral administration. The pH in the stomach (<3) is quite different from the neutral pH in the intestine, and such a difference is large enough to elicit

pH-dependent behavior of polyelectrolyte hydrogels. For polycationic hydrogels, the swelling is minimal at neutral pH, thus minimizing drug release from the hydrogels. This property has been used to prevent release of foul-tasting drugs into the neutral pH environment of the mouth. When caffeine was loaded into hydrogels made of copolymers of methyl methacrylate and N,N'-dimethylaminoethylmethacrylate (DMAEM), it was not released at neutral pH, but released at zero-order at pH 3-5 where DMAEM become ionized [218]. Polycationic hydrogels in the form of semi-IPN have also been used for drug delivery in the stomach. Semi-IPN of crosslinked chitosan and PEO showed more swelling under acidic conditions (as in the stomach). This type of hydrogels would be ideal for localized delivery of antibiotics, such as amoxicillin and metronidazole, in the stomach for the treatment of *Helicobacter pylori* [242].

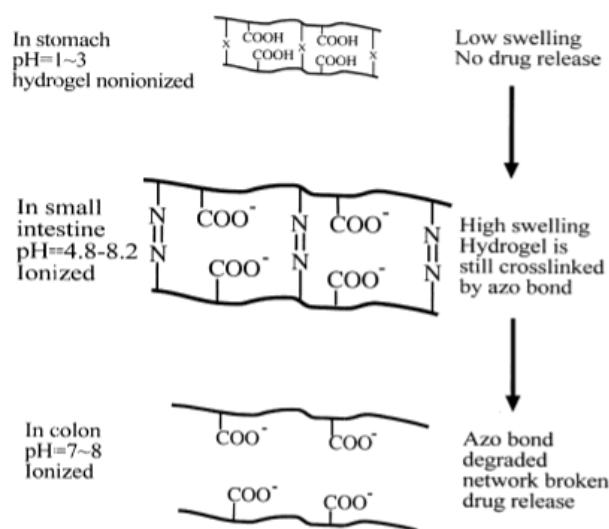


**Figure 2.9 :** Schematic Illustration of Oral Colon-specific Drug Delivery Using Biodegradable and pH-sensitive Hydrogels. The Azoaromatic Moieties in the Crosslinks are Designated by  $-N=N-$ .

Hydrogels made of PAA or poly(methacrylic acid (PMA) can be used to develop formulations that release drugs in a neutral pH environment [243,244]. Hydrogels made of polyanions (e.g. PAA) crosslinked with azoaromatic crosslinkers were developed for colon-specific drug delivery. Swelling of such hydrogels in the stomach is minimal and thus, the drug release is also minimal. The extent of swelling increases as the hydrogel passes down the intestinal tract due to increase in pH leading to ionization of the carboxylic groups. But, only in the colon, can the azoaromatic cross-links of the hydrogels be degraded by azoreductase produced by

the microbial flora of the colon [245,246], as shown in Figure 2.9. The degradation kinetics and degradation pattern (e.g. surface erosion or bulk erosion) can be controlled by the crosslinking density [245]. The kinetics of hydrogel swelling can be controlled by changing the polymer composition [246]. The polymer composition can be changed as the pH of the environment changes. Some pendant groups, such as N-alkanoyl (e.g. propionyl, hexanoyl and lauroyl) and O-acylhydroxylamine moieties can be hydrolyzed as the pH changes from acidic to neutral values, and the rate of side-chain hydrolysis is dependent on the length of the alkyl moiety.

pH-sensitive hydrogels were placed inside capsules [247] or silicone matrices [248,249] to modulate the drug release. The swelling-shrinking of hydrogels is controlled by changing pH, instead of temperature. In the silicone matrix system [248,249], medicated pH-dependent hydrogel particles made of semi-IPN of PAA and PEO were used. The release patterns of several model drugs having different aqueous solubilities, and partitioning properties (including salicylamide, nicotinamide, clonidine HCl and prednisolone) were correlated with the pH-dependent swelling pattern of the semi-IPN. At pH 1.2, the network swelling was low and the release was limited to an initial burst. At pH 6.8, the network became ionized and higher swelling resulted in increased release.

Normally, the selected drug is physically loaded in the swollen thermo-responsive hydrogel and the drug release is controlled by the external temperature changes due to the thermo-reversible properties of the PNIPAAm hydrogel. Generally regarded, the drug exhibits a Fickian release [237], which depends on the swelling ratio of the hydrogel. As the temperature is increased above the LCST, PNIPAAm hydrogel may shrink and quickly form a dense, thick skin layer [250,251], which leads to the burst release initially and then the release of the drug in the network matrix is stopped. A typical release pattern was reported by Kim's research group [217] and an on-off release pattern of the model drug, indomethacin, was achieved by regulating the temperature between 20 and 30°C. A series of investigations based on the thermo-responsive hydrogels was carried out and much useful data were obtained [211,217,252-254]. In this case thermo-responsive hydrogels provided a negative temperature-responsibility to the drug release, i.e. slow drug release at increased temperature and rapid drug release at decreased temperature. In some cases, a positive controlled release pattern, i.e. rapid drug release at increased temperature

and slow drug release at decreased temperature, is urgently needed when drug delivery system (DDS) is specially designed to respond to an increase in the body temperature resulting from diseases, such as inflammation or cancers etc (Figure 2.10).

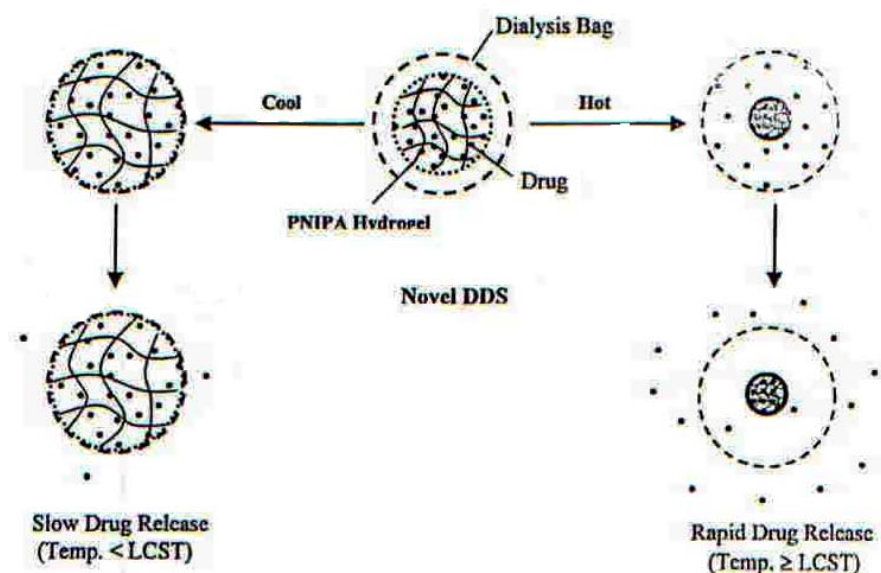


**Figure 2.10 :** Schematic Illustration of the Novel, Thermo-responsive DDS to give a Positive Drug Release by Modulating the External Temperature.

Equilibrium water content ( $W_{\infty}$ ) is a basic property of hydrogels because most of their applications depend on its value; the bigger  $W_{\infty}$ , the better permeability and biocompatibility of the gel. This higher permeability allows controlled drug release from hydrogels. However, exceedingly high water content results in very poor mechanical properties of the hydrogel. It is therefore necessary to look for an adequate balance in the hydrophilic and hydrophobic components to make hydrogels useful for particular applications without loss of their mechanical properties. A hydrogel LCST can be changed by modifying the side-chain substituent of the polymer or, in the case of copolymers, by varying their composition using comonomers which are more or less hydrophilic [96,255]. The same effect can be achieved by increasing the hydrophobic part of a hydrophilic monomer [256]. Katime et al [257] were preparation of hydrogels made of NIPAAm copolymerized with IA, their swelling kinetics, equilibrium water content and kinetics of aminophylline release, as a function of the hydrogel composition.

Hydrogels based on NIPAAm and its copolymers have been used to develop temperature-modulated drug release systems. The release of a drug entrapped in the

polymer network depends strongly on the permeability of the network, i.e. on the degree of swelling of the gel. Therefore, the swelling/collapse process can be used to switch the release of the drug on and off, presenting a pulsatile release control [125,181,247,258-261]. Additionally, the presence of ionic components may provide pH-sensitive hydrogels, which are particularly useful, for example, in the delivery of drugs or peptides to a specific site in the gastrointestinal tract [262] or in response to small changes in the pH of blood stream [263] or tissues [264] in a pathological situation, such as a clot or cancer.

## 2.7. Mechanical Strength of the Gels

The mechanical strength of the gels is important for biomedical applications such as selective membranes, enzyme activity controlling and drug delivery systems. PNIPAAm is the most widely used member of this type of polymer system. Pure NIPAAm hydrogels crosslinked by using hydrophilic tetrafunctional BIS and octafunctional glyoxal bis(diallyl acetal) (GLY) as crosslinker have low mechanical strength in the swollen state, i.e., below LCST [265]. The combination of large swelling and high mechanical performance within the same gel structure is important for both industrial and biomechanical applications. The formation of hydrophobically modified copolymers, nanocomposite gels and double networks by incorporation of hydrophobic components into the hydrogel structure can be given as the main examples of the methods, which are used to improve the mechanical properties [266-269].

Yıldız et al. [270] hydrogels composed of NIPAAm, BIS, VTPDMS and IA as hydrophobic monomer, hydrophilic crosslinker, hydrophobic crosslinker and weakly ionizable comonomer, respectively, were prepared to investigate the effect of hydrophobic component, i.e., VTPDMS on the compression moduli of the samples attained equilibrium swollen state in distilled-deionized water at 25°C. For mechanical strength analysis, conventional rubber elasticity and swelling theories for networks formed in the presence of diluent were adopted. The second one deals with neutral polymer chains. From the swelling and compression measurements, effective crosslinking density  $\nu_e$ , average molecular weight between crosslinks  $M_c$  and polymer-water interaction parameter  $\chi$ , which can be used to characterize the structures of the hydrogels, were calculated.

The equilibrium water content of the gel is a basic property, given that several useful applications require suitable water content. Hydrogels with higher water content are generally more advantageous because they show a higher permeability and biocompatibility. However, on increasing the water content the mechanical strength of the hydrogel decreases. To obtain a gel with high water content and an acceptable mechanical strength, a composite molecular structure is necessary. This structure will consist of a hydrophilic component that absorbs large amounts of water and hydrophobic component that improves the mechanical strength [271].

In recent years different types of hydrogels sensitive to temperature or pH have been synthesized. Variations in these parameters raise interesting structural changes that could eventually be important for biomedical applications. Several hydrogels of N-substituted AAm derivatives, such as PNIPAAm [117,236,243], poly(N,N-dimethylacrylamide) [173], poly(N-methylacrylamide) [244], and practically hydrolyzed PAAm [237] belong to the group of thermosensible hydrogels. Copolymerization is also an important aspect in this field because the transition temperature range can be modified by incorporating a more hydrophilic monomer to the hydrogel [127,245].

Quintana et al [246], study of hydrogels of NIPAAm copolymerized with IA as a possible drug-delivery system. In this investigation they have studied the mechanical properties of several poly(NIPAAm-co-IA) gels were synthesized with different compositions and crosslinking grades. Oscillatory shear measurements were carried out at two temperatures, 22°C and 37°C.

### 3. EXPERIMENTAL SECTION

#### 3.1. Materials

##### 3.1.1. N-isopropylacrylamide (NIPAAm)

NIPAAm was purchased from Aldrich Chemical Company Inc. The molecular weight is 113.16 g/mol and it was used without any purification.

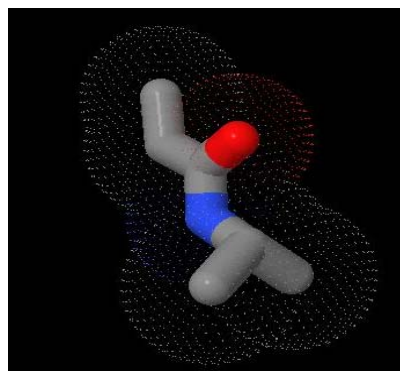
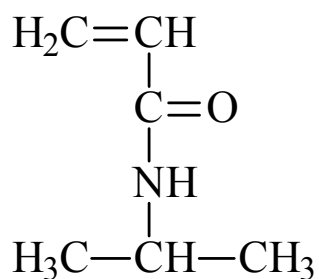


**Figure 3.1:** Structural Formula of N-isopropylacrylamide

##### 3.1.2. Itaconic acid (IA)

IA was purchased from Fluka. The molecular weight is 130.10 g/mol and it was used without any purification.

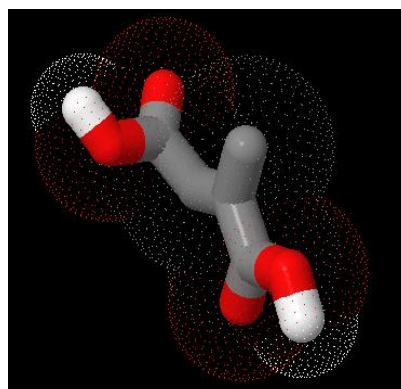
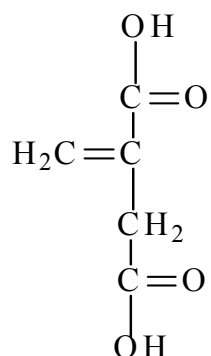


**Figure 3.2:** Structural Formula of Itaconic Acid



### 3.1.6. Azobis(isobutyronitrile) (AIBN)

AIBN (Merck A.G.) was recrystallized from chloroform then dried in vacuum oven at room temperature. It has a melting point of 102-104°C. Its molecular weight is 164 g/mol.

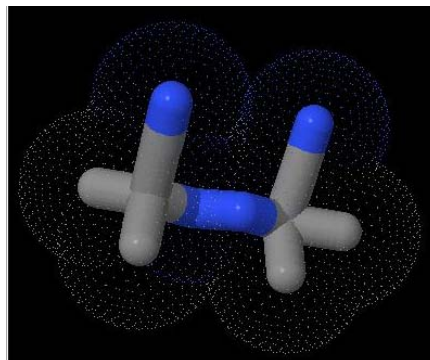
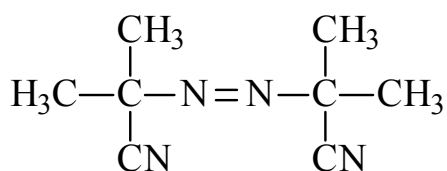


**Figure 3.5:** Structural Formula of Azobis(isobutyronitrile)

### 3.1.7. Dimethyl itaconate (DMI)

DMI was purchased from Fluka. The molecular weight is 158.16 g/mol and it was used without any purification.

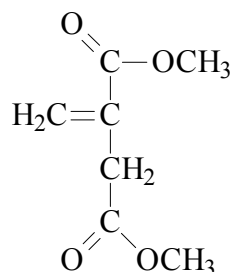


**Figure 3.6:** Structural Formula of Dimethyl Itaconate

### 3.1.8. $\alpha,\omega$ -acryloxyorganofunctional poly(dimethylsiloxane) vinyl terminated PDMS (VTPDMS)

VTPDMS-V-Si-2150 was used as a hydrophobic macrocrosslinker. It was the product of Gold Schmidt Chemical Corporation. Tegomer V-Si 2150, its molecular weight is 1000 gr/mol, ( $n \sim 10$ ,  $5 < m < 10$ ). It was dried at 30°C in vacuum for >48 h before use.

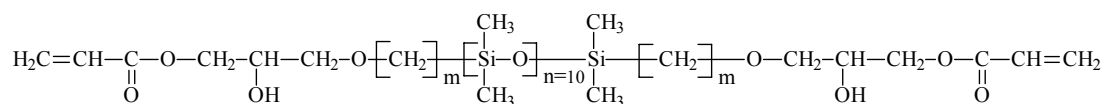


**Figure 3.7:** Structural Formula of  $\alpha,\omega$ -acryloxyorganofunctional Poly(dimethylsiloxane)

### 3.1.9. $\alpha,\omega$ -acryloxyorganofunctional poly(dimethylsiloxane) vinyl terminated PDMS (VTPDMS)

VTPDMS-V-Si-2250 was used as a hydrophobic macrocrosslinker. agent. It was the product of Gold Schmidt Chemical Corporation. Tegomer V-Si 2250, its molecular weight is 2000 gr/mol, ( $n\sim 20$ ,  $5 < m < 10$ ). It was dried at  $30^\circ\text{C}$  in vacuum for  $>48$  h before use.

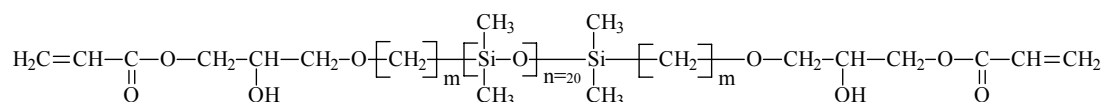


**Figure 3.8:** Structural Formula of  $\alpha,\omega$ -acryloxyorganofunctional Poly(dimethylsiloxane)

### 3.1.10. Acetyl chloride (AcCl)

AcCl was purchased from Merck A.G. and used without any purification. Its molecular weight is 82.5 g/mol

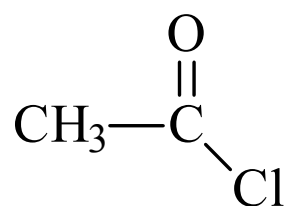


**Figure 3.9:** Structural Formula of Acetyl Chloride

### 3.1.11. Theophylline (THP)

THP was purchased from Sigma, and used without any purification. Its molecular weight is 180.17 g/mol and melting point  $271^\circ\text{C}$ .

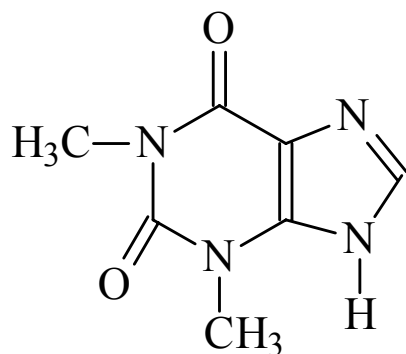


**Figure 3.10:** Structural Formula of Theophylline

### 3.1.12. Chloroform (CHCl<sub>3</sub>)

Chloroform was purchased from Merck A.G. The molecular weight is 119.38 g/mol, and it was used without any purification.

### 3.1.13. 1,4-Dioxane

1,4-Dioxane was purchased from Riedel-de Haen. The molecular weight is 88.11 g/mol, and it was used without any purification.

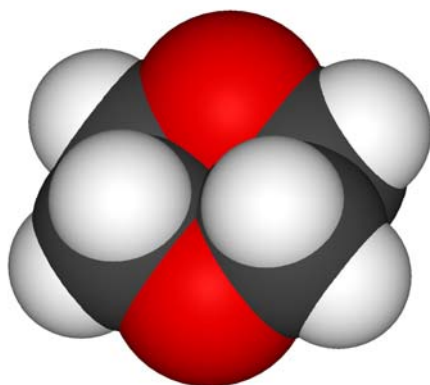


**Figure 3.11:** Structural Formula of 1,4-Dioxane

### 3.1.14. Benzene (C<sub>6</sub>H<sub>6</sub>)

Benzene was purchased from Merck A.G. The molecular weight is 78.11 g/mol, and it was used without any purification.

### 3.1.15. n-Heptane

n-Heptane was purchased from Merck A.G. The molecular weight is 100.21 g/mol, and it was used without any purification.

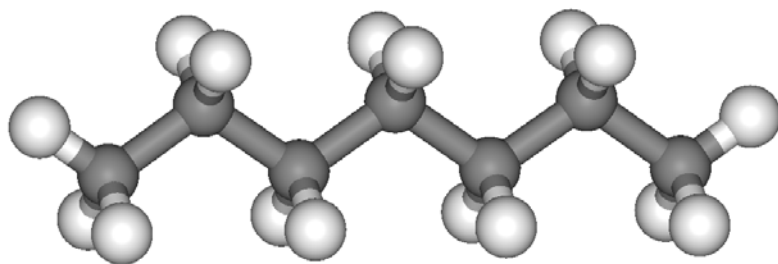


**Figure 3.12:** Structural Formula of n-Heptane

### 3.1.16. Methanol (MetOH)

Methanol was purchased from Merck A.G. The molecular weight is 32.04 g/mol, and it was used without any purification.

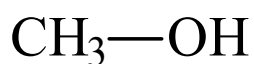


**Figure 3.13:** Structural Formula of Methanol

### 3.1.17. Octyl alcohol (C<sub>8</sub>H<sub>18</sub>O)

Octyl alcohol was purchased from Merck A.G. The molecular weight is 130.23 g/mol, and it was used without any purification.



**Figure 3.14:** Structural Formula of Octyl Alcohol

### 3.1.18. Cetyl alcohol (C<sub>16</sub>H<sub>34</sub>O)

Cetyl alcohol was purchased from Merck A.G. The molecular weight is 242.45 g/mol, and it was used without any purification.

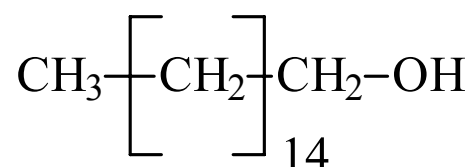


**Figure 3.15:** Structural Formula of Cetyl Alcohol

### 3.1.19. Butyl alcohol (C<sub>4</sub>H<sub>10</sub>O)

Butyl alcohol was purchased from Fluka. The molecular weight is 74.12 g/mol, and it was used without any purification.



**Figure 3.16:** Structural Formula of Butyl Alcohol

### 3.1.20. Sodium chloride (NaCl)

NaCl was purchased from Merck A.G. The molecular weight is 58.44 g/mol, the purity 99.5 % and it was used without any purification.

### 3.1.21. Potassium chloride (KCl)

KCl was purchased from Riedel-de Haen. The molecular weight is 74.55 g/mol, and it was used without any purification.

### 3.1.22. Potassium dihydrogen phosphate (KH<sub>2</sub>PO<sub>4</sub>)

KH<sub>2</sub>PO<sub>4</sub> was purchased from Riedel-de Haen. The molecular weight is 136.09 g/mol, and it was used without any purification.

### 3.1.23. Disodium hydrogen phosphate (Na<sub>2</sub>HPO<sub>4</sub>)

Na<sub>2</sub>HPO<sub>4</sub> was purchased from Merck A.G. The molecular weight is 177.97 g/mol, and it was used without any purification.

### 3.1.24. Citric acid monohydrate (C<sub>6</sub>H<sub>8</sub>O<sub>7</sub>·H<sub>2</sub>O)

C<sub>6</sub>H<sub>8</sub>O<sub>7</sub>·H<sub>2</sub>O was purchased from Fluka. The molecular weight is 210.14 g/mol, and it was used without any purification.

### 3.1.25. Phosphoric acid (H<sub>3</sub>PO<sub>4</sub>)

H<sub>3</sub>PO<sub>4</sub> was purchased from Riedel-de Haen. The purity 85%, and it was used without any purification.

### 3.1.26. Boric acid (H<sub>3</sub>BO<sub>3</sub>)

H<sub>3</sub>BO<sub>3</sub> was purchased from Fluka. The molecular weight is 61.83 g/mol, and it was used without any purification.

### **3.1.27. Sodium hydroxide (NaOH)**

NaOH was purchased from Carlo Erba. The molecular weight is 39.997 g/mol, and it was used without any purification.

### **3.1.28. Hydrochloric acid (HCl)**

HCl was purchased from Merck A.G. The purity 37 %, melting point 271°C, and it was used without any purification.

### **3.1.29. Distilled-deionized water (DDW)**

Distilled-deionized water was supplied from Analytical Chemistry Lab. with.

### **3.1.30. Phosphate buffer (PBS)**

Isotonic saline solution was prepared dissolving hydrogen (0.92 g of Na<sub>2</sub>HPO<sub>4</sub>) and dihydrogen phosphates (0.2 g of KH<sub>2</sub>PO<sub>4</sub>), and potassium (0.2 g of KCl) and sodium chloride (5.85 g of NaCl) salts. Final volume was brought up to one liter with deionized water. pH of the buffer solution was adjusted to 7.5 with 0.1 N of HCl.

### **3.1.31. Citrate buffer (CB)**

Citrate buffer solutions were prepared according to following recipe; 7.0 g of citric acid monohydrate, 3.83 g of phosphoric acid (85% wt solution) and 3.54 g of boric acid, were dissolved in 343.0 mL of NaOH (1.0 M) solution, and deionized water were added up to 1 liter. In order to adjust pH of the citrate buffer solution a set of HCl solutions (0.1 N, 0.5 N, and 1.0 N) were prepared and using these solutions pH values of the citrate buffer solutions adjusted to pH of 2.0, 4.0, 6.0, 8.0, 10.0 and 12.0. Adding 5.85 g of NaCl can finely do ionic strength adjustment to 0.1M.

## **3.2. Experimental Set-up and Equipment**

### **3.2.1. Thermostated water bath**

A thermostated water bath was used for providing a constant temperature during the gel preparations and LCST measurements.

### **3.2.2. Vacuum oven**

A vacuum oven (BINDER model) was used for removal of solvents from hydrogel and linear polymer samples. It includes a digital temperature control system and manometer. A pump (KNF model) is used to provide vacuum.

### **3.2.3. Oven**

An oven (BINDER) includes a digital temperature control system.

### **3.2.4. Digital compass**

The diameters of the cylindrical gel samples were measured using a calibrated digital compass. (Metr ISO) The device had a measuring range between 0-150 mm with an accuracy of  $\pm 0.02$  mm.

### **3.2.5. Tubes**

Internal diameter and heights of glass were used in the gelation experiments were 2.5-3.5 mm (and 10.5-11.5 mm) and 10.0 cm, respectively.

### **3.2.6. FT-IR spectrophotometer**

FT-IR spectra of the samples were recorded on Perkin Elmer Spectrum One Model Spectrophotometer (FT-IR-reflectance, universal ATR with diamond and ZnSe), using the sample in the powder form.

### **3.2.7. UV-visible spectrophotometer**

The absorbance measurements of the linear (for LCST measurements) and crosslinked copolymer (for theophylline) samples were done at 400 nm and 500 nm for linear polymers, and 266 nm and 274 nm for hydrogels on a UV-visible recording spectrophotometer (Shimadzu UV-160 A), equipped with a temperature controlled cell.

### 3.2.8. Compressive testing



**Figure 3.17:** Photograph of Compressive Testing Machine

Compressive experiments were performed on the Hounsfield HK5-S Model tensile testing machine, equipped with uniaxial compression chin. Before the compression measurements, the gel samples were maintained in DDW at 23°C and 37°C to achieve swelling equilibria. Motion was set for compression at a speed of 1.00 cm/s, a distance for 10.00 mm. The units for force and displacement were measured in N and mm, respectively.

### 3.2.9. Conductometer and pH-meter

WTW-LF 2000 model conductometer and WTW 523 model pH meter were used for the conductivity and pH-value measurements.

### 3.2.10. Differential scanning calorimetry (DSC)

The DSC measurements were performed on a Metler Toledo DSC 821 under nitrogen atmosphere with a flow rate 30 ml/min. and heating rate of 10°C/min. The temperature range exported from 40–150°C.

### 3.2.11. Gel permeation chromatography (GPC)

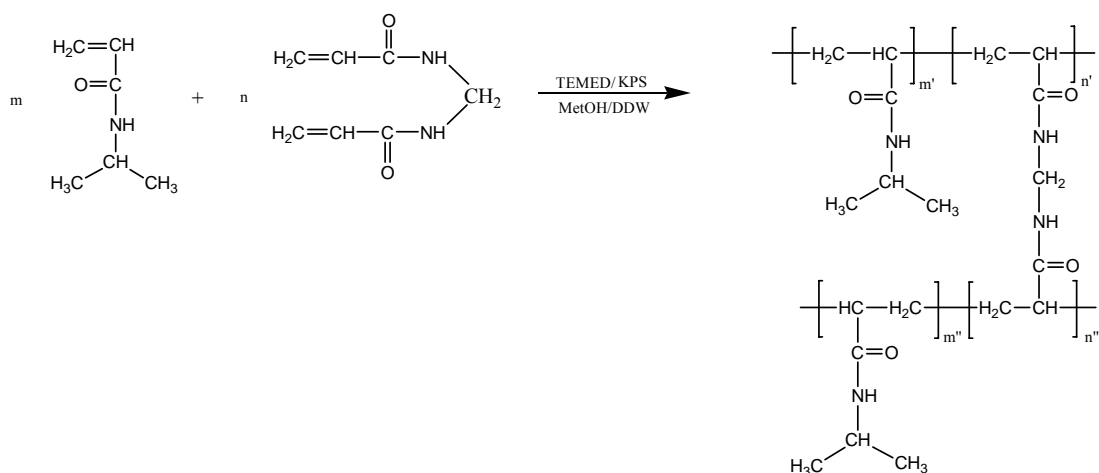
GPC analyses were carried out with a set up consisting of the Agilent pump and refractive-index detector (Model 1100) and four Waters Styragel Columns (HR 5E, HR 4E, HR 3, and HR2). THF was used as the eluent at a flow rate of 0.3 ml/min at 30°C. The molecular weights of the polymers were calculated with the aid of methylmethacrylate standards.

### 3.3. Synthesis and Characterization of Crosslinked and Linear PNIPAAm

#### 3.3.1. Synthesis of PNIPAAm hydrogels crosslinked with VTPDMS

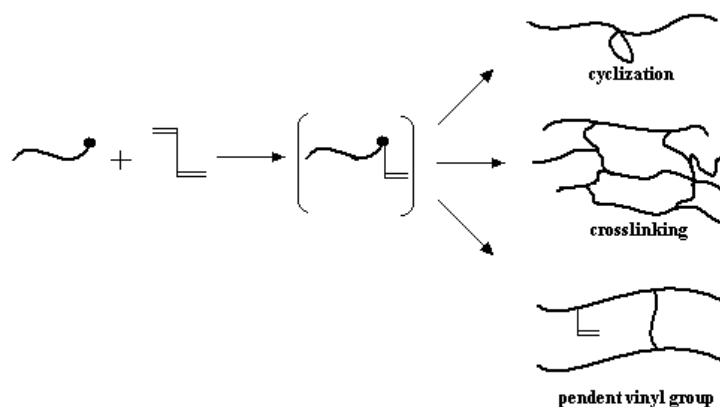
Hydrophobic/hydrophilic monomer (NIPAAm, 0.7 and 2.0 mol/L), hydrophilic and weakly acidic comonomer (IA,  $pK_1 = 3.85$  and  $pK_2 = 5.45$ ), hydrophobic macrocrosslinkers (vinyl terminated PDMS (VTPDMS); Tegomer V-Si 2250 ( $n \sim 20$ ,  $5 < m < 10$ ) and Tegomer V-Si 2150 ( $n \sim 10$ ,  $5 < m < 10$ )), hydrophilic crosslinker (BIS), were used without any purification. TEMED and KPS were used as activator (or cointiator) and initiator, respectively, for the polymerizations in DDW and DDW/MetOH mixture. AIBN was chosen as initiator for the crosslinking reactions in 1,4-dioxane.

Three types of NIPAAm gels were prepared: **(1)** The networks made of neutral NIPAAm chains and crosslinked with hydrophilic tetrafunctional constituent (BIS); **(2)** the neutral NIPAAm hydrogels containing hydrophobic and tetra functional macrocrosslinker (VTPDMS); **(3)** negatively ionizable hydrogels containing 1.0-7.5 mol % of IA with respect to total principal monomer, i.e., NIPAAm.



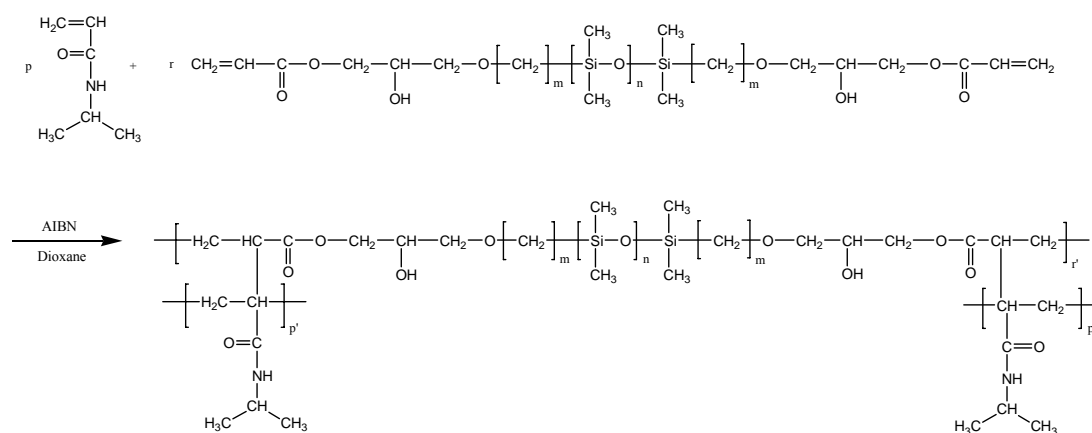
**Scheme 3.1a.** Polymerization Reaction of Neutral NIPAAm Hydrogel.

**(1)** The gelation solutions containing NIPAAm (0.7 and 2.0 mol/L), BIS ( $1.25 \times 10^{-2}$  and  $2.50 \times 10^{-2}$  mol/L) and KPS/TEMED ( $1.50 \times 10^{-2}$  mol/L, for each constituent of redox initiator pair) were prepared using a 40/60 mixture of DDW/MetOH (v/v %) as a polymerization solvent. The pre-gel solutions introduced into glass tubes of  $\sim 10$  mm inner diameter were placed vertically in a large glass tube that was closed tightly with a rubber cap, and then filled oxygen-free nitrogen by using a syringe, and placed in a thermostat at  $25^\circ\text{C}$  for 72h (Scheme 3.1a).



**Scheme 3.1b.** Possible Reactions of a Pendant Vinyl Group in Free Radical Crosslinking Polymerization

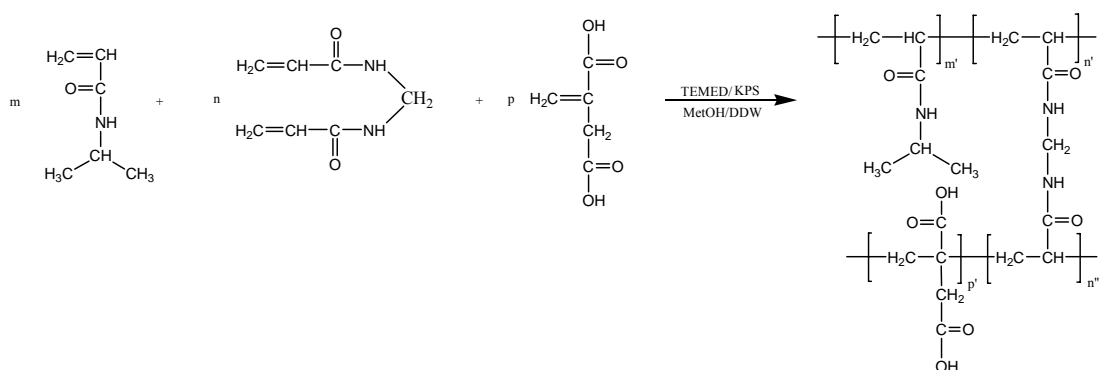
The free radical solution copolymerization of a monomer containing one polymerizable double bond with a crosslinking agent having at least two polymerizable double bonds is the most frequently used technique for hydrogel synthesis. After the crosslinking agent is incorporated into the growing polymer chain by one double bond, the pendant vinyl group may react in at least three ways (Scheme 3.1b): (a) react with another growing polymer chain, resulting in the formation of a crosslink; (b) react with the radical on the same macromolecule, forming a short cycle; or (c) remain unreacted. The structure of the crosslinking agent, e.g., the number of atoms separating the double bonds and conditions of copolymerization, e.g., amount of solvent during copolymerization, influence the extents of double bonds reacting with the same polymer chain (cyclization).



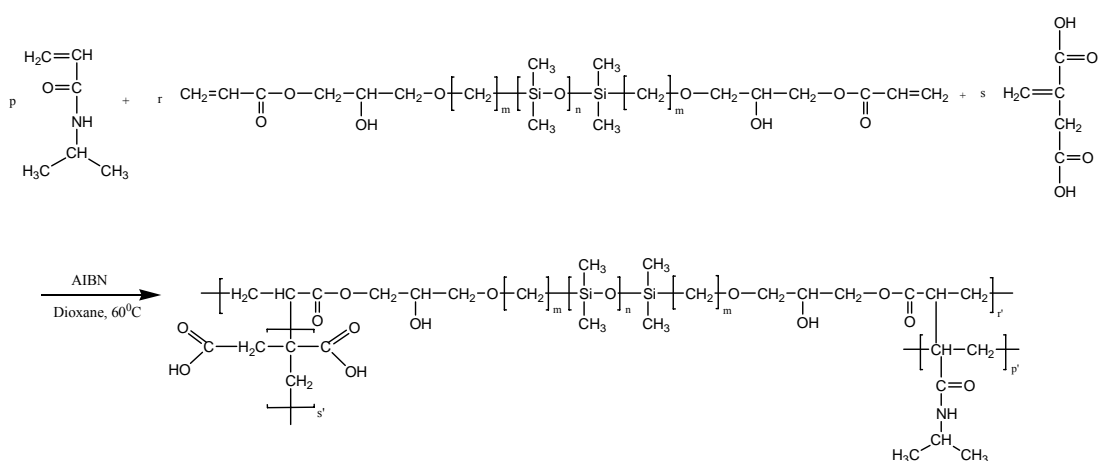
**Scheme 3.2.** Schematic Representation of the Polymerization of PNIPAAm Hydrogel Crosslinked with PTPDMS.

(2) The gels were prepared by free radical crosslinking polymerizations at 60°C under nitrogen atmosphere for 72 h. Monomer (2.0 mol/L), VTPDMS ( $1.25 \times 10^{-2}$  and  $2.50 \times 10^{-2}$  mol/L) and AIBN ( $5.8 \times 10^{-3}$  mol/L) were dissolved in 1,4-dioxane. The polymerization mixtures loaded in test tubes with ~10 mm diameter were inserted into large glass tubes equipped with a rubber cap and a syringe (Scheme 3.2).

(3) IA (1.0, 2.5, 5.0 and 7.5 mol % of total NIPAAm concentration (0.7 mol/L and 2.0 mol/L) was added into the pre-gel solutions of Type (1) and Type (2), and they were gelled in the same manner used for (1) and (2) (Scheme 3.3 and Scheme 3.4).



**Scheme 3.3.** Schematic Representation of the Polymerization of P(NIPAAm-co-IA) Hydrogel Crosslinked with BIS.



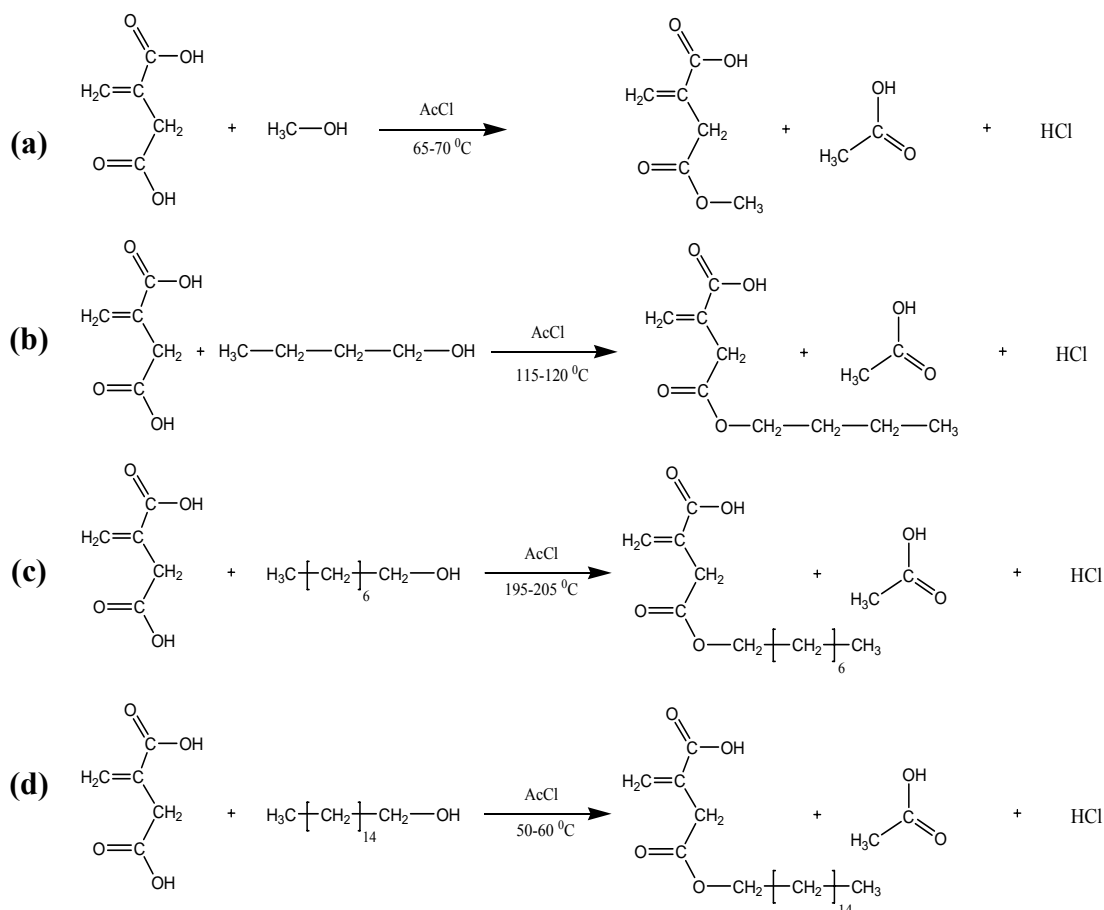
**Scheme 3.4.** Schematic Representation of the Polymerization of P(NIPAAm-co-IA) Hydrogel Crosslinked with VTPDMS.

After the reaction periods needed to complete gelation processes, each test tube was broken and the hydrogels were immersed in DDW for Types (1) and (3), and in 1,4-dioxane for Types (2) and (3) to remove linear polymer chains and unreacted constituents. Type (1) and Type (2) include neutral NIPAAm hydrogels crosslinked with BIS (hydrophilic crosslinker) and VTPDMS (hydrophobic macrocrosslinker), respectively. However, Type (3) represents ionic NIPAAm hydrogels. The difference in the washing process of resulting gels is due to hydrophobic (VTPDMS) and hydrophilic (BIS) nature of the crosslinkers. For BIS-crosslinked samples (Samples HB14 – HB17, Type 3), ionic NIPAAm hydrogels were immersed in an excess amount of deionized water while for VTPDMS-crosslinked samples (Samples HV3 – HV9 Type 3), ionic NIPAAm hydrogels were extracted with 1,4-dioxane to remove uncrosslinked water-insoluble compound, i.e., VTPDMS. A final wash of all samples was with deionized water for 1 week.

### **3.3.2. Synthesis of monoesters of itaconic acid**

1 mole of itaconic acid and 3-4 mol of alcohol was added acetyl chloride as a catalyst, with shaking. The mixture was refluxed on the steam-bath for 20-180 minutes, solution taking place at the boiling point. The excess alcohol was immediately evaporated in vacuum. The residue was recrystallized and chilling to 0°C and the products were dried in vacuum [247-249]. Their melting points and yields (%) were determined using Electrothermal model machine, and by gravimetrically, respectively. Table 3.1 summarizes the synthesis conditions, melting points and yields of monoesters of IA. Scheme 3.5 illustration of the synthesis procedure of monoitaconates.

The synthesized the monoitaconates, i.e. monoesters of IA were used as hydrophilic/hydrophobic comonomers for both linear and crosslinked NIPAAm copolymers.



**Scheme 3.5.** Chemical Structures and Reaction Mechanisms of Monoitaconates.  
 (a) MMI, (b) MBuI, (c) MOcI, (d) MCEI

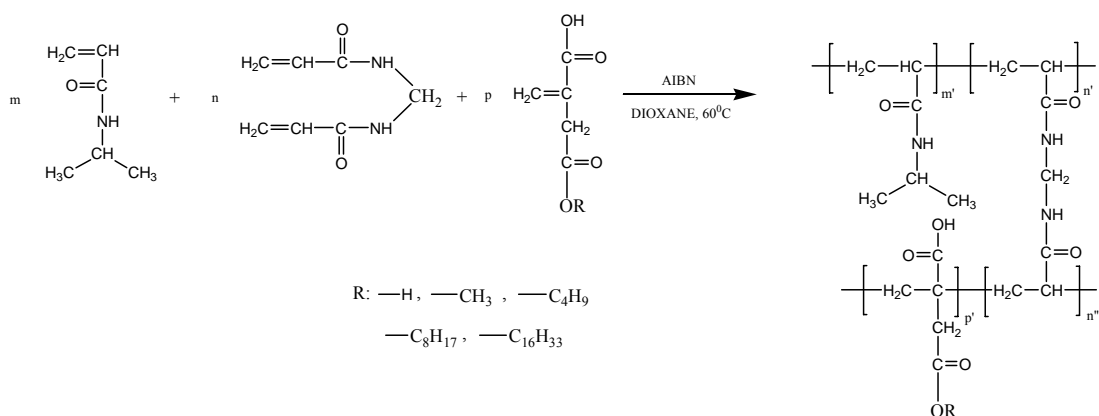
**Table 3.1 :** Synthesis Conditions, Melting Points and Yields of Monoitaconates.

	Reaction time (min)	Recrys.	Melting point (°C)		Yield (%)		MW (gr/mol)
			Litature	This work	Litature	This work	
MMI	20	B/H	66-68 <sup>(a)</sup>	67-70	84 <sup>(a)</sup>	86	144
MBuI	20	B/H	40 <sup>(b)</sup>	37-38	-	84	286
MCEI	150	M	-	43-44	-	55	354
MOcI	120	M	55-56 <sup>(c)</sup>	54-56	35 <sup>(c)</sup>	34	242

**B:** Benzene, **M:** Methanol, **H:** n-Heptane

<sup>(a)</sup>: Reference [272], <sup>(b)</sup>: Reference [273], <sup>(c)</sup>: Reference [274],





**Scheme 3.7.** Schematic Representation of the Polymerizations of P(NIPAAm-co-IA), P(NIPAAm-co-MBuI), P(NIPAAm-co-MOCl) and P(NIPAAm-co-MCeI) Hydrogels.

(3) NIPAAm (2.0 mol/L), MOCl (2.5 and 5.0, mol %), BIS ( $2.50 \times 10^{-2}$  and  $3.75 \times 10^{-2}$  mol/L) and TEMED ( $1.39 \times 10^{-2}$  mol/L), all of these reagents were dissolved in 3.0 mL of MetOH. An initiator solution was also prepared by dissolving KPS ( $1.5 \times 10^{-2}$  mol/L) in 2.0 ml of DDW. The KPS solution was added to the monomer solution; immediately after complete mixing, the pregel solution was transferred into a test tube, which had been inserted into a large glass tube that was closed tightly with a rubber cap, and then filled oxygen-free nitrogen by using a syringe, and placed in a thermostat at 25°C for 72h.

To obtain perfect network structures, the gels were left in the tubes for 72 h. After this reaction period, the gels were taken out of the tubes and immersed in MetOH, MetOH/DDW mixture, DDW and 1,4-dioxane (depending on the composition of polymerization solutions) to remove unreacted molecules.

### 3.3.4. Synthesis of linear PNIPAAm, its copolymers and terpolymers with itaconic acid, its monoitaconates and dimethyl itaconate

PNIPAAm, poly(dimethyl itaconate) (PDMI), copolymers of NIPAAm with IA, DMI, MMI, MBuI, MOCl and MCeI and terpolymers with IA and DMI were obtained by free radical solution polymerization using AIBN and KPS/TEMED redox pair, as initiators in 1,4-Dioxane and in MetOH/DDW mixture (MetOH/DDW: 60/40, v/v %), respectively, with total monomer concentrations of 0.7 mol/L. The reaction mixtures were purged with nitrogen for 10 min and then allowed to react in an air oven at 25°C and 60°C (in DDW and in 1,4-Dioxane, respectively) for 72 h

under nitrogen. The polymers were precipitated in n-hexane (or water). To purify the solid products, they were dissolved in cold water and then collapsed by heating.

Synthesis procedures of homopolymers, copolymers and terpolymers are classified as follows:

- (1) PNIPAAm, KPS ( $1.5 \times 10^{-2}$  mol/L) in MetOH/DDW mixture (60/40, v/v %)
- (2) PNIPAAm, AIBN ( $5.0 \times 10^{-3}$  mol/L) in 1,4-dioxane
- (3) PDMI, KPS ( $1.5 \times 10^{-2}$  mol/L) in MetOH/DDW mixture (60/40, v/v %)
- (4) PDMI, AIBN ( $5.0 \times 10^{-3}$  mol/L) in 1,4-dioxane,
- (5) NIPAAm with IA (1.0, 2.5, 5.0, 7.5, 10.0 mole % of IA in the feed), (TEMED/KPS ( $1.39 \times 10^{-3}$  mol/L /  $1.5 \times 10^{-2}$  mol/L) in MetOH/DDW mixture (60/40, v/v %) and AIBN ( $5.0 \times 10^{-3}$  mol/L) in 1,4-dioxane,
- (6) NIPAAm with DMI (5.0, 10.0 mole % of DMI in the feed), TEMED/KPS ( $1.39 \times 10^{-3}$  mol/L /  $1.5 \times 10^{-2}$  mol/L) in MetOH/DDW mixture (60/40, v/v %), and AIBN ( $5.0 \times 10^{-3}$  mol/L) in 1,4-dioxane,
- (7) NIPAAm with MMI (10.0 mole % of MMI in the feed), (TEMED/KPS ( $1.39 \times 10^{-3}$  mol/L /  $1.5 \times 10^{-2}$  mol/L) in MetOH/DDW mixture (60/40, v/v %), and AIBN ( $5.0 \times 10^{-3}$  mol/L) in 1,4-dioxane,
- (8) NIPAAm with MBuI (10.0 mole % of MBuI in the feed), (TEMED/KPS ( $1.39 \times 10^{-3}$  mol/L /  $1.5 \times 10^{-2}$  mol /L) in MetOH/DDW mixture (60/40, v/v %), and AIBN ( $5.0 \times 10^{-3}$  mol /L) in 1,4-dioxane,
- (9) NIPAAm with MOcI (1.0, 2.5, 5.0 mole % of MOcI in the feed), AIBN ( $5.0 \times 10^{-3}$  mol/L) in 1,4-dioxane,
- (10) NIPAAm with MCeI (1.0 mole % of MCeI in the feed), AIBN ( $5.0 \times 10^{-3}$  mol/L) in 1,4-dioxane,
- (11) NIPAAm/IA/DMI terpolymers (9.0 mole % of IA and 1.0 mole % DMI, 7.5 mole % of IA and 2.5 mole % DMI, 5.0 mole % of IA and 5.0 mole % DMI, 2.5 mole % of IA and 7.5 mole % DMI, 1.0 mole % of IA and 9.0 mole % DMI, in the feed) initiated with AIBN ( $5 \times 10^{-3}$  mol/L) in 1,4-dioxane.

### **3.4. Drug Loading and Release**

#### **3.4.1. Standard absorbance curve**

The standard calibration curve of the absorbance as a function of the Theophylline concentration was studied at 266 nm on the UV spectrophotometer [275].

#### **3.4.2. Drug loading and drug delivery system (DDS) preparation**

The swollen PNIPAAm and its copolymer hydrogels samples crosslinked with BIS and VTPDMS were dried in vacuum overnight until its weight remained unchanged. The vacuum dried PNIPAAm hydrogels were immersed in the 0.1 and 0.3 wt. % of Theophylline in the PBS (pH=7.5) solution at 25°C for 96 h to reach the equilibrated state. During this period, the drug diffused into the hydrogel network along with the PBS. Then, drug-loaded hydrogels were dried in vacuum until its weight remained unchanged for to measure the loading capacity of drug (in mg) in the gel and then this dried drug-loaded hydrogel used for drug release study.

#### **3.4.3. Drug release study**

Dried PNIPAAm and its copolymer hydrogels samples crosslinked with BIS and VTPDMS were cut into small pieces, being approximately was 0.0200 – 0.0300 g. The hydrogels were equilibrated at 21°C for 4 days in excess PBS solutions containing a proper amount of Theophylline (pH=7.5). Two different concentrations of Theophylline in PBS were used: 0.1 and 0.3 wt %. The hydrogels loaded with Theophylline were placed in quartz cells containing 4 mL of PBS solutions. The release amount of drugs was measured from the changes in the absorbance values at 266 nm by means of a UV spectrophotometer (Shimadzu UV-160 A). The release experiments were carried out at 37°C. The measurements were conducted as a function of time, and the results are given in relative units  $M_t/M_p$  and  $M_t/M_\infty$ , where  $M_t$  is the instantaneous mass of the drug released at time  $t$ ,  $M_p$  is the mass of the dry hydrogel, and  $M_\infty$  is the total mass of drug released at equilibrium.

### 3.5. Characterization methods

#### 3.5.1. Measurements of gel diameter

The hydrogel samples obtained were inserted into the DDW. During the measurements, the temperature was controlled by circulating thermostatted water through the water-jacket around the cell. The gel diameter was determined as a function of temperature by using a digital compass. The accuracy of the gel diameter was within 3 %. In addition, each swelling ratio in this work is an average of two separate swelling measurements performed in parallel. After equilibration at one temperature, the gel diameter  $d$  was measured and the volume  $V_s$  was estimated by cubing the diameter, and then the sample was re-equilibrated at another temperature.

#### 3.5.2. Gravimetric and volumetric measurement

The volume swelling ratio, defined as the reciprocal of polymer volume fraction was calculated gravimetrically using the following equations:

$$\frac{1}{v_{2s}} = 1 + \left[ \frac{w_1 \rho_2}{w_2 \rho_1} \right] \quad (3,1)$$

$$\frac{1}{v_{2r}} = 1 + \left[ \frac{w_1 \rho_2}{w_2 \rho_1} \right] \quad (3,2)$$

where  $w_2$  and  $w_1$  are the weight of the dried gel sample and the solvent absorbed by the sample during the swelling (or gelation) processes, respectively. Subscripts **s** and **r** signify swelled and relaxed states (corresponding to gelation) of hydrogels, respectively.  $\rho_1$  and  $\rho_2$  define the densities of the solvent used for swelling (or gelation) experiments and the dried hydrogel, respectively. The densities of all dried polymers prepared in this work were taken as  $1.1 \times 10^3 \text{ kg/m}^3$ .

The gravimetric measurements were also used to calculate the volumetric compositions of the hydrogels. Assuming that the gels swell isotropically and dividing equation (3,1) into equation (3,2)

$$\frac{V_s}{V_r} = \frac{v_{2r}}{v_{2s}} = \left( \frac{d}{d_0} \right)^3 \quad (3,3)$$

Here,  $V_s$  and  $V_r$  are the hydrogel sample volumes after and before equilibrium swelling, respectively.  $d$  and  $d_0$  indicate the equilibrium and original diameters of the hydrogels.

### 3.5.3. Compression-strain measurements

In order to characterize the network structure of the hydrogels, uniaxial compression measurements were performed using a tensile testing system (Model H5K-S, Hounsfield). The cylindrical gels were cut in pieces, 1.0 cm (0.5 cm) in height. Before the compression measurements, the gel samples were maintained in DDW at 23°C and 37°C to achieve swelling equilibria. Hounsfield H5K-S model tensile testing machine, settled a crosshead speed of 1.0 cm/min and a load capacity of 5N was used to perform uniaxial compression experiments on the samples of each type of hydrogel.

The compression modulus of each network was determined from the slope of the linear portions of compression stress-strain curves, using the following equation:

$$\tau = \frac{F}{A_0} = G(\lambda - \lambda^{-2}) \quad (3,4)$$

Where,  $\tau$  is the applied force per unit area of the sample, i.e., pressure in Pa to compress the undeformed swollen specimen to the required relative deformation,  $\lambda$ . The effective crosslinking density,  $\nu_e$  was calculated from the compression modulus ( $G$ ), i.e., slope of the linear portion using the equation:

$$\nu_e = \frac{G}{(RT\nu_{2s}^{1/3}\nu_{2r}^{2/3})} \quad (3,5)$$

where  $\nu_{2s}$  and  $\nu_{2r}$  are the polymer volume fractions in the equilibrium-swollen system and in the relaxed state, i.e., just after polymerization completed, but before swelling.

From the values of  $\nu_e$ ,  $\nu_{2r}$ ,  $\nu_{2s}$  and  $\rho_2$  the polymer-solvent interaction parameter,  $\chi$  and average molecular weight between crosslinking points,  $M_c$  can be calculated via equation (3,6) and equation (3,7).

$$\chi = - \frac{\left[ \ln(1 - \nu_{2s}) + \nu_{2s} + \nu_e V_1 \nu_{2r} \left\{ \left( \frac{\nu_{2s}}{\nu_{2r}} \right)^{1/3} - \left( \frac{\nu_{2s}}{\nu_{2r}} \right) \left( \frac{1}{2} \right) \right\} \right]}{\nu_{2s}^2} \quad (3,6)$$

$$M_c = \frac{\rho_2}{\nu_e} \quad (3,7)$$

where  $V_1$  is the molar volume of the solvent. These equations derived by using the phantom network model are valid for neutral networks in the highly swollen state.

#### 3.5.4. Measurement of swelling kinetics

Dynamic swelling studies were undertaken to elucidate the mechanism of water and drug diffusion into the hydrogel samples as determined by the dynamic portion of the gravimetric curve. The sample were dried at room temperature in air initially and then under vacuum. Dried gels were left to swell in DDW ( $23 \pm 0.1^\circ\text{C}$ ) in a thermostated water bath. To obtain the mass swelling data of the gels, the samples were removed from the water bath at various time intervals and dried with filter paper for the removal of excess water on hydrogel surface, then weighed, and placed were in the same bath. The mass swelling percentages [**S% (m)**] for water diffusion and drug loading experiments were calculated from the following relation:

$$S\% = \left[ \frac{(m_t - m_0)}{m_0} \right] \times 100 \quad (3,8)$$

where  $m_0$  is the mass of the dry gel at the beginning ( $t=0$ ), and  $m_t$  is the mass of the swollen gel at time  $t$ . The swelling rate constants of the hydrogels were calculated from the following relation [276]:

Percentage mass swelling

$$[\mathbf{S\% (m)}] = k_{sr}t \quad (3,9)$$

where  $k_{sr}$  is the swelling rate constant.

Water transport in polymer networks, i.e., swelling-time curves may be described by the following equation [277]:

$$M_t / M_\infty = kt^n \quad (3,10)$$

In this expression,  $k$  is proportionality constant related to the structure of the network,  $n$  is a diffusion exponent;  $M_t$  and  $M_\infty$  are the amounts of water absorbed at time  $t$  and at equilibrium, respectively. This equation was applied to the first 60 % of the total amount of absorbed water.

Drug diffusion in the hydrogel kinetics was also evaluated using the same equation (3,10) [278]:

$$F = \frac{M_t}{M_\infty} = kt^n \quad (3,11)$$

Here,  $F$  is the fractional uptake,  $M_t / M_\infty$  where  $M_t$  is the amount of drug uptake at time  $t$ ,  $M_\infty$  is the maximum amount absorbed drug,  $k$  is a constant incorporating characteristic of hydrogel-drug system,  $n$  is the diffusional exponent, which is indicative of the transport mechanism.

### 3.5.5. Measurement of deswelling kinetics

The kinetics of deswelling behavior of the hydrogels was measured at 37°C. Before the measurement of deswelling kinetics, the hydrogels were reached to swollen equilibria in DDW at 23°C in advance. After wiping off water on the surfaces with filter paper, the weights of the gels were recorded during the course of deswelling at each regular time interval. The deswelling ratio (**DSR**) (%) is defined as following equation (3.12) [279]:

$$DSR(\%) = \left[ \frac{m_t - m_0}{m_{t,eq} - m_0} \right] \times 100 \quad (3.12)$$

where  $m_0$  is the mass of the dry gel at the beginning ( $t=0$ ),  $m_t$  is the mass of the shrunken gel at time  $t$  ( $T = 37^\circ\text{C}$ ),  $m_{t,eq}$  is the mass of the swollen gel at equilibria ( $T = 23^\circ\text{C}$ ).

### **3.5.6. Determination of monoitaconate content in linear NIPAAm copolymers**

Acidic comonomer contents of NIPAAm copolymers were determined by conductometric titration method. WTW-LF 2000 model conductometer was used for the conductivity and pH value measurements. The conductometric titrations were carried out in a glass cell kept at constant temperature of 25°C. For each titration experiment, the cell was filled with 10.0 ml 0.1 N NaOH solution in which 0.5 g of solid NIPAAm copolymer was dispersed by magnetic stirring. After the NIPAAm copolymer completely dissolved, the solution was titrated with 0.1N HCl, which was added from a microburette. Acidic comonomer content in polymers, i.e. copolymer composition was calculated from the inflection points.

### **3.5.7. Cloud point measurements**

The solutions of the PNIPAAm, its copolymers and terpolymers (2 g/L) were prepared in citrate buffer (CB) at pH 4 and in phosphate buffered saline (PBS) at pH 7.4 while the pHs of the polymer solutions prepared in DDW were adjusted with NaOH and HCl standard solutions. Absorbance measurements were done at 400 nm on a UV-visible recording spectrophotometer (Shimadzu UV-160A), equipped with a temperature-controlled cell.

Cloud points were taken as the initial break points in the resulting absorbance versus temperature curves. Furthermore, the cloud points, i.e., LCSTs of the polymer solutions in the range of pH 1-7 were determined visually by noting the temperature at which turbidity first appears upon slowly heating the aqueous solution by a water bath.

## 4. RESULTS AND DISCUSSION

### 4.1. Compressive Elastic Moduli of Poly(NIPAAm) Hydrogels Crosslinked with VTPDMS

In this part of this thesis, hydrogels composed of NIPAAm, BIS, VTPDMS and IA as hydrophobic monomer, hydrophilic crosslinker, hydrophobic crosslinker and weakly ionizable comonomer, respectively, were prepared to investigate the effect of hydrophobic component, i.e., VTPDMS on the compression moduli of the samples attained equilibrium swollen state in DDW at 25°C. For mechanical strength analysis, conventional rubber elasticity and swelling theories for networks formed in the presence of diluents were adopted. The second one deals with neutral polymer chains. From the swelling and compression measurements, effective crosslinking density  $\nu_e$ , average molecular weight between crosslinks  $M_c$  and polymer-water interaction parameter  $\chi$ , which can be used to characterize the structures of the hydrogels, were calculated.

In general, heterogeneous NIPAAm hydrogels are obtained by conventional method in water above the LCST. The inhomogeneity, being considered as a factor decreasing mechanical strength, may be optimized or removed by the choice of synthesis method, comonomer and crosslinker structure [64,152,259,272,273]. In the present study, it has been observed that the mechanical performance of NIPAAm hydrogels could be improved by using hydrophobic macrocrosslinker, i.e., VTPDMS with two different molecular weights. These commercial products were composed of soft and hydrophobic segments of dimethylsiloxane ( $n \sim 10$  and  $n \sim 20$  for V-Si 2150 and 2250, respectively) and  $-\text{CH}_2$  units ( $5 < m < 10$ ).

Compression moduli of neutral and ionic NIPAAm hydrogels crosslinked with BIS and VTPDMS equilibrated in water at 25°C were determined by means of a Hounsfield H5K-S model tensile testing machine. Any loss of water and changing in temperature during the measurements was not observed because of the compression period being less than 1 min. Figures 4.1 and 4.2 show a comparison of the behaviors

**Table 4.1** : Polymerization Conditions, Polymer Volume Fractions ( $v_{2r}$ ,  $v_{2s}$ ), Compression Moduli (G) and Polymer-water Interaction Parameters ( $\chi$ ) at Swelling Equilibria at 25°C for Neutral PNIPAAm Hydrogels Prepared in the Presence of Two Different Crosslinker

Sample No	Crosslinker ( $\times 10^{-2}$ mol/L)	Comonomer (mole %)	$v_{2s}$	$v_{2r}$	G (Pa)	$v_e$ (molm <sup>-3</sup> )	C.E	$\chi$	Mc (kg/mol)
HB9	BIS, 1.25	-	0.0221	0.0818	101	0.77	0.06	0.506	1429
HB10 <sup>a</sup>	BIS, 2.50	-	0.0361	0.0716	422	2.99	0.12	0.511	368
HB11 <sup>b</sup>	BIS, 2.50	-	0.0646	0.1729	7132	23.12	0.92	0.513	47.6
HB12 <sup>b</sup>	BIS, 1.25	-	0.0487	0.3102	3558	8.57	0.69	0.508	128.4
HB13 <sup>b</sup>	BIS, 1.25	-	0.0289	0.2532	755	2.48	0.19	0.504	444.3
HB14 <sup>a</sup>	BIS, 2.50	IA, 2.50	0.0154	0.2235	1858	8.17	0.33	-	134.6
HB15 <sup>a</sup>	BIS, 2.50	IA, 5.00	0.0028	0.0868	415	6.05	0.24	-	181.8
HB16 <sup>b</sup>	BIS, 1.25	IA, 2.50	0.0279	0.3089	2196	6.39	0.51	-	172.1
HB17 <sup>b</sup>	BIS, 2.50	IA, 2.50	0.0581	0.2170	9084	26.19	1.05	-	42.0
HP1 <sup>*</sup>	VTPDMS, 1.25	-	0.1935	0.2158	40115	77.77	6.22	0.571	14.1
HP2 <sup>■</sup>	VTPDMS, 1.25	-	0.1149	0.1976	12879	31.50	2.52	0.537	34.9
HP3 <sup>*</sup>	VTPDMS, 1.25	IA, 1.00	0.1385	0.2257	20946	44.05	3.52	-	24.9
HP4 <sup>*</sup>	VTPDMS, 1.25	IA, 2.50	0.1198	0.2686	10896	21.41	1.71	-	51.4
HP5 <sup>*</sup>	VTPDMS, 1.25	IA, 7.50	0.0904	0.3761	7482	12.90	1.03	-	85.3
HP6 <sup>*</sup>	VTPDMS, 2.50	IA, 7.50	0.2516	0.2068	65274	119.29	4.77	-	9.2
HP7 <sup>■</sup>	VTPDMS, 1.25	IA, 1.00	0.0659	0.2794	3969	9.27	0.74	-	118.7
HP8 <sup>■</sup>	VTPDMS, 1.25	IA, 2.50	0.0456	0.3895	1523	3.22	0.26	-	341.6
HP9 <sup>■</sup>	VTPDMS, 1.25	IA, 7.50	0.0108	0.3729	206	0.73	0.06	-	1517.2

<sup>a</sup> [NIPAAm]= 0.7 M, <sup>b</sup> [NIPAAm]= 2.0 M, C.E = Crosslinking efficiency ( $v_e/v_{e,t}$ ).  $v_{e,t}$  is taken as initial concentration of crosslinker

\*Tegomer V-Si 2250; M.W = 2000 gmol<sup>-1</sup>, ■Tegomer V-Si 2150; M.W = 1000 gmol

of neutral NIPAAm hydrogels crosslinked with BIS and VTPDMS, under uniaxial compression. Figures 4.3-4.5 show the measured force (F) for compressing samples (HB10 – HB13), (HP1, HP3-HP5), (HP2, HP7- HP9) at 25°C, respectively.

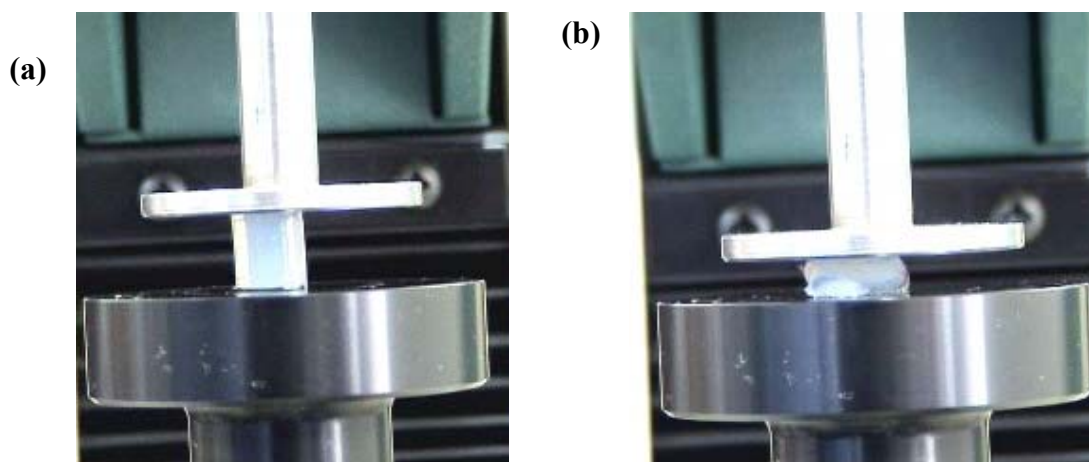


**Figure 4.1 :** Compression Process of Sample HB11 in Table 4.1: (a) Initial (F = 0.0 N) and (b) Final States (F = 5.0 N).

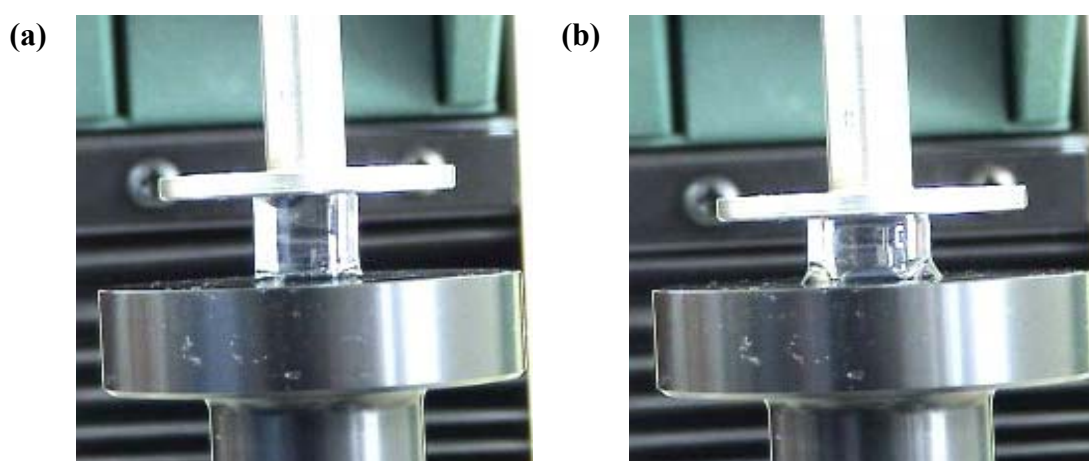


**Figure 4.2 :** Compression Process of Sample HP1 in Table 4.1: (a) Initial (F = 0.0 N) and (b) Final States (F = 5.0 N).

Forces (N) or loads corresponding to compressions (mm) were obtained from the original curves of uniaxial compression experiments. Figures 4.1(a) and 4.2(a) correspond to initial states, i.e., zero load and, Figures 4.1(b) and 4.2(b) point out the heights at 5.0 N, i.e., final states of the F (N) - compression (mm) curves of the samples HB11 and HP1 in Figures 4.2 and 4.3, respectively. Both the curves indicated above and the photographs corresponding to their behaviors during the compression processes show that the resistance to compression of the NIPAAm hydrogels crosslinked with VTPDMS is greater than the ones crosslinked with BIS in the range of 0.0–5.0 N. Pressure (Pa) – linear deformation factor  $(-\lambda - \lambda^2)$  plots of all samples were drawn by using the data obtained from the linear portions of F(N) –

compression curves (Figures 4.6-4.8) . The slopes of these straight lines, i.e., compression moduli and equation (3,5) were used to compute the effective network concentration,  $\nu_e$ .

To understand the effect of structure, molecular weight, concentration of crosslinker, and monomer concentration on the mechanical performance and swelling properties of neutral NIPAAm hydrogels, the parameters  $\nu_{2r}$ ,  $\nu_{2m}$ ,  $\nu_e$ ,  $\chi$  and  $M_c$ , which were used to describe the polymer-solvent systems, was calculated from equations 3,4 – 3,7. Table 4.1 summarizes the synthesis conditions, swelling and mechanical properties of neutral NIPAAm hydrogels crosslinked with hydrophilic and hydrophobic tetrafunctional monomer and macromer, respectively. The data belonging to ionic NIPAAm hydrogels prepared in the presence of two different concentrations of BIS, Tegomer V-Si 2250 and Tegomer V-Si 2150 are listed in Tables 4.1.

As can be seen from Table 4.1, the much lower effective crosslinking densities and crosslinking efficiencies were obtained for the NIPAAm hydrogels crosslinked with BIS than for the ones crosslinked with VTPDMS. In another words, the compression moduli of the latter samples were approximately seven times greater than those of the first ones. To be sure of this unexpected increase in mechanical strength, the syntheses of neutral NIPAAm hydrogels containing hydrophobic macromers as a crosslinker were repeated.

Both of the tetrafunctional components were incorporated covalently into the gel structures by free radical solution copolymerization method. The effect of increasing monomer and crosslinker content in reducing the swelling and in increasing the compression modulus was an expected result for the conventional crosslinking agents, i.e., for BIS-crosslinked gels.

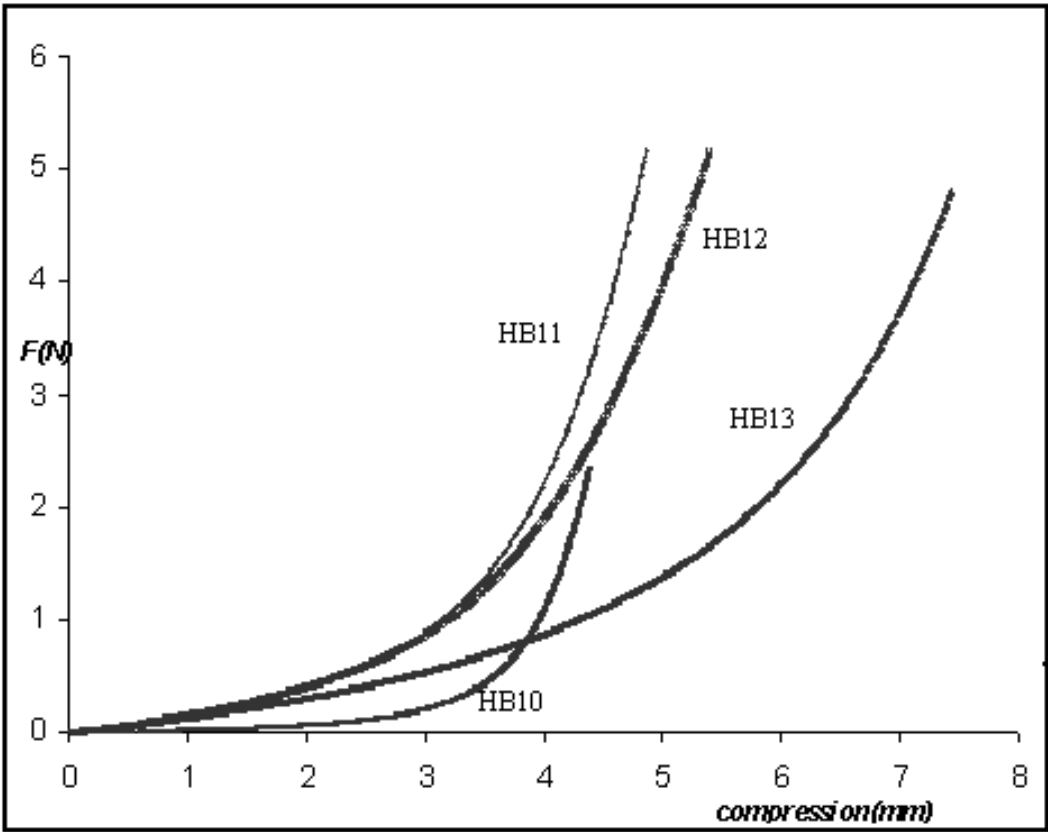


**Figure 4.3 :** Measured Force,  $F$  (N) as a Function of Compression (mm) for Samples HB10 – HB13 Given in Table 4.1.

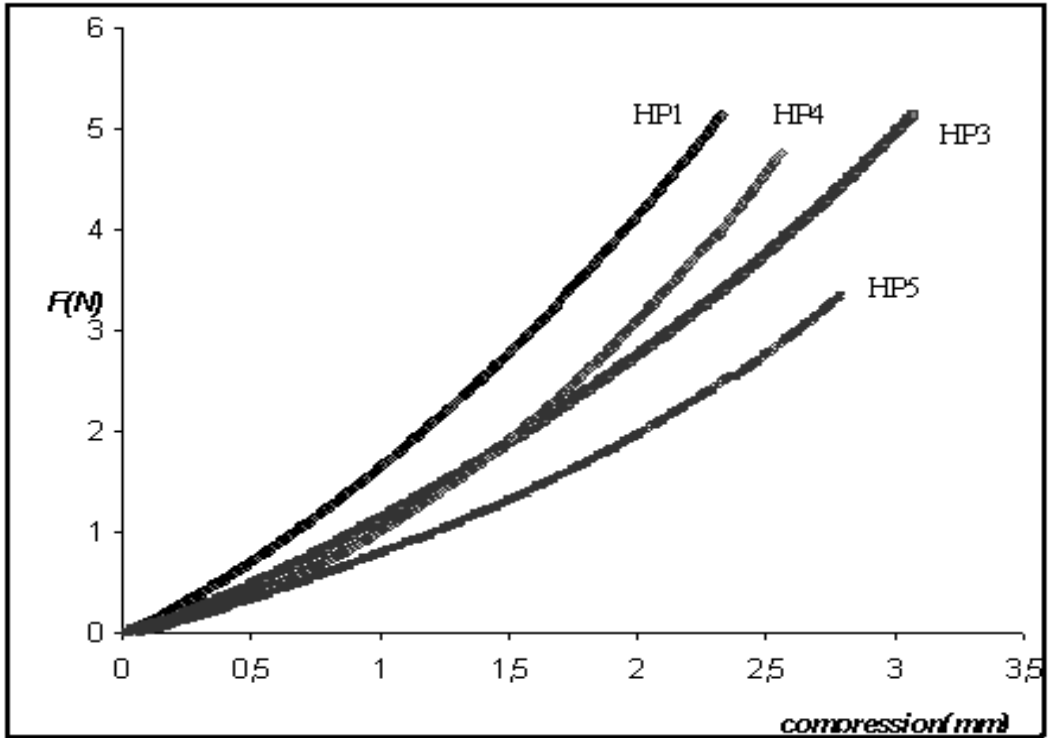


**Figure 4.4 :** Measured Force,  $F$  (N) as a Function of Compression (mm) for Samples HP1, HP3 – HP5 Given in Table 4.1.

However, the effective crosslinking densities of NIPAAm hydrogels containing VTPDMS (Tegomer V-Si 2250) chains were nearly seven times greater than the theoretical ones calculated from the feed composition. The reason for high crosslinking efficiency for VTPDMS-crosslinked gels can be the strong hydrophobic interactions between the methyl groups on the siloxane portions of macromer. In another words, the unusual value of effective crosslinking for the VTPDMS-crosslinked NIPAAm hydrogels arises from the contribution of physical crosslinks to the crosslinking efficiencies. Furthermore, the increases in  $\nu_{2s}$  and  $\chi$  produced by increasing molecular weight of VTPDMS showed that the hydrophobicity of neutral NIPAAm hydrogels increase with increasing length of siloxane portions, as expected. The inverse relation between the number of dimethylsiloxane units and the crosslinking efficiencies of Tegomer V-Si 2250 and 2150 supports the interpretation based on mainly hydrophobic interactions (Samples HP1 and HP2 in Table 4.1).

Tables 4.1 summarize the physical parameters such as  $\mathbf{G}$ ,  $\nu_e$  and  $\mathbf{M}_c$ , defining the mechanical properties of ionic NIPAAm hydrogels crosslinked with BIS and VTPDMS. From the comparison of the data in these Tables with the ones in Table 4.1 and Figures 4.5-4.7, it was seen that the ionic NIPAAms containing 2.50 mol% of IA in the feed and crosslinked with BIS (Samples HB14, HB17) exhibited higher compression moduli than those of the neutral ones, whereas all of the ionic NIPAAm hydrogels crosslinked with VTPDMS tetramers (Samples HP3 – HP6 for Tegomer V-Si 2250; Samples HP7 – HP9 for Tegomer V-Si 2150) showed higher swelling degrees and lower compression moduli than the corresponding neutral ones (Samples HP1 and HP2 for Tegomer V-Si 2250 and V-Si 2150, respectively). In the case of NIPAAm hydrogels containing 2.50 mol% of IA as acidic comonomer with two carboxyl groups and BIS as hydrophilic crosslinker, the presence of nonionized carboxyl groups in the structures of weakly ionized IA molecules in addition to –NHR and C=O groups in the molecular structures of BIS and NIPAAm units increase the strong of noncovalent intramolecular hydrophilic interactions, i.e., the number of hydrogen bonding between the NIPAAm chains. The lower compression modulus of NIPAAm hydrogel having 5.00 mol% of IA in the pregel solutions (Sample HB15) indicates that increasing number of carboxylate groups with increase in the mole content of IA causes to rise the electrostatic repulsive forces between the same type ions. It means that the increasing numbers of the intermolecular hydrogen

bonds between the  $-\text{COOH}$  groups with negative charged, i.e.,  $-\text{COO}^-$  groups and water molecules decrease the strength of the physical crosslinks between the  $-\text{COOH}$  groups and amide groups, resulting from the intramolecular interactions, and thus the strength of the mechanical performance.

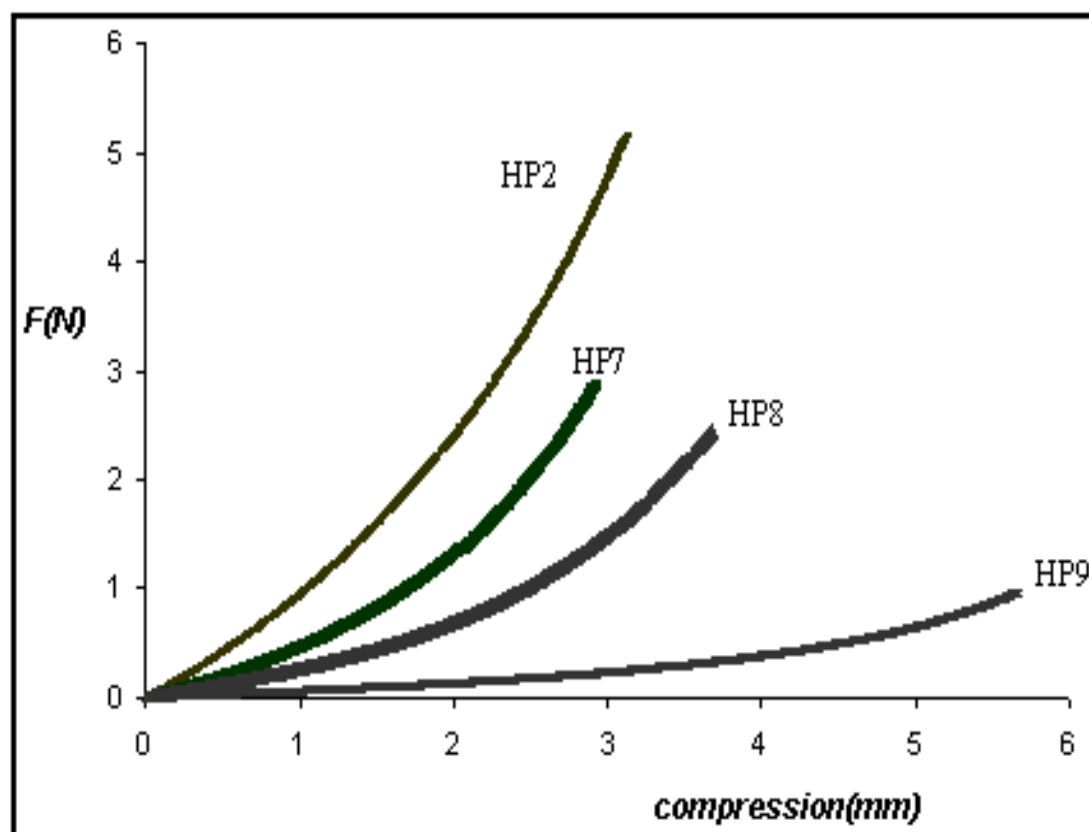


**Figure 4.5 :** Measured Force,  $F$  (N) as a Function of Compression (mm) for Samples HP2, HP7 – HP9 Given in Table 4.1.

The mechanical behaviors of neutral and ionic NIPAAm hydrogels crosslinked with hydrophobic macromers, Tegomer V-Si 2250 and V-Si 2150 are similar to those of the ones crosslinked with hydrophilic monomer, i.e., BIS. The main difference results from the nature of secondary forces, being highly affected on the degree of physical crosslinkings. On the contrary, neutral NIPAAm/BIS crosslinked samples, in the case of the NIPAAm hydrogels containing VTPDMS as a macro crosslinker, hydrophobic interactions between Tegomer molecules incorporated covalently into the gel structures were mainly responsible for their high compression moduli and crosslinking efficiencies. The lower mechanical responses of the hydrogels composed of temperature-sensitive NIPAAm molecules and less hydrophobic macrocrosslinker, i.e., Tegomer V-Si 2150, containing half of the dimethylsiloxane

units in the molecular structure of Tegomer V-Si 2250 also supported this interpretation.

For both Tegomer V-Si 2250 and Tegomer V-Si 2150, crosslinking efficiencies dependent on the compression moduli of the hydrogels were decreased sharply, with increasing IA content (Table 4.1). This effect can be explained by the fact that electrostatic repulsive forces between  $-\text{COO}-$  groups of weakly ionized IA units attached covalently on to the main chain structures of NIPAAm networks destroy the intramolecular hydrophobic interactions arising from the dimethylsiloxane units of VTPDMS chains. To support these findings and propose the optimum conditions for the materials having high mechanical strength and water absorption capacity, i.e., optimum combination of hydrophilic and hydrophobic constituents, Tegomer content of the products was increased while IA content was taken as constant for its highest value used in this work (Samples HP5, HP6).

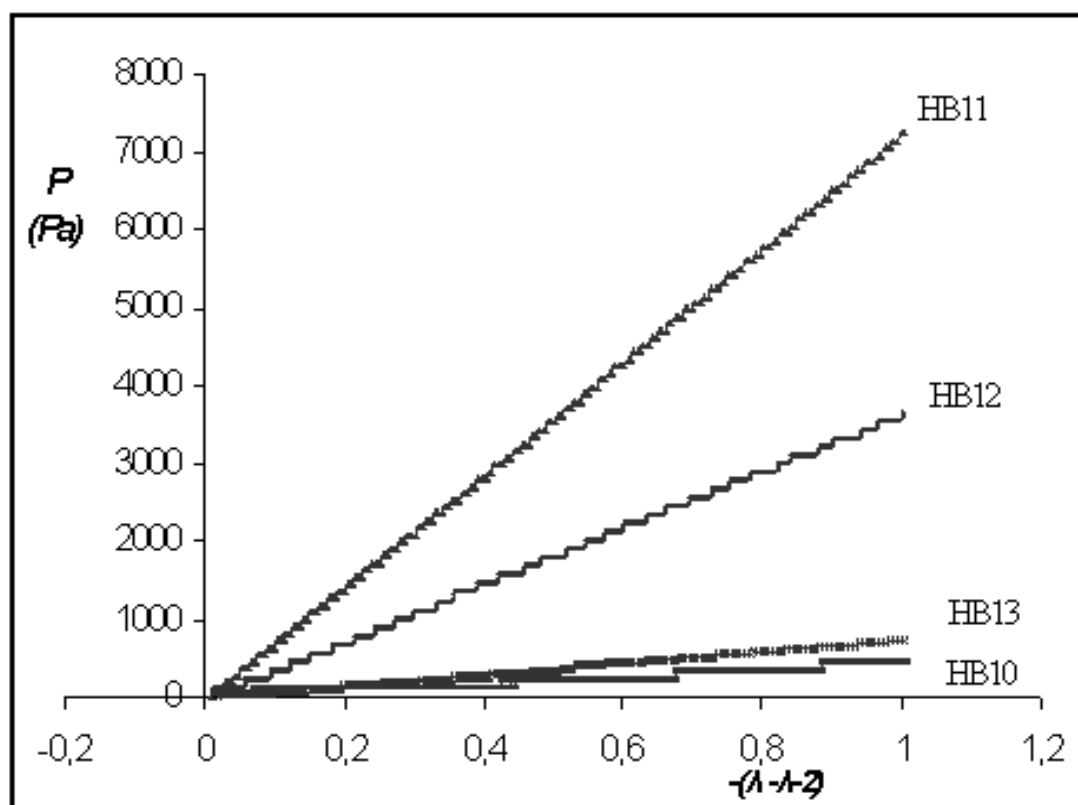


**Figure 4.6 :** Compression Stress-strain Curves (Pressure (Pa) vs.  $-(\lambda - \lambda^2)$ ) for Samples HB10 – HB13 Given in Table 4.1.

The results showed that the increase in the number of hydrophobic siloxane units suppressed the effect of physical crosslink-destroyers, i.e., -COO- groups. From the comparison of the compression moduli of the samples in Table 4.1 with the diameters of the corresponding ones in Table 4.2 (because they are used for the determination of the effective crosslinking densities), it was observed that the preparation of highly swollen, but mechanically stable NIPAAm hydrogels was mainly related to the ratio of hydrophilic/hydrophobic constituents. For example, the diameters of the neutral and so weakly swollen NIPAAm hydrogels were nearly stable during the observation period chosen as 3 months whereas in the case of the ionic hydrogels crosslinked with hydrophobic crosslinker, surprisingly, the diameters of the samples increased in the course of time, except Samples HP3 and HP6. The results indicate that for these two samples hydrophobic interactions are balanced with the hydrophilic ones.

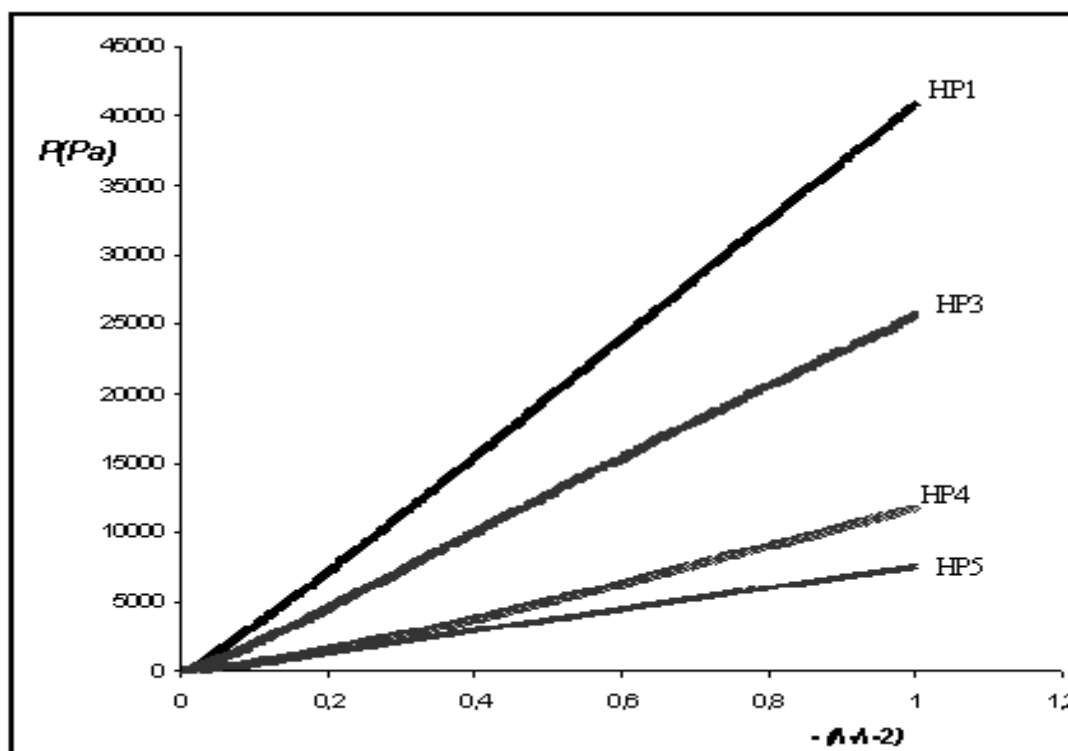


**Figure 4.7 :** Compression Stress-strain Curves (Pressure (Pa) vs.  $-(\lambda-\lambda^2)$ ) for Samples HP1, HP3 – HP5 Given in Table 4.1.

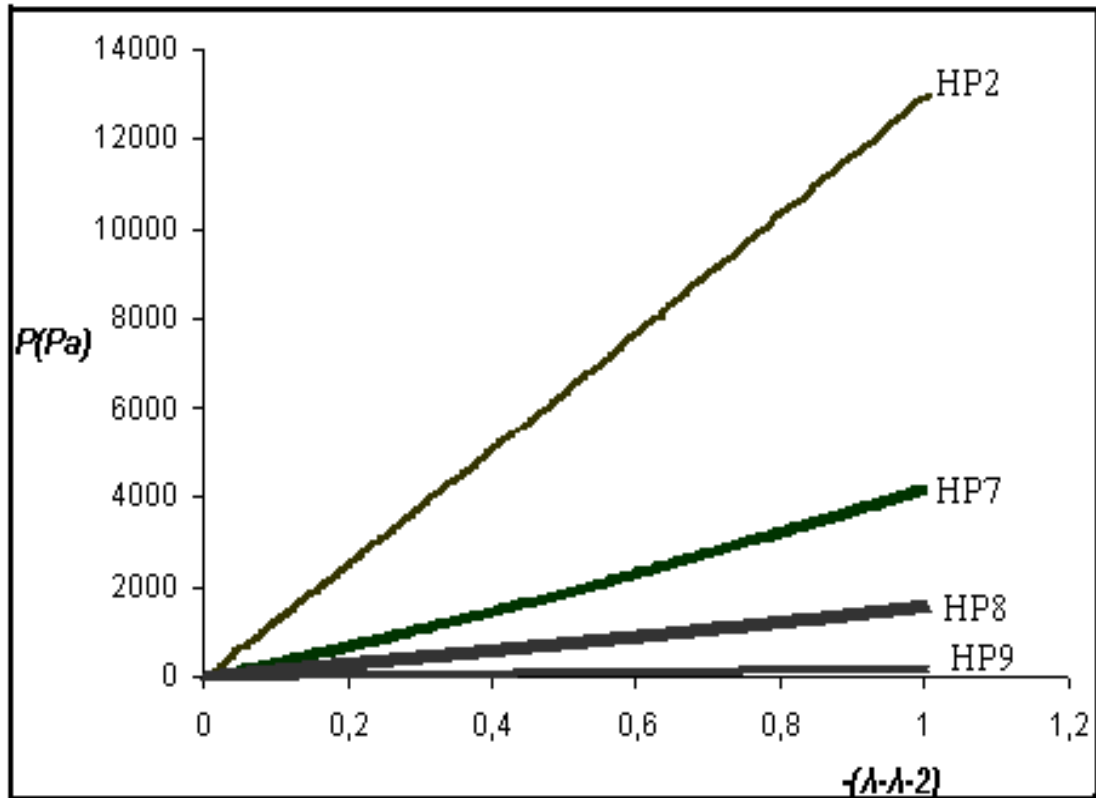


**Figure 4.8** : Compression Stress-strain Curves (Pressure (Pa) vs.  $-(\lambda-\lambda^2)$ ) for Samples HP2, HP7 – HP9 Given in Table 4.1.

We studied the effects of VTPDMS, being a hydrophobic macrocrosslinker on the physical parameters such as polymer volume fraction ( $v_{2s}$ ), effective crosslinking density ( $v_e$ ), polymer-solvent interaction parameter,  $\chi$  and average molecular weight between crosslinking points ( $M_c$ ) of neutral and ionic NIPAAm hydrogels, in comparison with those of the ones crosslinked with BIS. It was revealed that the compressive elastic moduli of VTPDMS-crosslinked neutral NIPAAm hydrogels were 50 times higher than those of the ones crosslinked with conventional tetra functional monomer, i.e., BIS in 1,4-dioxane. The lower mechanical responses of the neutral NIPAAm hydrogels crosslinked with Tegomer V-Si 2150, having half of the dimethylsiloxane units in the molecular structure of Tegomer V-Si 2250 supported the importance of the nature of secondary forces, being highly effected on the degree of physical crosslinkings. For both Tegomer V-Si 2250 and Tegomer V-Si 2150, the compression moduli of the ionic NIPAAm hydrogels were decreased sharply, with increasing IA content.

**Table 4.2 :** Swollen Diameters of the Samples Given in Tables 4.1

Sample no.	Crosslinker (x10 <sup>-2</sup> mol/L)	Comonomer (mole %)	d (mm) (at swelling equilibrium)	d (mm) (3 months later)
HB11	BIS, 2.50	-	8.40	8.21
HB12	BIS, 1.25	-	9.29	9.37
HB13	BIS, 1.25	-	22.35	21.62
HP1 <sub>1</sub> *	VTPDMS, 1.25	-	11.20	11.17
HP2 <sub>1</sub> *	VTPDMS, 1.25	-	14.36	14.38
HP3 <sub>2</sub> *	VTPDMS, 1.25	IA, 1.00	12.71	15.71
HP6 <sub>2</sub> *	VTPDMS, 2.50	IA, 7.50	11.42	15.59
HP5*	VTPDMS, 1.25	IA, 7.50	17.45	33.45
HP4*	VTPDMS, 1.25	IA, 2.50	14.20	18.60
HP7*	VTPDMS, 1.25	IA, 1.00	17.56	25.35

[NIPAAm] = 2.0 molL<sup>-1</sup>

\*Tegomer V-Si 2250; M.W = 2000 gmol<sup>-1</sup>

•Tegomer V-Si 2150; M.W = 1000 gmol<sup>-1</sup>

(Subscripts 1 and 2 indicate the results of two different synthesizes carried out with the same experimental procedure)

As for these results, the electrostatic repulsive forces between the ionized carboxyl groups of IA units destroyed the strong intramolecular hydrophobic interactions arising from the dimethylsiloxane units of VTPDMS chains. From the starting point of these findings, it can be said that the most productive combinations of the hydrophilic component which absorbed large amount of water and the hydrophobic component which improved the mechanical performance are necessary to designate the materials having the right balance of repulsive and attractive forces, being responsible for swelling and mechanical behaviors of the networks. For this study, the indicated combinations of hydrophobic and hydrophilic constituents correspond to the ratios of VTPDMS 2250 (1.25×10<sup>-2</sup> mol/L) / IA (1.0 mol %) for Sample HP3 and VTPDMS 2250 (2.50×10<sup>-2</sup> mol/L)/IA (7.50 mol %) for Sample HP6. The absorption capacities of these hydrogels and their applications in drug delivery are subject to further studies.

## 4.2. Synthesis and Characterization of Monoitaconates

The mono-n-alkyl itaconates selected for this work were methyl (M), butyl (Bu), octyl (Oc) and cetyl (Ce). These hydrophobic/hydrophilic, i.e., amphiphilic comonomers were prepared by esterification of itaconic acid with the corresponding alcohols using acetyl chloride as a catalyst to ensure slightly acidic conditions.

Monoitaconates were characterized by FTIR spectroscopy as can be seen in Figure 3.1. The following characteristic peaks of IA and its mono itaconates could be found: C=O stretching at 1700-1750  $\text{cm}^{-1}$  (for acids and esters), C=C stretching at 1600-1650  $\text{cm}^{-1}$ , H-bonded OH groups in the 3200-2500  $\text{cm}^{-1}$  region (broad band) and C-H stretching modes at 2800-3000  $\text{cm}^{-1}$ .

These monoitaconates include a carboxylic acid group and an ester group in each repeat unit. Therefore, the most interesting spectral regions in Figure 3.1 are the carbonyl and hydroxyl stretching bands. In the case of IA, the hydroxyl stretching region band shows a very wide band due to free hydroxyl groups. It occurs at about 3500  $\text{cm}^{-1}$  and has a maximum at 3200  $\text{cm}^{-1}$ . Another characteristic feature in this region is the wide band with lower intensity at 2600  $\text{cm}^{-1}$ . This band is attributed to the combinations of O-H and O...H stretching bands. The intensity of these peaks decrease with increase in the length of alkyl groups.

As to the reported data, ester groups occurs at 1735  $\text{cm}^{-1}$ . The carboxylic acid groups of IA is in the form of carboxylic acid dimers ( band at about 1700  $\text{cm}^{-1}$  in Figure 4.9(a) ). The spectra (b) and (c) in Figure 4.9 show that as the alkyl group lengths of monoitaconates increase, relative absorptions due to C-H and C=O stretching modes for ester groups increase.

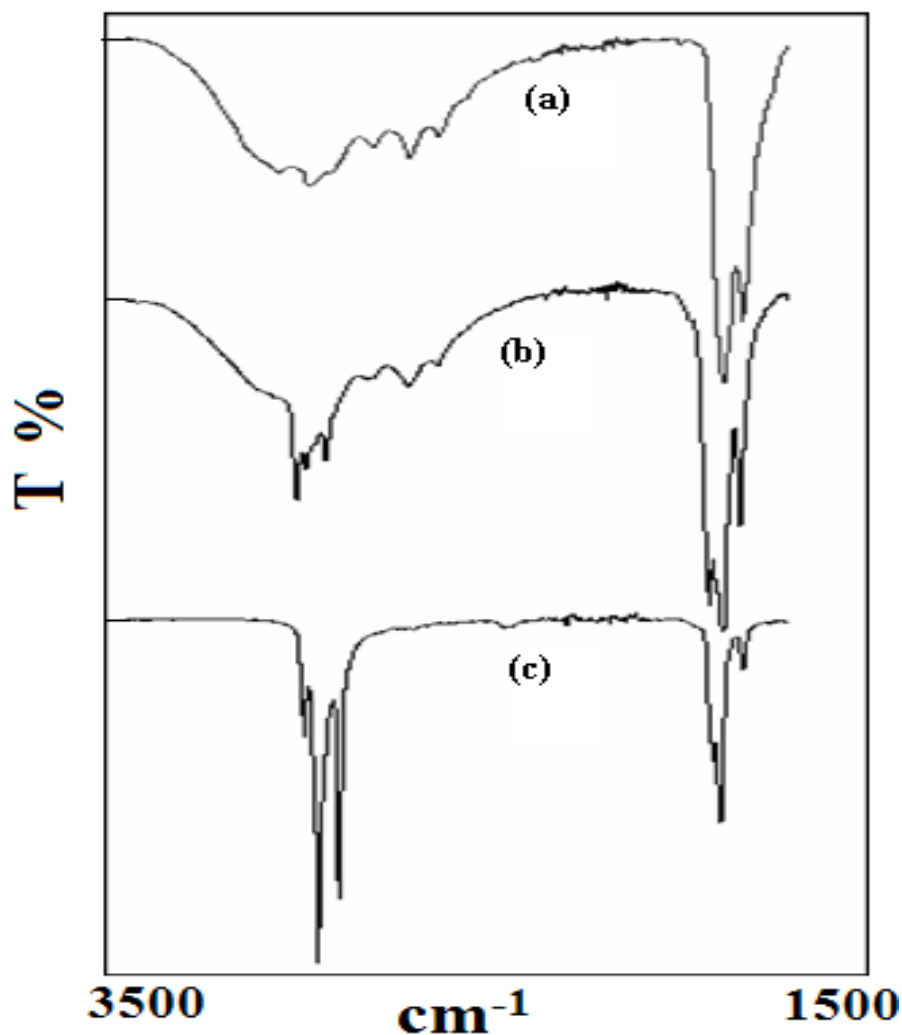


**Figure 4.9.** FTIR Spectra of (a) IA, (b) MBuI and (c) MCEI.

The inflection point of potentiometric titration curve of MMI monomer was approximately equal to the half of the one obtained from the aqueous solutions of IA monomer, having two carboxylic acid group. Conductometric and potentiometric titration results proved that the acid-base titration method was the most sensitive and the simple way for the quantitative determination of carboxylic acid groups (Figure 4.10 and Figure 4.11 respectively).

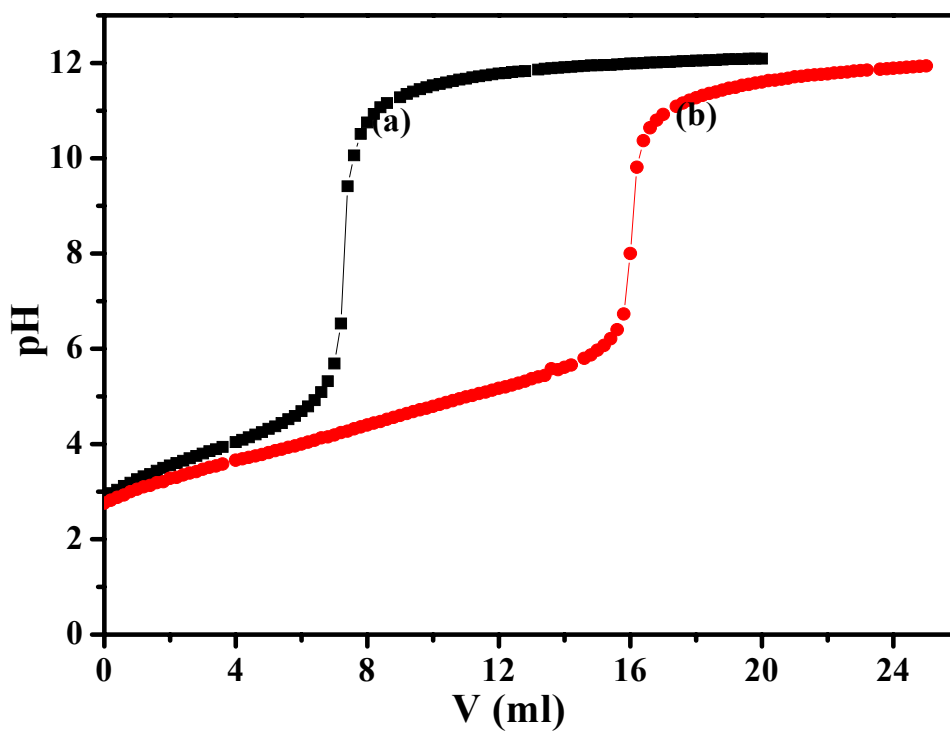


Figure 4.10 : Potentiometric Titration Curves of (a) MMI and (b) IA

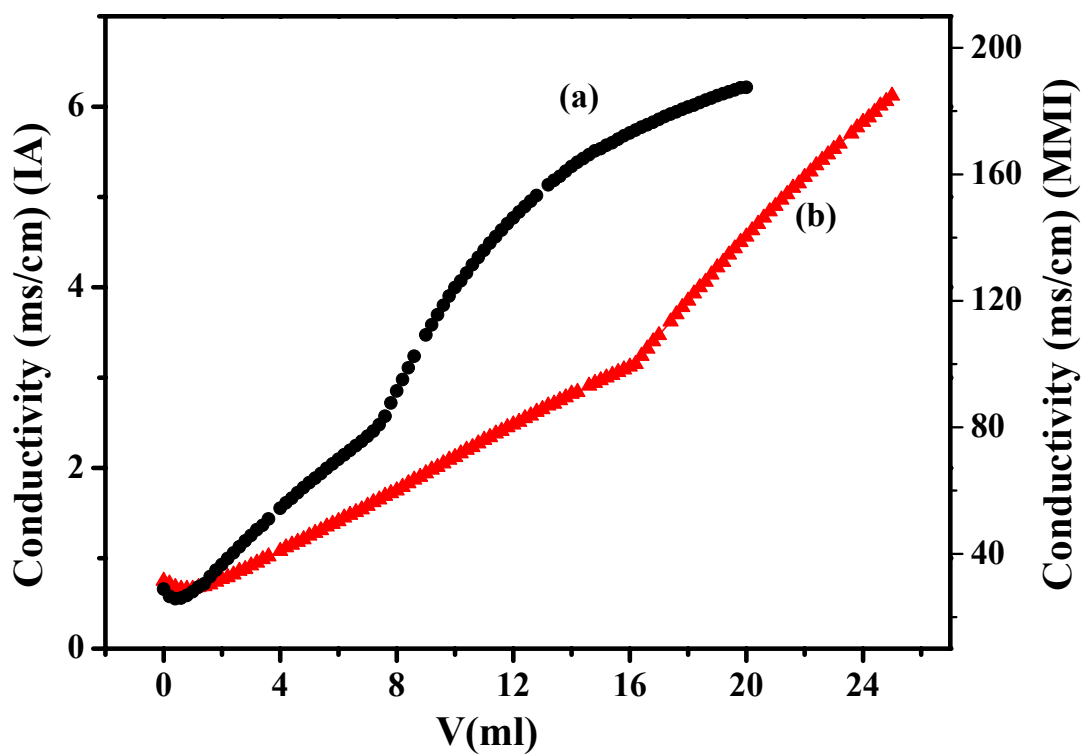


Figure 4.11 : Conductometric Titration Curves of (a) MMI and (b) IA

### 4.3. Compressive Elastic Moduli of NIPAAm Copolymer Hydrogel: the Effects of Crosslinker Concentration, Temperature and, Type and Concentration of Monoitaconates on the Swelling Equilibria and Mechanical Properties.

The effect of the comonomer concentration and type on the volume swelling ratio ( $V/V_0$ ) and phase transition temperatures of hydrophobically modified and ionizable PNIPAAm gels are given in Table 4.3 and Figure 12-19.

**Table 4.3 :** Type and Comonomer Concentration of Monoitaconates in NIPAAm Hydrogels ( $T=23\pm 2^\circ\text{C}$ )

Sample No:	Monomer	Comonomer type	Comonomer Concentration (mole %)
HB18	NIPAAm	-	-
HB19	NIPAAm	IA	1.0
HB20	NIPAAm	IA	1.5
HB21	NIPAAm	IA	2.5
HB22	NIPAAm	IA	5.0
HB23	NIPAAm	IA	10.0
HB24	NIPAAm	DMI	1.0
HB25	NIPAAm	DMI	2.5
HB26	NIPAAm	DMI	5.0
HB27	NIPAAm	DMI	10.0
HB28	NIPAAm	MMI	1.0
HB29	NIPAAm	MMI	2.5
HB30	NIPAAm	MMI	5.0
HB31	NIPAAm	MMI	7.5
HB32	NIPAAm	MMI	10.0
HB33	NIPAAm	MBuI	1.0

[NIPAAm]=0.7 mol/L, [BIS]= $2.5 \times 10^{-2}$ ,  $T=25^\circ\text{C}$ , in MetOH/DDW

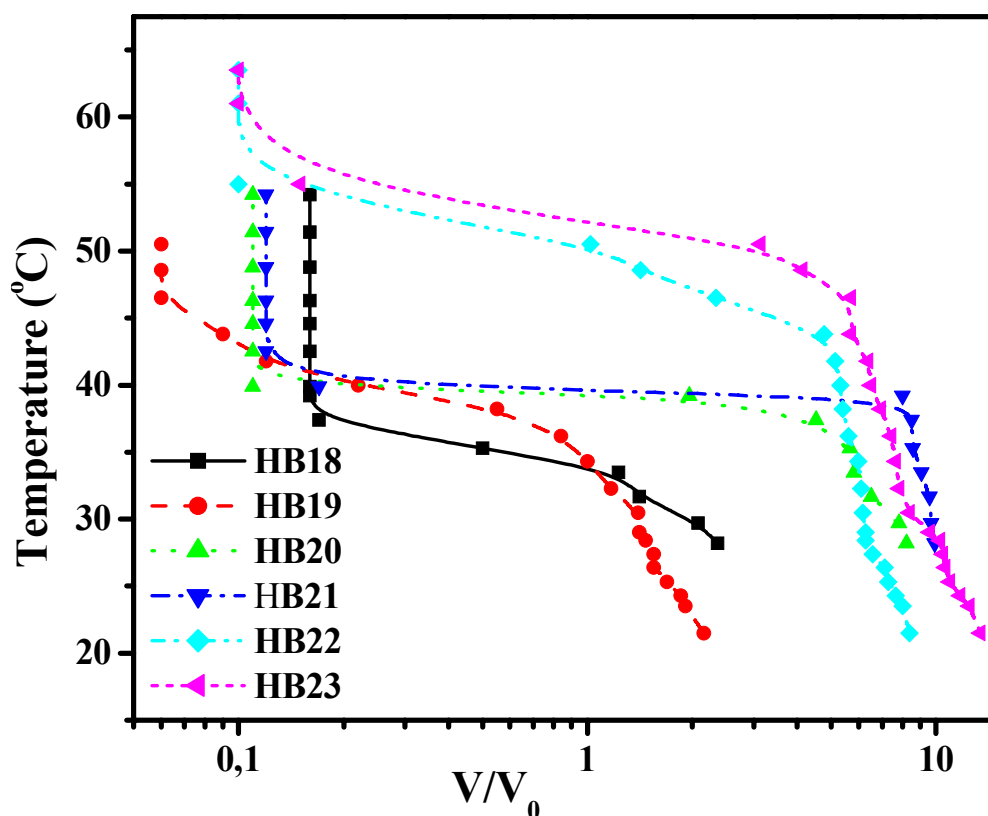


**Figure 4.22** : Temperature Dependence of the Volume Swelling Ratios of the PNIPAAm and Ionic NIPAAm/IA Copolymer Gels Identified in Table 4.3.

Figure 4.12 shows the swelling curves of the non-ionic PNIPAAm and ionic NIPAAm/IA copolymer gels containing 1.0, 1.5, 2.5, 5.0 and 10.0 mole % of IA in the feed (sample HB18 and samples HB19-HB23), which are described in Table 4.3. It can be clearly seen from Figure 4.12 that IA content of NIPAAm/IA hydrogels affects both the swelling ratio in the completely expanded and collapsed regions and the phase transition temperature of temperature-sensitive NIPAAm hydrogels. The temperature vs. volume swelling ratio curves of these samples indicate that the one having 2.5 mole % of IA in the feed can be suggested for drug release experiments because of discontinuous and larger volume change during the phase transition.

The samples HB24-HB27 were prepared by using 1.0, 2.5, 5.0, 10.0 mole % of DMI, respectively, to increase the hydrophobicity of the NIPAAm hydrogel. DMI has two side-chains and these side-chains contain small hydrophobic moieties ( $-\text{CH}_3$  groups) at the end of the hydrophilic carboxylate groups. The phase transition curves of NIPAAm/DMI copolymer gels in Figure 4.13 indicate the phase transition temperatures of the samples decrease slightly with increase in DMI content in the feed.

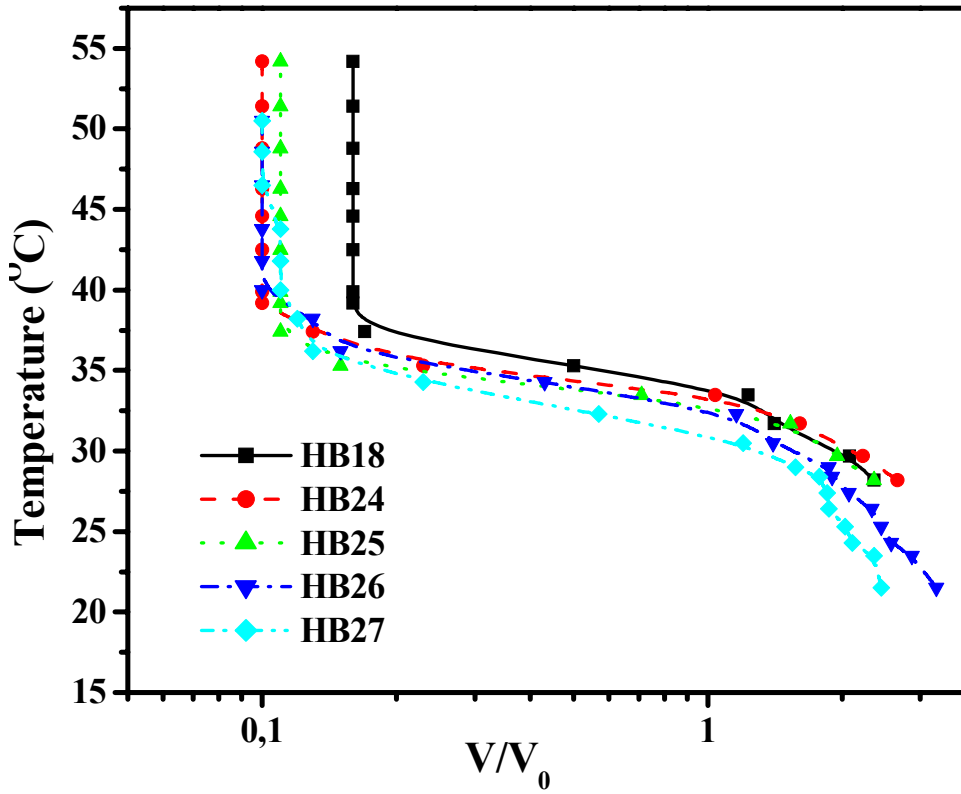


Figure 4.12 : Temperature Dependence of the Volume Swelling Ratios of the PNIPAAm and NIPAAm/DMI Copolymer Gels Identified in Table 4.3.

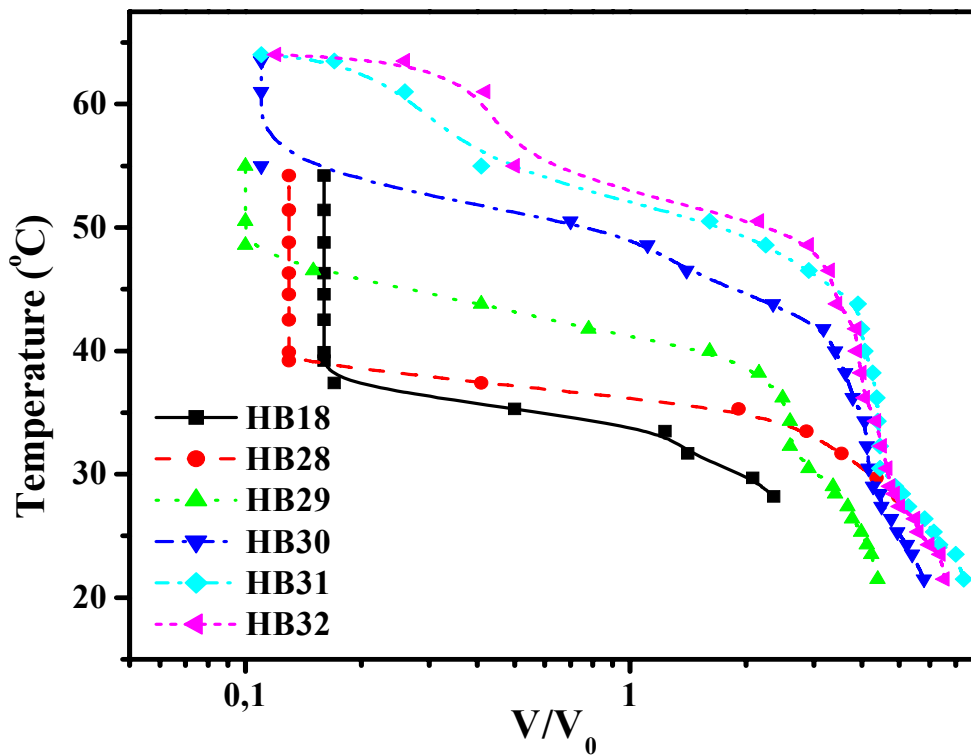
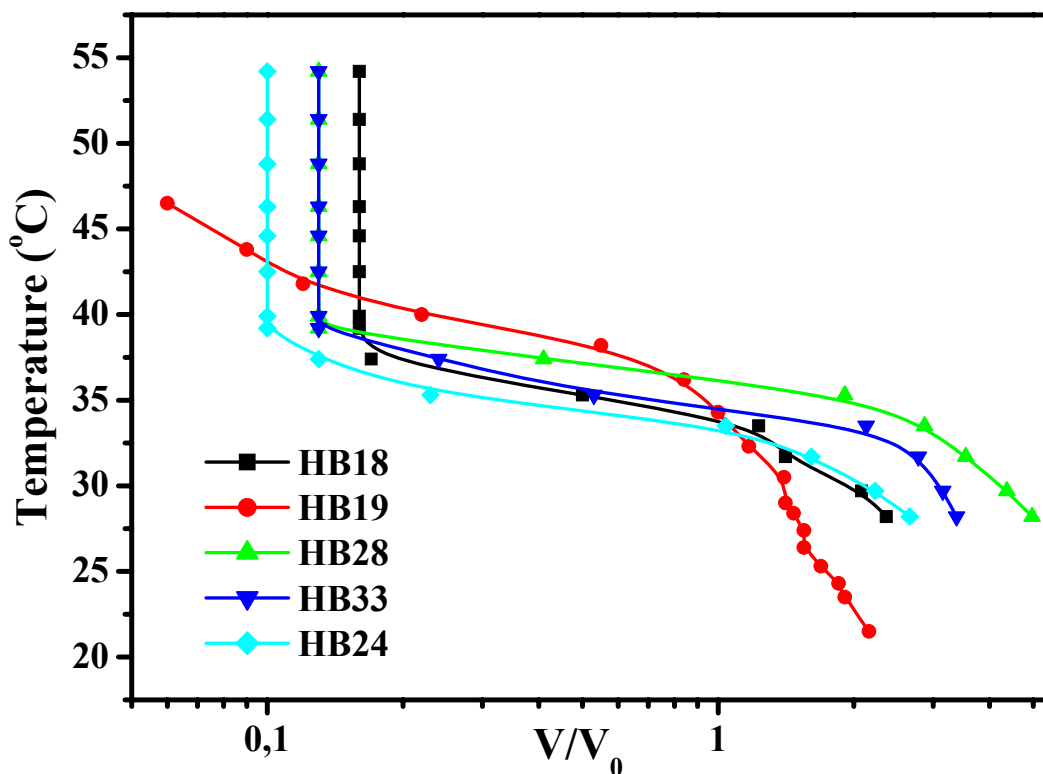


Figure 4.13 : Temperature Dependence of the Volume Swelling Ratios of the PNIPAAm and NIPAAm/MMI Copolymer Gels Identified in Table 4.3.

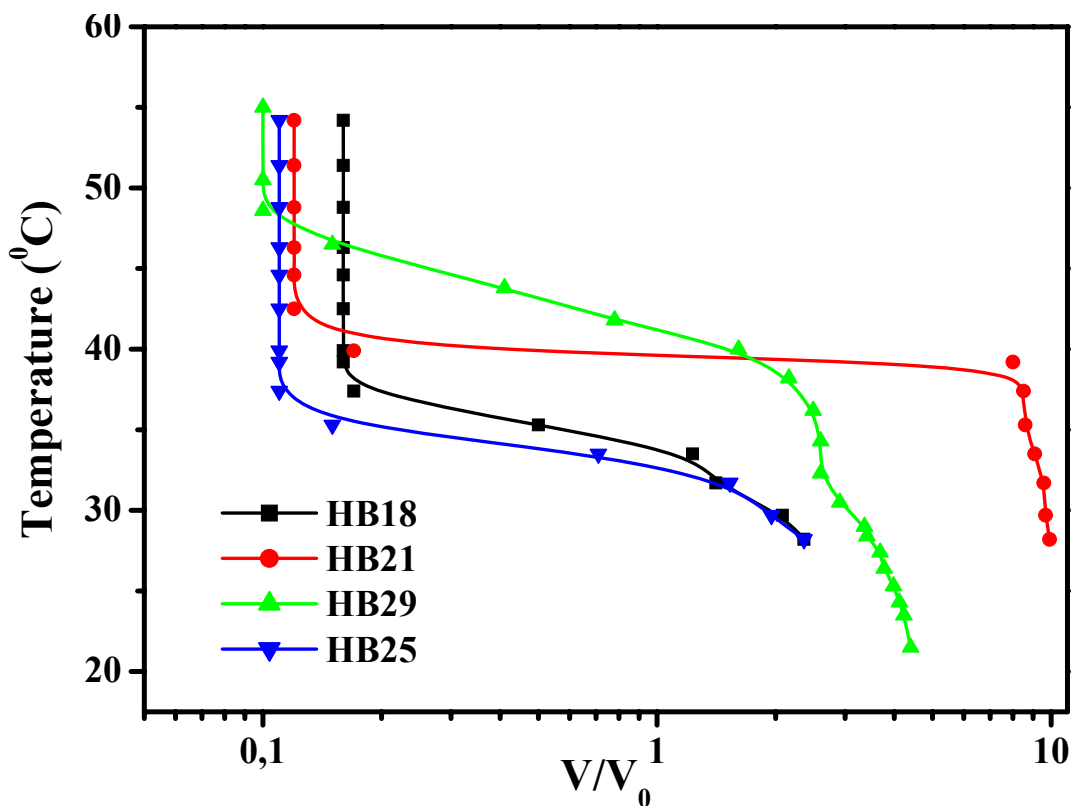


**Figure 4.15** : Temperature Dependence of the Volume Swelling Ratios of the PNIPAAm, NIPAAm/IA, NIPAAm/MMI, NIPAAm/MBuI, NIPAAm/DMI Gels Having 1.0 mole % of Comonomer, Which is Identified in Table 4.3.

Figure 4.14 shows the swelling curves of the non-ionic PNIPAAm and NIPAAm/MMI copolymer gels containing 1.0, 2.5, 5.0, 7.5 and 10.0 mole % of MMI in the feed (sample HB18 and samples HB28-HB32), which are described in Table 4.3. The phase transition behaviors (i.e. the swelling ratios in the completely expanded and collapsed regions and the phase transition temperature) of NIPAAm/MMI copolymer hydrogels containing hydrophobically modified IA, i.e. MMI is slightly different from the once the NIPAAm/IA hydrogels having higher than 2.50 mole % of IA. This difference observed with increasing amount of MMI can be explained as the dilution effect of hydrophobic methyl groups on ionization degree of  $-\text{COOH}$  groups.

The curves for Samples HB18, HB19, HB28, HB33 and HB24 plotted in Figure 4.15 showing the temperature dependence of the volume swelling ratio of the PNIPAAm, NIPAAm/IA, NIPAAm/MMI, NIPAAm/MBuI, NIPAAm/DMI gels, having 1.0 mole % comonomer in the feed, reveal that the increasing hydrophobicity of comonomer mainly affects both the phase transition temperature and volume

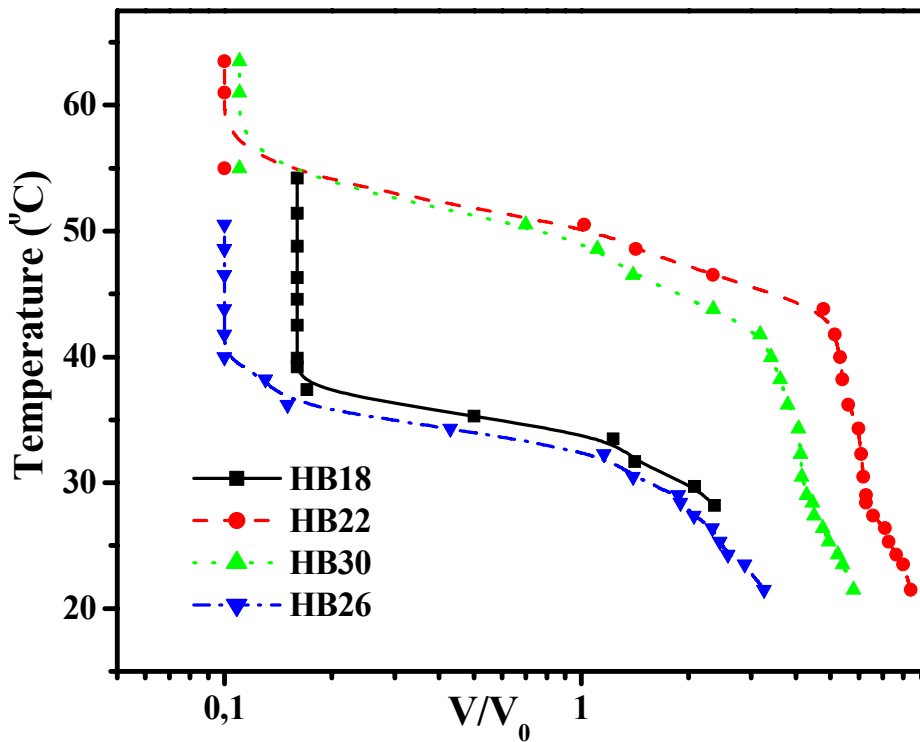
swelling ratio in the expanded and collapsed regions. Further, this figure indicates that the phase transition temperature of the samples decrease with increase in the hydrophobic nature of the comonomer (DMI > MBuI > MMI > IA).



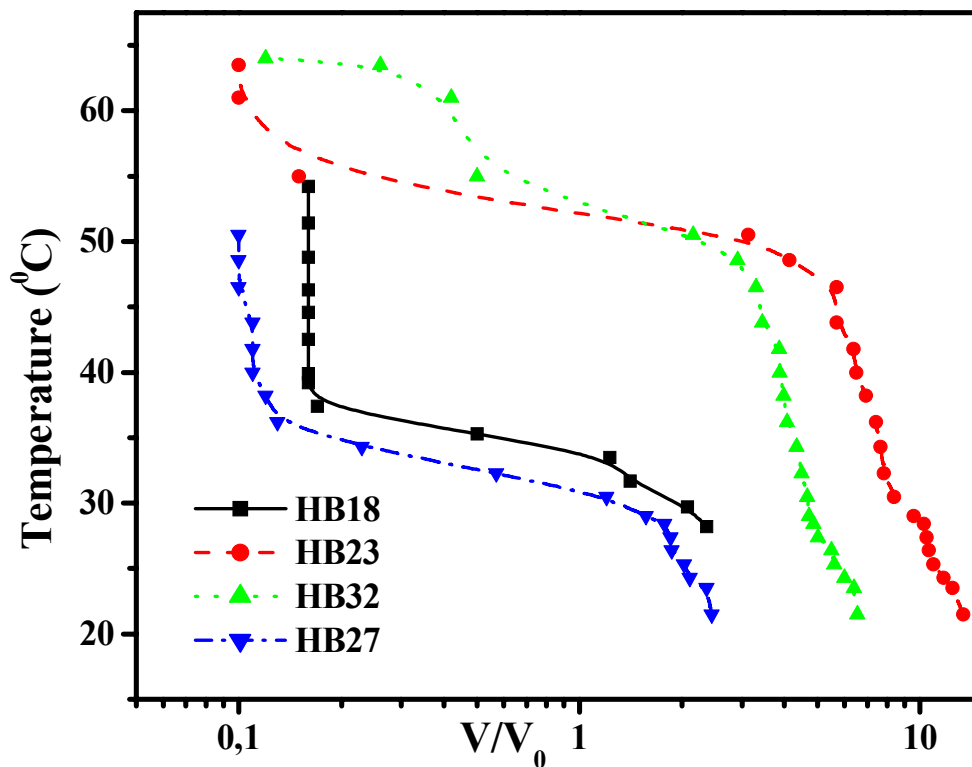
**Figure 4.16 :** Temperature Dependence of the Volume Swelling Ratios of the PNIPAAm, NIPAAm/IA, NIPAAm/MMI, NIPAAm/DMI Copolymer Gels Having 2.50 mole % of Comonomer, Which is Identified in Table 4.3.

Figure 4.16-4.18 shows the swelling curves of the PNIPAAm, NIPAAm/IA, NIPAAm/MMI, NIPAAm/DMI copolymer gels having 2.50, 5.0, 10.0 mole % comonomer in the feed, which are described in Table 4.3. These figures indicates that the phase transition temperature of the samples decrease with increase in the ionic nature and the content of the comonomer (IA > MMI > DMI).

Figure 4.19 shows the effect of crosslinker type and concentration on the swelling behavior of PNIPAAm hydrogels. It is seen that the crosslinkers (VTPDMS V-Si 2150 and V-Si 2250) having hydrophobic structure (HB2 and HB1) reduces both the phase transition temperatures and the volume swelling ratios of the gels. Further, the bubbles around the surface of PNIPAAm hydrogels crosslinked with VTPDMS (the photographs in Figure 4.21) support the effect of hydrophobic constituent on the swelling/shrinking behaviors of network structures.



**Figure 4.17** : Temperature Dependence of the Volume Swelling Ratios of the PNIPAAm, NIPAAm/IA, NIPAAm/MMI, NIPAAm/DMI Copolymer Gels Having 5.0 mole % of Comonomer, Which is Identified in Table 4.3.



**Figure 4.18** : Temperature Dependence of the Volume Swelling Ratios of the PNIPAAm, NIPAAm/IA, NIPAAm/MMI, NIPAAm/DMI Copolymer Gels Having 10.0 mole % of Comonomer, Which is Identified in Table 4.3.

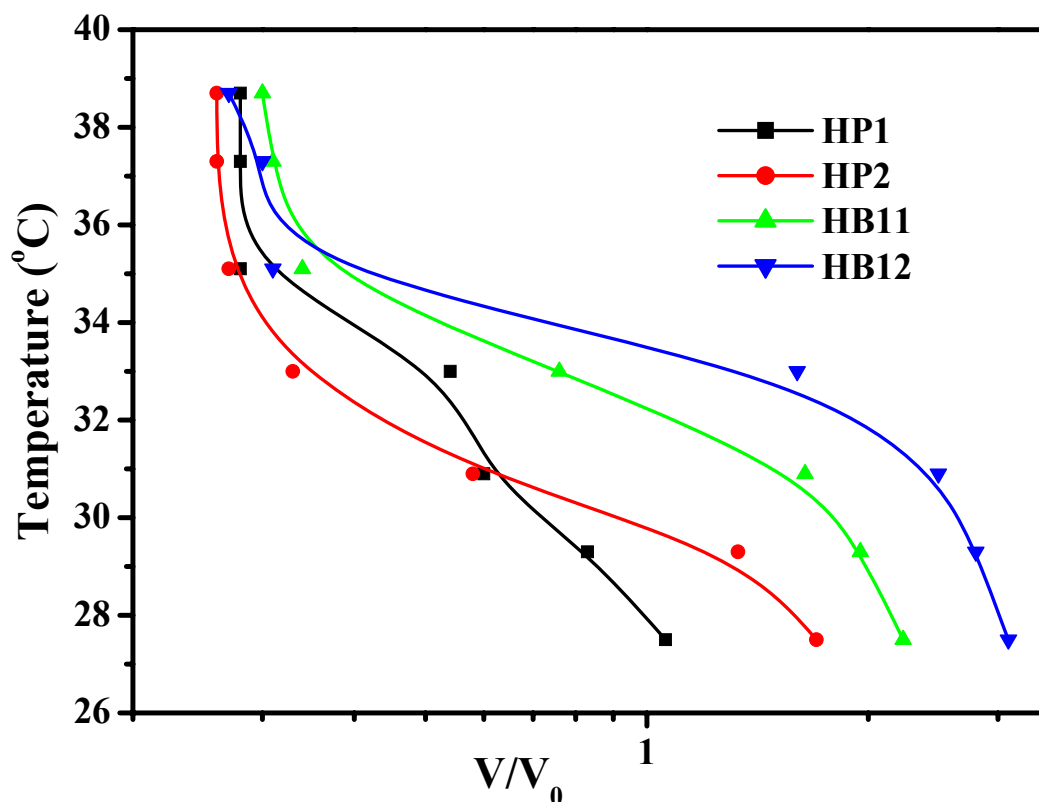


**Figure 4.19** : Temperature Dependence of the Volume Swelling Ratios of the Effect of Crosslinker Type and Concentration on the Swelling Behavior of PNIPAAm Hydrogels

NIPAAm hydrogels composed of NIPAAm, BIS, IA and/or its monoesters (MMI, MBuI, MOcI and MCEI) as hydrophobic/hydrophilic monomer (depending on the temperature), hydrophilic crosslinker, weakly ionizable comonomer, and hydrophobically modified comonomer, respectively, were prepared to investigate the effect of hydrophobic component on the compression moduli of the samples attained equilibrium swollen and shrinking states in DDW at 23°C and 37°C. For mechanical strength analysis, conventional rubber elasticity and swelling theories for networks formed in the presence of diluent were adopted. From the swelling and compression measurements, effective crosslinking density  $\nu_e$ , average molecular weight between crosslinks  $M_c$  and polymer-water interaction parameter  $\chi$ , which can be used to characterize the structures of the hydrogels, were calculated.

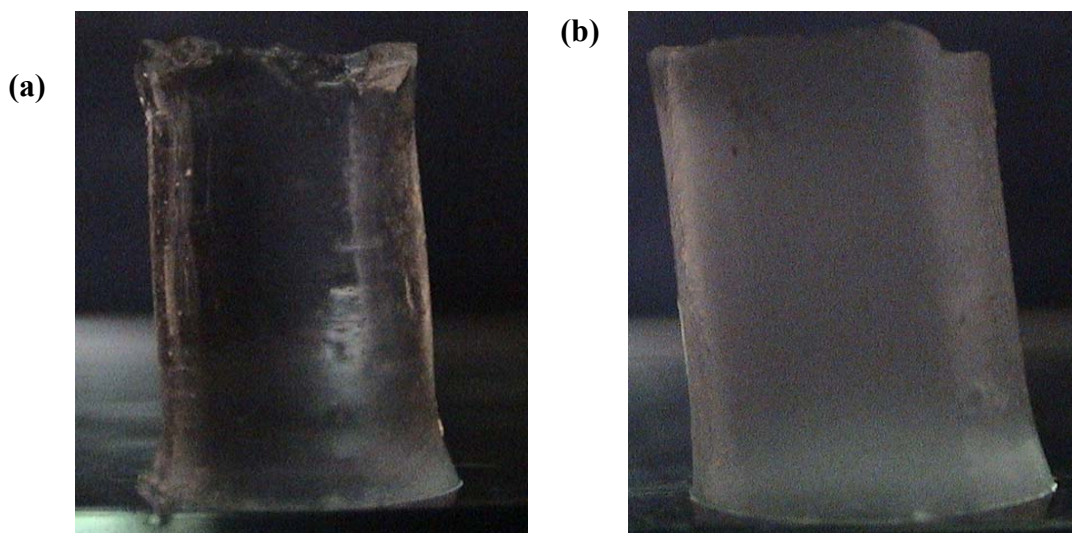


**Figure 4.20** : Photographs of PNIPAAm Hydrogels Crosslinked with BIS and Equilibrated in DDW: (a) Sample HB11, (b) Sample HB12

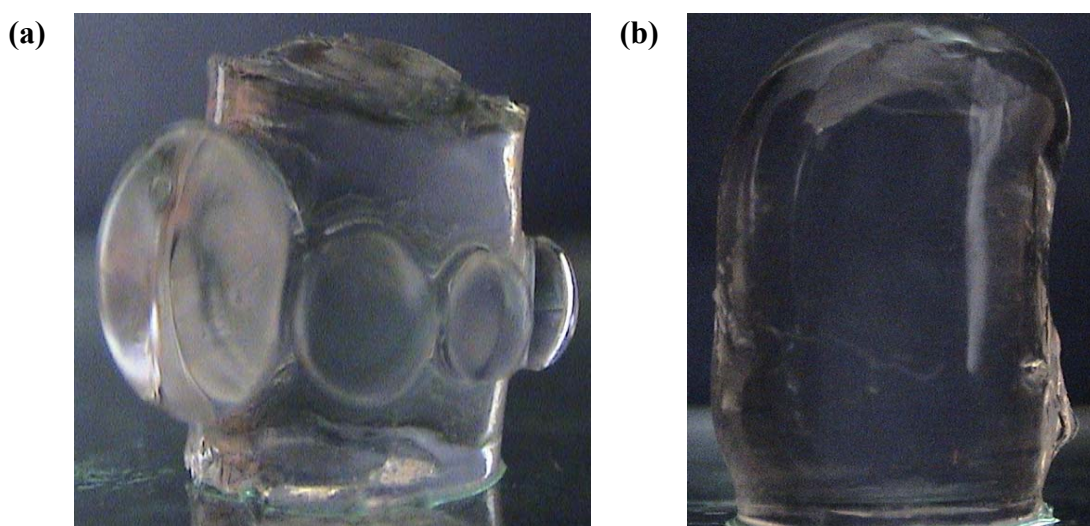


**Figure 4.21** : Photograph Showing the Morphology of PNIPAAm Hydrogel Crosslinked with VTPDMS and Equilibrated in DDW: (a) Sample HP2, (b) Sample HP1

Tables 4.4-4.6 summarize the synthesis conditions, swelling and mechanical properties of NIPAAm copolymer hydrogels crosslinked with hydrophilic tetrafunctional monomer, BIS.

**Table 4.4 :** Polymer Volume Fractions ( $v_{2r}$ ,  $v_{2s}$ ), Compression Moduli (G) and Polymer-water Interaction Parameters ( $\chi$ ) at 23°C for PNIPAAm, NIPAAm/IA, and NIPAAm/monoitaconate (MBuI, MOcI, MCEI) Hydrogels Prepared Using BIS ( $2.50 \times 10^{-2}$  mol/L and  $3.75 \times 10^{-2}$  mol/L) and AIBN as Crosslinker and Initiator

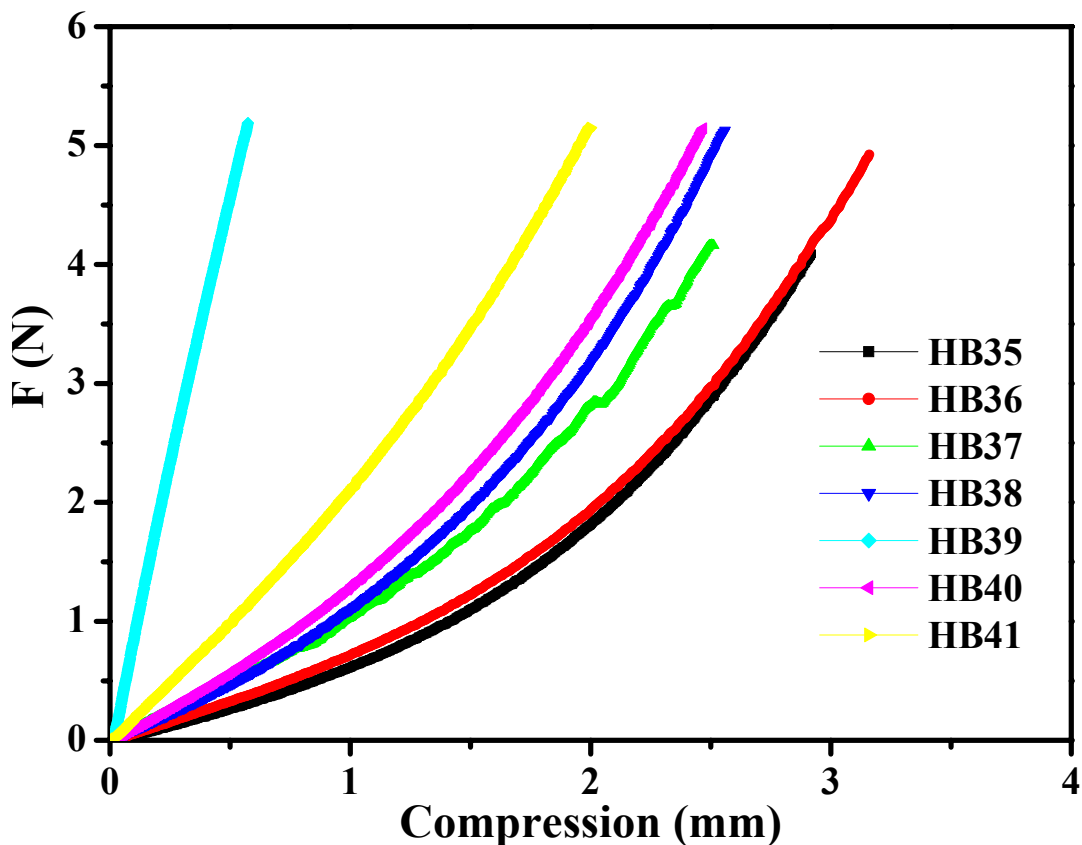
Sample No	Comonomer (mol %)	* $v_{2r}$	* $v_{2s}$	*G (Pa)	* $v_e$ (molm <sup>-3</sup> )	*C.E.	* $M_c$ (kg/mol)	* $\chi$
HB35 <sup>a</sup>	-	0.1704	0.0644	4694.3	15.43	0.62	71.29	0.52
HB36 <sup>a</sup>	MBuI, 2.50	0.1704	0.0305	4490.6	18.89	0.76	58.23	0.51
HB37 <sup>a</sup>	MBuI, 5.0	0.1704	0.0261	5292.5	23.44	0.94	46.93	0.39
HB38 <sup>a</sup>	MOcI, 2.50	0.1704	0.2337	14322	30.77	1.23	35.75	0.60
HB39 <sup>a</sup>	MOcI, 5.0	0.1704	0.4731	247923	422.08	16.88	2.61	0.75
HB40 <sup>a</sup>	MCEI, 2.50	0.1704	0.1279	16116	42.25	1.69	26.04	0.54
HB41 <sup>a</sup>	MCEI, 5.0	0.1704	0.1978	36012	81.89	3.28	14.43	0.58
HB42 <sup>b</sup>	-	0.1704	0.0802	11000	33.64	0.90	32.7	0.52
HB43 <sup>b</sup>	MBuI, 2.50	0.1704	0.0586	9280	31.47	0.84	34.95	0.51
HB44 <sup>b</sup>	MBuI, 5.0	0.1704	0.0460	9438	34.67	0.92	31.73	0.50
HB45 <sup>b</sup>	MOcI, 2.50	0.1704	0.2628	29286	60.53	1.61	18.17	0.61
HB46 <sup>b</sup>	MOcI, 5.0	0.1704	0.5314	548552	898.75	23.97	1.22	0.80
HB47 <sup>b</sup>	MCEI, 2.50	0.1704	0.1612	33582	81.56	2.17	13.49	0.56
HB48 <sup>b</sup>	MCEI, 5.0	0.1704	0.2138	36247	80.20	2.14	13.72	0.58
HB49 <sup>a</sup>	IA, 2.50	0.1704	0.0185	3692.1	18.32	0.73	60.04	0.51
HB50 <sup>b</sup>	IA, 2.50	0.1704	0.0323	7277.1	30.04	0.80	36.62	0.44

\* Measurements Temperature= 23 °C, <sup>a</sup> [BIS] =  $2.50 \times 10^{-2}$  mol/L, <sup>b</sup> [BIS] =  $3.75 \times 10^{-2}$  mol/L

**Table 4.5 :** Polymer Volume Fractions ( $v_{2r}$ ,  $v_{2s}$ ), Compression Moduli (G) and Polymer-water Interaction Parameters ( $\chi$ ) at 37 °C for PNIPAAm, and NIPAAm/monoitaconate (MBuI, MOcI, MCEI) Hydrogels Prepared Using BIS ( $2.50 \times 10^{-2}$  mol/L and  $3.75 \times 10^{-2}$  mol/L) and AIBN as Crosslinker and Initiator

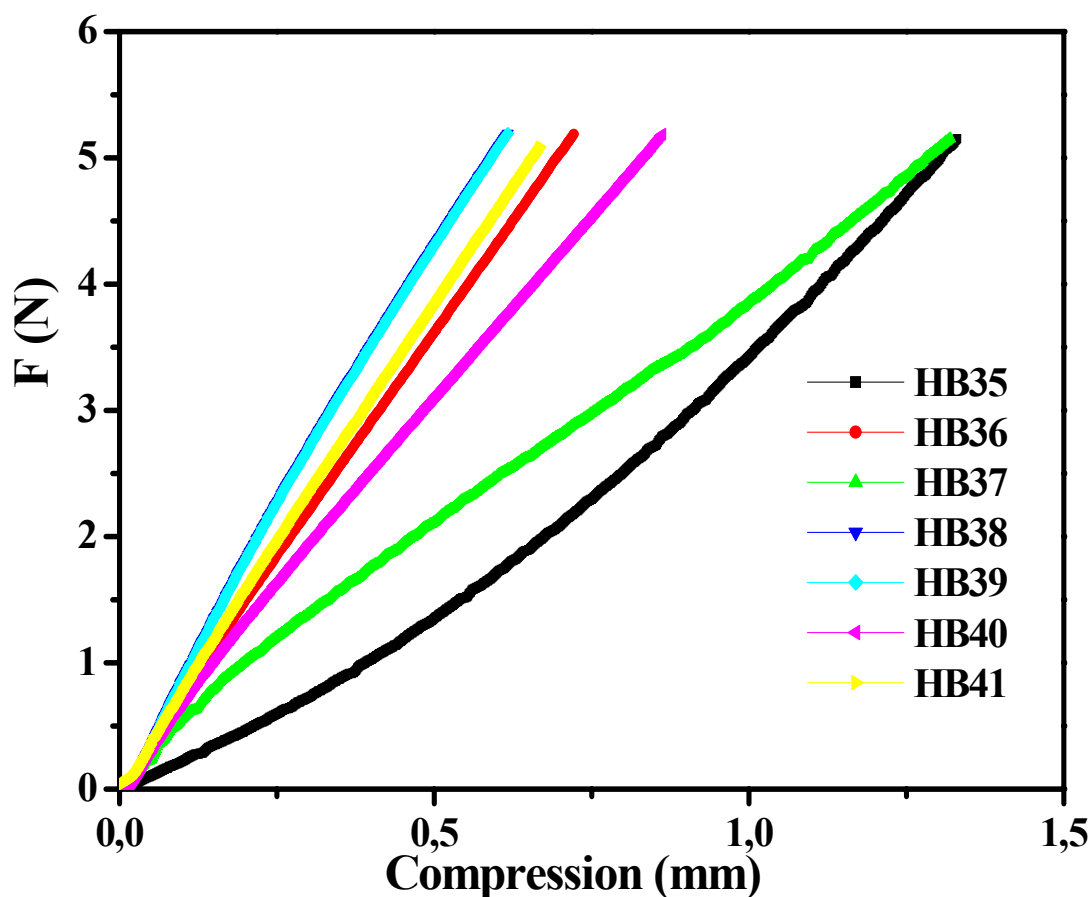
Sample No	Comonomer (mol %)	* $v_{2r}$	* $v_{2s}$	*G (Pa)	* $v_e$ (molm <sup>-3</sup> )	*C.E.	*M <sub>c</sub> (kg/mol)	* $\chi$
HB35 <sup>a</sup>	-	0.1704	0.0644	4694.3	15.43	0.62	71.29	0.52
HB36 <sup>a</sup>	MBuI, 2.50	0.1704	0.0305	4490.6	18.89	0.76	58.23	0.51
HB37 <sup>a</sup>	MBuI, 5.0	0.1704	0.0261	5292.5	23.44	0.94	46.93	0.39
HB38 <sup>a</sup>	MOcI, 2.50	0.1704	0.2337	14322	30.77	1.23	35.75	0.60
HB39 <sup>a</sup>	MOcI, 5.0	0.1704	0.4731	247923	422.08	16.88	2.61	0.75
HB40 <sup>a</sup>	MCEI, 2.50	0.1704	0.1279	16116	42.25	1.69	26.04	0.54
HB41 <sup>a</sup>	MCEI, 5.0	0.1704	0.1978	36012	81.89	3.28	14.43	0.58
HB42 <sup>b</sup>	-	0.1704	0.0802	11000	33.64	0.90	32.7	0.52
HB43 <sup>b</sup>	MBuI, 2.50	0.1704	0.0586	9280	31.47	0.84	34.95	0.51
HB44 <sup>b</sup>	MBuI, 5.0	0.1704	0.0460	9438	34.67	0.92	31.73	0.50
HB45 <sup>b</sup>	MOcI, 2.50	0.1704	0.2628	29286	60.53	1.61	18.17	0.61
HB46 <sup>b</sup>	MOcI, 5.0	0.1704	0.5314	548552	898.75	23.97	1.22	0.80
HB47 <sup>b</sup>	MCEI, 2.50	0.1704	0.1612	33582	81.56	2.17	13.49	0.56
HB48 <sup>b</sup>	MCEI, 5.0	0.1704	0.2138	36247	80.20	2.14	13.72	0.58

\* Measurements Temperature= 37 °C, <sup>a</sup>[BIS] =  $2.50 \times 10^{-2}$  mol/L, <sup>b</sup>[BIS] =  $3.75 \times 10^{-2}$  mol/L



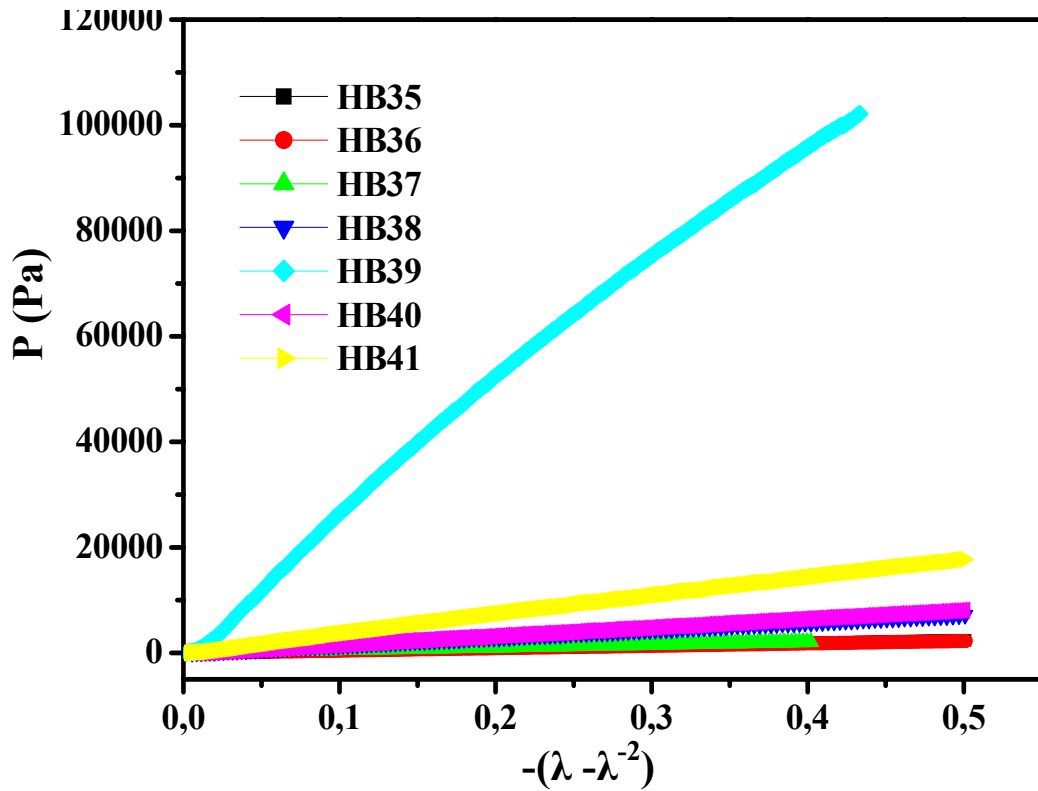
**Figure 4.22** : Measured Force,  $F$  (N) as a Function of Compression (mm) for Samples HB35, HB36, HB37, HB38, HB39, HB40, and HB41 are Given in Table 4.4. ( $T_{\text{swelling}} = 23^{\circ}\text{C}$ )

Figure 4.22-4.27 and, Table 4.4 and 4.5 show a comparison of the mechanical behaviors and network parameters of NIPAAm/monoesters of IA copolymer hydrogels crosslinked with BIS ( $2.50 \times 10^{-2}$  mol/L), under uniaxial compression. Figure 4.22 and 4.23 show measured force ( $F$ ) for compressing Samples HB35-HB41 at  $23^{\circ}\text{C}$  and  $37^{\circ}\text{C}$ , respectively. Force ( $F$ ) or loads corresponding to compressions (mm) were obtained from the original curves of uniaxial compression experiments. Pressure ( $\text{Pa}$ ) – Linear deformation factor,  $-(\lambda - \lambda^2)$  plots of all samples were drawn by using the data obtained from the linear portions of Load (N) versus compression (mm) curves (Figure 4.24 and 4.25). The slope of these straight lines, i.e. compression moduli (or shear moduli)  $G$  were calculated from equation (3,4), polymer volume fractions at equilibrium and relaxed states and equation (3,5) were used to compute the effective network concentration,  $\nu_e$ .



**Figure 4.23** : Measured Force,  $F$  (N) as a Function of Compression (mm) for Samples HB35, HB36, HB37, HB38, HB39, HB40, HB41 Given in Table 4.5 ( $T_{\text{swelling}} = 37^{\circ}\text{C}$ )

From the data in Table 4.4 and 4.5 it was seen that the compression moduli and crosslinking densities of NIPAAm hydrogels containing 2.50 and 5.0 mole % of monoesters of IA in the feed and crosslinked with BIS ( $2.50 \times 10^{-2}$  mol/L) increase with temperature and alkyl chain length in the order of MCEI > MOcI > MBuI. Both the temperature ( $37^{\circ}\text{C}$ ) being higher than the LCST ( $\sim 32^{\circ}\text{C} - 34^{\circ}\text{C}$ ), and the increase in the length of the alkyl chain results in an increase of hydrophobicity and so the mechanical strength of the gels.



**Figure 4.24** : Compression Stress-strain Curves (Pressure (Pa) vs.  $-(\lambda-\lambda^{-2})$ ) for Samples HB35, HB36, HB37, HB38, HB39, HB40, and HB41 are Given in Table 4.4. ( $T_{\text{swelling}} = 23^{\circ}\text{C}$ )

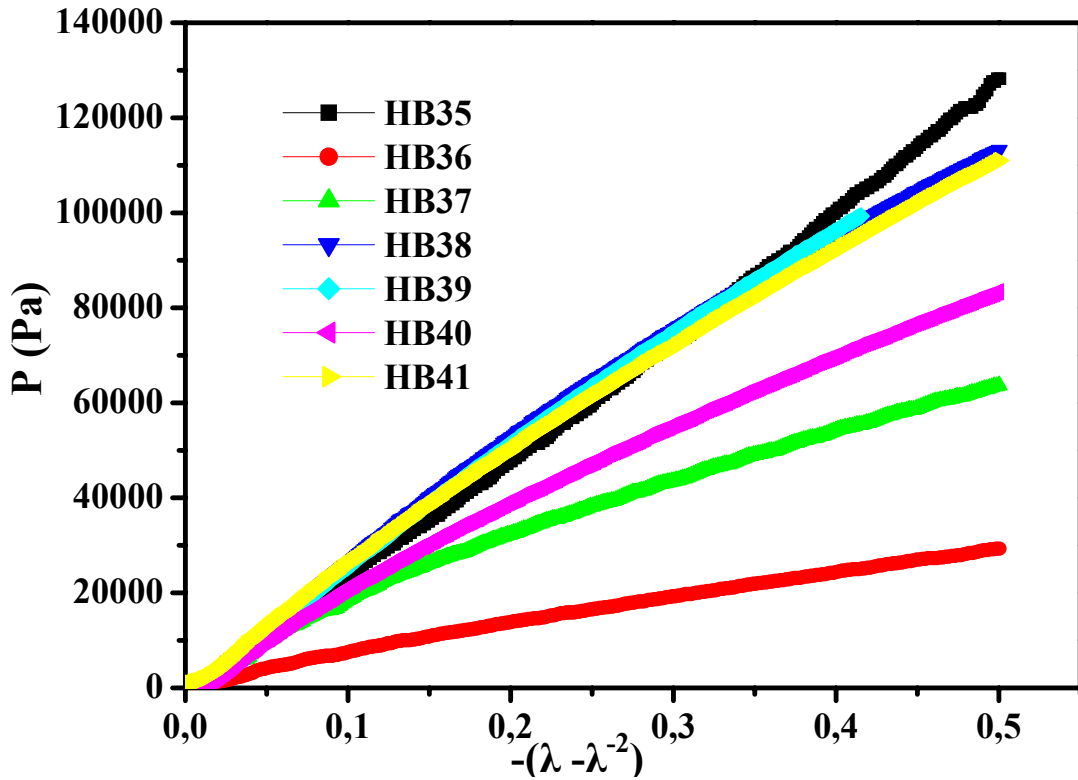


**Figure 4.25** : Compression Stress-strain Curves (Pressure (Pa) vs.  $-(\lambda-\lambda^{-2})$ ) for Samples HB35, HB36, HB37, HB38, HB39, HB40, and HB41, Given in Table 4.5. ( $T_{\text{swelling}} = 37^{\circ}\text{C}$ )

The photographs in Figure 4.26 shows the changes in morphologies of the hydrogels during the shrinking process. The bubble formation on the surfaces of the gels was observed, for the ones containing hydrophobic modified comonomer, i.e. monoesters of itaconic acid. Both shrinking degree and the bubbles were increased with increasing length of alkyl chains of monoitaconates.

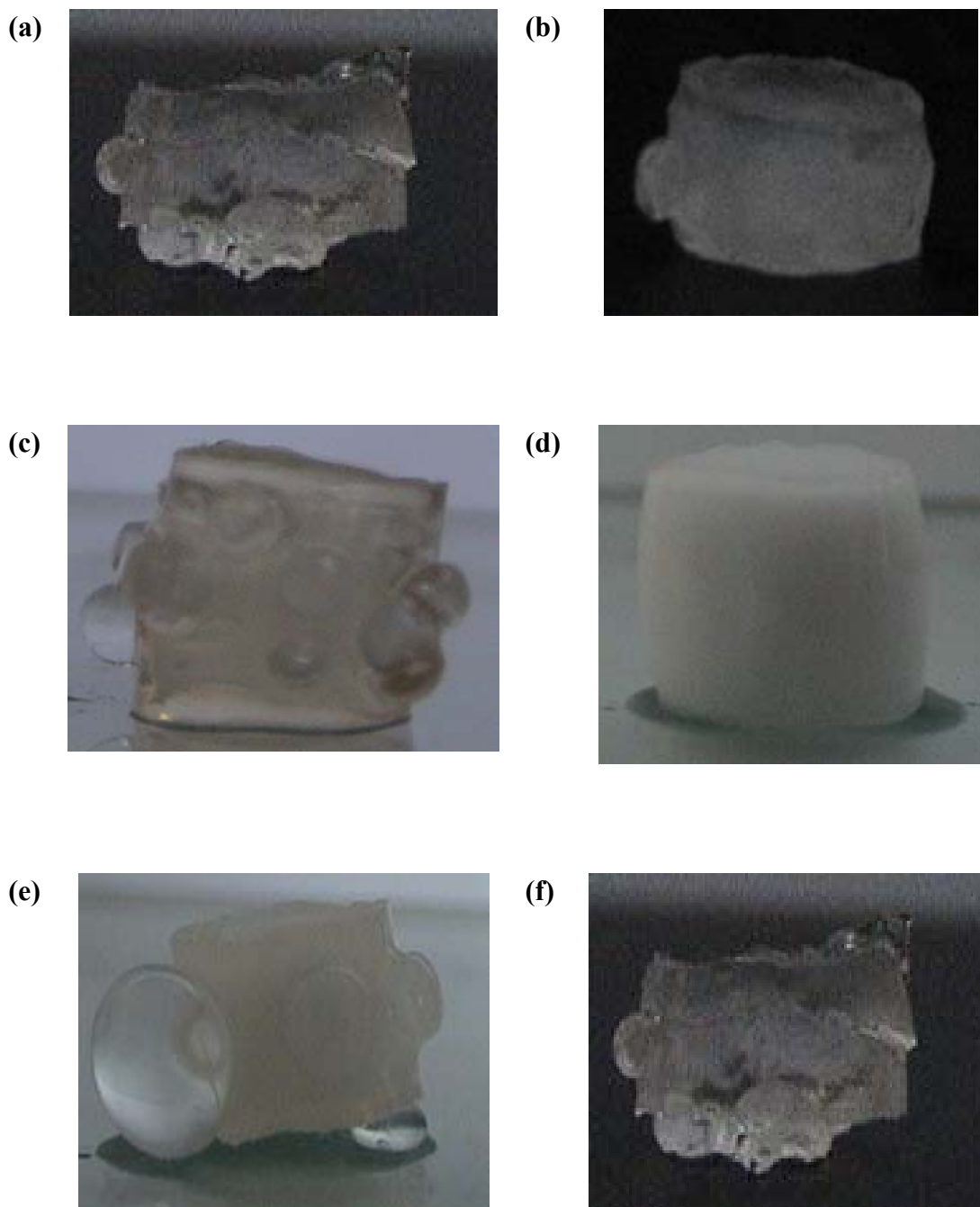


**Figure 4.36** : Series of Photograph Showing the Morphology of PNIPAAm Hydrogels Equilibrated in DDW 37°C, (a) HB36, (b) HB37, (c) HB38, (d) HB39, (e) HB40, (f) HB41.

Figure 4.27-4.30 and, Table 4.4 and 4.5 show a comparison of the shrinking behavior and network parameters of PNIPAAm and NIPAAm/monoesters of IA copolymer hydrogels crosslinked with BIS ( $3.75 \times 10^{-2}$  mol/L), under uniaxial compression. Figure 4.27 and 4.28 show measured force (**F**) for compressing Samples HB42 - HB48 at 23°C and 37°C, respectively. Force (**F**) or loads corresponding to compressions (mm) were obtained from the original curves of uniaxial compression experiments. Pressure (**Pa**) – Linear deformation factor,  $-(\lambda-\lambda^2)$  plots of all samples were drawn by using the data obtained from the linear portions of Load (**N**) versus compression (mm) curves (Figure 4.29 and 4.30). The slope of these straight lines, i.e. compression moduli (or shear moduli) **G** were calculated from equation (3,4), polymer volume fractions at equilibrium and relaxed states and equation (3,5) were used to compute the effective network concentration,  $v_e$ .

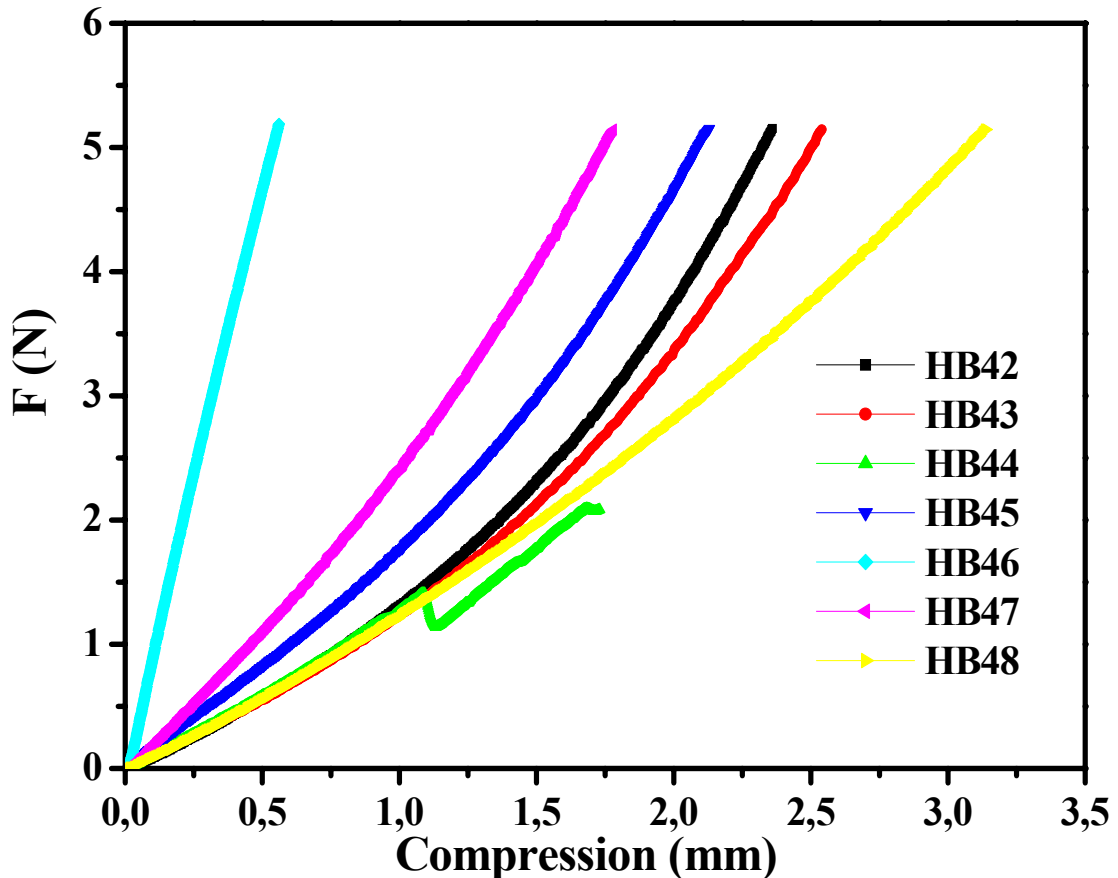


**Figure 4.27** : Measured Force, F (N) as a Function of Compression (mm) for Samples HB42, HB43, HB44, HB45, HB46, HB47, HB48 Given in Table 4.4 ( $T_{\text{swelling}} = 23^\circ\text{C}$ )

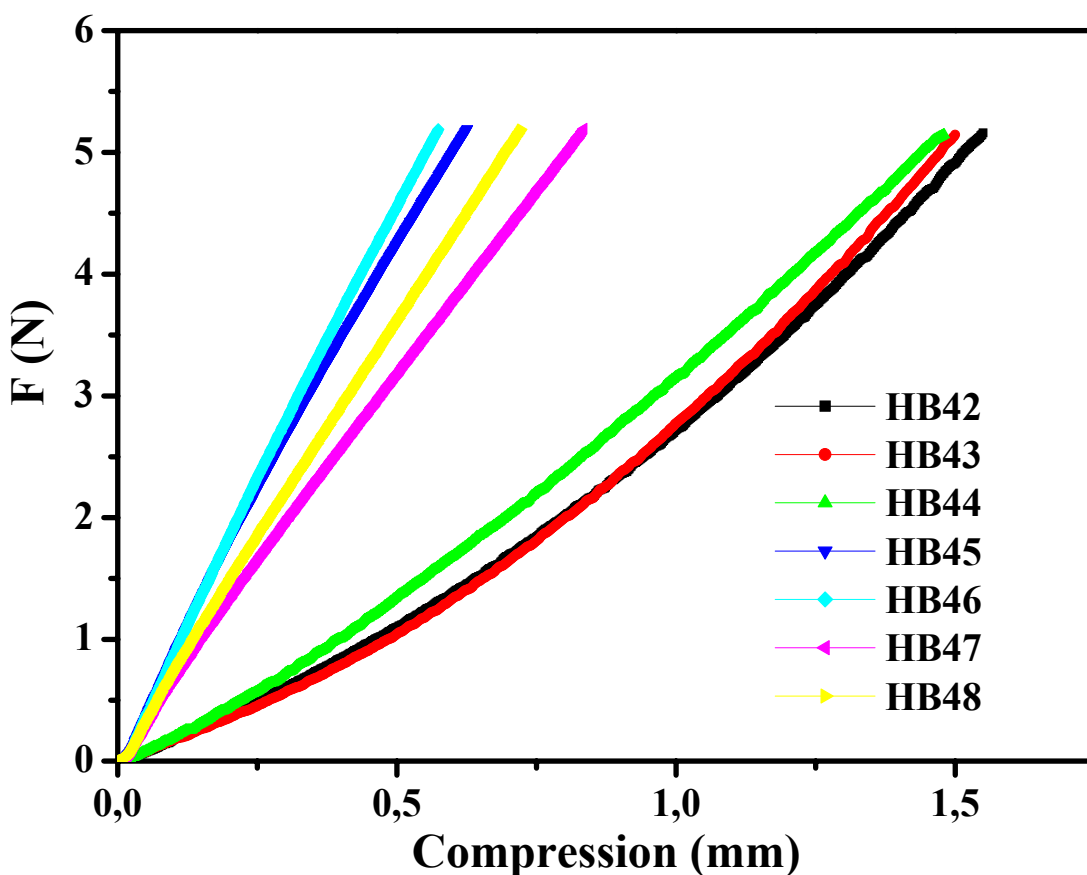


**Figure 4.28** : Measured Force,  $F$  (N) as a Function of Compression (mm) for Samples HB42, HB43, HB44, HB45, HB46, HB47, HB48 Given in Table 4.5 ( $T_{\text{swelling}} = 37^{\circ}\text{C}$ )

From the data in Table 4.4 and 4.5 it was seen that the compression moduli and crosslinking densities of NIPAAm hydrogels containing 2.50 and 5.0 mole % of monoesters of IA in the feed and crosslinked with BIS ( $3.75 \times 10^{-2}$  mol/L) increase with temperature and alkyl chain length in the order of MCEI > MOCI > MBUI. Both the temperature ( $37^{\circ}\text{C}$ ) being higher than the LCST ( $\sim 32^{\circ}\text{C} - 34^{\circ}\text{C}$ ), and the increase in the length of the alkyl chain results in an increase of hydrophobicity and so the mechanical strength of the gels.

The compression moduli and crosslinking densities of the gels containing 5.0 mole % of MOCI crosslinked with concentrated solution of BIS ( $3.75 \times 10^{-2}$  mol/L) were highly greater than those of the ones synthesized with  $2.5 \times 10^{-2}$  mol/L concentration of BIS. The results indicate that both covalent bonds (primary interactions) between the NIPAAm chains and hydrophobic interactions resulting from the hydrophobic octyl chains (secondary interactions) depends on the optimum conditions of crosslinker concentration and n-alkyl chain length.

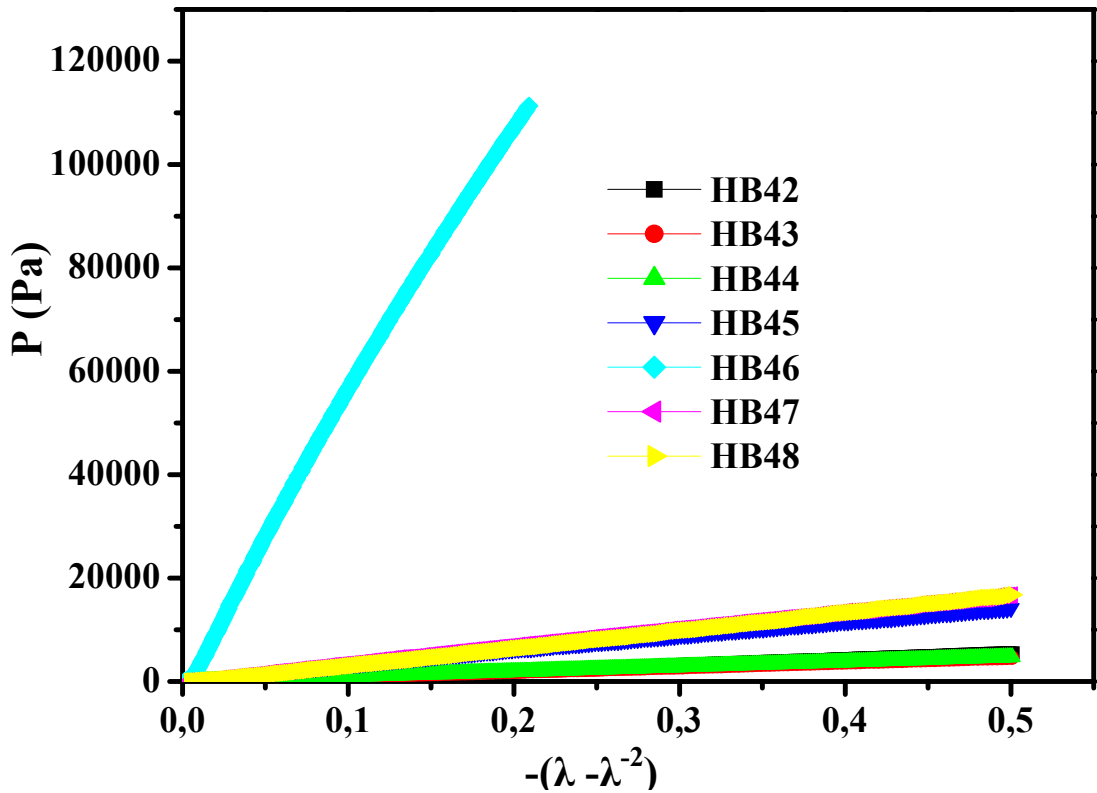


**Figure 4.29** : Compression Stress-strain Curves (Pressure (Pa) vs.  $-(\lambda-\lambda^{-2})$ ) for Samples HB42, HB43, HB44, HB45, HB46, HB47, and HB48 Given in Table 4.4. ( $T_{\text{swelling}} = 23^{\circ}\text{C}$ )

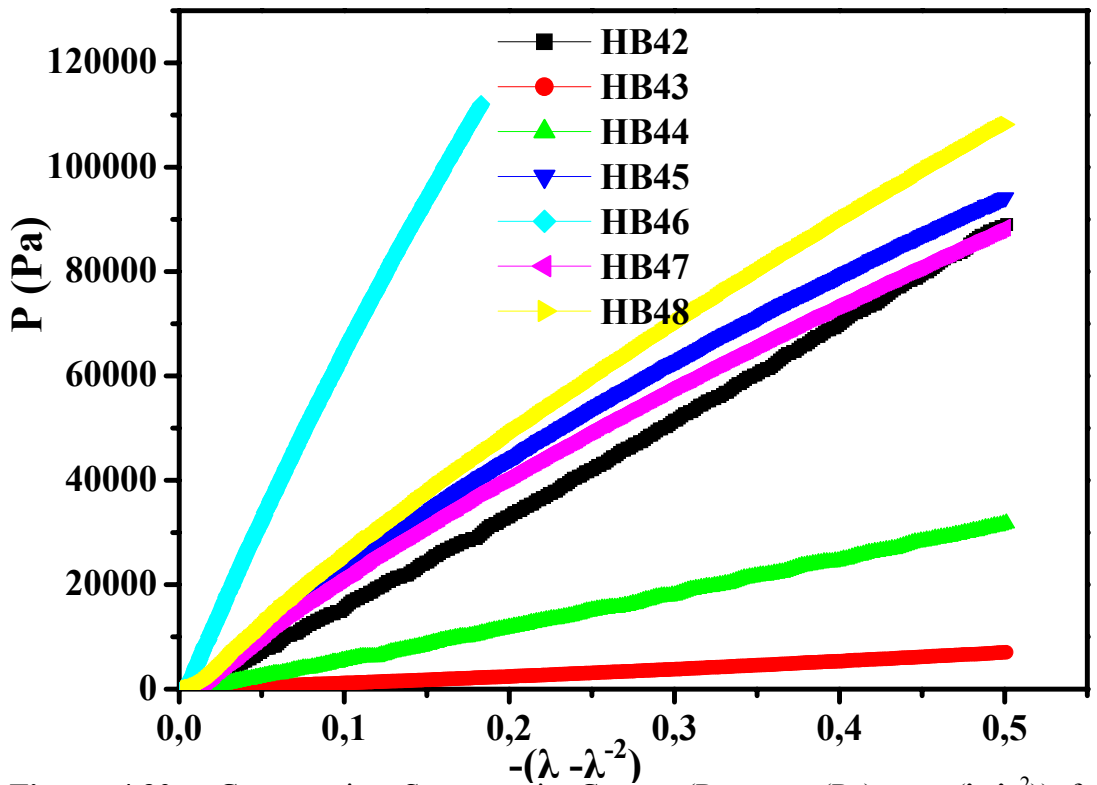


**Figure 4.30** : Compression Stress-strain Curves (Pressure (Pa) vs.  $-(\lambda-\lambda^{-2})$ ) for Samples HB42, HB43, HB44, HB45, HB46, HB47, and HB48 Given in Table 4.5. ( $T_{\text{swelling}} = 37^{\circ}\text{C}$ )

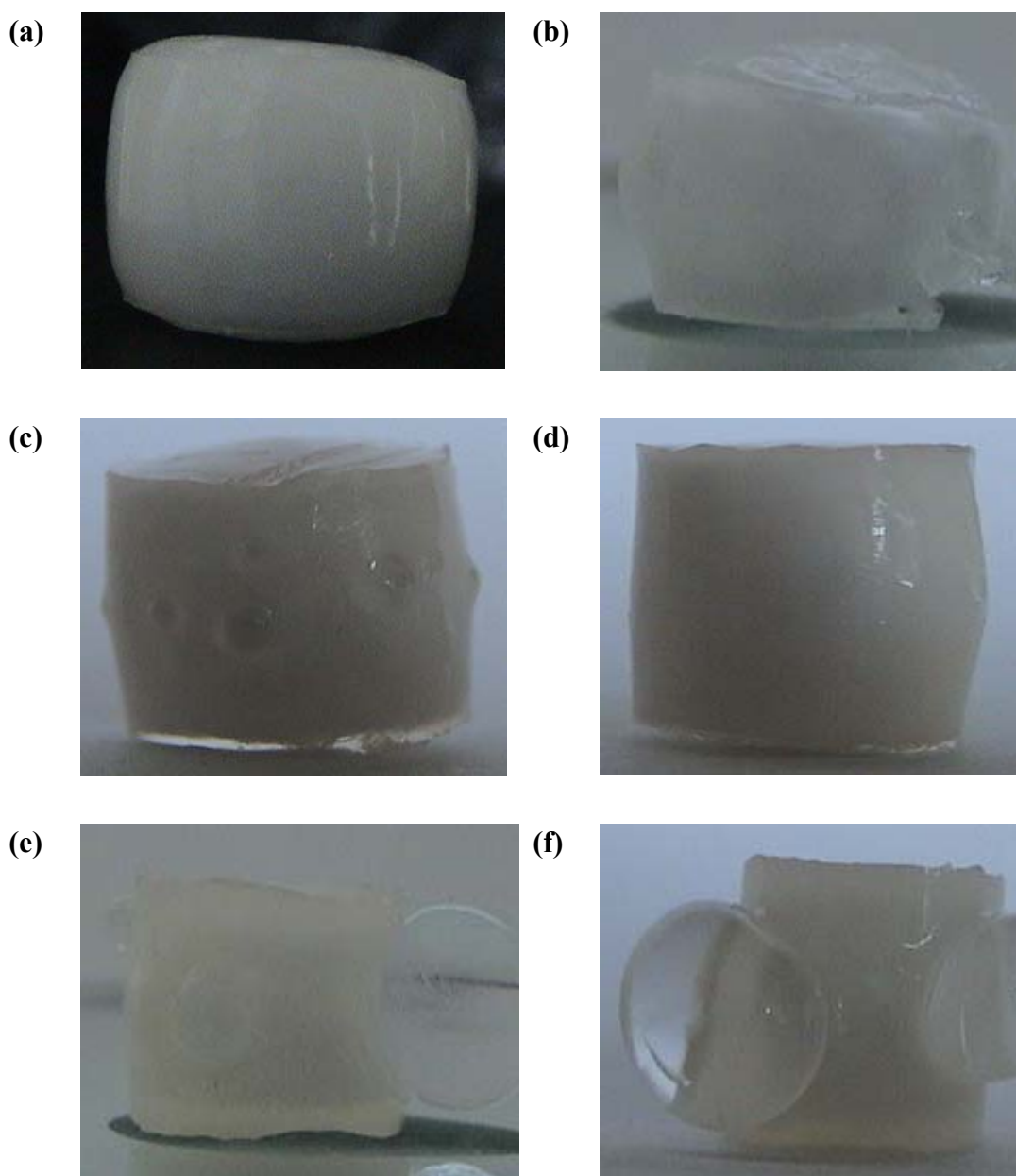


**Figure 4.31** : Series of Photograph Showing the Morphology of NIPAAm/monoitaconate Hydrogels Crosslinked with  $3.75 \times 10^{-2}$  mol/L Concentration of BIS in DDW at  $37^{\circ}\text{C}$ : (a) HB42, (b) HB43, (c) HB45, (d) HB46, (e) HB47, (g) HB48

The photographs in Figure 4.31 shows the changes in morphologies of the hydrogels during the shrinking process. The bubble formation on the surfaces of the gels was observed, for the ones containing hydrophobic modified comonomer, i.e. monoesters of itaconic acid. Both shrinking degree and the bubbles were increased with increasing length of alkyl chains of monoitaconates.

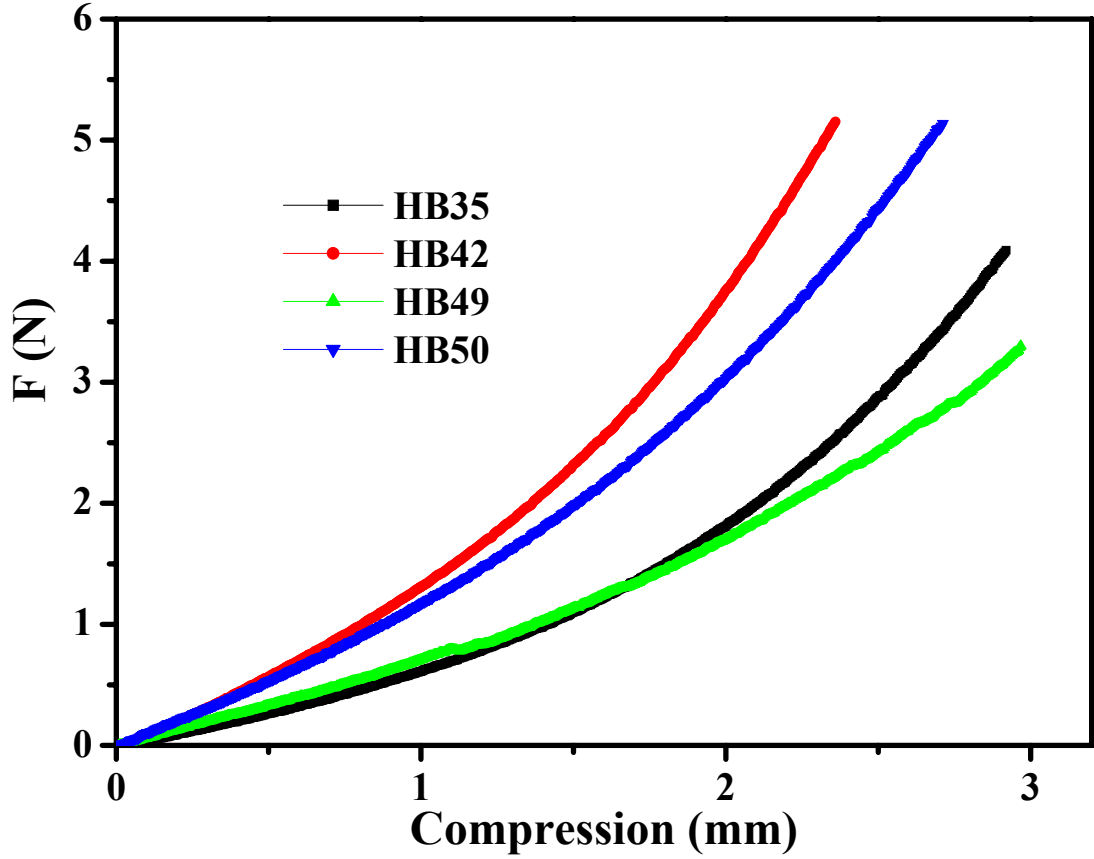


**Figure 4.32** : Measured Force,  $F$  (N) as a Function of Compression (mm) for Samples HB35, HB42, HB49, HB50 Given in Table 4.4 ( $T_{\text{swelling}} = 23^{\circ}\text{C}$ )

Figure 4.32-4.33 and, Table 4.14 show a comparison of the mechanical behaviors and network parameters of PNIPAAm and NIPAAm/IA copolymer hydrogels crosslinked with two different concentrations of BIS ( $2.50 \times 10^{-2}$  mol/L and  $3.75 \times 10^{-2}$  mol/L), under uniaxial compression. Figure 4.32 shows the measured force ( $F$ ) for compressing Samples HB35-HB42, HB49 and HB50 at  $23^{\circ}\text{C}$ . Force ( $F$ ) or loads corresponding to compressions (mm) were obtained from the original curves of uniaxial compression experiments.

Pressures (Pa) – Linear deformation factor,  $-(\lambda - \lambda^2)$  plots of all samples were drawn by using the data obtained from the linear portions of Load (N) versus compression (mm) curves (Figure 4.33). The slope of these straight lines, i.e. compression moduli (or shear moduli)  $G$  were calculated from equation (3,4), polymer volume fractions at equilibrium and relaxed states and equation (3,5) were used to compute the effective network concentration,  $\nu_e$ .

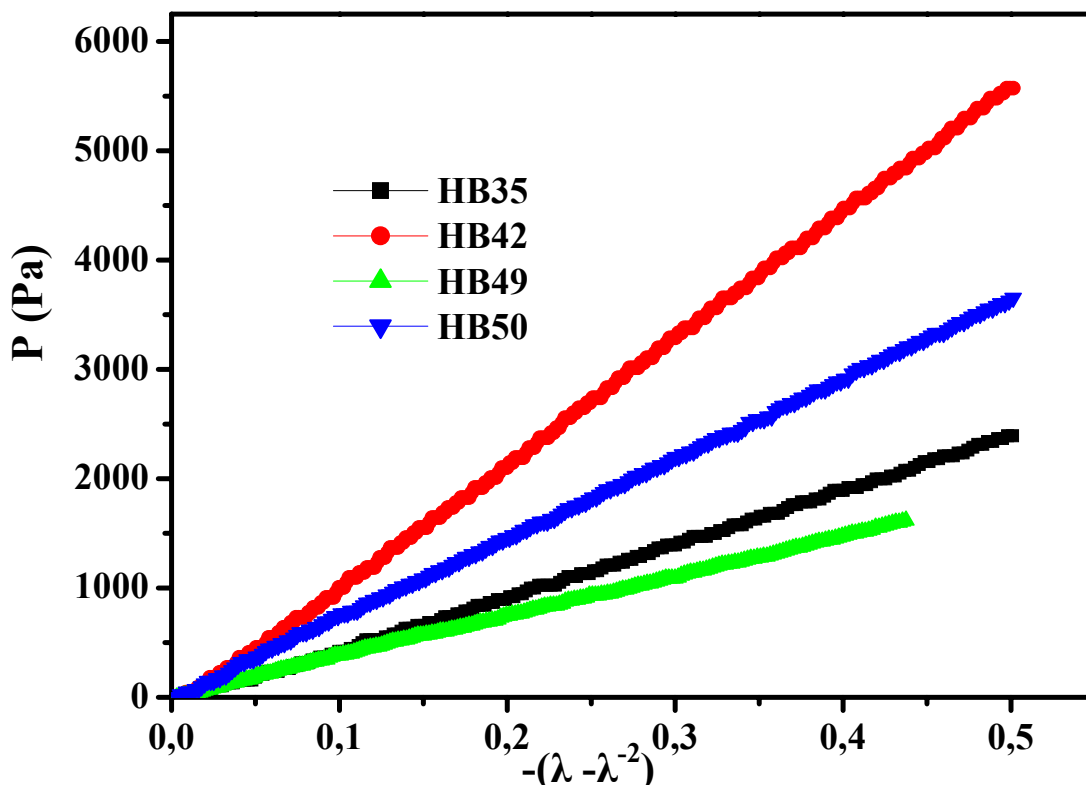


**Figure 4.33** : Compression Stress-strain Curves (Pressure (Pa) vs.  $-(\lambda - \lambda^{-2})$ ) for Samples HB35, HB42, HB49, and HB40 Given in Table 4.4. ( $T_{\text{swelling}} = 23^{\circ}\text{C}$ )

From the data in Table 4.4 it was seen that the compression moduli and crosslinking densities of PNIPAAm hydrogels and NIPAAm/IA copolymer hydrogels containing 2.50 mole % of IA in the feed and crosslinked with two different concentrations of BIS ( $2.50 \times 10^{-2}$  mol/L and  $3.75 \times 10^{-2}$  mol/L) increase with increase in the crosslinker concentration of, i.e. primary interactions between the NIPAAm chains. On the other hand, the presence of IA (hydrophilic and ionic  $-\text{COOH}$  and  $-\text{COO}^-$  groups) decreased the mechanical strength of the network structures because of the repulsive forces between the  $-\text{COO}^-$  groups.

**Table 4.6 :** Polymer Volume Fractions ( $v_{2r}$ ,  $v_{2s}$ ), Compression Moduli (G) and Polymer-water Interaction Parameters ( $\chi$ ) at 23 °C and 37 °C for PNIPAAm and NIPAAm/MOcI Hydrogels Prepared Using BIS and  $K_2S_2O_8$  as Crosslinker and Initiator

Sample No.	$d_0$ (mm)	$d$ (mm)	Cr.linker ( $\times 10^{-2}$ mol/L)	Comon. (mole %)	$v_{2r}$	$v_{2s}$	G (Pa)	$v_e$ (molm <sup>-3</sup> )	C.E.	$M_c$ (kg/mol)	$\chi$
HB11	6.25	8.46	BIS, 2.50	-	0.1704	0.0623	7864.6	26.14	1.05	33.28	0.51
HB51	10.63	14.06	BIS, 2.50	MOcI, 2.50	<sup>a</sup> 0.1704	<sup>a</sup> 0.0736	<sup>a</sup> 724.1	<sup>a</sup> 2.28	<sup>a</sup> 0.09	<sup>a</sup> 381.58	<sup>a</sup> 0.52
HB52	10.75	12.80	BIS, 3.75	MOcI, 2.50	<sup>a</sup> 0.1704	<sup>a</sup> 0.1009	<sup>a</sup> 736.8	<sup>a</sup> 2.09	<sup>a</sup> 0.06	<sup>a</sup> 416.27	<sup>a</sup> 0.54
HB53	10.93	13.50	BIS, 2.50	MOcI, 5.0	<sup>a</sup> 0.1704	<sup>a</sup> 0.0904	<sup>a</sup> 2981.3	<sup>a</sup> 8.76	<sup>a</sup> 0.35	<sup>a</sup> 99.32	<sup>a</sup> 0.60
HB54	10.87	11.83	BIS, 3.75	MOcI, 5.0	<sup>a</sup> 0.1704	<sup>a</sup> 0.1322	<sup>a</sup> 8300.2	<sup>a</sup> 21.52	<sup>a</sup> 0.57	<sup>a</sup> 40.43	<sup>a</sup> 0.55
HB51	10.63	9.48	BIS, 2.50	MOcI, 2.50	<sup>b</sup> 0.1704	<sup>b</sup> 0.2402	<sup>b</sup> 7144.1	<sup>b</sup> 14.52	<sup>b</sup> 0.58	<sup>b</sup> 59.92	<sup>b</sup> 0.60
HB52	10.75	9.51	BIS, 3.75	MOcI, 2.50	<sup>b</sup> 0.1704	<sup>b</sup> 0.2461	<sup>b</sup> 7009.7	<sup>b</sup> 14.14	<sup>b</sup> 0.38	<sup>b</sup> 61.53	<sup>b</sup> 0.60
HB53	10.93	9.33	BIS, 2.50	MOcI, 5.0	<sup>b</sup> 0.1704	<sup>b</sup> 0.2740	<sup>B</sup> 44839	<sup>b</sup> 87.29	<sup>b</sup> 3.49	<sup>b</sup> 9.97	<sup>b</sup> 0.65
HB54	10.87	9.28	BIS, 3.75	MOcI, 5.0	<sup>b</sup> 0.1704	<sup>b</sup> 0.2739	<sup>b</sup> 30162	<sup>b</sup> 58.72	<sup>b</sup> 1.57	<sup>b</sup> 9.81	<sup>b</sup> 0.61

[NIPAAm] = 2.0 mol/L, <sup>a</sup> 23 °C, <sup>b</sup> 37 °C

Figure 4.34-4.37 and, Table 4.6 show a comparison of the mechanical behaviors and network parameters of PNIPAAm and NIPAAm/MOCl copolymer hydrogels containing 2.50 and 5.0 mole % of MOCl and crosslinked with two different concentration of BIS ( $2.50 \times 10^{-2}$  mol/L and  $3.75 \times 10^{-2}$  mol/L) using  $K_2S_2O_8$  / TEMED redox pair as initiator in DDW, under uniaxial compression. Figure 4.34 and 4.35 show measured force (**F**) for compressing Samples HB11, HB51-HB54 at 23°C and 37°C, respectively. Force (**F**) or loads corresponding to compressions (mm) were obtained from the original curves of uniaxial compression experiments. Pressure (**Pa**) – Linear deformation factor,  $-(\lambda-\lambda^2)$  plots of all samples were drawn by using the data obtained from the linear portions of Load (**N**) versus compression (mm) curves (Figure 4.36 and 4.37). The slope of these straight lines, i.e. compression moduli (or shear moduli) **G** were calculated from equation (3,4), polymer volume fractions at equilibrium and relaxed states and equation (3,5) were used to compute the effective network concentration,  $v_e$ .

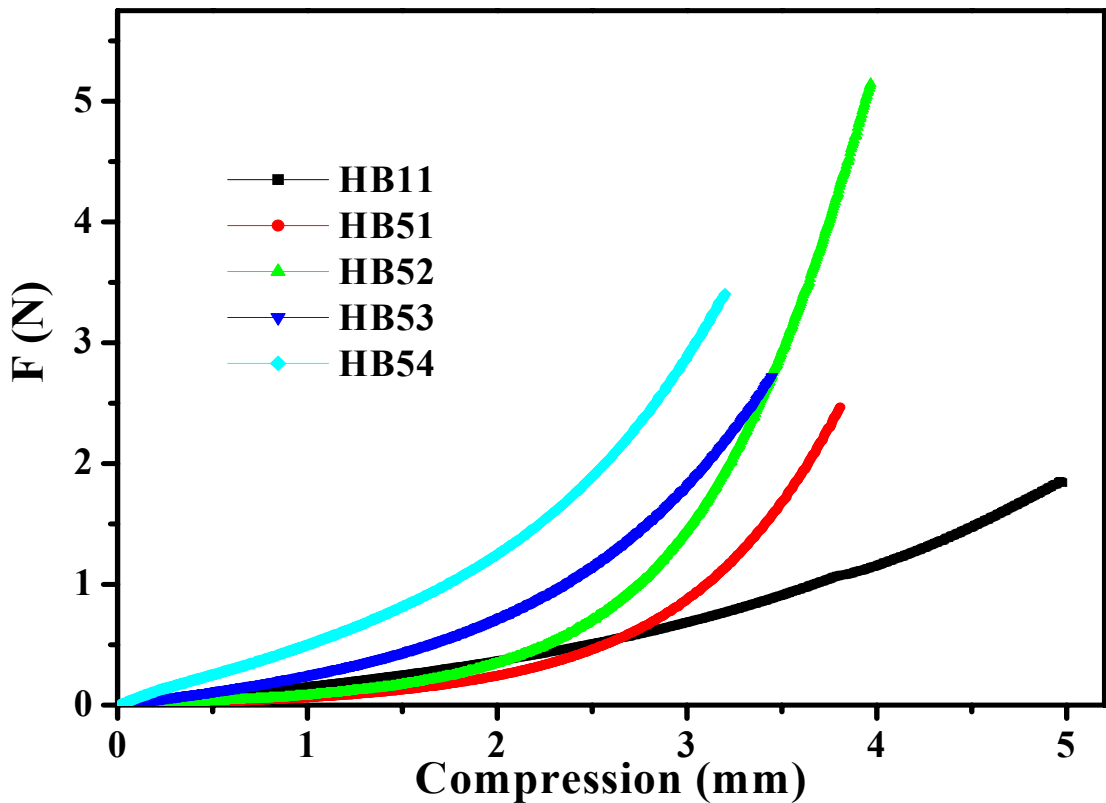


**Figure 4.34:** Measured Force, **F** (N) as a Function of Compression (mm) for Samples HB11, HB51, HB52, HB53, and HB54 Given in Table 4.6. ( $T_{\text{swelling}} = 23^\circ\text{C}$ )

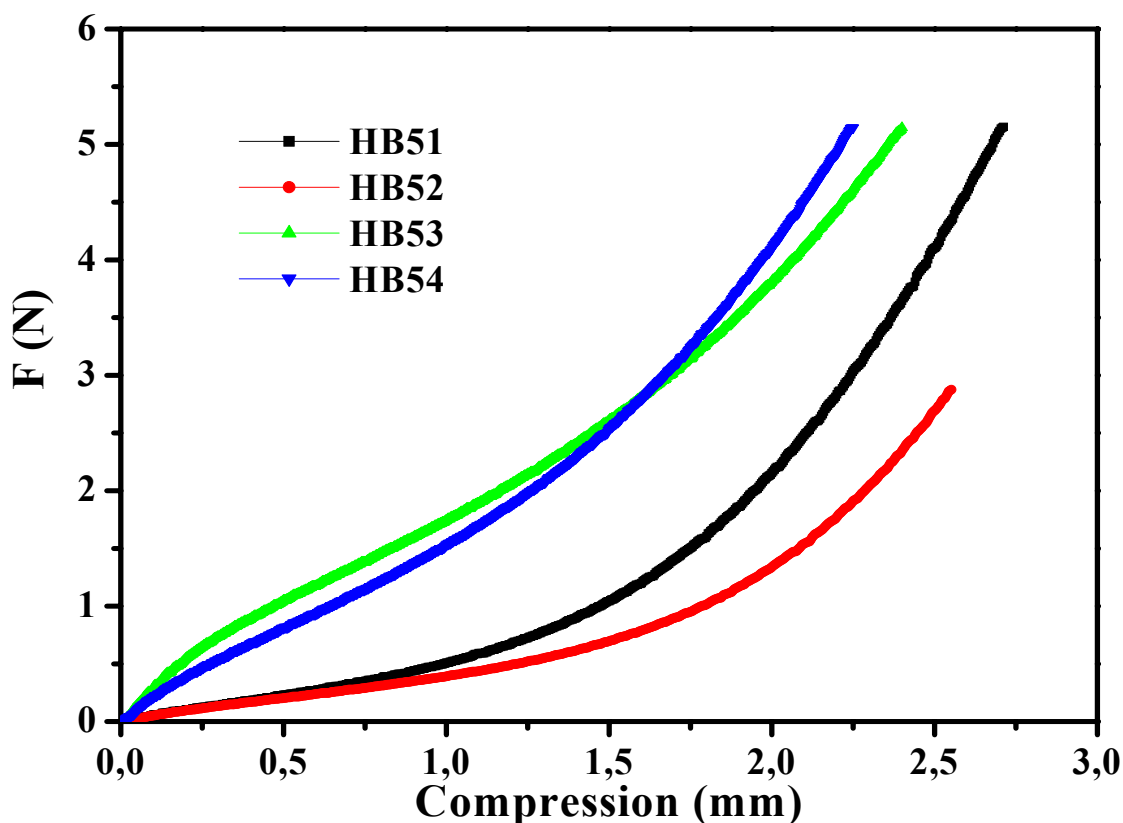


**Figure 4.35** : Measured Force,  $F$  (N) as a Function of Compression (mm) for Samples HB11, HB51, HB52, HB53, HB54 Given in Table 4.16 ( $T_{\text{swelling}} = 37^{\circ}\text{C}$ )

The compression moduli and crosslinking densities of the gels containing 2.50 and 5.0 mole % of MOcI and crosslinked with two different concentration of BIS ( $2.50 \times 10^{-2}$  mol/L and  $3.75 \times 10^{-2}$  mol/L) using  $\text{K}_2\text{S}_2\text{O}_8$  / TEMED redox pair as initiator at  $25^{\circ}\text{C}$  in DDW, were enormously lower greater than those of the ones initiated with AIBN at  $60^{\circ}\text{C}$  in 1,4-Dioxane. The results indicate that both covalent bonds (primary interactions) between the NIPAAm chains, i.e. crosslinking efficiency and reactivity of MOcI with long alkyl chain depends on the type of initiator and polymerization medium

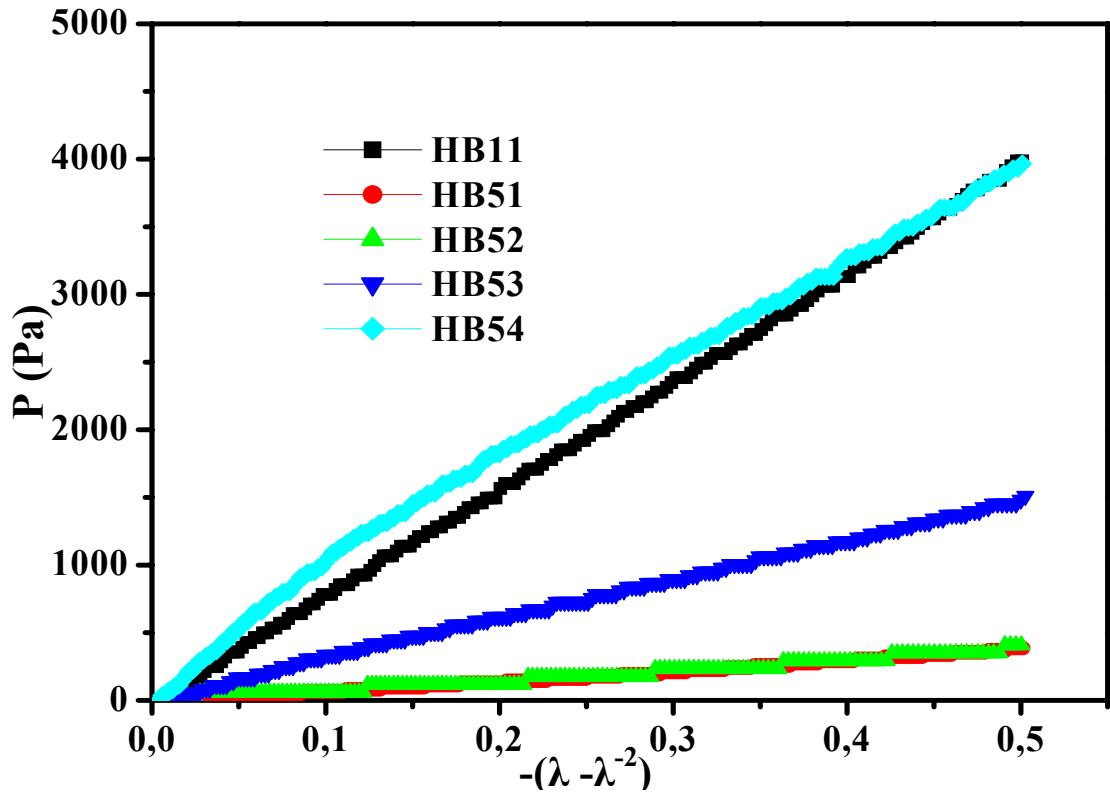


**Figure 4.36** : Compression Stress-strain Curves (Pressure (Pa) vs.  $-(\lambda-\lambda^{-2})$ ) for Samples HB11, HB51, HB52, HB53, and HB54 Given in Table 4.6. ( $T_{\text{swelling}} = 23^{\circ}\text{C}$ )

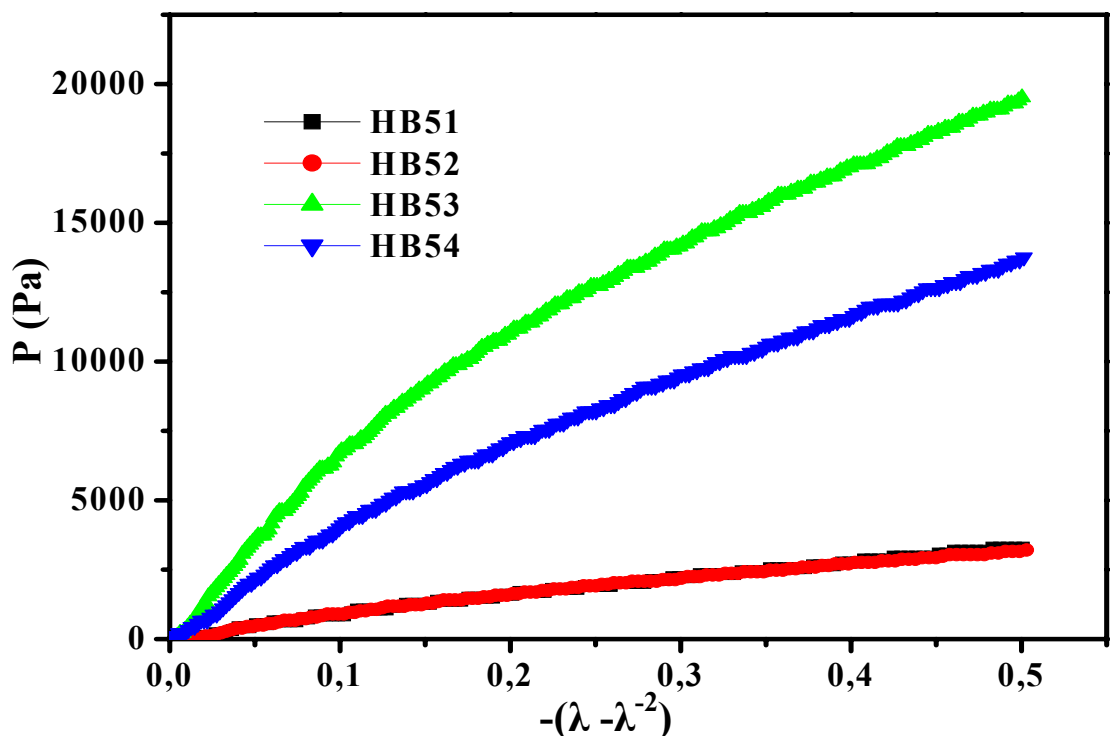


**Figure 4.37** : Compression Stress-strain Curves (Pressure (Pa) vs.  $-(\lambda-\lambda^{-2})$ ) for Samples HB51, HB52, HB53, and HB54 Given in Table 4.6. ( $T_{\text{swelling}} = 37^{\circ}\text{C}$ )

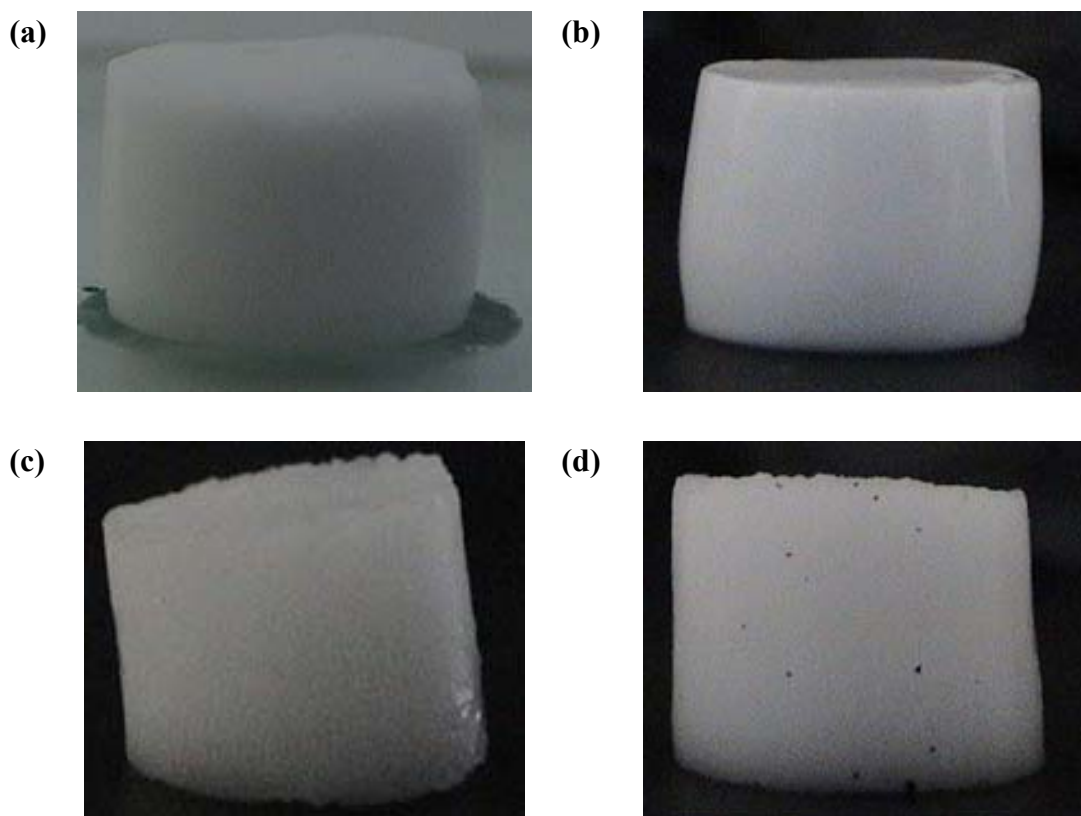


**Figure 4.38** : Series of Photograph Showing the Morphology of PNIPAAm Hydrogels in DDW at 37°C, (a) HB51, (b) HB52, (c) HB53, (d) HB54

The photographs in Figure 4.38 show the changes in morphologies of the hydrogels, which are identified in Table 4.6 during the shrinking process. The bubble formation on the surfaces of the gels was not observed, for the ones containing hydrophobically modified comonomer MOcI but synthesized with  $K_2S_2O_8$  / TEMED redox pair as initiator at DDW. From the relation between network parameters and external views of the hydrogels, network structure are estimated as follows, water decrease the solubilities of hydrophobic components and the hydrogels synthesized in water can have inhomogeneous network in the presence of MOcI as hydrophobically modified comonomer while the hydrogels synthesized in 1,4-Dioksane can exhibit heterogeneous external view but strongly increased mechanical strength, resulting from the hydrophobic interactions between octyl groups.

As can be seen from all of these tables and figures, higher effective crosslinking densities and crosslinking efficiencies are obtained for the NIPAAm copolymer hydrogels modified hydrophobically, using monoesters of IA. This means that to designate the materials having the right balance of repulsive and attractive forces,

being responsible for swelling and mechanical behaviors of the networks, it is necessary to control of the type and concentration of initiator crosslinker, and reaction medium and, the type and content of hydrophobic component, which improved the mechanical performance of the material.

#### 4.4. Drug release of Theophylline from PNIPAAm and its Copolymer Hydrogels Crosslinked with BIS and VTPDMS

The phase transition temperatures of NIPAAm hydrogels (corresponding to the LCSTs of linear polymers) are changed by increasing the hydrophobic part of a hydrophilic monomer. The same effect can be achieved by varying the compositions, in the case of copolymers, using comonomers, which are more or less hydrophilic.

PNIPAAm hydrogels show a volume phase transition in water at 34°C, going from a swollen to an unswollen state. This behavior could allow its use in intelligent systems for drug release. In this part, kinetics of theophylline loading and release, as a function of the hydrogel composition are described.

**Table 4.7 :** Initial Slope ( $k_{sr}$ ), Diffusional Exponent ( $n$ ) and Diffusion Parameter ( $k$ ) Values of PNIPAAm and PNIPAAm/IA Copolymeric Hydrogels at 25°C in DDW.

Sample No	Comonomer (mol %)	Crosslinker ( $\times 10^{-2}$ mol/L)	Initiator	$k_{sr}$	$k$	$n$
HB12	-	BIS, 1.25 <sup>a,c</sup>	K <sub>2</sub> S <sub>2</sub> O <sub>8</sub>	37,67	3,32	0,43
HB16	IA, 2.50	BIS, 1.25 <sup>a,c</sup>	K <sub>2</sub> S <sub>2</sub> O <sub>8</sub>	150,89	3,76	0,66
HP1	-	VTPDMS, 1.25 <sup>b,d</sup>	AIBN	14,04	2,28	0,31
HP3	IA, 1.00	VTPDMS, 1.25 <sup>b,d</sup>	AIBN	62,01	3,99	0,54
HP4	IA, 2.50	VTPDMS, 1.25 <sup>b,d</sup>	AIBN	127,95	5,53	0,75
HP6	IA, 7.50	VTPDMS, 2.50 <sup>b,d</sup>	AIBN	125,04	5,17	0,75

[NIPAAm]= 2.0 mol/L, <sup>a</sup> MetOH/DDW, <sup>b</sup> 1,4-Dioxane, <sup>c</sup> T=25°C, <sup>d</sup> T= 60 °C

**Table 4.8** : Initial Slope ( $k_{sr}$ ), Diffusional Exponent ( $n$ ) and Diffusion Parameter ( $k$ ) Values of PNIPAAm and PNIPAAm/IA Copolymeric Hydrogels at 25°C in pH 7.50 Phosphate Buffer

Sample No	Comonomer (mol %)	Crosslinker ( $\times 10^{-2}$ mol/L)	Initiator	$k_{sr}$	$k$	$n$
HB12	-	BIS, 1.25 <sup>a,c</sup>	$K_2S_2O_8$	37,96	3,36	0,44
HB16	IA, 2.50	BIS, 1.25 <sup>a,c</sup>	$K_2S_2O_8$	45,25	3,61	0,46
HP1	-	VTPDMS, 1.25 <sup>b,d</sup>	AIBN	11,74	2,15	0,27
HP3	IA, 1.00	VTPDMS, 1.25 <sup>b,d</sup>	AIBN	38,02	2,99	0,44
HP4	IA, 2.50	VTPDMS, 1.25 <sup>b,d</sup>	AIBN	44,63	3,42	0,49
HP6	IA, 7.50	VTPDMS, 2.50 <sup>b,d</sup>	AIBN	45,59	3,28	0,51

[NIPAAm]= 2.0 mol/L, <sup>a</sup> MetOH/DDW, <sup>b</sup> 1,4-Dioxane, <sup>c</sup> T=25°C, <sup>d</sup> T= 60 °C

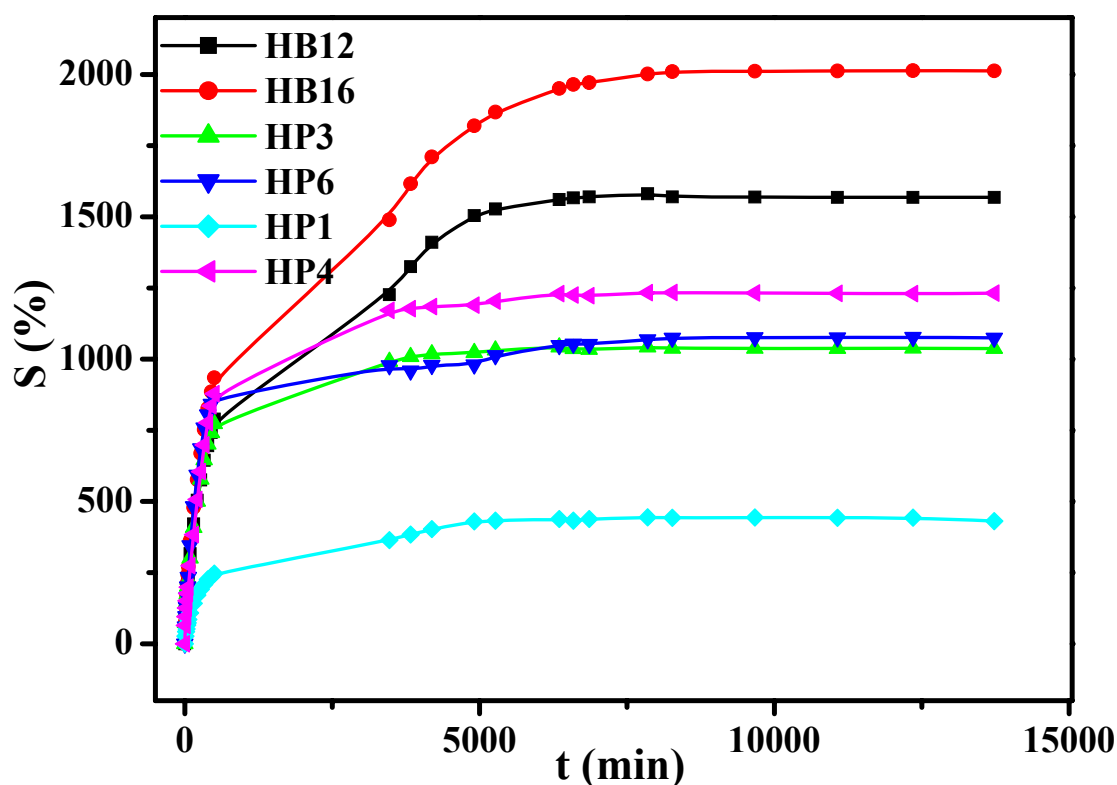


**Figure 4.39** : Percentage Mass Swelling as a Function of Time for the Series of NIPAAm Hydrogels at 25°C in pH 7.5 Phosphate Buffer

Figures 4.39 and 4.41 show the dynamic water and phosphate buffer swelling plots of PNIPAAm (HB 12) and NIPAAm/IA (HB 16) (2.5 mol % of IA) copolymers crosslinked with BIS ( $1.25 \times 10^{-2}$  mol/L) and initiated with KPS/TEMED redox pair in DDW/MetOH mixture and, PNIPAAm (HP 1) and NIPAAm/IA (HB 3, 4 and 6) (1.0, 2.5 and 7.5 mol % of IA) copolymers crosslinked with VTPDMS ( $1.25 \times 10^{-2}$  mol/L) and initiated with AIBN in 1,4-Dioxane. As can be seen from the figures, equilibrium percentage mass swelling in both water and phosphate buffer of PNIPAAm crosslinked with BIS is higher than the one crosslinked with VTPDMS. This result supports the effect of hydrophobic crosslinker on the diffusion process of solvent in to the hydrogel. For the samples containing ionizable comonomer IA, equilibrium percentage mass swelling increased with increasing repulsive forces resulting from  $-\text{COO}^-$  groups. In the presence of VTPDMS as crosslinker, the percentages in water are higher than in phosphate buffer.

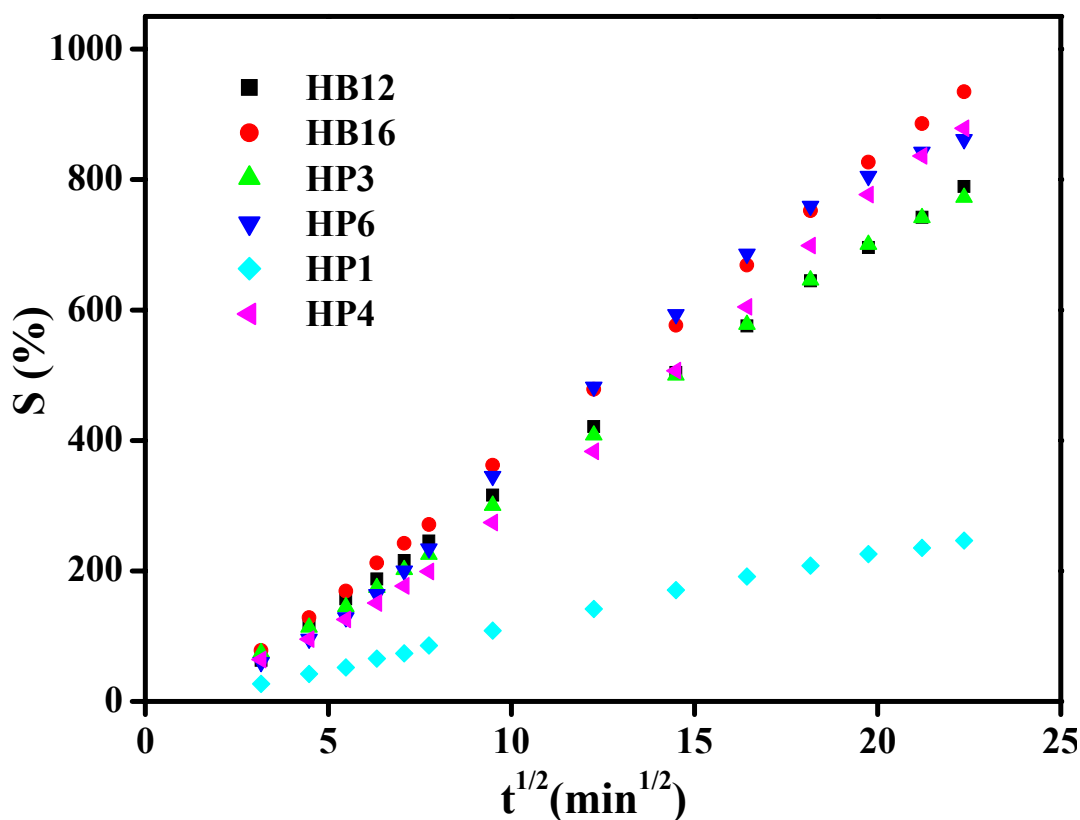


**Figure 4.40** : The Plot of Percentage Mass Swelling vs Square Root of Time for NIPAAm Hydrogels at 25°C in pH 7.5 Phosphate Buffer

The swelling curves of PNIPAAm and NIPAAm/ IA copolymer hydrogels in phosphate water and in water were used for the calculation of a certain diffusion characteristics.

Swelling rate curves of the PNIPAAm and NIPAAm/IA copolymer hydrogels are shown in Figures 4.40 and 4.42. The swelling rate constants of the hydrogels were calculated from equation (3,9) and the initial slopes ( $k_{sr}$ ) were presented in Tables 4.7 and 4.8. The results show that the initial slopes of the curves increase with the increase of IA concentration: this is a result of the electrostatic repulsion of the next  $-COO^-$  groups in the hydrogel structure. On the other hand, diffusion media and the ratio of hydrophobic/hydrophobic components affect the rate of diffusion.

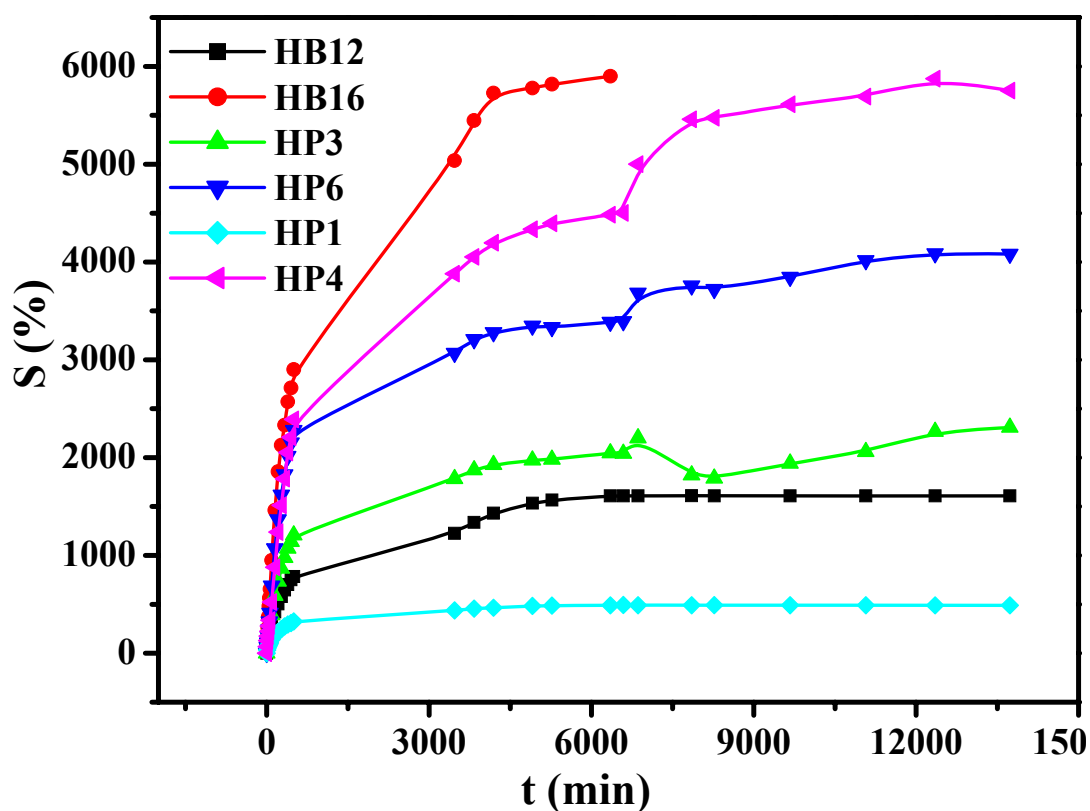


**Figure 4.41** : Percentage Mass Swelling as a Function of Time for the Series of NIPAAm Hydrogels at 25°C in Distilled Water

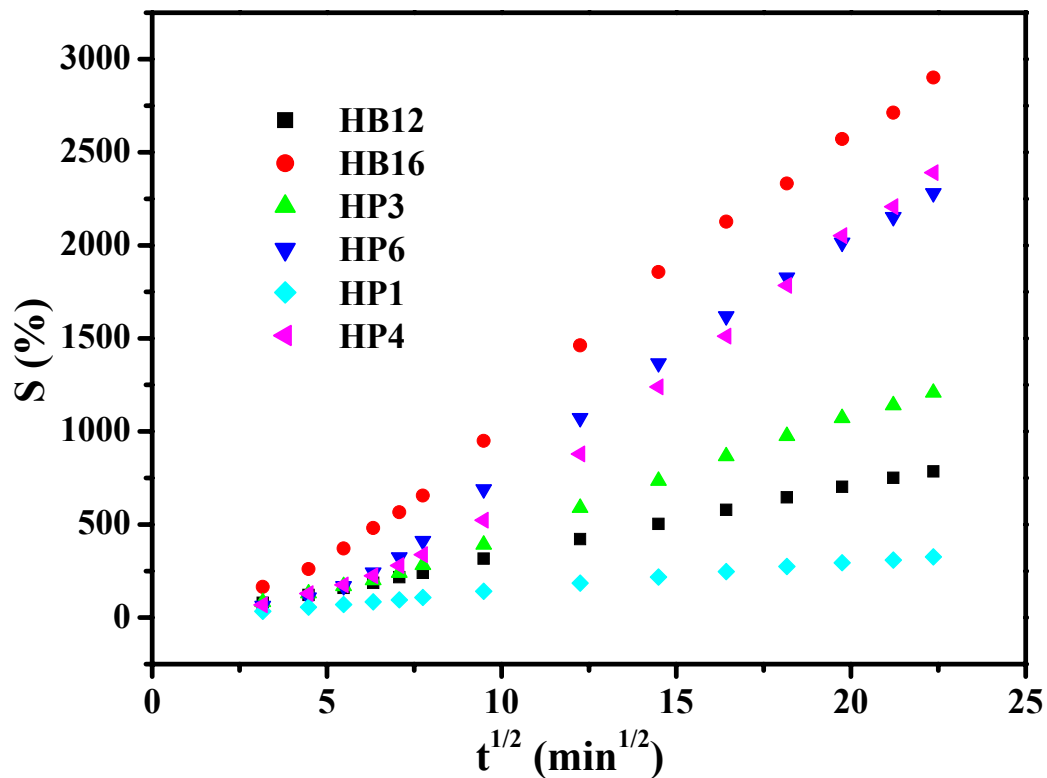


**Figure 4.42 :** The Plot of Percentage Mass Swelling vs Square Root of Time for NIPAAm Hydrogels at 25°C in Distilled Water

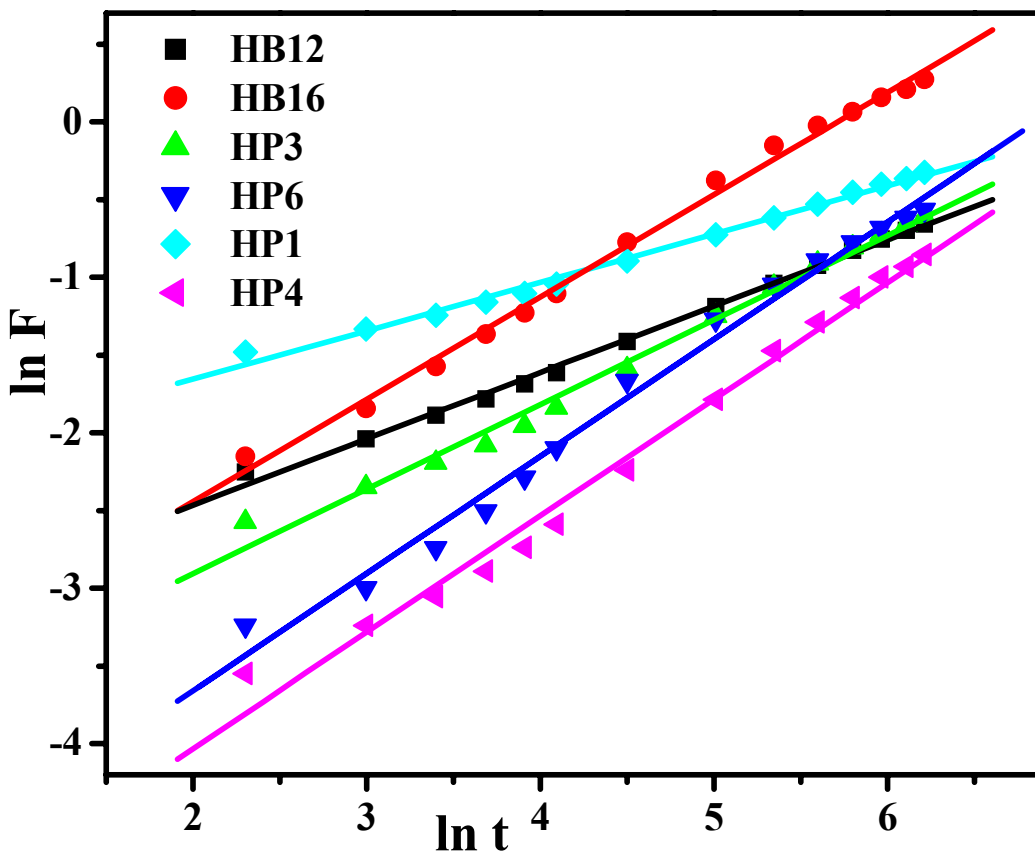


**Figure 4.43 :** The Plot of  $\ln F$  vs  $\ln t$  for the series of NIPAAm Hydrogels at Different Comonomer Concentration at 25°C in Distilled Water

To better understand the solvent absorption behavior of these hydrogels, equations (3,10) and (3,11) were used. The plots of  $\ln F$  versus  $\ln t$  for the series of PNIPAAm and NIPAAm/IA copolymer hydrogels crosslinked with BIS and VTPDMS are shown in Figures 4.43 and 4.44. The exponents  $k$  and  $n$  values were calculated from the slope and intercept of the lines, respectively, and are presented in Tables 4.7 and 4.8. It is clear from the analysis that as the itaconic acid content in the hydrogel structure increases the diffusional release kinetics exponent  $n$ , which is indicative of the transport mechanism, increases from 0.30 to 0.75 for PNIPAAm and NIPAAm/IA hydrogels with different IA content and crosslinker structure.

For Fickian kinetics in which the rate of penetrate diffusion is rate limiting,  $n = 0.5$ , whereas values of  $n$  between 0.5 and 1.0 indicate the contribution of non-Fickian processes, depending on the polymer relaxation.

The results in Tables 4.7 and 4.8 indicate that the swelling transport mechanism was transferred from Fickian to non-Fickian transport with increasing IA content and changing of hydrophilic/hydrophobic component ratio and diffusion medium.

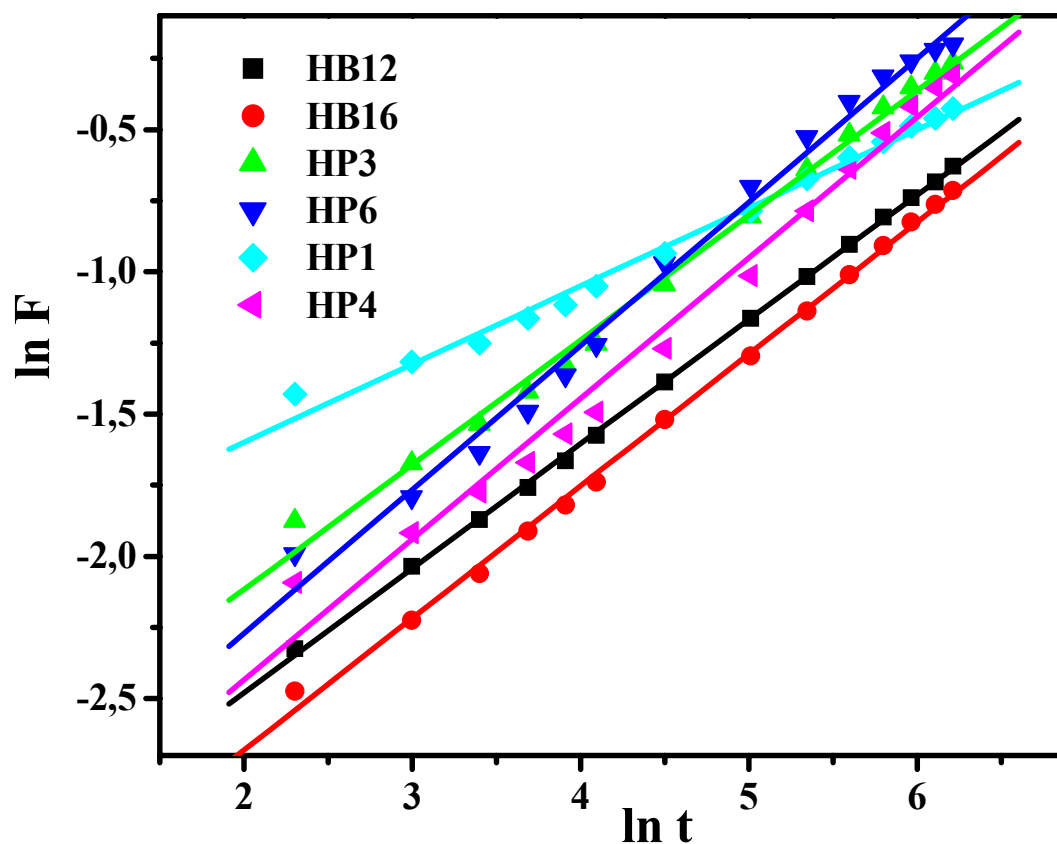


**Figure 4.44** : The Plot of  $\ln F$  vs  $\ln t$  for the Series of NIPAAm Hydrogels at Different Comonomer Concentration at 25°C in pH 7.5 Phosphate Buffer

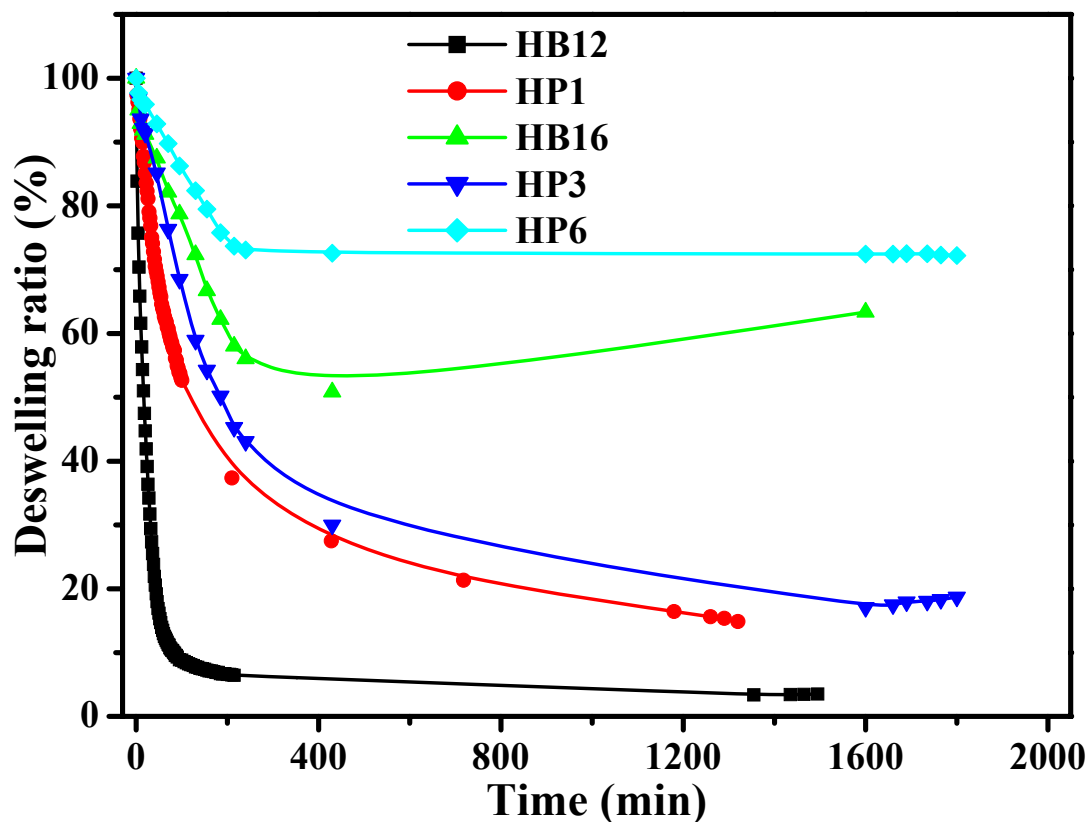
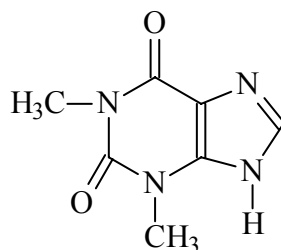


**Figure 4.45** : Deswelling Ratio as a Function of Time for the NIPAAm and NIPAAm/IA Copolymeric Hydrogels (Sample HB12, HP1, HB16, HP3, and HP6) at 37°C in DDW

The effect of the hydrophilic comonomer content (IA) and hydrophobic crosslinker (VTPDMS) on the deswelling ratio for the copolymeric hydrogels at 37°C was shown in Figure 4.45. The deswelling rates of the curves suggest the importance of hydrogel composition and, the intermolecular interactions between the hydrogel components and loading/release media.

Theophylline was used as a drug for controlled-release of PNIPAAm and NIPAAm/IA copolymer hydrogels crosslinked with BIS and VTPDMS.



Theophylline and its close relatives aminophylline, caffeine and chocolate, are members of the methylxanthine group of chemicals. Caffeine was the first of this

group to be found helpful to asthmatic humans but had some unpleasant side effects. Other derivatives were quickly produced in hope of minimizing side effects and maximizing the airway relaxant properties that are so helpful in airway disease.

The calibration curve of the absorbance as a function of the Theophylline concentration at 266 nm is shown in Figure 4.46. It has a linear relationship with a correlation coefficient (r) of 0.9998. This linear relationship can be quantitatively described as the following equation:

$$A = (51.18c + 20.90) \times 10^{-3} \quad (4.1)$$

where A is the absorbance and c is the concentration ( $\times 10^6$  g/ml) of the drug (Theophylline).

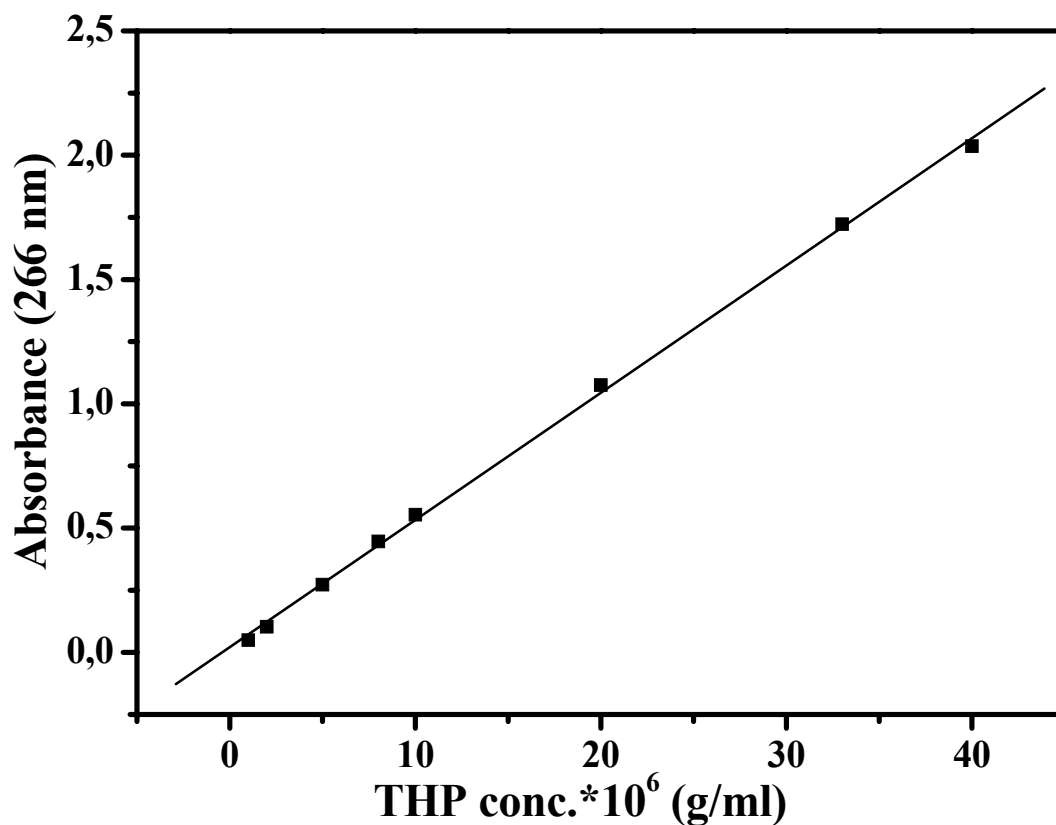


**Figure 4.46 :** The Standart Calibration Curve of the Absorbance as a Function of the Theophylline Concentration at 266 nm.

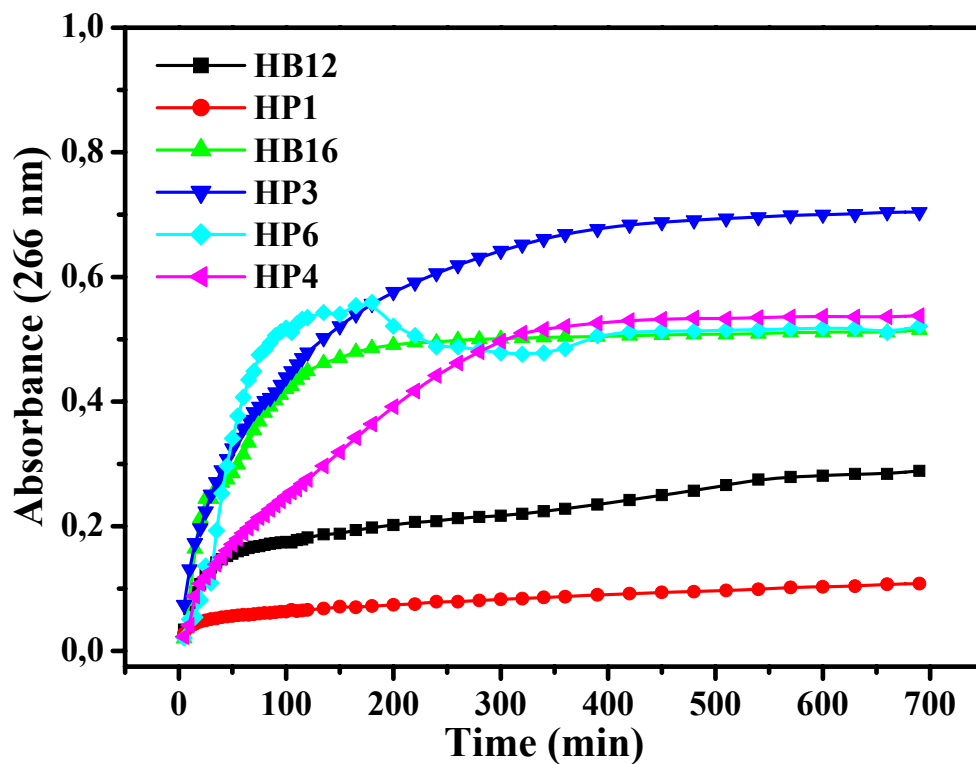


Figure 4.47 : Absorbance (at 266 nm) vs Time of Theophylline Release ( $C = 0.1$  g/L) for the PNIPAAm and NIPAAm / IA Copolymer Hydrogels

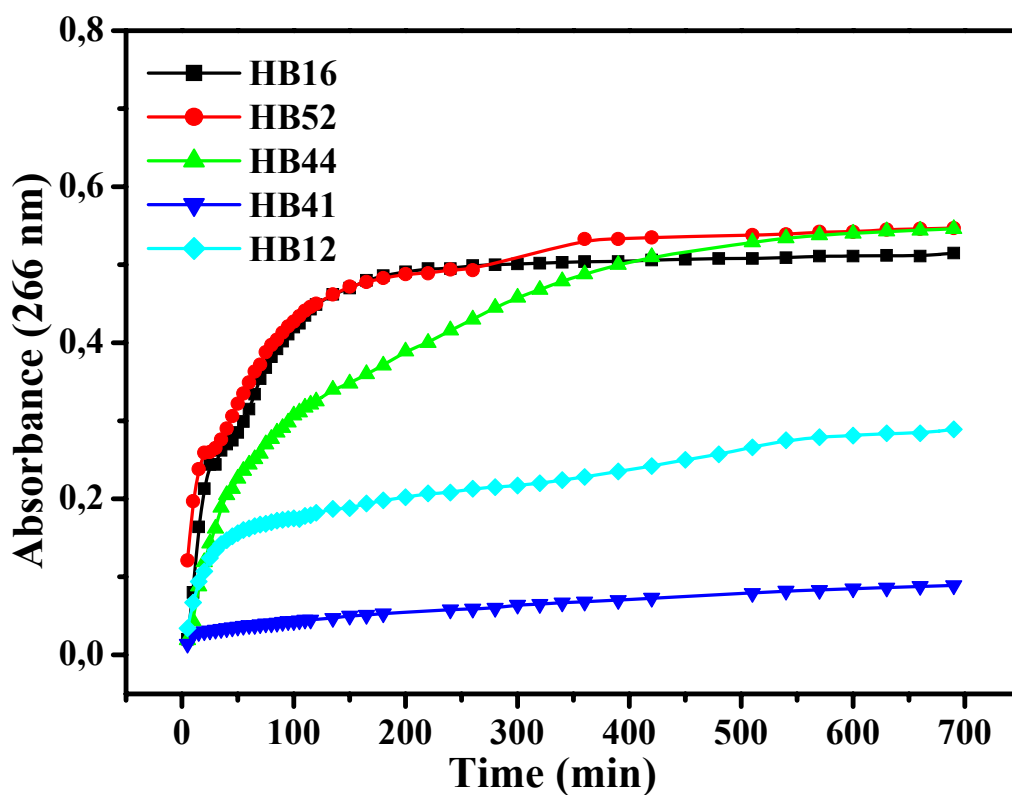
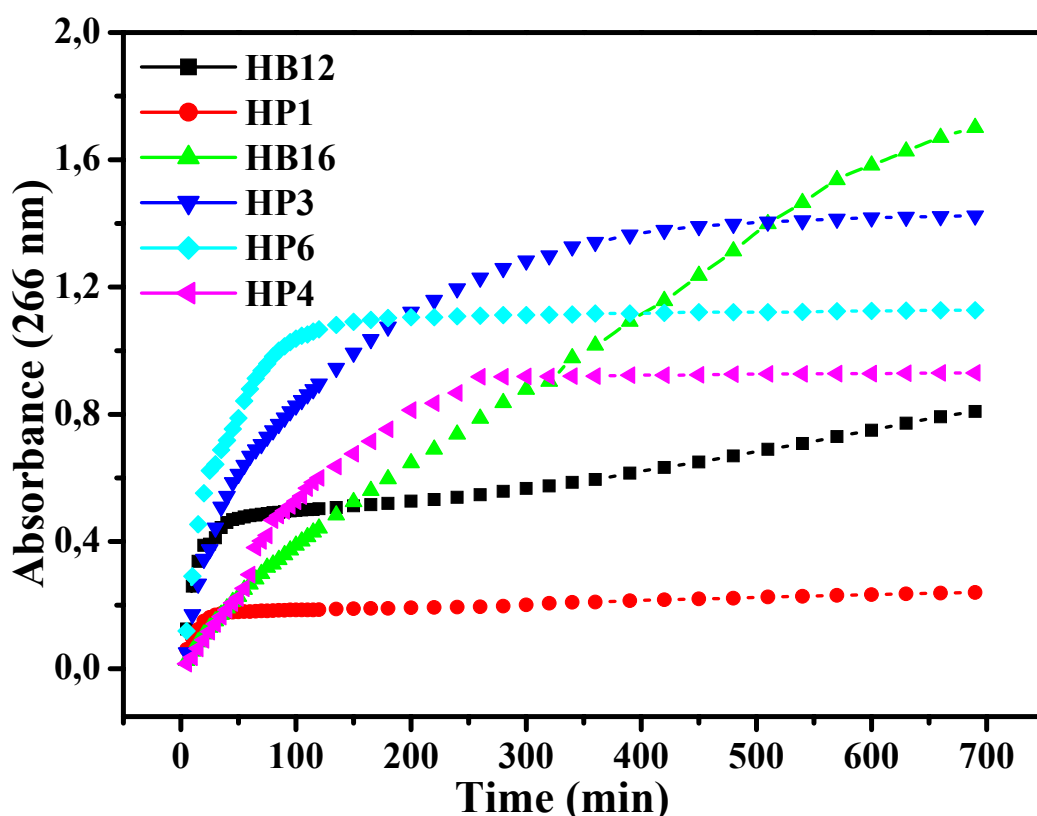


Figure 4.48 : Absorbance (at 266 nm) vs Time of Theophylline Release ( $C = 0.1$  g/L) for the PNIPAAm, NIPAAm / IA, NIPAAm / MBuI, NIPAAm / MOCl and NIPAAm / MCeI Copolymer Hydrogels

Figure 4.47 and 4.49 show the controlled-release plots of PNIPAAm and NIPAAm / IA copolymer hydrogels for two different Theophylline concentrations in phosphate buffer at pH 7.5. As can be seen from these curves, both drug concentration and composition of the hydrogels affect the drug loading / release capacities and mechanisms of hydrogels. PNIPAAm hydrogel crosslinked with VTPDMS has the lowest drug release capacity because of the unressemble structures to each other. This means that, Theohylline, being a water-soluble drug and having hydrophilic structure does not prefer to intermolecular interaction with hydrophobic dimethyl siloxane groups and so drug loadind/release capacity decrease. The presence of hydrophilic and ionizable IA molecules in the structures of NIPAAm hydrogels increases the release capacities and rates of hydrogels crosslinked with BIS or VTPDMS because repulsive forces between the  $-\text{COO}^-$  groups controls the shrinking rate at  $37^\circ\text{C}$  and so the drug molecules do not trap in the polymeric network.



**Figure 4.49** : Absorbance (at 266 nm) vs Time of Theophylline Release ( $C = 0.3$  g/L) for the PNIPAAm and NIPAAm / IA Copolymer Hydrogels

Figure 4.48 and 4.50 show the controlled-release plots of PNIPAAm, NIPAAm / IA, NIPAAm / MBuI, NIPAAm / MOcI and NIPAAm / MCeI copolymer hydrogels for two different Theophylline concentrations in phosphate buffer at pH 7.5. As can be

seen from these curves, both drug concentration and composition of the hydrogels affect the drug loading / release capacities and mechanisms of hydrogels. NIPAAm/MCeI copolymer hydrogel crosslinked with BIS has the lowest drug release capacity because of the unressemble structures to each other. This means that, Theohylline, being a water-soluble drug and having hydrophilic structure does not prefer to intermolecular interaction with hydrophobic and long alkyl chains and so drug loadind/release capacity decrease. The presence of both hydrophilic and ionizable –COOH and, butyl groups, which do not prevent the hydrophilic and electrostatic effects of ionic groups in the structure of monoester, in the structures of networks increases the release capacities and changes the release kinetics of hydrogels.

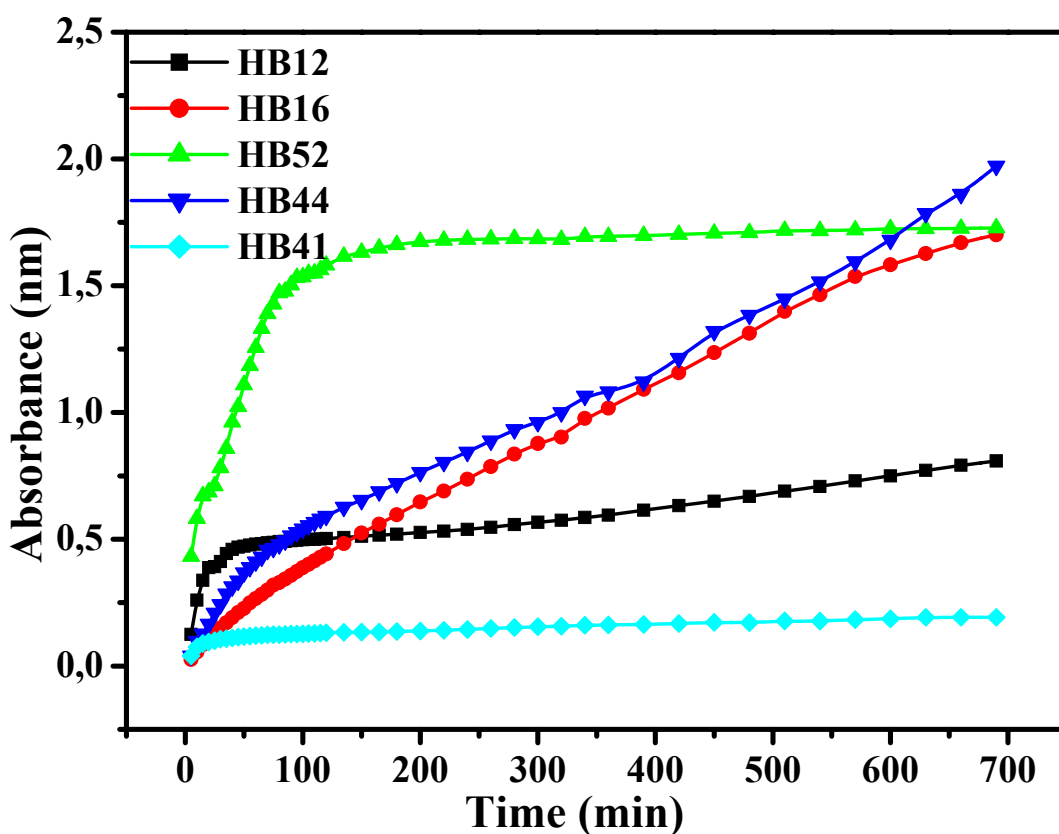


**Figure 4.50:** Absorbance (at 266 nm) vs Time of Theophylline Release ( $C = 0.3$  g/L) for the PNIPAAm, NIPAAm / IA, NIPAAm / MBuI, NIPAAm / MOcI and NIPAAm / MCeI Copolymer Hydrogels

Sample HB 52 contains 2.50 mol % of MOcI as hydrophobically modified ionizable comonomer in the feed. The results of drug release experiments of these hydrogel give the most optimum conditions like its mechanical strength and LCST measurements.

#### 4.5. Solution Behavior of NIPAAm/Monoitaconate Copolymers and NIPAAm/Itaconic Acid/Dimethyl Itaconate Terpolymers

PNIPAAm, poly(dimethyl itaconate) (PDMI) and, copolymers and terpolymers of NIPAAm with IA, DMI, MMI, MBuI, MOcI and MCEI were obtained by free radical solution polymerization using AIBN and KPS/TEMED redox pair, as initiator, in 1,4-Dioxane and in MetOH/DDW mixture ( MetOH/DDW: 60/40, v/v %) with a total monomer concentration of 0,7 mol/L.

**Table 4.9** : Synthesis Conditions, GPC and DSC Results of PNIPAAm, PDMI and NIPAAm/monoitaconate Copolymers

Sample	Polymer	Solvent Type	Tg (°C)	M <sub>n</sub> x 10 <sup>-3</sup> (g/mol)	M <sub>w</sub> x 10 <sup>-3</sup> (g/mol)	M <sub>w</sub> / M <sub>n</sub>
L-1	PNIPAAm	M/W	139,0	90.3	314.0	3.47
L-2	PNIPAAm	D	137,2	33.4	122.0	3.64
L-3*	IA / NIPAAm	M/W	153	-	-	-
L-4*	IA / NIPAAm	D	158.2	111.0	138.0	1.24
L-5*	MMI / NIPAAm	M/W	148,0	7.54	14.2	1.88
L-6*	MMI / NIPAAm	D	150,0	3.27	6.81	2.09
L-7*	DMI / NIPAAm	M/W	128,5	53.4	221.0	4.14
L-8*	DMI/ NIPAAm	D	130,0	31.3	101.0	3.22
L-9	PDMI	M/W	50,0	25.5	3.89	1.52
L-10	PDMI	D	32,0	27.2	4.26	1.56
L-11*	MBuI/ NIPAAm	M/W	135,5	14.6	24.4	1.67
L-12*	MBuI/ NIPAAm	D	141,0	89.9	32.5	3.62

\* for the samples containing 10.0 mol % of comonomers in the feed.

[NIPAAm] = 0.7 mol/L, D: 1,4-Dioxane, T=60°C and AIBN as initiator, M/W: methanol/destile-deionize water (60/40 v/v %), T=25°C and KPS/TEMED redox pair as initiator

General procedure: Monomer (NIPAAm), comonomer (or comonomers, in the range of 1-10 mole % in the feed) and AIBN (or KPS/TEMED)) were dissolved in 1,4-dioxane (or in MetOH/DDW mixture). The reaction mixture was purged with nitrogen for 10 min and allowed to react in an air oven at 60°C for 72 h under nitrogen. The polymers were precipitated in n-hexane (or in water, depending on the composition of polymers). To purify the solid products, they were dissolved in cold water and then collapsed by heating. Synthesis conditions, molecular weight and glass transition temperatures of PNIPAAm, PDMI and NIPAAm/DMI, NIPAAm/MMI, NIPAAm/MBuI, NIPAAm/IA copolymers containing 10.0 mole % of comonomer are given in Table 4.9.

FTIR spectra of mono-N-alkyl itaconates, PNIPAAm and NIPAAm/IA/DMI terpolymers were recorded on Perkin Elmer Spectrum One Model Spectrophotometer (FTIR-reflectance, universal ATR with diamond and ZnSe), using the samples in the powder form. To determine the compositions of the copolymers with IA and its monoesters bearing methyl, butyl, octyl and cetyl groups, the copolymers (0.5 g) were dissolved in an excess of 0.1N NaOH (10 mL). After the deprotonation of the carboxyl groups, the excess of NaOH was titrated with 0.1N HCl.

Gel permeation chromatography was used to determine the molecular weights of NIPAAm and DMI homopolymers, NIPAAm/IA, NIPAAm/MMeI, NIPAAm/MBuI and NIPAAm/DMI copolymers employing a Waters instrument (equipped with a Model 1100 refractive index detector) in tetrahydrofuran. The elution rate was 0.3 ml/min. Waters styrogel columns (HR 5E, HR 4E, HR 3 and HR 2) were used. GPC was calibrated using polystyrene standards. The DSC measurements were performed on a Metler Toledo DSC 821 under nitrogen atmosphere with a flow rate 30 ml/min and a heating rate of 10 °C/min. The temperature range was exported from 40–150 °C.

Synthesis condition, and glass transition temperatures of and NIPAAm/DMI, NIPAAm/IA, NIPAAm/MOcI and NIPAAm/MCeI copolymers and NIPAAm/DMI/IA terpolymers containing 5.0 and 10.0 mole % of comonomer are given in Table 4.10.

**Table 4.10** : DSC Results of NIPAAm Copolymers and Terpolymers

Sample	Reaction media	Comonomer 1 (mole %)	Comonomer 2 (mole %)	Tg (°C)
L-4	D	IA, 10.0	-	158.2
L-13*	D	IA, 9.0	DMI, 1.0	156.9
L-14*	D	IA, 5.0	DMI, 5.0	151.9
L-15*	D	IA, 1.0	DMI, 9.0	146.0
L-8	D	DMI, 10	-	130.0
L-17	D	DMI, 5.0	-	142.5
L-16	D	IA, 5.0	-	156.3
L-18	M/W	MOcI, 5.0	-	135.9
L-19	D	MOcI, 5.0	-	138.1
L-20	D	MCEI, 5.0	-	136.2

\*For terpolymer samples, total mole fraction of comonomers in the feed was 10 mole %,

[NIPAAm] = 0.7 mol/L, **D**: 1,4-Dioxane, T=60°C and AIBN as initiator,  
**M/W**: methanol/destile-deionize water (60/40 v/v %), T=25°C and KPS/TEMED redox pair as initiator

Figures 4.51 and 4.52 shows the DSC curves of the linear copolymer and terpolymer samples, which are the identified in Tables 4.9 and 4.10. Copolymerization is a well-known procedure to adjust the glass transition temperature (T<sub>g</sub>) of polymers. As seen in Tables 4.9 and 4.10 and Figure 4.51 and 4.52, an increase in both the chain length of alkyl groups attached to the monoitaconates and the contents of the mono- and dialkyl itaconates in the copolymer and terpolymers decrease the T<sub>g</sub>s.

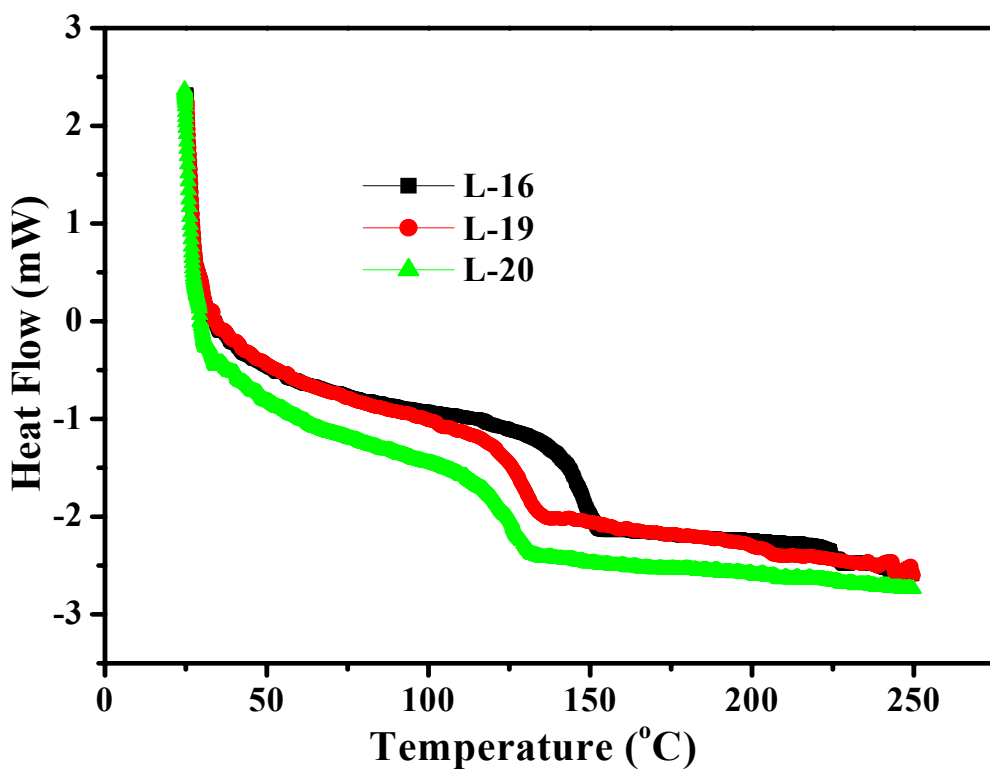


**Figure 4.51:** DSC Thermograms of NIPAAm/IA (L-16), NIPAAm/MOCl (L-19), NIPAAm/MCeI (L-20) Copolymers Containing 5.0 mole % of Comonomer in the Feed.

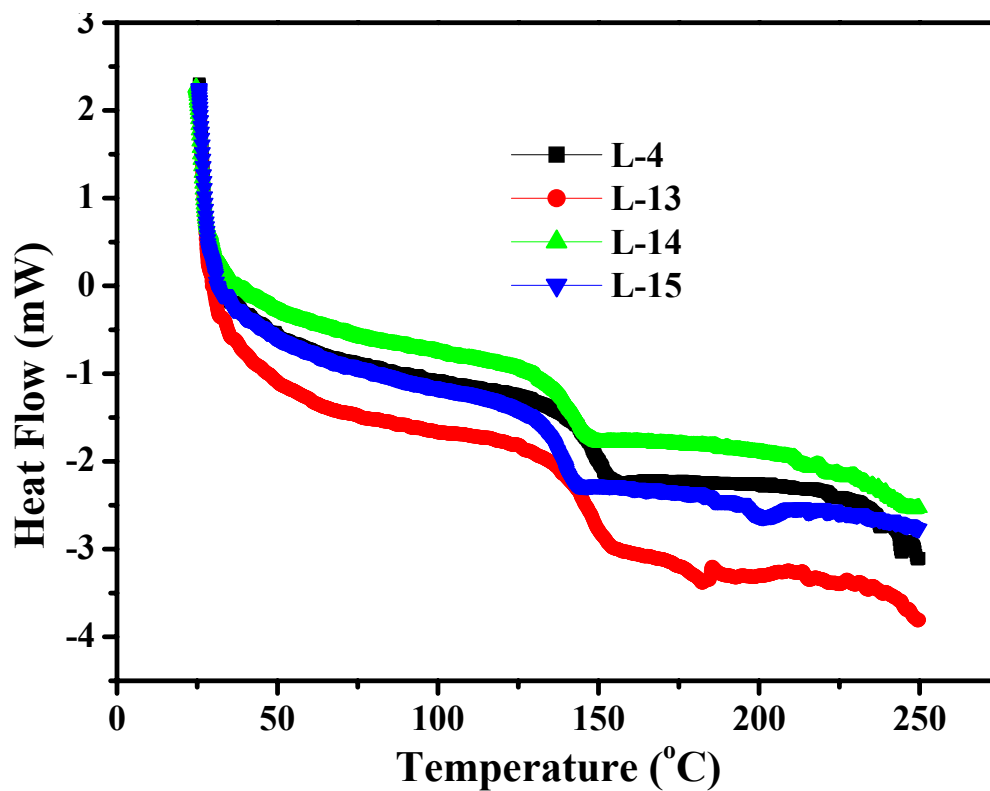


**Figure 4.52:** DSC Thermograms of NIPAAm/IA (L-4), NIPAAm/DMI/IA Terpolymers Containing 10.0 mole % of Total Comonomer Content in the Feed.

**Table 4.11** : Feed and Copolymer Compositions of NIPAAm Copolymers

<b>Sample</b>	<b>Feed composition (in mol %)</b>	<b>Polymer composition<sup>*</sup> (in mol %)</b>
<b>L-6</b>	10.0 % MMI	18.0 %
<b>L-12</b>	10.0 % MBuI	12.4 %
<b>L-21</b>	1.0 % IA	0.5 %
<b>L-22</b>	2.5 % IA	1.5 %
<b>L-16</b>	5.0 % IA	2.1 %
<b>L-23</b>	7.5 % IA	3.3 %
<b>L-4</b>	10.0 % IA	8.2 %
<b>L-24</b>	1.0 % MOcI	1.0 %
<b>L-25</b>	2.5 % MOcI	5.3 %
<b>L-19</b>	5.0 % MOcI	5.6 %
<b>L-26</b>	1.0 % MCeI	0.9 %

\* obtained by acid-base titration.

In the case of IA/NIPAAm and MMI/NIPAAm copolymers, the presence of the carboxylic groups forming hydrogen bonds increases the T<sub>g</sub> while the monoalkyl and dialkyl itaconates such as MBuI, MOcI, MCeI and DMI lead to a decrease in T<sub>g</sub>s of copolymer and terpolymer because of the destructions of intermolecular interactions (resulting from the -COOH and -COO<sup>-</sup> groups) through the longer alkyl spacers.

To determine the compositions copolymers with IA and its monoesters bearing methyl, butyl, octyl and cetyl groups, the copolymers (0.5 g) were dissolved in 10 mL of standard sodium hydroxide (0.1 N NaOH) to deprotonate the carboxyl groups. The excess of NaOH was titrated with standard hydrochloric acid (0.1 N HCl). The amount of acidic comonomer units was calculated from the amount of NaOH required to deprotonate the carboxylic acid groups. The copolymer compositions calculated from the end points of acid-base titrations are summarized in Table 4.11. From the comparison of the feed compositions of the copolymers with

the corresponding copolymer compositions, obtained from the acid-base titrations it can be discussed that the reactivities of monoitaconates are higher than that of IA and increase with increasing length of alkyl chain.

From the comparison of the feed compositions of the copolymers with the corresponding copolymer compositions, obtained from the acid-base titrations it can be concluded that the reactivities of monoitaconates are higher than that of IA acid and increase with increasing length of alkyl chain.

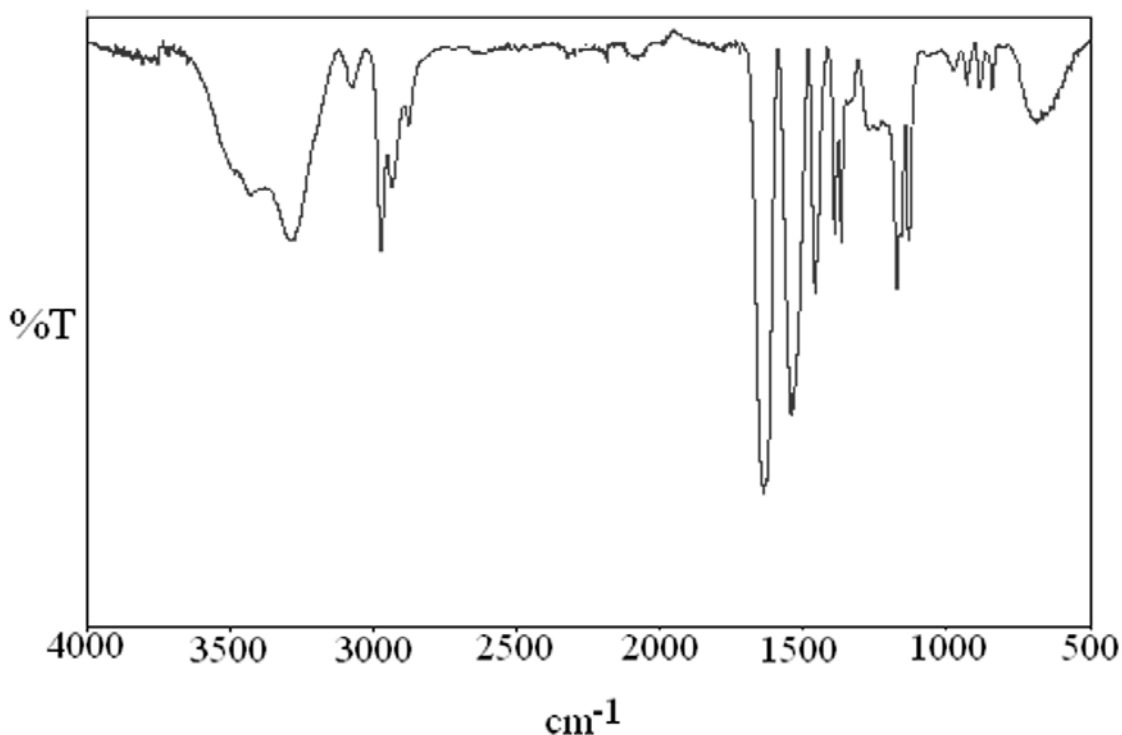


**Figure 4.53:** FTIR Spectrum of PNIPAAm

FTIR spectra of PNIPAAm, its copolymers and terpolymers are shown in Figure 4.53 - 4.55. Figure 4.53 shows the characteristic absorption peaks of PNIPAAm (-C=O stretching at 1660 cm<sup>-1</sup>, -NH bending at 1640 cm<sup>-1</sup> and 1540 cm<sup>-1</sup> for primary and secondary amides, respectively). The appearance of C=O stretching belonging to carboxyl group of itaconic acid and (at 1750 cm<sup>-1</sup>), along with the absorption peaks of PNIPAAm show the presence of itaconic acid in the chains. The intensity of this peak increased with an increase in the IA acid content of copolymers and terpolymers (Figures 4.54 and 4.55).

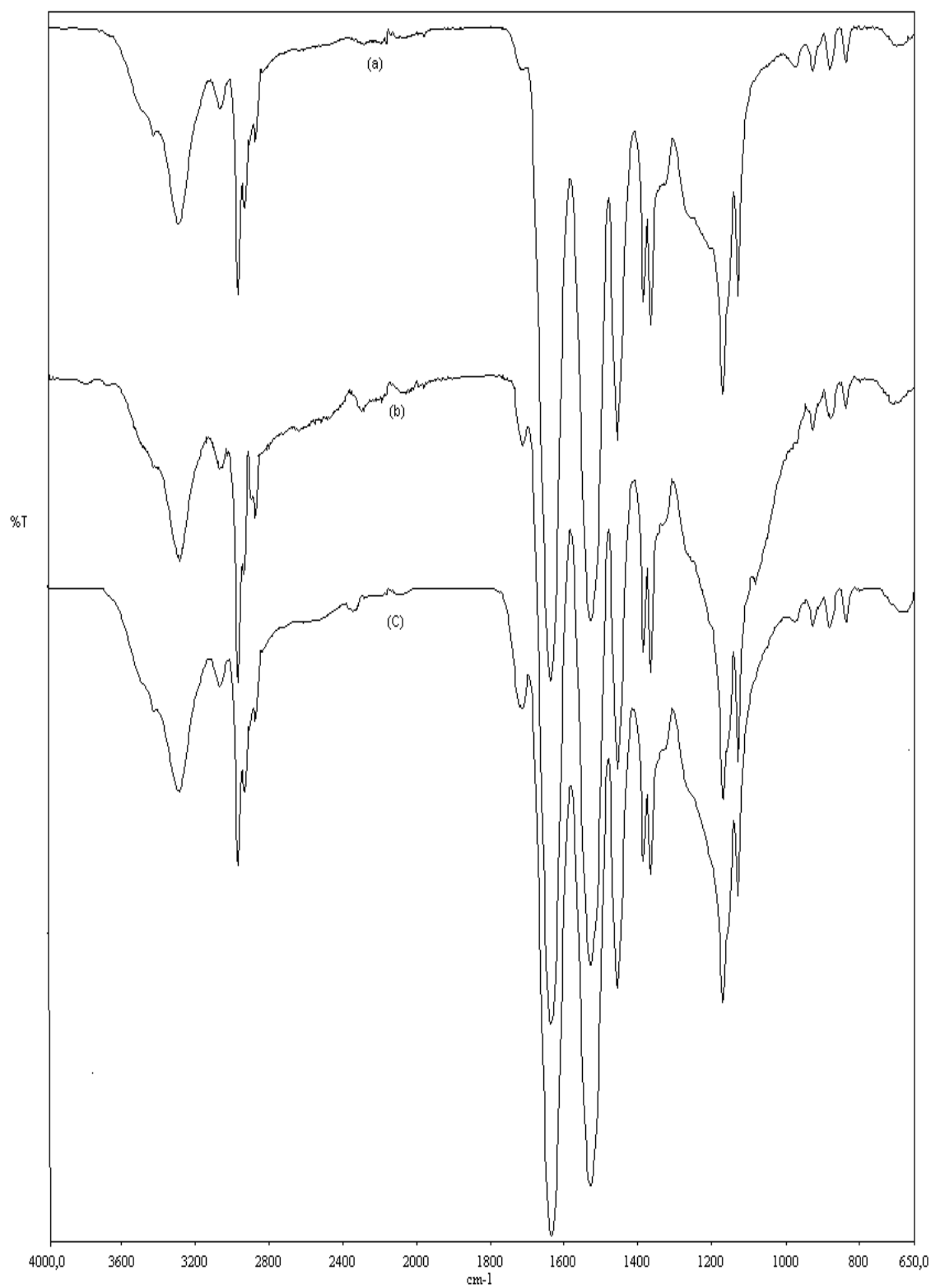


**Figure 4.54:** FT-IR Spectra of NIPAAm/IA Copolymers. IA Content in the Feed (a) 2.5 mole %, (b) 5.0 mole %, (c) 7.5 mole % (in 1,4-Dioxane)

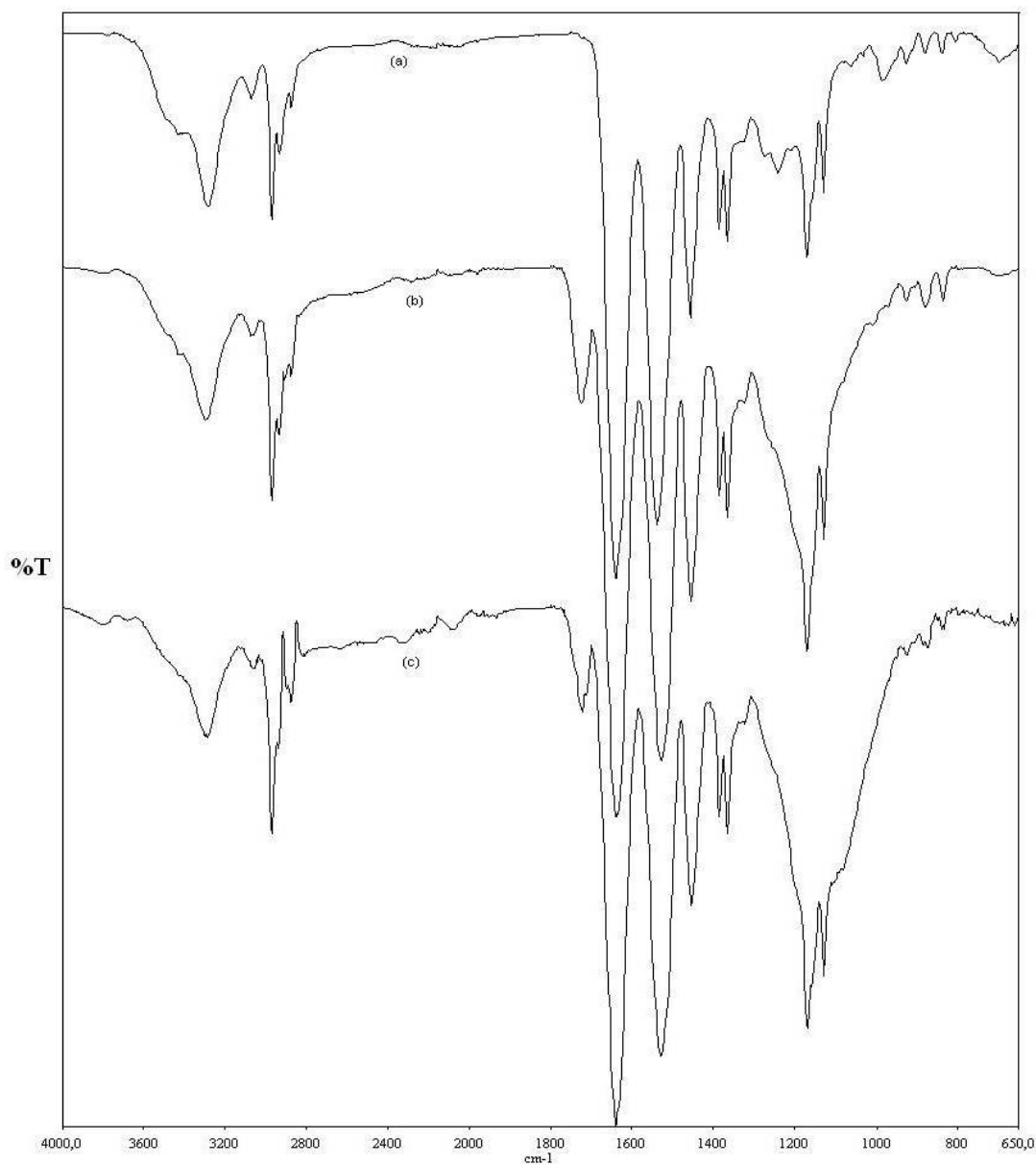


**Figure 4.55:** FTIR Spectra of NIPAAm/DMI/IA Terpolymers. (a) PNIPAm, (b) 2.5 mole % of IA+7.5 mole % of DMI, (c) 5.0 mol % of IA+5.0 mole % of DMI (in 1,4-Dioxane)

#### 4.5.1. Cloud point (LCST) measurements

Cloud point measurements were carried out in a Shimadzu UV-160A UV-visible spectrophotometer equipped with a temperature controlled cell. The temperature of the polymer solutions (2 g/L) was increased from 15°C to 60°C in increments of 0.5 - 1°C/min and the absorbance was observed at 400 nm. LCSTs were taken as the initial break points in the resulting absorbance versus temperature curves. The pH of these solutions was controlled by using phosphate (PBS, Na<sub>2</sub>HPO<sub>4</sub>-KH<sub>2</sub>PO<sub>4</sub> in 0.10

M NaCl at pH 7.4) and citric acid (CB, sodium citrate-citric acid at pH 4) buffer systems while the pHs of the polymer solutions prepared in DDW were adjusted with NaOH and HCl.

Visual determination of cloud points, i.e., LCSTs of the polymer solutions in the range of pH 1-9 were done by noting the temperature at which turbidity first appears upon slowly heating the aqueous solution by a water bath.

The temperature was raised from 15°C to 60°C at heating rate of 1°C/5 min. The LCST was defined as the temperature at the inflection point on the absorbance versus temperature curve. Furthermore, the cloud points, i.e., LCSTs of the polymer solutions in the range of pH 1-7 were determined visually by noting the temperature at which turbidity first appears upon slowly heating the aqueous solution by a water bath.

**Table 4.12** : pH and Solvent Dependence of LCST for PNIPAAm, NIPAAm/IA and NIPAAm/MBuI Copolymers, Containing 10.0 mol % of Comonomer in the Feed

Sample	pH 2 <sup>(1)</sup>	pH 4 <sup>(1)</sup>	pH 7 <sup>(1)</sup>	pH 4 <sup>(2)</sup>	pH 2 <sup>(3)</sup>	pH 4 <sup>(3)</sup>	pH 6 <sup>(3)</sup>	PH 7 <sup>(4)</sup>
L-3	29,2	31,0	>60,0	36,3	32,5	35,5	38,5	37,0
L-4	29,7	29,2	>60,0	32,5	30,5	33,5	36,5	36,5
L-1	30,3	-	28,3	34,5	33,5	33,5	33,5	-
L-2	29,3	-	26,7	34,2	32,5	32,5	32,5	-
L-11	<20,0	24,3	46,9	26,4	-	-	-	43,4
L-12	<20,0	19,5	48,2	22,5	-	-	-	44,5

**L-3:** 10 mole % of IA (MetOH/DDW), **L-4:** 10 mole % of IA (1,4 Dioxane), **L-1:** PNIPAAm (MetOH/DDW), **L-2:** PNIPAAm (1,4-Dioxane), **L-11:** 10 mole % of MBuI ((MetOH/DDW), **L-12:** 10 mole % of MBuI (1,4-Dioxane)

- <sup>(1)</sup> in CB (at 400 nm)
- <sup>(2)</sup> in DDW (at 400 nm)
- <sup>(3)</sup> in DDW (for visual)
- <sup>(4)</sup> in PBS (at 400 nm)

The results related with the measurements of the phase (or coil-globule) transition temperatures are given in Table 4.12 and shown in Figures 4.59-4.65. As can be seen from the indicated Figures and Table, it is possible to adjust the LCST over a wide range of temperatures by changing the type of the comonomers ( IA, MMeI, MBuI, MOcI, MCEI and DMI), polymerization medium (Meth/DDW, 60/40 v/v % or 1,4 Dioxane) and the solvent, which is used for cloud point measurements (DDW, CB and PBS), the composition of NIPAAm copolymers ( containing 1.0 - 10.0 mol % of comonomer in the feed) and NIPAAm/IA/DMI terpolymers (synthesized using 10.0 mol % of IA+DMI comonomer mixtures), and the pH of the solution.

Cloud point determination by absorbance measurements is a widely used method. In Figures 4.56-4.58 the absorbance versus temperature curves of two copolymers and two terpolymers are shown. For the polymer chains containing both hydrophilic and hydrophobic units, phase separation behaviours in DDW and in CB at pH 4 were excellent (Figures 4.56(a) and 4.57). For NIPAAm/MBuI copolymer and NIPAAm/IA/DMI terpolymer containing 9.0 mol % of DMI in CB at pH 4, also a sharp phase transition can be observed, but also some clouding occurs 5°C above the phase transition temperature (Figures 4.56(b) and 4.58). An explanation for these second inflection points at higher temperatures might be the intermolecular interactions between DMI, MBuI units and CB components. It can also be seen in Table 4.12 that the composition of the solutions which are used for LCST measurements, along with comonomer-type, comonomer-content and solution-pH are important to the shift in the temperatures of coil-to-globule transitions.

Further, in the case of Figure 4.56(b), the second inflection points at higher temperatures indicate the heterogeneous distribution of Sample L-12 while the absorbance versus temperature curve of Sample L-4 in Figure 4.56(a) displayed a sharp phase transition pointed out the existence of the more homogeneous copolymer chains than the Sample L-12 . The polydispersity index results which are given in Table 4.9 ( $M_w / M_n = 3.62$  and 1.24 for Samples L-12 and L-4, respectively) support these findings.

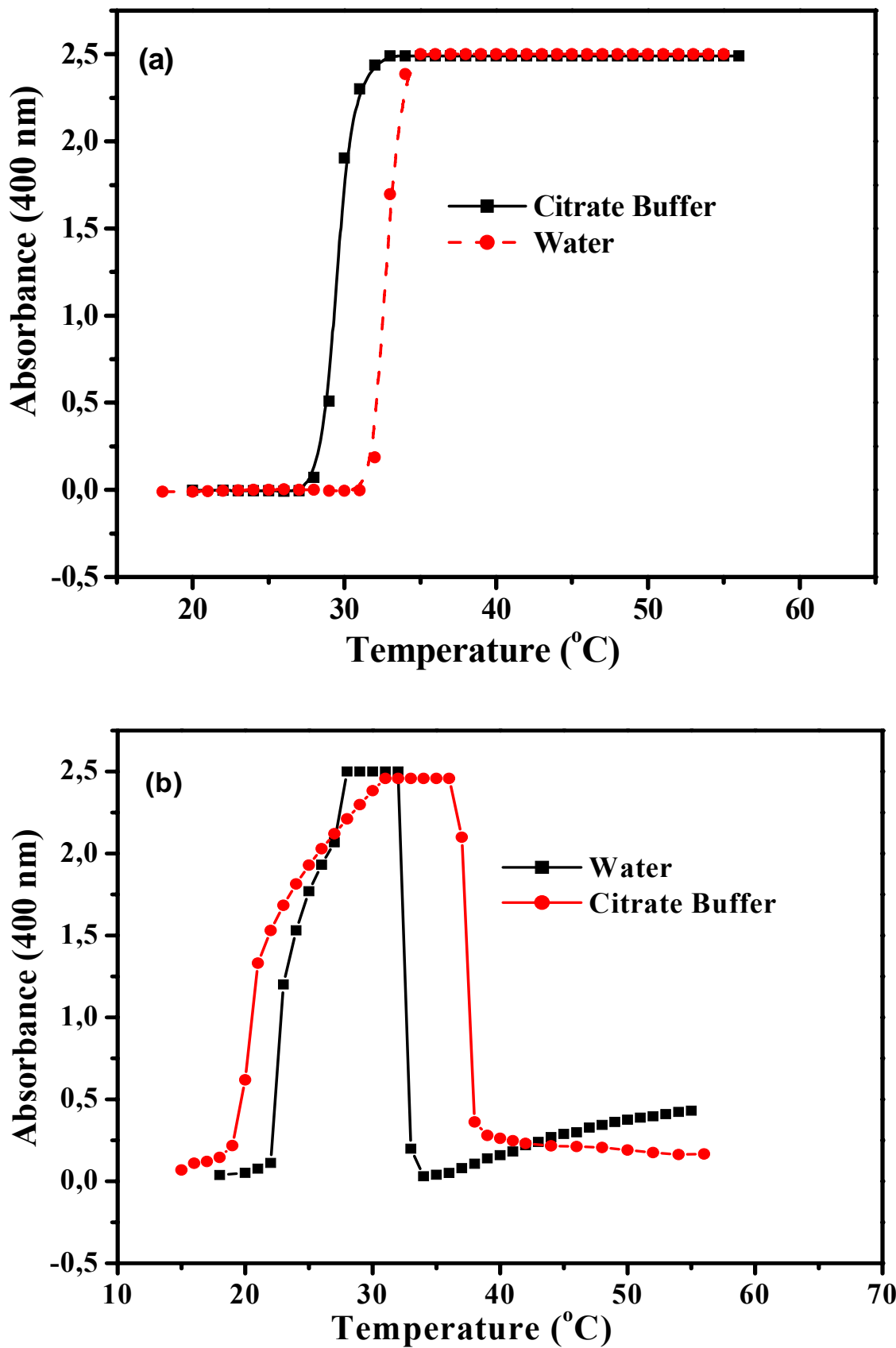


**Figure 4.56:** Absorbance of the NIPAAm/IA (a) and NIPAAm/MBuI (b) Copolymer Solutions as a Function of Temperature (in DDW and in CB at pH4; Comonomer Content: 10.0 mol %, in the Feed)

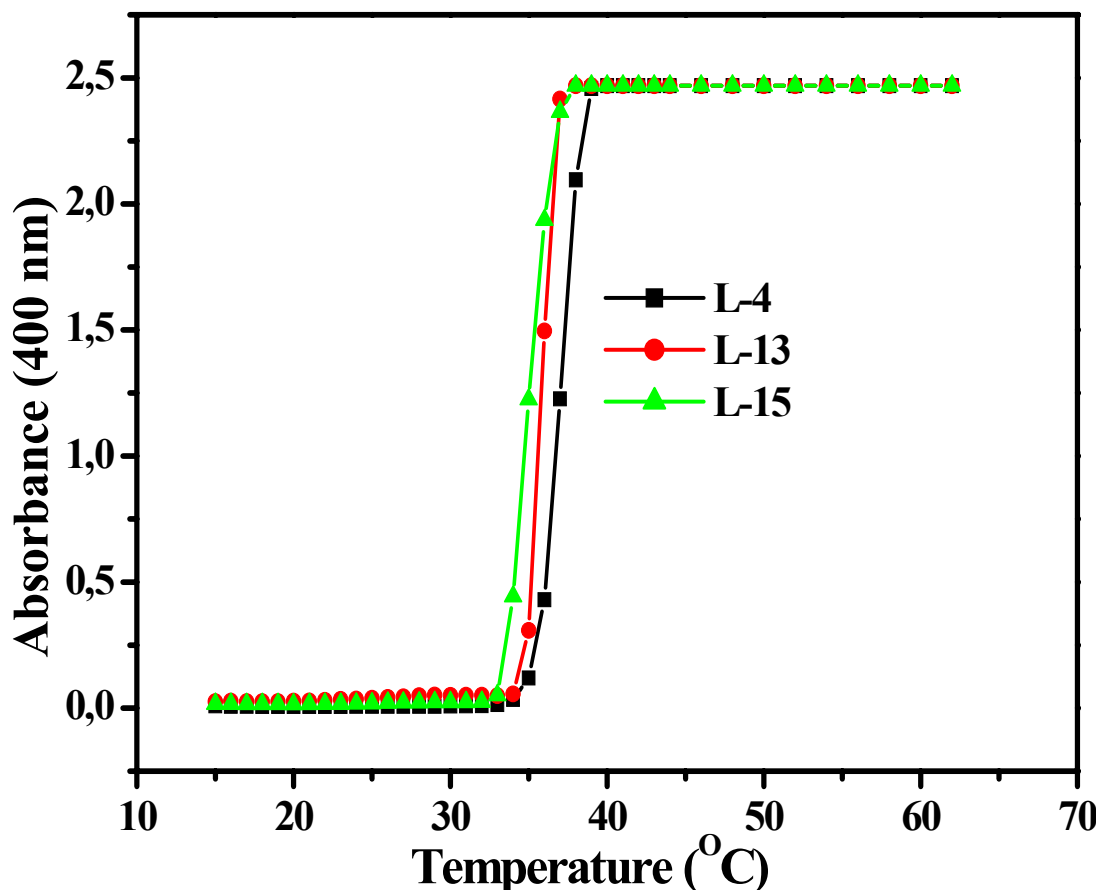


**Figure 4.57 :** Absorbances ( $\lambda = 400 \text{ nm}$ ) of the NIPAAm/IA (10 mole % of IA) (L-4); NIPAAm/DMI/IA (9.0 mole% of IA+1.0 mole % of DMI) (L-13) and 1.0 mole % of IA+9.0 mole % of DMI (L-15) Copolymer and Terpolymer Solutions as a Function of Temperature (in DDW at pH4 in 1,4-Dioxane)

Figures 4.57 and 4.58 and, Table 4.12 summarize the effects of solvent type used for polymerizations and cloud point measurements on the LCSTs of linear NIPAAm copolymers and terpolymers. It is seen that the intermolecular interactions between DMI units and the components of citrate buffer decrease the LCST of the terpolymer having higher content of DMI (Figures 4.57 and 4.58). Further, similar molecular interactions were observed for PNIPAAm and its copolymers with IA and MBuI. It was assumed that the structure of synthesis solvent (MetOH/DDW and 1,4-Dioxane) affect the molecular arrangement of polymer chains whereas the compositions of the buffered solutions change the intermolecular interactions between the chains and so the LCST of the samples (Table 4.12)

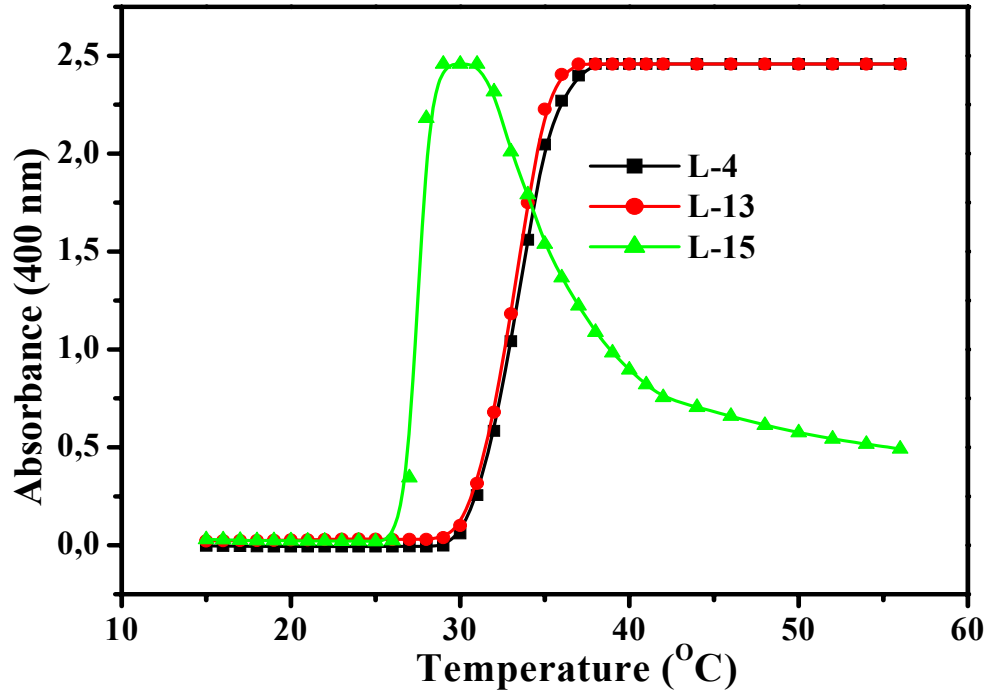


**Figure 4.58 :** Absorbances ( $\lambda = 400 \text{ nm}$ ) of the NIPAAm/IA (10 mole % of IA) (L-4); NIPAAm/DMI/IA (9.0 mole% of IA+1.0 mole % of DMI) (L-13) and 1.0 mole % of IA+9.0 mole % of DMI (L-15) Copolymer and Terpolymer Solutions as a Function of Temperature (in CB at pH4, in 1,4-Dioxane)

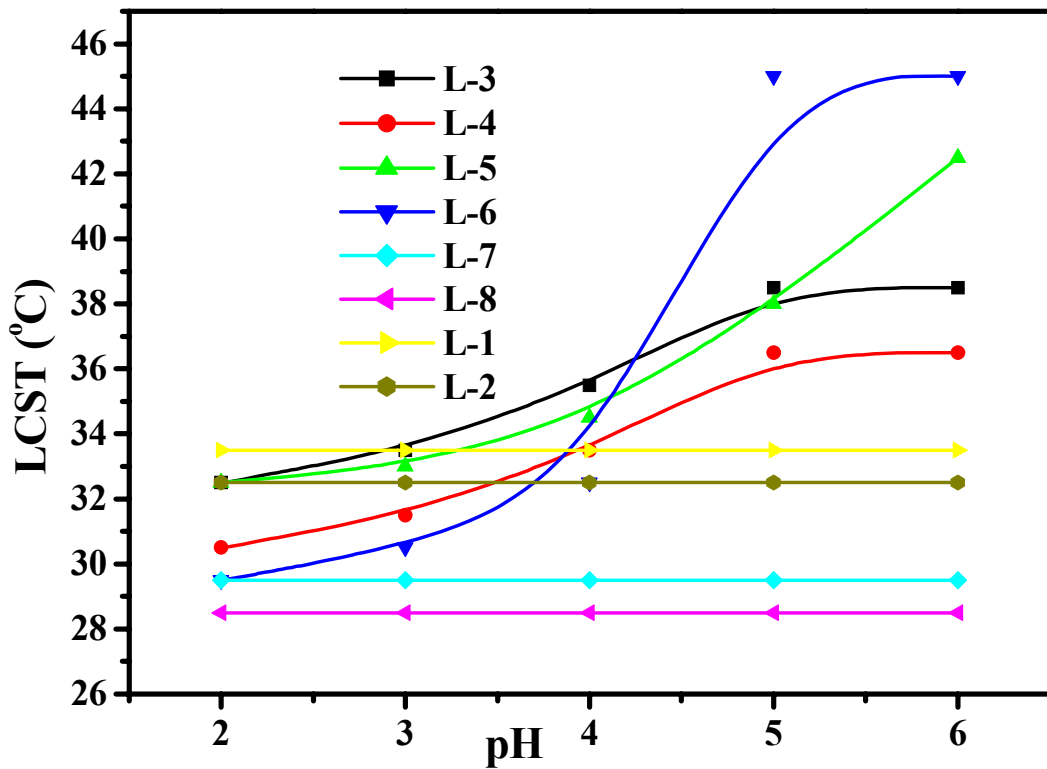


**Figure 4.59:** Changes in Cloud Points as a Function of pH for Solutions of the PNIPAAm, and NIPAAm/monoester and NIPAAm/diester of IA Copolymers (measured as visual, in DDW). The Samples are Described in Tables 4.9

Figures 4.59 and 4.60 show temperature versus pH, LCST vs comonomer content curves of PNIPAAm, NIPAAm/DMI, NIPAAm/IA and NIPAAm/MMeI copolymers and, NIPAAm/IA/DMI terpolymers synthesized in two different media. The combination of pH-sensitive and/or hydrophobically modified comonomers such as IA and MMeI, hydrophobic comonomer DMI and thermo-sensitive monomer, NIPAAm in the copolymer or terpolymer structures leads to a polymer that respond to both temperature and pH. Both the pure PNIPAAm chains (Samples L-1 and L-2 in Figure 4.59) and the NIPAAm/DMI copolymer chains (Samples L-7 and L-8 in Figure 4.59) exhibit pH-independent phase transitions. In the case of DMI comonomer, the presence of the methyl groups in the chain structure results in a decrease in LCST. Figure 4.59 and, Tables 4.9 and 4.10 also indicate that the polymerization medium is affected on both the  $T_g$ s and the LCSTs of the samples.

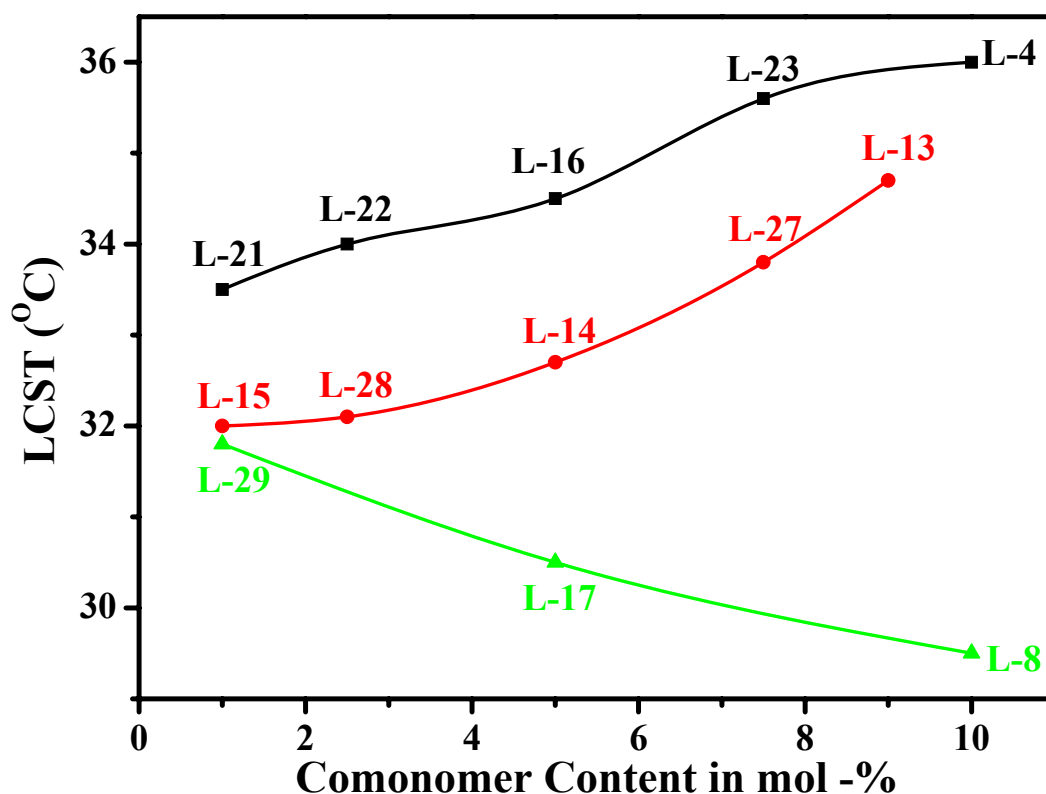
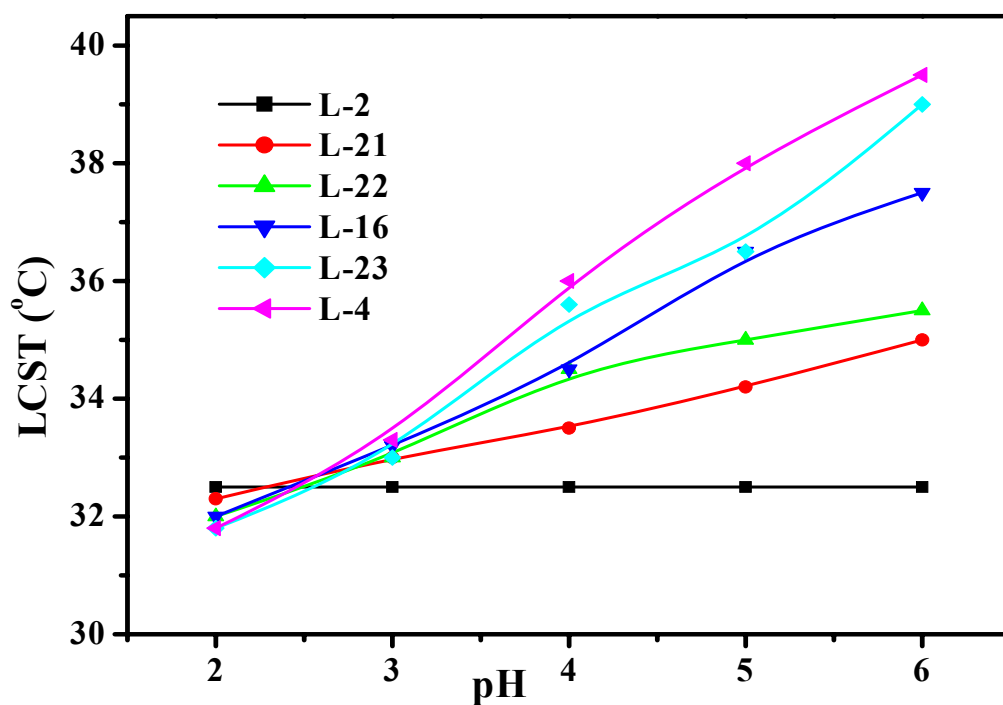


**Figure 4.60:** Changes in Cloud Points as a Function of Comonomer Content of the NIPAAm/IA, NIPAA/DMI and NIPAAm/DMI/IA Copolymers and Terpolymers (measured as visual, in DDW). The Samples are Described in Tables 4.9-4.11 (L-21) 1.0 % IA, (L-22) 2.5 % IA; (L-16) 5.0 mole % of IA; (L-23) 7.5 mole % of IA; (L-4) 10.0 mole % of IA ; (L-13) 9.0 mole % of IA-1.0 mole % of DMI; (L-27) 7.5 mole % of IA-2.5 mole % of DMI; (L-14) 5.0 mole % of IA-5.0 mole % of DMI; (L-28) 2.5 mole % of IA-7.5 mole % of DMI; (L-15) 1.0 mole % of IA-9.0 mole % of DMI; (L-8) 10.0 mole % of DMI; (L-17) 5.0 mole % of DMI; (L-29) 1.0 mole % of DMI.

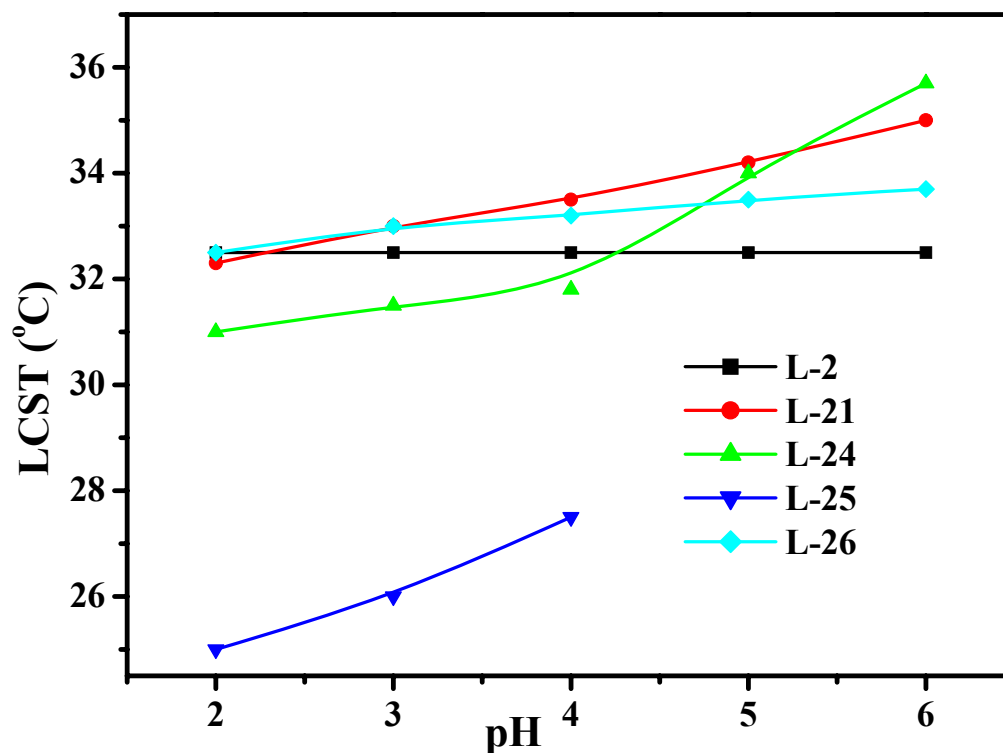
Figure 4.60 shows the effect of the comonomer content and type on the LCSTs of NIPAAm copolymers and terpolymers in DDW at pH 4. The samples are described in Tables 4.9 and 4.10. Curve 1 is for NIPAAm / IA copolymers in the range of 1.0 – 10.0 mol % of IA in the feed. Middle one is for terpolymers of NIPAAm / IA / DMI (IA/DMI contents, in mol %: 1.0/9.0; 2.5/7.5; 5.0/5.0; 7.5/2.5; 9.0/1.0). Curve 3 represents the LCSTs of NIPAAm / DMI copolymers for 1.0, 5.0 and 10.0 mole % of DMI. For the NIPAAm/IA/DMI terpolymers in Figure 4.60, the higher the DMI content the lower the LCST, in the range of pH 2-6. This means that the higher DMI content the greater hydrophobicity and the decrease the affinity of the terpolymer chains towards water.

It is known that IA ( $pK_1 = 3.85$  and  $pK_2 = 5.45$ ) is a weak acid. There exists a pair of carboxyl groups separated by two carbon atoms. Below pH 2 the aqueous solutions of IA contain only undissociated acid molecules. The carboxylate ion concentrations increase as the hydroxyl ion concentration in the solution is increased. The monoanion concentrations are maximum at pH 4-5 but above pH 8 IA exists completely in the dianion form. Therefore, the LCSTs of the NIPAAm / IA copolymers containing in the range of 1.0-10.0 mol % of IA increase greatly around pH 6. These pH-dependent phase transitions arise from the change in both IA content and ionization states of carboxyl groups (curve 1 in Figure 4.60).

The effect of pH changes, which should result in different degrees of ionization for the IA, MOcI and MCeI units, is shown in Figure 4.61 for the NIPAAm copolymers. These results show that, upon increased content and ionization degree of carboxyl groups, and length of alkyl chains, cloud points are shifted to higher temperatures. This means that with increase in the length of hydrophobic alkyl chain in the monoitaconates intramolecular interactions between the carboxyl groups are suppressed and LCSTs increase. The pH-dependent cloud point measurements of NIPAAm/MMeI copolymer (Figure 4.59) are similar to those of the NIPAAm copolymers with MOcI and MCeI. Its phase transition temperatures higher than that of the NIPAAm/IA copolymer (10.0 mol % of IA in the feed) also support the effect of the presence of alkyl chains on the ionization degree of carboxyl groups.

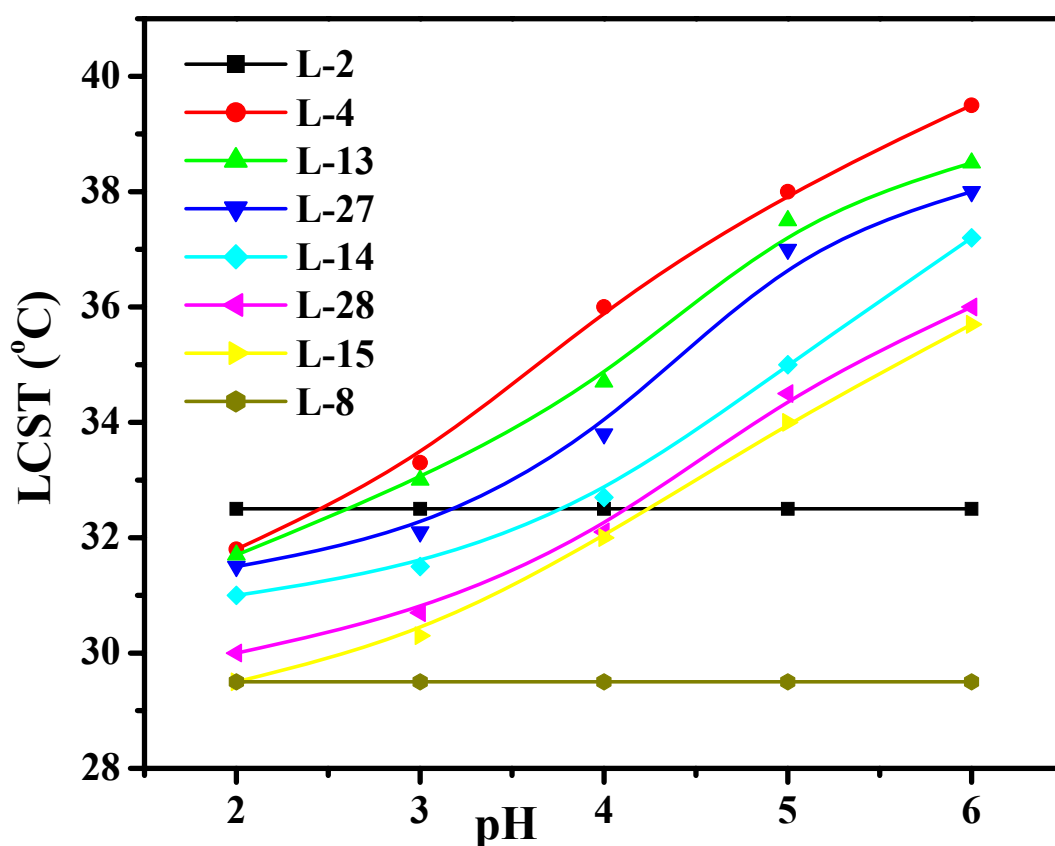


**Figure 4.61** : Changes in Cloud Points as a Function of pH for Solutions of the NIPAAm / IA Copolymers (measured as visual, in DDW). The Samples are Described in Tables 4.9-4.11.



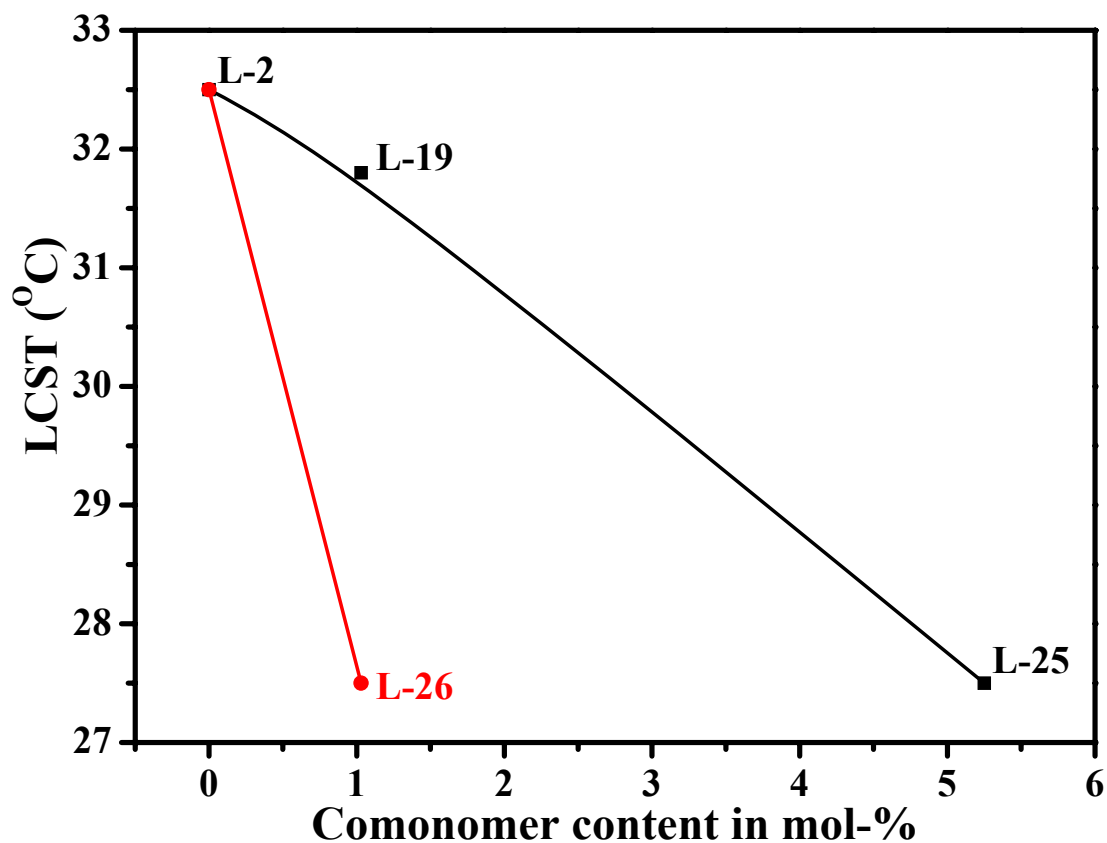
**Figure 4.62** : Changes in LCSTs as a Function of pH for the Aqueous Solutions of PNIPAAm (L-2), NIPAAm / IA (L-21), NIPAAm/MOCl (L-24), NIPAAm / MOCl (L-25, 2.5 mole % of MOCl) and NIPAAm/MCEI (L-26) Copolymers Containing 1.0 mole % of Comonomer (except Sample L-25) in the Feed (measured as visual, in DDW). Copolymer Compositions of the Samples are Described in Table 4.11.

Figure 4.62 shows the pH-sensitive solution behaviours of linear thermosensitive-PNIPAAms copolymerized with monoesters of itaconic acid. As to the LCST vs. pH curves of NIPAAm / MOcI copolymers containing the 1.0 mol % of MOcI in the feed, MOcI behaves as hydrophobic comonomer in the range of pH 2-4, while at higher pHs, hydrophilic and ionic effects of  $-\text{COO}^-$  groups suppress the hydrophobic interactions between the long alkyl chains of MOcI. On the other hand, in the case of the 2.5 mol % of MOcI hydrophobic groups prevent the ionization of  $-\text{COOH}$  groups and cause the LCST of linear PNIPAAm to decrease. The solution behaviours of linear NIPAAm/MOcI copolymers are similar to the NIPAAm/MOcI copolymer hydrogels. Both cloud point and glass transition measurements, and mechanical measurements of linear and crosslinked materials, respectively, indicated that octyl chains had the most effective alkyl chain lengths for the hydrophobic modifications of NIPAAm polymers.



**Figure 4.63:** Changes in Cloud Points as a Function of pH for Solutions of the PNIPAAm, NIPAAm/IA, NIPAA/DMI and NIPAAm/DMI/IA Copolymers and Terpolymers (measured as visual, in DDW). The Samples are Described in Tables 4.9-4.11

Figure 4.63 illustrates that the phase transition temperatures for the terpolymers change from the LCST of the NIPAAm/IA copolymer to the one of the NIPAAm/DMI copolymer. LCSTs above pH 3-4 shift to temperatures higher than those observed for PNIPAAm while for below pH 3 or 4 they show the lower value of LCST than that of PNIPAAm, by depending on the IA/DMI ratio in the terpolymers. The results shown in Figure 4.63 reveal that, even if the terpolymer hydrophobicity is increased by adding DMI units, the presence of IA units overcomes this decrease in hydrophilicity of the terpolymers. This is due to the ionization of IA carboxylic groups, which start to become partially charged for pH values above pH 3.



**Figure 4.64:** Effect of MOcI and MCEI Contents on the LCSTs of the Polymers PNIPAAm (measured as visual in DDW at pH 4). The polymer Compositions of Samples L-2 (PNIPAAm), L-19 (1.0 mole % of MOcI, in the feed), L-25 (2.5 mole % of MOcI, in the feed) and L-26 (1.0 mole % of MCEI, in the feed) are Described in Table 4.10.

The presence of DMI units in the terpolymers balances the hydrophilic character of IA. The LCSTs of PNIPAAm and NIPAAm/DMI copolymer (containing 10 mol % of DMI in the feed) do not change with solution pH but, for all terpolymers and NIPAAm/IA copolymer (containing 10 mol % of IA in the feed), LCST increases as the pH is increased.

Figure 4.64 show that the hydrophilic/hydrophobic balance of the copolymers and terpolymers and their LCSTs can be adjusted sensitively by controlling alkyl chain lengths, comonomer (or comonomers) contents and combinations. In conclusion, the sensitivity of these NIPAAm copolymers and terpolymers to change in pH and temperature suggest that they could be useful in biotechnology and drug delivery applications where small changes in pH and temperature.

## 5. CONCLUSION

The effects of comonomer type and concentration, crosslinker type and concentration on the solution behaviours and mechanical strengths of linear and crosslinked with NIPAAm copolymers have been investigated as a function of temperature and pH.

Effects of VTPDMS, being a hydrophobic macrocrosslinker on the physical parameters such as polymer volume fraction ( $v_{2s}$ ), effective crosslinking density ( $v_e$ ), polymer-solvent interaction parameter,  $\chi$  and average molecular weight between crosslinking points ( $M_c$ ) of neutral and ionic NIPAAm hydrogels, in comparison with those of the ones crosslinked with BIS. It was revealed that the compressive elastic moduli of VTPDMS-crosslinked neutral NIPAAm hydrogels were 50 times higher than those of the ones crosslinked with conventional tetra functional monomer, i.e., BIS in 1,4-dioxane. The lower mechanical responses of the neutral NIPAAm hydrogels crosslinked with Tegomer V-Si 2150, having half of the dimethylsiloxane units in the molecular structure of Tegomer V-Si 2250 supported the importance of the nature of secondary forces, being highly effected on the degree of physical crosslinkings. For both Tegomer V-Si 2250 and Tegomer V-Si 2150, the compression moduli of the ionic NIPAAm hydrogels were decreased sharply, with increasing IA content.

The compression moduli and crosslinking densities of NIPAAm hydrogels containing 2.50 and 5.0 mole % of monoesters of IA in the feed and crosslinked with BIS ( $2.50 \times 10^{-2}$  mol/L) increase with temperature and alkyl chain length in the order of  $M_{CeI} > M_{OcI} > M_{BuI}$ . Both the temperature ( $37^\circ\text{C}$ ) being higher than the LCST ( $\sim 32^\circ\text{C} - 34^\circ\text{C}$ ), and the increase in the length of the alkyl chain results in an increase of hydrophobicity and so the mechanical strength of the gels.

The compression moduli and crosslinking densities of the gels containing 5.0 mole % of MOcI crosslinked with concentrated solution of BIS ( $3.75 \times 10^{-2}$  mol/L) were highly greater than those of the ones synthesized with  $2.5 \times 10^{-2}$  mol/L concentration of BIS. The results indicate that both covalent bonds (primary interactions) between

the NIPAAm chains and hydrophobic interactions resulting from the hydrophobic octyl chains (secondary interactions) depends on the optimum conditions of crosslinker concentration and n-alkyl chain length.

As for these results, the electrostatic repulsive forces between the ionized carboxyl groups of IA units destroyed the strong intramolecular hydrophobic interactions arising from the dimethylsiloxane units of VTPDMS chains. From the starting point of these findings, it can be said that the most productive combinations of the hydrophilic component which absorbed large amount of water and the hydrophobic component which improved the mechanical performance are necessary to designate the materials having the right balance of repulsive and attractive forces, being responsible for swelling and mechanical behaviors of the networks.

By the use of IA, DMI and mono-N-alkylitaconates as comonomers, temperature- and pH-sensitive copolymers and terpolymers based on NIPAAm could easily be synthesized by free radical solution polymerization. From the comparison of the feed compositions of the copolymers with the corresponding copolymer compositions, obtained from the acid-base titrations it was seen that the reactivities of monoitaconates were higher than that of IA and increased with increasing length of alkyl chain. Thermal analysis was conducted by DSC to see how the introduction of hydrophobic alkyl chains affects the  $T_g$ s of NIPAAm chains.

The hydrophilic/hydrophobic balance of the copolymers and terpolymers and their LCSTs could be adjusted sensitively by controlling alkyl chain lengths, comonomer (or comonomers) contents and combinations. With increasing length of hydrophobic alkyl chains in the mono-N-alkylitaconates, intramolecular interactions between the carboxyl groups were suppressed and LCSTs increased.

The sensitivity of these NIPAAm copolymers and terpolymers to change in pH and temperature suggest that they could be useful in biotechnology and drug delivery applications where small changes in pH and temperature.

The temperature vs. volume swelling ratio and mass swelling vs time curves of the NIPAAm copolymer hydrogels crosslinked with VTPDMS and/or BIS indicate that the one having 2.5 mole % of IA in the feed can be suggested for drug release experiments because of discontinuous and larger volume change during the phase transition.

Equilibrium percentage mass swelling in both water and phosphate buffer of PNIPAAm crosslinked with BIS was higher than the NIPAAm hydrogel crosslinked with VTPDMS. This result supports the effect of hydrophobic crosslinker on the diffusion process of solvent in to the hydrogel. For the samples containing ionizable comonomer IA, equilibrium percentage mass swelling increased with increasing repulsive forces resulting from  $-\text{COO}^-$  groups. In the presence of VTPDMS as crosslinker, the percentages in water were higher than in phosphate buffer.

PNIPAAm, NIPAAm/IA and NIPAAm/monoitaconate copolymer hydrogels were used for drug release experiments Both Theophylline concentration and composition of the hydrogels affects the drug loading/release capacities and mechanisms of hydrogels.

PNIPAAm hydrogel crosslinked with VTPDMS has the lowest drug release capacity because of the unressemble structure to drug molecules. This means that, Theohylline, being a water-soluble drug and having hydrophilic structure does not prefer to intermolecular interaction with hydrophobic dimethyl siloxane groups and so drug loading/release capacity decrease. The presence of hydrophilic and ionizable IA molecules in the structures of NIPAAm hydrogels increases the release capacities and rates of hydrogels crosslinked with BIS or VTPDMS because repulsive forces between the  $-\text{COO}^-$  groups controls the shrinking rate at  $37^\circ\text{C}$  and so the drug molecules do not trap in the polymeric network.

The results of drug release experiments of NIPAAm copolymer hydrogel crosslinked with BIS and containing 2.50 mol % of MOcI in the feed as hydrophilic crosslinker and hydrophobically modified ionizable comonomer, respectively gave the most optimum conditions like its mechanical strength and LCST measurement results.

## REFERENCES

- [1] **Jeong, B., Gutowska, A.**, 2002, Trends Biotechnol., **20**, 305
- [2] **Hoffman, A.S., Stayton, P.S., Bulmus, V., Chen, G., Jinping, C., Chueng, C.**, 2000, J Biomed Mater Res, **52**, 577..
- [3] **Galaev, I.Yu., Mattiasson, B.**, Trends Biotechnol., **17**, 335
- [4] **Kikuchi, A., Okano, T.**. 2002, Prog. Polym. Sci., **27**, 1165
- [5] **Qiu, Y., Park, K.**, 2001, Adv. Drug. Deliv. Rev.**53**, 321.
- [6] **Okano, T., Dusek, K.**, 1993, editor. Responsive gels: volume transitions, vol. II. Berlin: Springer;. p. 180-197
- [7] **Twaites, B.R., Alarcon, C.H., Cunliffe, D., Lavigne, M., Pennadam, S., Smith, J.R.**, 2004, J. Control. Release, **97**, 551
- [8] **Lomadze, N., Schneider, H-J.**, 2005, Tetrahedron Lett., **46**, 751
- [9] **Kabanov, VA.**, 1994, Polym. Sci., **36**, 143
- [10] **Leclercq, L., Boustta, M., Vert, M.**, 2003, J. Drug Target, **11**, 129
- [11] **Chiantore, O., Guaita, M., Trossarelli, L.**, 1979, Macromolec. Chem., **180**, 969.
- [12] **Winnik, F.M., Ringsdorf, H., Venzmer, J.**, 1991, Macromolecules, **24**, 1678
- [13] **Wooten, W.C., Blanton R.B., Coover, H.W.** 1957, J.Polym. Sci., **XXV.**, 403.
- [14] **Otake, K., Inomata, H., Konno M., Saito, S.**, 1990, Macromolecules, **23**, 283.
- [15] **Schild, H.G., Tirrell, D.A.**, 1991, Macromolecules, **24**, 948.
- [16] **Schild, H.G., Tirrell, D.A.**, 1990, J. Phys. Chem., **94**, 4352.
- [17] **Inomata, H., Yagi, Y., Otake, K., Konno M., Saito, S.**, 1989, Macromolecules, **22**, 3494.
- [18] **Yan, L., Zhu, Q., Kenkare, P.U.**, 2000, J. Appl. Polym. Sci., **78**, 1971

- [19] **Chilkoti, A., Dreher, M.R., Meyer, D.E., Raucher, D.**, 2002, *Adv. Drug Deliv. Rev.*, **54**, 613
- [20] **Kobayashi, J., Kikuchi, A., Sakai, K., Okano, T.**, 2002, *J. Chromatogr. A*, **958**, 109
- [21] **Anastase-Ravion, S., Ding, Z., Pelle, A., Hoffman, A.S., Letourneur, D.**, 2001, *J. Chromatogr B.*, **761**, 247
- [22] **Kushida, A., Yamato, M., Isoi, Y., Kikuchi, A., Okano T.**, 2005, *Eur. Cells Mater.*, **10**,23
- [23] **Tighe, B.R.**, 1986, *Polym. J.*, **8**, 18
- [24] **Pedley, G., Shelley, P.J., Tighe, B.J.**, 1980, *Polym. J.*, **12**, 99.
- [25] **Brazel, C.S., Peppas, N.A.**, 1996, *J. Controlled Release*, **39**, 57-64
- [26] **Lee, P. I.**, 1985, *Eur. Pat. Appl.*, **11**, 31.
- [27] **Lee, P. I.**, 1985, *J. Controlled Release*, **2**, 277.
- [28] **Andrade, J. D.**, 1976, *Hydrogels for Medical and Related Applications*, ACS Symposium Series, **31**, American Chemical Society.
- [29] **Pelton, R.H., Chibante, P.**, 1986, *Colloids Surf.* **20**, 247
- [30] **Wu, X., Pelton, R.H., Hamielec, A.E., Woods, D.R., McPhee, W.**, 1994, *Colloid Polym. Sci.*, **272**, 467.
- [31] **Bokias, G., Durand, A., Hourdet, D.**, 1998, *Macromol. Chem. Phys.*, **199**, 1387
- [32] **Dusek, K., Prins, W.**, 1969, *Adv. Polym. Sci.*, **6**, 1
- [33] **Weiss, N., Van Vliet, T., Silberberg, A.**, 1979, *J. Polym. Sci. Phys.*, **17**, 2229
- [34] **Bastide, J., Picot, C., Candau, S.**, 1981, *J. Macromol. Sci. Phys. B*, **19**, 13
- [35] **Richards, E.G., Temple, C.J.**, 1971, *Nature*, **230**, 92
- [36] **Hsu, T., Ma, D., Cohen, C.**, 1983, *Polymer*, **24**, 1273
- [37] **Pusey, P.N., van Megen, W.**, 1989, *Physica*, **A157**, 705
- [38] **Klonowski, W.**, 1985, *J. Apply. Phys.* **58**, 2883
- [39] **Tran-Cong, Q., Nagaki, T., Nakagawa, T., Yano, O., Soen, T.**, 1989, *Macromolecules*, **22**, 2720
- [40] **Bahar,I., Erbil,Y.,Baysal B.,Erman, B.**, 1987, *Macromolecules*, **20**, 1353

- [41] **Swislow, G., Sun, S.T., Nishio, I., Tanaka, T.**, 1980, *Phys. Rev. Lett.*, **44**, 796
- [42] **Amiya, T., Tanaka, T.**, 1987, *Macromolecules*, **20**, 1162
- [43] **Zrinyi, M., Horkay, F.**, 1989, *Macromolecules*, **22**, 394
- [44] **Zrinyi, M., Horkay, F.**, 1989, *Macromolecules*, **17**, 2805
- [45] **Marchetti, M., Prager, S., Cussler, E.**, 1990, *Macromolecules*, **23**, 1760
- [46] **Otake, K., Inomata, H., Konno, M., Saito, S.**, 1990, *J. Chem. Phys.*, **91**, 1345
- [47] **Mark, J. E., Erman, B.**, 1988, *Rubberlike Elasticity a Molecular Primer*. Wiley, New York
- [48] **Konak., Bansil, C.**, 1989, *Polymer*, **30**, 677
- [49] **Hassa, J., Ilavsky, M., Dusek, M.**, 1975, *J. Polym. Sci. Polym. Phys.*, **13**, 253
- [50] **Weiss, N., Silberberg, A.**, 1975, *Polym. Prepr. Am. Chem. Soc., Div. Polym. Chem.*, **16**, 289
- [51] **Siegel, R.A., Frestone B.A.**, 1988, *Macromolecules*, **21**, 3254
- [52] **Hirokawa, Y., Tanaka, T., Katayama, S.**, 1984, In *Life Sciences Research Rep.* **31**, 77
- [53] **Beltran, S., Hooper, H.H., Blanch, W.H., Prausnitz, J.M.**, 1990, *J. Chem. Phys.*, **92**, 2061
- [54] **Ohmine, I, Tanaka, T.**, 1982, *J. Chem. Phys.*, **77**, 5725
- [55] **Osada, Y., Umezawa, K., Yamauchi, A.**, 1988, *Macromol. Chem.*, **189**, 597
- [56] **Katayama, S., Ohata, A.**, 1985, *Macromolecules*, **18**, 2781
- [57] **Pinkrah, V.T., Snowden, M.J., Mitchell, J.C., Seidel, J., Chowdhry, B.Z., Fern, G.R.**, 2003, *Langmuir*, **19**, 585
- [58] **Peng, T., Cheng, Y.L.**, 2001, *Polymer*, **41**, 2091
- [59] **Bignotti, F., Penco, M., Sartore, L., Peroni, I., Mendichi, R., Casolaro, M.**, 2000, *Polymer*, **41**, 8247.
- [60] **Kurisawa, M., Yui, N.**, 1998, *J. Control. Release*, **54**, 191
- [61] **Miyata, T., Asami, N., Uragami, T.**, 1999, *Nature*, **399**, 766

- [62] **Ulijn, R.V.**, 2006, *J. Mater. Chem.*, **16**, 2217
- [63] **Kang, S., Bae, Y.H.**, 2003, *J. Control. Release*, **86**, 115
- [64] **Erbil, C., Yıldız, Y., Uyanık, N.**, 2000, *Polym. Int.*, **49**, 795
- [65] **Tokuyama, H., Ishihara, N., Sakohara, S.**, 2007, *Europ. Polym. J.*, **43**, 4975
- [66] **Wu, C., Zhou, S.Q.**, 1997, *Macromolecules*, **30**, 574.
- [67] **Wu, C., Zhou, S.Q.**, 1995, *Macromolecules*, **28**, 381.
- [68] **Shibayama, M., Fujikawa, Y., Nomura, S.**, 1995, *Macromolecules*, **28**, 381.
- [69] **Wu, C., Zhou, S.Q.**, 1996, *Macromolecules*, **29**, 1574.
- [70] **Shibayama, M., Morimoto, M., Nomura, S.**, 1994, *Macromolecules*, **27**, 5060.
- [71] **Shibayama, M., Fujikawa, Y., Nomura, S.**, 1996, *Macromolecules*, **29**, 535.
- [72] **Shibayama, M., Morimoto, M., Nomura, S.**, 1994, *Macromolecules*, **27**, 5060.
- [73] **Casolaro, M.**, 1995, *Macromolecules*, **28**, 2351.
- [74] **Shibayama, M., Mizutani, S.Y., Nomura, S.**, 1996, *Macromol.* **29**, 2019.
- [75] **Boutris, C., Chatzi, E.G., Kiparissides, C.**, 1997, *Polymer*, **38**, 2567.
- [76] **Lim, Y.H., Kim, D., Lee, D.S., Casolaro, M.**, 1997, *Polymer*, **36**, 4827.
- [77] **Staikos, G.**, 1995, *Macromol. Rapid Commun.*, **16**, 913.
- [78] **Wu, C., Zhou, S.Q., Yeung, S.C.F.A., Jiang, S.H.**, 1996, *Angew. Makromol. Chem.*, **240**, 123.
- [79] **Snowden, M.J., Chowdhry, B.A., Vincent, B., Morris, G.E.**, 1996, *J.Chem. Soc. Faraday Trans.*, **92**, 5013.
- [80] **Ringsdorf, H., Venzmer, J.**, 1991, *J. Macromol.*, **24**, 1678
- [81] **Li, M., Jiang, M., Zhang, Y.X., Fang, Q.**, 1997, *Macromolecules*, **30**, 470,
- [82] **Winnik, F.M.**, 1990, *Macromolecules*, **23**, 233.
- [83] **Shibayama, M., Tanaka, T., Han, C.C.**, 1992, *J. Chem. Phys.*, **97**, 6842.
- [84] **Shibayama, M., Tanaka, T.**, 1995, *J. Chem. Phys.*, **102**, 9392.

- [85] **Yoo, M.K., Sung, Y.K., Cho, C.S., Lee, Y.M.**, 1997, *Polymer*, **38**, 2759.
- [86] **Bansil, R., Gupta, M.K.**, 1980, *Ferroelectrics*, **30**, 63
- [87] **Mallam, S., Hetch, A., Geissler, E., Pruvost, P.**, 1989, *J. Chem. Phys.*, **91**, 6447
- [88] **Guth, E., Mark, H.**, 1934, *Monats. Chem.* **65**, 93
- [89] **Weiss, N., Silberberg, A.**, 1977, *Br. Polym. J.*, **9**, 144
- [90] **Candau, S.J., Young, C.Y., Tanaka, T., Bastide, J.**, 1979, *J. Chem. Phys.*, **70**, 4694
- [91] **Hirotsu, S.**, 1987, *J. Phys. Soc. Jpn.*, **56**, 233
- [92] **Nishio, I., Swislow, G., Sun, S.T., Tanaka, T.**, 1982, *Nature*, **300**, 243
- [93] **Taylor, L. D., Cerankowski, L. D.**, 1975, *J. Polym. Sci. Polym. Chem.*, **13**, 2551
- [94] **Ray, B.; Isobe, Y., Morioka, K., Habaue, S., Okamoto, Y., Kamigaito, M.; Sawamoto, M.**, 2003, *Macromolecules*, **36**, 543.
- [95] **Ray, B., Isobe, Y., Matsumoto, K., Habaue, S., Okamoto, Y., Kamigaito, M., Sawamoto, M.**, 2004, *Macromolecules*, **37**, 1702.
- [96] **Fujishige, S.; Kubota, K.; Ando, I.** 1989, *J. Phys. Chem.*, **93**, 3311.
- [97] **Tiktopulo, E. I., Uversky, V. N., Lushchik, V. B., Klenin, S. I., Bychkova, V.E., Ptitsyn, O. B.**, 1995, *Macromolecules*, **28**, 7519.
- [98] **Takei, Y., Aoki, T., Sanui, K., Ogata, N., Okano, T., Sakurai, Y.**, 1993, *Bioconjugate Chem.*, **4**, 42.
- [99] **Ding, Z., Chen, G., Hoffman, A.**, 1996, *Bioconjugate Chem.*, **7**,121.
- [100] **Tong, Z., Zeng, F., Zheng, X., Sato, T.**,1999, *Macromolecules*, **32**, 4488.
- [101] **Zheng, X., Tong, Z., Xie, X., Zeng, F.**, 1998, *Polym. J.*, **30**, 284
- [102] **Baltes, T., Garret-Flaudy, F., Freitag, R.**, 1999, *J. Polym. Sci: Part A: Polym. Chem.*, **37**, 2977.
- [103] **Xia, Y., Yin, X., Burke, N. A. D., Stover, H. D. H.**, 2005, *Macromolecules*, **38**, 5937.
- [104] **Furyk, S., Zhang, Y., Ortiz-Acasto, D., Cremer, P.S., Bergbreiter, D.E.**, 2006, *J. Polym. Sci: Part A: Polym. Chem.*, **44**, 1492.
- [105] **Uchida, K; Saka, K., Ito, E., Kikuchi, A., Yamato, M., Okana, T.**, 2000, *Biomaterials*, **21**, 923-929.

- [106] **Eliassaf, J.**, 1987, *J. Appl. Polym. Sci.*, **22**, 873-874
- [107] **Rochev, Y., Golubeva, T., Gorelow, A., Allen, L., Gallagher, W.M. Selezneva, I., Gavrilyuk, B., Dawson, K.**, 2001, *Prog. Colloid Polym. Sci.*, **118**, 153-156
- [108] **Winnik, F M., Ringsdorf, H., Venzmer, J.**, 1990, *Macromolecules* **23**, 2415.
- [109] **Seker, F., Ellis, A. B.**, 1998, *J. Polym. Sci., Part A: Polym. Chem.*, **36**, 2095
- [110] **Wu, X. Y., Pelton, R. H., Tam, K. C., Woods, D. R., Hamielec, A. E.**, 1993, *J. Polym. Sci., Part A: Polym. Chem.*, **31**, 957.
- [111] **Djokpe, E., Vogt, W.**, 2001, *Macromol. Chem. Phys.*, **202**, 750.
- [112] **McPheem, W., Tam, K.C., Pelton, R.**, 1993, *J. Colloids Interface Sci.*, **146**, 24.
- [113] **Park, T. G., Choi, H. K.**, 1998, *Macromol. Rapid Commun.* **19**, 167.
- [114] **De Rossi, D., Kajiwara, K., Osada, Y., Yamadin, A.**, 1991. Plenum Press, New York
- [115] **Vidakovic, P., Rondelez, F.**, 1984, *Macromolecules* **17**, 418.
- [116] **Lifshitz, I., Grosberg, A., Khokhlov, A. R.**, 1978, *Rev. Mod. Phys.* **50**, 683
- [117] **Heskins, M., Guillet, J.E.**, 1968, *J. Macromol. Sci. Chem.*, **A2**, 1441
- [118] **Kato, N., Takahashi, F.**, 1997, *Bull. Chem. Soc. Jpn.*, **70**, 1289
- [119] **Chu, B., Xu, R., Wang, Z., Zuo, J.**, 1988, *J. Appl. Crystallogr.*, **21**, 707
- [120] **Xue, W., Hamley, I.W.**, 2002, *Polymer*, **43**, 3069.
- [121] **Volpert, E., Selb, J., Candau, F.**, 1996, *Macromolecules*, **29**, 1452.
- [122] **Etsuo, K., Zhang, Y.Q., Toyochi, T., Mamada, A.**, 1993, *Macromolecules*, **26**, 1053.
- [123] **Edward Glass, J.**, 1996, *Hydrophilic Polymers*, American Chemical Society, Washington, DC,
- [124] **Spafford, M., Polozava, A., Winnik, F.W.**, 1998, *Macromolecules*, **31**, 7099
- [125] **Meyer, D.E., Shin, B.C., Kong, G.A., Dewhirst M.W., Chilkoti, A.**, 2001, *J. Control, Release*, **74**, 213

- [126] **Brazel, C.S., Peppas, N.A.**, 1995, *Macromolecules*, **28**, 8016
- [127] **Hirotsu, S., Hirokawa, Y., Tanaka, T.**, 1987, *J. Chem. Phys.*, **87**, 1392
- [128] **Schild, H.G., Sung, Y.K., Cho, C.S., Lee, Y.M.**, 1997, *Polymer*, **38**, 2759
- [129] **Erbil, C., Akpınar, F.D., Uyanık, N.**, 2000, *Macromol Chem. Phys.*, **200**, 2448.
- [130] **Ganorkar, C.R., Liu, R., Baudys M., Kim, S.W.**, 1999, *J. Control. Release*, **59**, 287
- [131] **Durand, A., Hourdet, D.**, 1999, *Polymer*, **40**, 4941,
- [132] **Durand, A., Hourdet, D.**, 2000, *Polymer*, **41**, 545
- [133] **Chen, G., Hoffman, A.S.** 1995, *Nature*, **373**, 49
- [134] **Kawasaki, H., Sasaki, S., Maeda, H.**, 1997, *J. Phys. Chem. B*, **26**, 101
- [135] **Chen, G., Hoffman, A. S.**, 1995, *Macromol. Chem. Phys.*, **196**, 1251
- [136] **Lowe, L.T., Tenhu, H.**, 1998, *Macromolecules*, **31**, 1590.
- [137] **Yoshida, R., Okuyama, R., Sakai, Y., Okana, T., Sakurai, Y.**, 1994, *J. Membr. Sci.*, **89**, 267.
- [138] **Kaneko, Y., Yoshida, R., Sakai, K., Sakurai, Y., Okana, T.**, 1995, *J. Membr. Sci.* **101**,13.
- [139] **Faes, H., Schryver, F.C.D., Sein, A., Bijma, K., Kevelam, J., Engberts, J.B.F.N.**, 1996, *Macromolecules*, **29**, 3875.
- [140] **Turner, K., Zhu, P.W., Napper, D.H.**, 1996, *Colloid Polym. Sci.*, **274**, 622
- [141] **Bromberg, L.**, 1996, *Macromol. Rapid Commun.*, **17**, 481.
- [142] **Lee, W.F., Hugh, G.C.**, 1997, *J. Appl. Polym. Sci.*, **64**, 1477.
- [143] **Taniguchi, T., Kuraki, M., Miyashita, T.**, 1996, *Colloid Polym. Sci.*, **274**, 717.
- [144] **Lu, T., Vesterinen, E., Tenhu, H.**, 1998, *Polymer*, **39**, 641.
- [145] **Lim, Y.H., Kim, D., Lee, D.S.**, 1997, *J. Appl. Polym. Sci.*, **64**, 2647
- [146] **Hoffman, A.S., DeRossi, D., Kajiwara, K., Osada, Y., Yamauchi, A.**, 1991, *Plenum Press, New York*, p.289

- [147] **Ratner, B.D., Hoffman, A.S.**, 1976, American Chemical Society, Washington.
- [148] **Schroder, U.P., Oppermann, W.**, 1996, John Wiley&Sons,
- [149] **Jones, M.C., Ranger, M., Leroux, J-C.**, 2003, Bioconj. Chem., **14**, 774
- [150] **Dufresne, M.H., Garrec, D.L., Sant, V., Leroux, J-C., Ranger, M.**, 2004, Int. J. Pharm., **277**, 81
- [151] **Dong, L.C., Hoffman, A.S.**, 1989, Trans. 15th. Ann. Myg. Soc.Biomater., 169
- [152] **Dong, L.C., Hoffman, A.S.**, 1990, J. Controlled Release, **13**, 21
- [153] **Kuhn, W.**, 1934, Kolloid Z. **68**, 2-15
- [154] **Kuhn, W.**, 1936, Kolloid Z. **76**, 258-271
- [155] **Treloar, L.R.G.**, 1947, Trans. Faraday Soc., **43**, 591
- [156] **James, H.M., Guth, E., J.** 1943, Chem. Phys., **11**, 455
- [157] **Wall, F.T.**, 1942, J. Chem. Phys., **10**, 132
- [158] **Flory, P.J., Rehner, Jr.**, 1943, J. Chem. Phys., **11**, 521
- [159] **M.L. Huggins, M.L.**, 1941, J. Chem. Phys., **9**, 440
- [160] **Dusek, K., Patterson, D.**, 1968, J. Polym. Sci., **6**, 1209
- [161] **Tanaka, T., Hocker, L.O., Benedek, G.B.**, 1973, J. Chem. Pyhs., **59**, 5151
- [162] **Tanaka, T., Ishiwata, S., Ishimota, C.**, 1977, Phys. Rev. Lett., **38**, 771
- [163] **Flory, P.J.**, 1953, Principle of Polymer Chemistry, Cornell University Press, Ithaca, New York
- [164] **Tanaka, T., Fillmore, T., Sun, S.T., Nishio, I., Swislow, G.**, 1980, Phys. Rev. Lett., **45**, 1636
- [165] **Osada, Y., Umezawa, K., Yamauchi, A.**, 1988, Macromol. Chem., **189**, 597
- [166] **Irie, M.**, 1986, Macromolecules, **19**, 2890
- [167] **Hirokawa, Y., Tanaka, T.**, 1985, Macromolecules, **18**, 2782
- [168] **Ricka, J., Tanaka, T.**, 1984, Macromolecules, **17**, 2916
- [169] **Firestone, B.A. , Siegel, R.A.**, 1988, Polym. Commun., **29**, 204

- [170] **Lee, H.B., John, N.S., Andrade, J.D.**, 1975, *J. Colloid Interface Sci.*, **51**, 225
- [171] **Takizawa, A., Kinoshita, T., Nomura, O., Tsujita, Y.**, 1985, *Polym. J.*, **17**, 747
- [172] **Al-Issa, M.A., Davis, T.P., Huglin, M.B., Rego, J.M., Rehab, M.M.**, 1990, *Macromol. Chem.*, **191**, 321
- [173] **Ilavsky, M., Hrouz, J., Havlicek, I.**, 1985, *Polymer*, **26**, 1514
- [174] **Kokufuta, E., Zhang, Y.Q., Tanaka, T.**, 1992, *Phase Trans.*
- [175] **Amiya, T., Hirokawa, Y., Hirose, Y., Li, Y., Tanaka, T.**, 1987, *J. Chem. Phys.*, **86**, 2375
- [176] **Hirotsu, S.**, 1990, *Macromolecules*, **23**, 903
- [177] **Strauss, U.P.**, 1989, *Am. Chem. Soc. Symp. Ser.* **223**, 317
- [178] **Peer, W.J.**, 1989, *Am. Chem. Soc. Symp. Ser.* **223**, 381
- [179] **Iliopoulos, I., Audebert, R., Quivoron, C.**, 1987, *Am. Chem. Soc. Symp. Ser.* **350**, 72
- [180] **Ilmain, F., Tanaka, T., Kokufuta, E.**, 1991, *Nature*, **349**, 400
- [181] **Okana, T., Bae, Y.H., Jacobs, H., Kim, S.W.**, 1990, *J. Contrl. Rel.* **11**, 255
- [182] **Heller, P.**, 1967, *Rept. Prog. Phys.*, **30**, 731
- [183] **Ma, S.K.**, 1976, *Modern Theory of Critical Phenomena*. Menlo Park, CA
- [184] **Li, Y., Tanaka, T.**, 1989, *J. Chem. Phys.*, **90**, 5161
- [185] **Hockberg, A., Tanaka, T., Nicoli, T.**, 1979, *Phys. Rev. Lett.*, **43**, 217
- [186] **Tabak, F., Corti, M., Pavesi, L., Rigamonti, A.**, 1987, *J. Phys.*, **C20**, 5691
- [187] **Ilavsky, M.**, 1981, *Polymer*, **22**, 1687
- [188] **Kramer, O.**, 1986, *Biological and Synthetic Polymer Networks*. New York
- [189] **Boyde, T.R.C.**, 1976, *J. Chromatogr.*, **124**, 219
- [190] **Veatch, R.W.**, 1983, *J. Pet. Technol.* April: 677
- [191] **Werner, G.**, 1984, *Allg. Vliesstoff-Rep.* **4**, 178

- [192] **Kossmelh, G., Klaus, N., Schafer, H.**, 1984, *Angew. Makromol. Chem.*, **123/124**, 2412
- [193] **Steinberg, I.Z., Oplatka, A., Katchalsky, A.**, 1966, *Nature*, **210**, 568
- [194] **Sussman, M.V., Katchalsky, A.**, 1970, *Science*, **167**, 45
- [195] **Horkay, F., Zrinyi, M.**, 1989, *Macromol. Chem. Macromol Symp.*, **30**, 133
- [196] **Fujiwuro, H., Shibayama, H., Chen, J.H., Nomura, S.**, 1989, *J. Appl. Polym. Sci.*, **37**, 1403
- [197] **De Rossi, D., Chiarelli, P., Buzzigoli, G., Domenici, C., Lazzeri, L.**, 1986, *Trans. Am. Soc. Artif. Intern. Organs*, **32**, 157
- [198] **Shiga, T., Hirose, Y., Okada, A., Kurauchi, T.**, 1989, *197th Am. Chem. Soc. Polym. Prep.*, p.310
- [199] **Suzuki, M.**, 1989, *Polym. Prep. Jpn.*, **46**, 603
- [200] **Osada, Y., Hasebe, M.**, 1985, *Chem. Lett.*, **9**, 1285
- [201] **Irie, M., Kungwachakun, D.**, 1985, *Macromol. Chem. Rapid Commun.* **5**, 829
- [202] **Yoshino, K., Nakao, K., Onado, M., Sugimoto, R.**, 1989, *Jpn. J. Appl. Polym.*, **28**, L682
- [203] **Yoshino, K., Nakao, K., Morita, S., Onado, M.**, 1989, *Jpn. J. Appl. Polym.*, **28**, L2027
- [204] **Osada, Y.**, 1987, *Adv. Polym. Sci.*, **82**, 1
- [205] **Kokufuto, E., Zhang, Y.Q., Tanaka, T.**, 1991, *Nature*, **351**, 302
- [206] **Freitas, R.F.S., Cussler, E.L.**, 1987, *Sep Sci Technol.*, **22**, 911
- [207] **Saitoh, K., Ozawa, T., Suzuki, N.**, 1976, *J. Chromatogr.*, **124**, 231
- [208] **Gehrke, S.H., Cussler, E.L.**, 1989, *Chem. Eng. Sci.*, **44**, 559
- [209] **Kou, J.H., Fleisher, D., Amidon, G.L.**, 199, *J. Control. Rel.*, **12**, 241
- [210] **Hasirci, V.N.**, 1982, *J. Appl. Polym. Sci.*, **27**, 33
- [211] **Hoffman, A.S.**, 1987, *J. Control. Rel.*, **6**, 297
- [212] **Park, T.G., Hoffman, A.S.**, 1988, *Appl. Biochem. Biotech.*, **19**, 1
- [213] **Park, T.G., Hoffman, A.S.**, 1990, *Biochem. Bioeng.*, **35**, 152
- [214] **Dong, L.C., Hoffman, A.S.**, 1987, *Am. Chem. Soc. Symp. Ser.*, **350**, 236

- [215] **Kokufuto, E., Tanaka, T.**, 1991, *Macromolecules*, **24**, 1605
- [216] **Bae, Y.H., Okana, T., Hsu, R., Kim, S.W.**, 1987, *Macromol. Chem. Rapid. Commun.*, **8**, 481
- [217] **Bae, Y.H., Okana, T., Kim, S.W.**, 1989, *J. Contrl. Rel.*, **9**, 271
- [218] **Siegel, R.A., Falamarzian, M., Firestone, B.A., Moxley, B.C.** 1988, *J. Contrl. Rel.*, **8**, 179
- [219] **Siegel, R.A., Firestone, B.A.**, 1990, *J. Contrl. Rel.*, **11**, 181
- [220] **Grimshaw, P.E., Grodzinsky, A.J.**, 1989, *Chem. Eng. Sci.*, **44**, 827
- [221] **Park, K., Park, H.**, 1999, *Polymeric Materials Encyclopedia*, 1476
- [222] **Hoffman, A.S.**, 1997, *Challenge and Strategies*, American Chemical Society, 485
- [223] **Bae, Y.H.**, 1997, *Challenge and Strategies*, American Chemical Society, 147
- [224] **Suzuki, M.**, 1991, *Polymer Gels*, Plenum Press, New York, 221
- [225] **Kishi, R., Ichijo, H., Hirasa, O.**, 1993, *J. Intelligent Mater. Sys. Struct.*, **4**, 533
- [226] **Kajiwara, K., Ross-Murphy, S.B.**, 1992, *Nature*, **355**, 208
- [227] **Osada, Y., Okuzaki, H., Hori, H.**, 1992, *Nature*, **355**, 242
- [228] **Ueoka, Y., Gong, J., Osada, Y.**, 1997, *J. Intelligent Mater. Syst. Struct.*, **8**, 465
- [229] **Dong, L.C., Hoffman, A.S.**, 1986, *J. Controlled Release*, **4**, 223
- [230] **Dong, L.C., Hoffman, A.S.**, 1987, *American Chemical Society*, Washington, DC, 236
- [231] **Shiroya, T., Tamura, N., Yasui, M., Fujimoto, K., Kawaguchi, H.**, 1995, *Colloids Surf.* **B4**, 267
- [232] **Park, T.G., Hoffman, A.S.**, 1990, *J. Biomed. Mater. Res.*, **21**, 24
- [233] **Park, T.G., Hoffman, A.S.**, 1993, *Enzyme Microb. Tech.*, **15**, 476
- [234] **Chen, J.P., Sun, Y.M., Chu, D.H.**, 1998, *Biotechnol. Prog.*, **14**, 473
- [235] **Park, T.G., Hoffman, A.S.**, 1991, *Biotechnol. Prog.*, **7**, 383
- [236] **Freitas, R.F.S., Cussler, E.L.**, 1987, *Chem. Eng. Sci.*, **42**, 97

- [237] **Cussler, E.L., Stokar, M., Varberg, J.E.**, 1984, *AICHe J.*, **30**, 578
- [238] **Feil, H., Bae, Y.H., Kim, S.W.**, 1991, *J. Memb. Sci.*, **64**, 283
- [239] **Gehrke, S.H., Andrews, G.P., Cussler, E.L.**, 1986, *Chem. Eng. Sci.*, **41**, 2153
- [240] **Trank, S.J., Johnson, D.W., Cussler, E.L.**, 1989, *Food Technol.*, **43**, 78
- [241] **Park, C., Orozco-Avila, I.**, 1992, *Biotechnol. Prog.*, **8**, 521
- [242] **Patel, V.R., Amiji, M.M.**, 1996, *Pharm. Res.*, **13**, 588
- [243] **Brannon-Peppas, L., Peppas, N.A.**, 1990, *Biomaterials*, **11**, 635
- [244] **Khare, A.R., Peppas, N.A.**, 1994, *J. Biomater. Sci. Polym. Ed.*, **6**, 598
- [245] **Ghandehari, H., Kopeckova, P., Kopecek, J.**, 1997, *Biomaterials*, **18**, 861
- [246] **Akala, E.O., Kopeckova, P., Kopecek, J.**, 1998, *Biomaterials*, **19**, 1037
- [247] **Gutawska, A., Bark, J.S., Kwon, I.C., Bae, Y.H., Kim, S.W.**, 1997, *J. Controlled Release*, **48**, 141
- [248] **Bilia, A., Carelli, V., Di Colo, G., Nannipieri, E.**, 1996, *Int. J. Pharm.*, **130**, 83
- [249] **Carelli, V., Coltelli, S., Di Colo, G., Nannipieri, E., Serafini, M.F.**, 1999, *Int. J. Pharm.*, **179**, 73
- [250] **Matsua, E.S., Tanaka, T.**, 1988, *J. Chem. Phys.*, **89**, 1695
- [251] **Kaneko, Y., Sakai, K., Kikuchi, A., Yoshida, R., Sakurai, Y., Okana, T.**, 1995, *Macromolecules*, **28**, 7717
- [252] **Okana, T., Yoshida, R., Sakai, K., Sakurai, Y.**, 1991, *Fundamentals and Biomedical Applications*. Plenum Press, New York, pp.299
- [253] **Kim, S.W., Bae, Y.H., Okana, T.**, 1992, *Pharm. Res.* **9**, 283
- [254] **Kim, I.S., Jeong, Y.I., Cho, C.S., Kim, S.H.**, 2000, *Int. J. Pharm.*, **211**, 1
- [255] **Priest, J.H., Nelson, R.G., Murray, S.L., Hoffman, A.S.**, 1987, *ACS Symposium Series*, **350**, 255
- [256] **Kugo, K., Grashin, J., Hoffman, A.S.**, 1988, *Trans. Third World Biomaterials Congress*,
- [257] **Katime, I., Valderruten, N., Quintana, J.R.**, 2001, *Polym. Int.*, **50**, 869

- [258] **Katono, H., Sanui, K., Ogata, N., Okana, T., Sakurai, Y.**, 1991, *Polym. J.*, **23**, 1179
- [259] **Jeong, B., Bae, Y.H., Lee, D.S., Kim, S.W.**, 1997, *Nature*, **388**, 860
- [260] **Yuk, S.H., Bae, Y.H.**, 1999, *Crit. Rev. Ther. Drug Carrier Syst.*, **16**, 385
- [261] **Peppas, N.A., Bures, P., Leobandung, W., Ichikawa, H.**, 2000, *Eur. J. Pharm. Biopharm.*, **50**, 27
- [262] **Serres, A., Baudys, M., Kim, S.W.**, 1996, *Pharm. Res.*, **13**, 196
- [263] **Vakkalanka, S.K., Brazel, C.S., Peppas, N.A.**, 1996, *J. Biomater. Sci. Polym. Ed.*, **8**, 119
- [264] **Narayani, R., Hermes, R.S., Rao, K.P.**, 1998, *Proc. IUPAC Int. Symp. Adv. Polym. Sci. Technol.*, **2**, 579
- [265] **Xue, W., Champ, S., Huglin, M.B.**, 2001, *Polymer*, **42**, 3665
- [266] **Gutowska, A., Bae, Y.H., Jacobs, H., Feijen, J., and Kim, S.W.**, 1994, *Macromolecules*, **27**, 4167
- [267] **Muniz, E.C., Geuskens, G.**, 2001, *Macromolecules*, **34**, 4480
- [268] **Tanaka, Y., Gong, J.P., Osada, Y.**, 2005, *Prog. Polym. Sci.*, **30**, 1
- [269] **Erbil, C., Kazancıoğlu, E., and Uyanık, N.**, 2004, *Eur. Polym. J.*, **40**, 1145
- [270] **Yıldız, Y., Uyanık, N., Erbil, C.**, 2006, *J. Macromol. Sci. Part:A, Pure and Appl. Chem.*, **43**, 1091
- [271] **Nagaoka, S.**, 1989, *Polym. J.*, **21**, 847
- [272] **Baker, B.R., Shaub R.E., Williams, G.H.**, 1952, *J. Org. Chem.*, **17**, 122
- [273] **Otsu, T., Yamagishi, K., Yoshioka, M.**, 1992, *Macromolecules*, **25**, 2713
- [274] **Gargallo, L., Radic, D.**, 1985, *Macromol. Chem.*, **186**, 1289
- [275] **Reddy, T.T., Lavenant, L., Lefebvre, J., Renard, D.**, 2006, *Biomacromolecules*, **7**, 323
- [276] **Urushizaki, F., Yamaguchi, H., Nakamura, K., Numajiri, S., Sugibayashi, K., Morimoto, Y.**, 1990, *Int J Pharm*, **58**, 135.
- [277] **Khare, A.R., Peppas, N.A.**, 1995, *Biomaterials*, **16**, 559
- [278] **Peppas, N. A.**, 1985, *Pharm. Acta. Helv.*, **60**, 110
- [279] **Lee, W., Yeh, Y.**, 2005, *European Polym. Journal*, **41**, 2488

## **BIOGRAPHY**

Yalçın Yıldız was born in Sakarya in 1974. After finishing primary, secondary and high school in Istanbul, he obtained his B. Sc. in Chemistry from Istanbul Technical University in Istanbul (1996).

He got his M. Sc. in Chemistry from Istanbul Technical University (1999) and he started his Ph. D. studies in Polymer Science and Technology program.

His research interests are mainly focus on polymer gels, polyurethanes and coloring.

He has worked for Aksoy Plastik as a research and development director in 2001-2003 and has been working as a research scientist in Flokser Tekstil since 2006.

## **Publications**

1. "Synthesis and Characterization of Poly -dimethyl siloxane- Containing Poly -vinyl pyrrolidinone- Block Copolymers" Nurseli UYANIK, Berrin KÖKER, Yalçın YILDIZ, J.Appl.Polym.Sci., 71, 1915-1922, 1999.
2. "Effect of Synthesis-Solvent Composition and Initiator Concentration on the Swelling Behaviours of Poly-N-isopropylacrylamide- -NIPAAM-, Poly-NIPAAM – co - dimethyl itaconate- and Poly-NIPAAM-co- itaconic acid- Gels" Candan ERBİL, Yalçın YILDIZ, Nurseli UYANIK, Polym. Int. 49:795-800, 2000.
3. "Effects of acetophenone-formaldehyde resin on the degradation of high-density polyethylene by UV-irradiation", Yalçın YILDIZ,, N. Uyanik, N. Kızılcın, Pigment & Resin Technology, 35, 5, 247-251, 2006.
4. "Compressive Elastic Moduli of Poly(N-isopropylacrylamide) Hydrogels Crosslinked with Poly(dimethyl siloxane)", Yalçın YILDIZ, Nurseli UYANIK, Candan ERBİL, Journal of Macromolecular Science, Part A: Pure and Applied Chemistry,43:1091-1106,2006.
5. "N-Isopropylacrylamide/monoalkyl itaconate copolymers and N-isopropylacrylamide/itaconic acid/dimethyl itaconate terpolymers", Candan Erbil, Yalçın Yıldız, Nurseli Uyanık, Polymer, Polym. Adv. Technol. 19, 1-8, 2008.

## **Presentations**

1. “Farklı Zincir Uzunluklarında Poli -Dimetil Siloksan- İçeren Makro Başlatıcılar Kullanılarak Sentezlenen ABA Tipi Polivinil Prolidinon Blok Kopolimerleri”, Yalçın YILDIZ, Nurseli UYANIK, Berrin KÖKER, XII. Ulusal Kimya Kongresi, Edirne, 1998.
2. “Yüksek Yoğunluklu Polietilenin Özel Katkı Maddelerinin Etkisi İle UV Işımasında Bozunması”, Yalçın YILDIZ, Nilgün KIZILCAN, Nurseli UYANIK, Güneri AKOVALI, XIII Ulusal Kimya Kongresi, Samsun, 1999.
3. “Başlatıcı Konsantrasyonunun Ve Sentezde Kullanılan Çözücü Bileşiminin Hidrofilik Ve İyonlaşabilen Gruplar İçeren Poli-N-İzopropilakrilamid- Kopolimer Jellerinin Faz Geçiş Davranışları Üzerindeki Etkilerinin İncelenmesi”, Candan ERBİL, Yalçın YILDIZ, Nurseli UYANIK, XIII Ulusal Kimya Kongresi, Samsun, 1999.
4. “Study of Ultraviolet Photooxidative Degradation of HDPE With a Special Photosensitizer”, Nurseli UYANIK , Yalçın YILDIZ, Nilgün KIZILCAN , Güneri AKOVALI, The 5th International Symposium of Scientists of Turkic Languages Countries on Polymers and PolymerComposites, ALMATY, September 1999.
5. “Solution Behaviours of NIPAAm/Monoitaconate Copolymers and NIPAAm/Itaconic acid/Dimethyl Itaconate Terpolymers”, Yalçın YILDIZ, Candan ERBİL, Nurseli UYANIK, 9th International Symposium on Polymers of Advanced Technologies (PAT), 22-25 October 2007, Shangai, China.